NEA/NSC/DOC(95)03/IV
Volume IV

SAND2016-9686R

LEU-COMP-THERM-097

TITANIUM AND/OR ALUMINUM ROD-REPLACEMENT EXPERIMENTS IN FULLY-REFLECTED WATER-MODERATED SQUARE-PITCHED U(6.90)O_2 FUEL ROD LATTICES WITH 0.67 FUEL TO WATER VOLUME RATIO (0.800 CM PITCH)

for publication in the
International Handbook of
Evaluated Criticality Safety Benchmark Experiments

Sandia National Laboratories is a multi-program laboratory managed and operated by Sandia Corporation, a wholly owned subsidiary of Lockheed Martin Corporation, for the U.S. Department of Energy's National Nuclear Security Administration under contract DE-AC04-94AL85000

NEA/NSC/DOC(95)03/IV
Volume IV

LEU-COMP-THERM-097

TITANIUM AND/OR ALUMINUM ROD-REPLACEMENT EXPERIMENTS IN FULLY-REFLECTED WATER-MODERATED SQUARE-PITCHED U(6.90)O_2 FUEL ROD LATTICES WITH 0.67 FUEL TO WATER VOLUME RATIO (0.800 CM PITCH)

Evaluator

Gary A. Harms
Sandia National Laboratories

Internal Reviewer
David E. Ames

Independent Reviewer

Nicolas Leclaire
Institut de Radioprotection et de Sûreté Nucléaire, IRSN

LEU-COMP-THERM-097

TITANIUM AND/OR ALUMINUM ROD-REPLACEMENT EXPERIMENTS IN FULLY-REFLECTED WATER-MODERATED SQUARE-PITCHED U(6.90)O_2 FUEL ROD LATTICES WITH 0.67 FUEL-TO-WATER RATIO (0.800 CM PITCH)

IDENTIFICATION NUMBER: LEU-COMP-THERM-097 SPECTRA

KEY WORDS: acceptable, aluminum, array, critical experiment, fuel rods, low enriched, square pitch, titanium, undermoderated, uranium, uranium dioxide, water-moderated, water-reflected

1.0 DETAILED DESCRIPTION

1.1 Overview of Experiment

The US Department of Energy (DOE) Nuclear Energy Research Initiative funded the design and construction of the Seven Percent Critical Experiment (7uPCX) at Sandia National Laboratories. The start-up of the experiment facility and the execution of the experiments described here were funded by the DOE Nuclear Criticality Safety Program. The 7uPCX is designed to investigate critical systems with fuel for light water reactors in the enrichment range above 5% ^{235}U. The 7uPCX assembly is a water-moderated and -reflected array of aluminum-clad square-pitched UO_2 fuel rods. The uranium is enriched to 6.90% by mass. Sets of 36 titanium and aluminum experiment rods with the same nominal outside diameter as the fuel rods were fabricated and used as replacements for fuel rods in the array. The twenty-four 7uPCX critical experiments reported here compare the effects of the titanium and aluminum replacement rods on nearly critical fuel rod arrays.

The fuel used in these experiments was fabricated using unirradiated UO_2 fuel pellets from fuel elements designed to be used in the internal nuclear superheater section of the Pathfinder boiling water reactor operated in South Dakota by the Northern States Power Company in the 1960s. The fuel elements were obtained from The Pennsylvania State University where they had been stored for many years. The fuel pellets in those fuel elements were removed from the original Incoloy cladding and reclad in 3003 aluminum tubes and end caps for use in the experiments reported here.

The nominal outside diameter of the fuel pellets is 0.207 in (0.52578 cm). The nominal outside diameter of the fuel rod cladding is 0.250 in (0.635 cm). The distance between the fuel rods in the square-pitched array is 0.315 in (0.8001 cm). This geometry gives a fuel-to-water volume ratio of 0.67 in the array.

The twenty-four critical experiments in this series were performed in 2015 and 2016 at the Sandia Critical Experiments Facility.

The first of the experiments had no replacement rods in the array and was intended to provide a baseline against which the experiments containing replacement rods could be compared. Eight critical experiments had titanium replacement rods in various numbers and arrangements near the center of the fuel array. Eight critical experiments had aluminum replacement rods in the same numbers and arrangements as in the eight experiments containing titanium experiment rods. In the final four experiments, fuel rods were removed from a central region of the array so that the pitch of the fuel rods in this part of the array was effectively doubled. This softened the neutron spectrum in the central part of the fuel array. Thirty-six replacement rods in different combinations of titanium and/or aluminum were placed in the interstices created in the center of the array.

All twenty-four critical experiments are judged to be acceptable as benchmark experiments.

1.2 Description of Experimental Configuration

1.2.1 Design of the Critical Assembly – An overall view of the critical assembly is shown in Figure 1. Figure 2 shows another view of the critical assembly. The assembly core resides in an elevated assembly tank that is connected to a moderator dump tank at a lower elevation. When the assembly is not being operated, the moderator resides in the dump tank. When the assembly is being brought to critical, the moderator is pumped from the dump tank into the assembly tank. The moderator can be released by gravity to the dump tank through two large-diameter pneumatically-operated normally-open dump valves. During operation, the moderator is continually circulated between the dump tank and the assembly tank. The level of the moderator in the assembly tank is maintained by overflow into one of two overflow standpipes. One is set at a fixed height that allows core tank to fill to a level that fully reflects the fuel in the critical assembly. The other overflow standpipe is remotely adjustable to set the water level in the core below the fully-reflected level. For the experiments described here, the adjustable standpipe was set to a level above that of the fixed standpipe. A heater is included in the dump tank to keep the moderator at a constant temperature set by a controller at the assembly control system. The purity of the water moderator is maintained by pumping it from the dump tank through clean-up loop consisting of a pump, two particulate filters, a resin bed, a resistivity water quality monitor, and the associated piping.

A cut-away view of the critical assembly is shown in Figure 3. The assembly fuel is supported in the assembly tank by two 1 in (2.54 cm) thick aluminum grid plates. A guide plate, used to align the fuel rods in the assembly during insertion, is located above the upper grid plate. The assembly core is situated in the tank to provide a 6.5 in (16.51 cm) thick water reflector below the lower grid plate. The diameter of the tank provides a radial water reflector around the assembly greater than 6 in (15.24 cm). The fixed assembly tank standpipe is set to provide an upper reflector approximately 6 in (15.24 cm) thick when the assembly tank is full.

The assembly has one control and two safety elements of identical design. Each of these elements has a B_4C-filled absorber section separated from a fuel follower by a polyethylene-filled decoupler section. When each of the elements is fully withdrawn, the fuel follower is in the assembly and the absorber is above the surface of the assembly moderator. The two types of elements are differentiated by the way in which they are used. During operations, the two safety elements are held in the most reactive position and provide a redundant shutdown mechanism that can be rapidly inserted by gravity drop. The control element is used to make fine adjustments to the reactivity of the assembly during operations. During the measurements reported here, all three elements were fully withdrawn to their most reactive positions. The three control/safety elements are attached to the control/safety element drives through electromagnets. The control/safety element drives are supported above the assembly tank by the drive support.

Figure 1. An Overall View of the Critical Assembly.

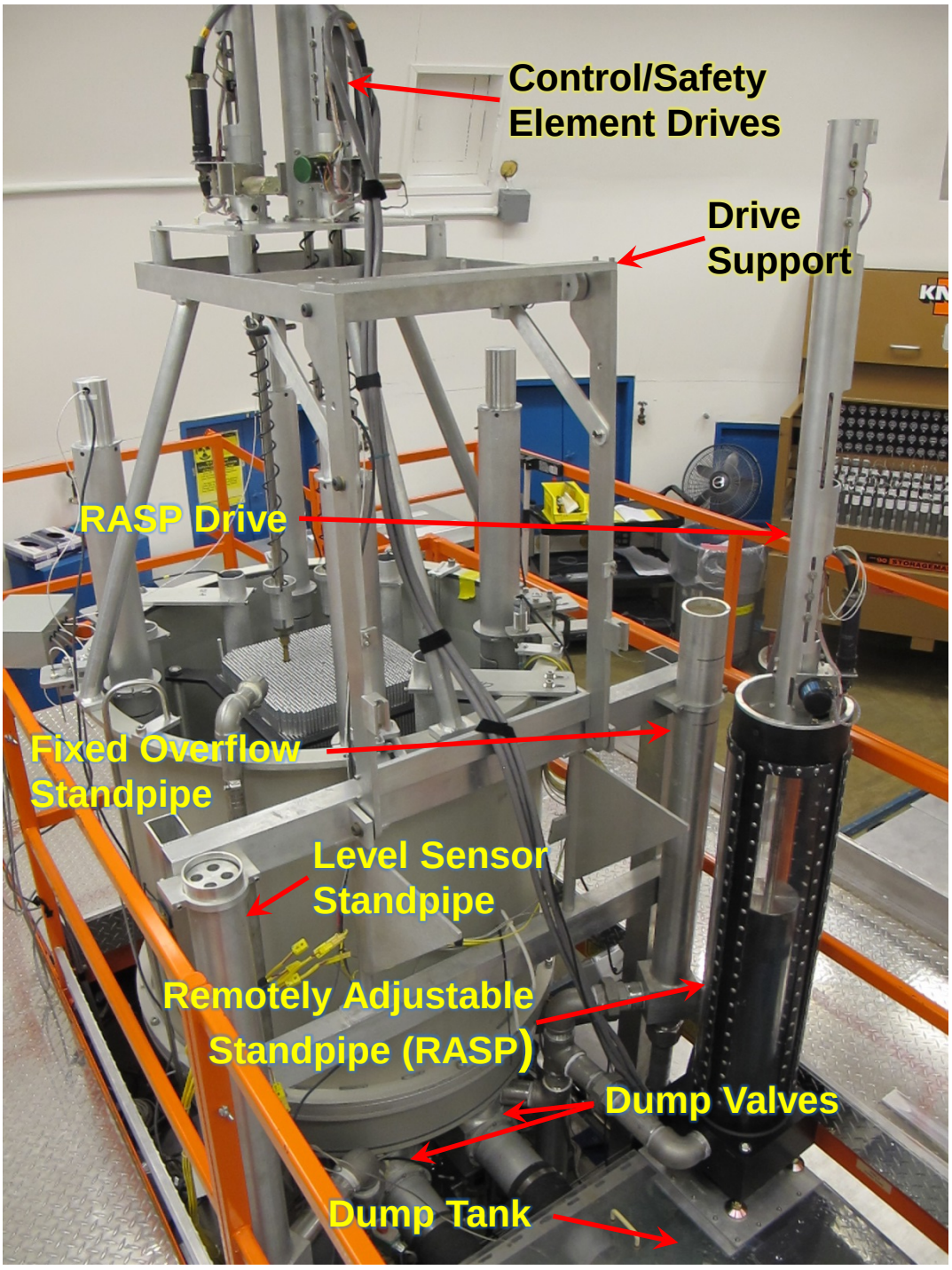

Figure 2. A Second View of the Critical Assembly.

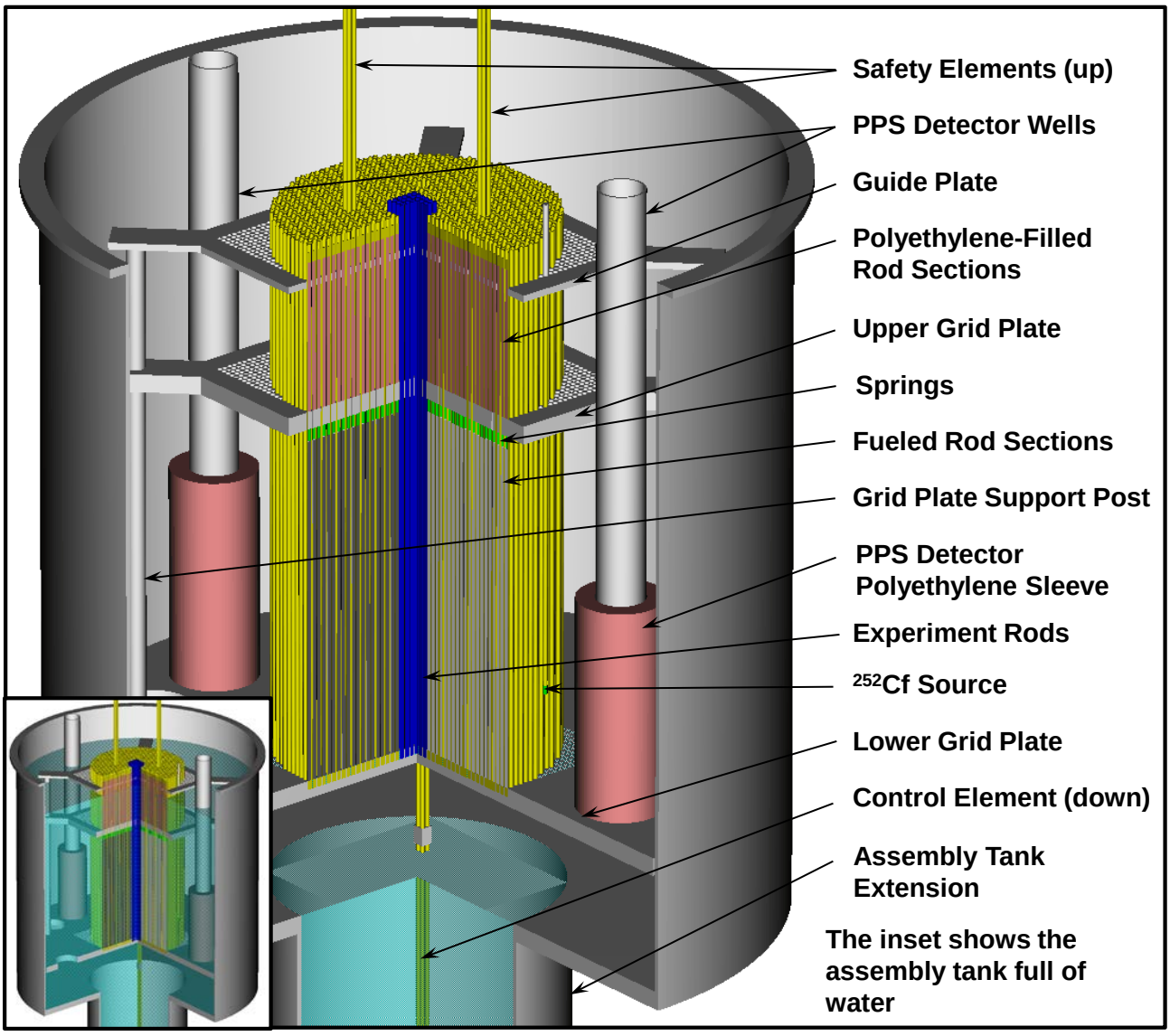

Figure 3. Cut-Away View of the Critical Assembly.

Figures 4 and 5 show photographs of two of the cores in the assembly. At the time that both photographs were taken, the moderator had been drained from the core tank. Figure 4 shows an overall view of the critical assembly core in the assembly tank. In this view, the control element is down and attached to the control element drive. Both safety elements are down and the safety element drives are withdrawn out of the picture. The lower grid plate is visible at the bottom of the tank with the upper grid plate above it. The guide plate is visible above the upper grid plate. The upper grid plate and the guide plate have checkerboard markings to aid in the placement of the fuel rods in the assembly grid. The guide plate has been etched so that each column and row in the grid pattern can be identified. The markings are visible in the figures. The two dry wells that house the fission chambers for the assembly instrumentation are visible in the picture. An array of 36 experiment rods, each slightly taller than the neighboring fuel rods, is located in the center of the fuel array.

Figure 5 shows a view of the top of the core for a different configuration. In this view, the control element is down and connected to the control element drive and the two safety elements are withdrawn from the core to their most reactive positions with the fueled sections in the core. The handle of the neutron source, which

stands above the tops of the fuel rods, is visible near the array of 36 experiment rods that are in the center of the fuel array.

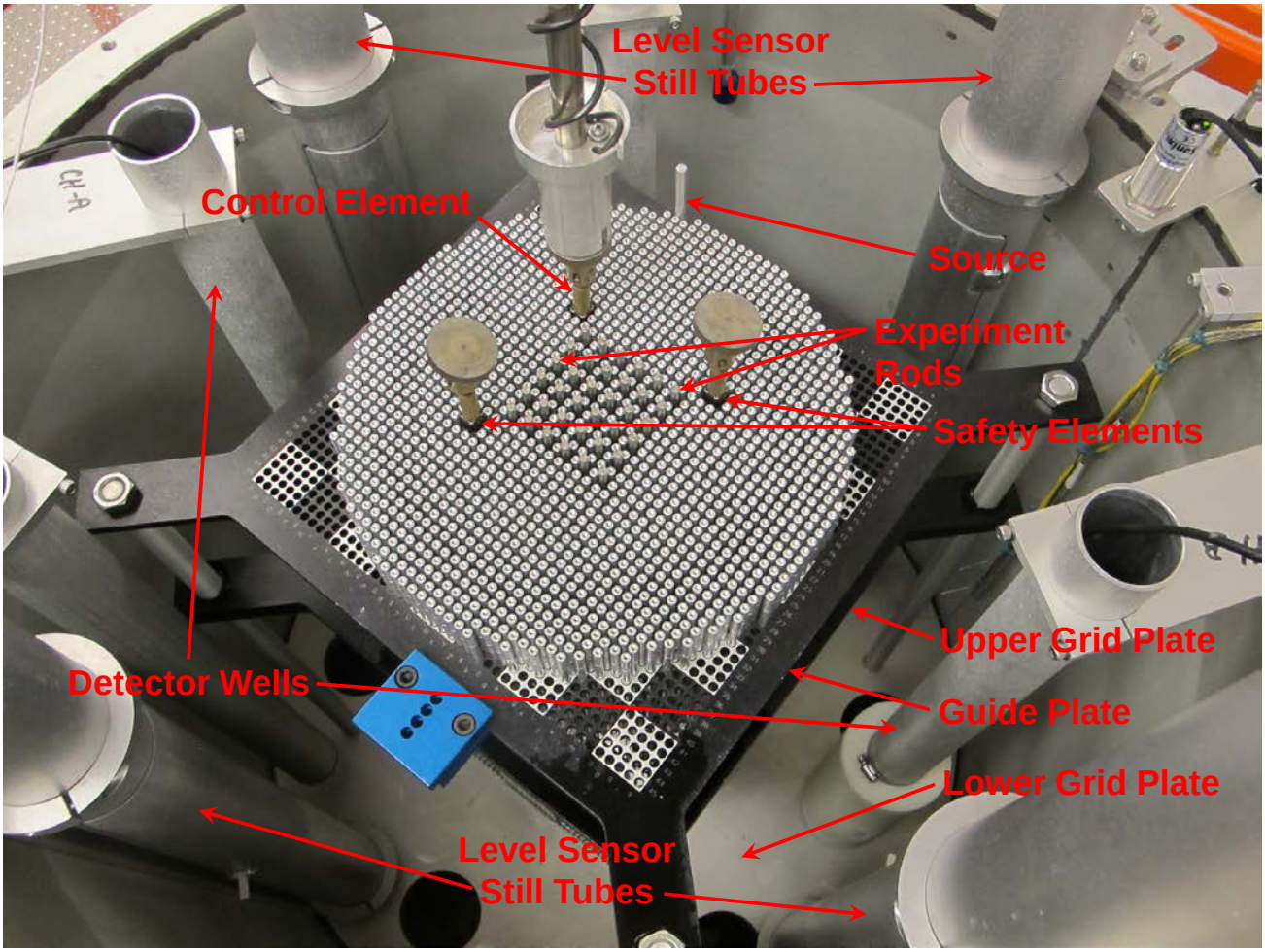

Figure 4. A View Inside the Core Tank with One of the Experiment Configurations (Case 8).

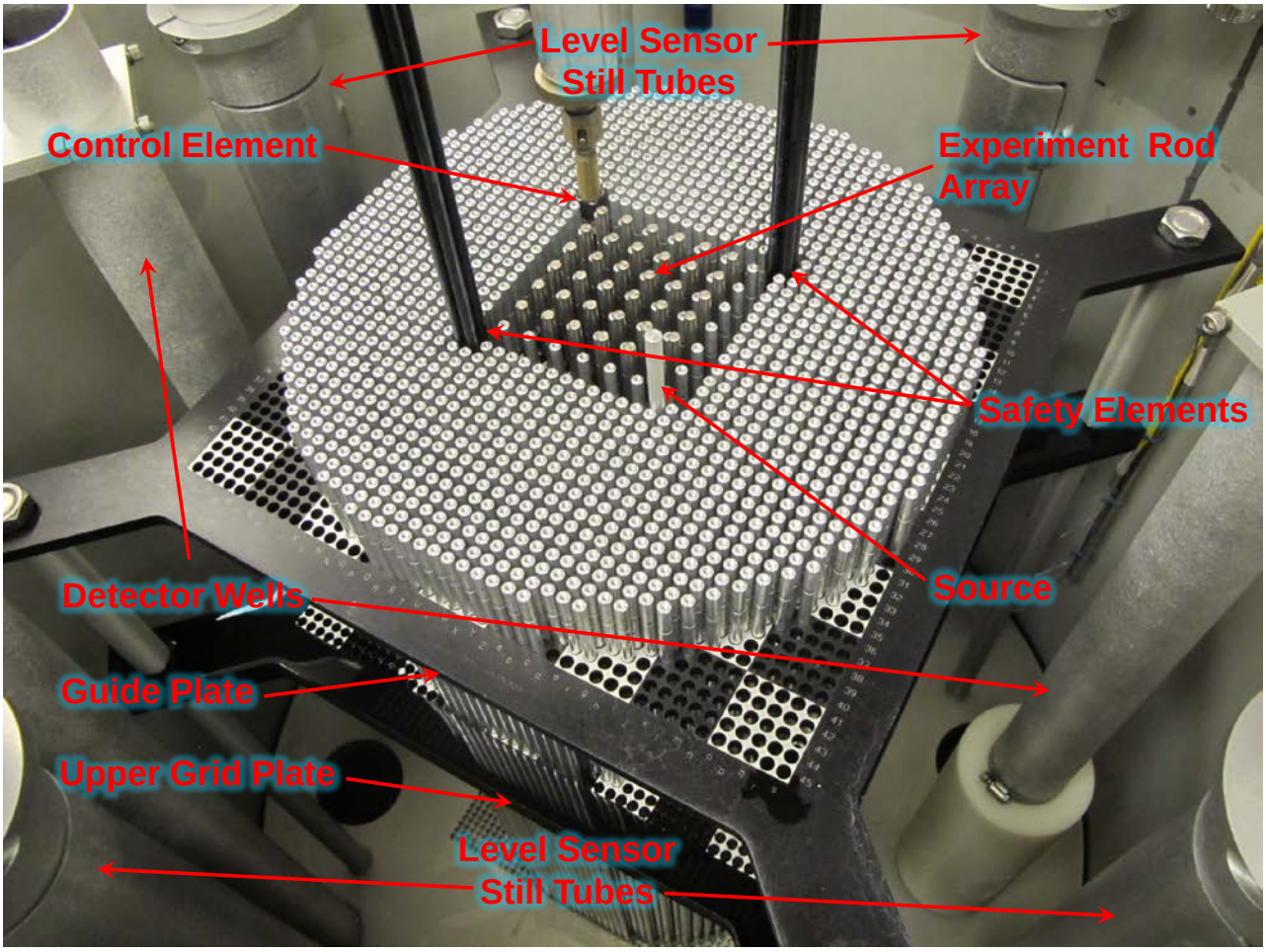

Figure 5. View of One of the Experiment Configurations (Case 24).

1.2.2 Reactor Room – The critical experiments were performed in the reactor building at the Sandia Pulsed Reactor Facility (SPRF). The reactor building is a large thick-walled, steel-reinforced concrete structure with a base in the shape of a cylinder having an inside diameter of approximately 30 ft (9.1 m) and capped with a hemispherical shell. A large steel and concrete door is present in the wall. Inside the building, the reactor room is lined on the walls and the dropped ceiling by 8 in (20.32 cm) of gypsum. The 4 in (10.16 cm) of gypsum that is nearest the concrete walls is borated. The floor is an 8 in (20.32 cm) thick concrete slab, the upper 4 in (10.16 cm) of which is borated. The ceiling is about 12 ft 5 in (378.46 cm) above the floor.

1.2.3 Assembly Tank - The assembly tank supports the assembly and contains the moderator during approach-to-critical experiments. The tank is cylindrical with a coaxial cylindrical projection out the bottom to accommodate the motion of the control/safety elements. The inside dimensions of the projection are 21.75 in (55.25 cm) tall by 15 in (38.1 cm) diameter. The radial wall thickness and floor thickness of the projection are both 0.25 in (0.635 cm). All parts of the tank were fabricated from 6061 aluminum.

The inside dimensions of the upper tank are 40 in (101.6 cm) tall by 36.88 in (93.6752 cm) diameter. The upper tank is 6061 aluminum. It has a radial wall thickness of 0.25 in (0.635 cm) and a bottom thickness of 1 in (2.54 cm). The upper assembly tank consists of two welded sections and the grid plate support ring.

The lower tank section has a 1 in (2.54 cm) thick floor that provides support for the assembly tank. The floor is drilled and tapped to accommodate the tank supports and has holes to connect to the two moderator dump valves. The floor also has a large central hole for the projection. The section has a flange at the top with an O-ring groove used for connection to the grid plate support ring.

The upper tank section is essentially a flanged tube. The lower flange is drilled to match the flange on the lower tank section and the grid plate support ring. The upper flange is drilled to connect to the support structure for the control/safety and source element drives.

The grid plate support ring fits between the upper and lower tank sections and has an O-ring groove in the surface that mates with the lower flange on the upper tank section. The lower grid plate attaches to the grid plate support ring.

The assembly tank is connected to two standpipes. One standpipe contains a linear moderator level sensor. The other contains an overflow pipe that determines the moderator level. The assembly tank also has a float switch used to indicate that the tank is full of moderator.

1.2.4 Grid Plates – The two 6061 aluminum grid plates support and maintain the spacing of the fuel rods in the critical assembly. A third guide plate, similar to but thinner than the upper grid plate, is located above the upper grid plate. The guide plate was fabricated from cast aluminum tooling plate, a standard aluminum product known for its dimensional stability. Both grid plates are 1 in (2.54 cm) thick while the guide plate is 0.375 in (0.9525 cm) thick. The lower grid plate is circular, 36.5 in (92.71 cm) in diameter, and is supported by the grid plate support ring that is part of the assembly tank. The lower grid plate has six 4.00 in (10.16 cm) diameter holes in it equally spaced on a 28 in (71.12 cm) diameter circle to allow passage of the moderator when the dump valves are opened. The upper grid plate is a 16.50 ± 0.06 in (41.91 ± 0.1524 cm) square with four support bosses at the corners. The support bosses are rectangular projections of the grid plates and are visible in Figures 4 and 5. The upper grid plate is supported above the lower grid plate by four 1 in (2.54 cm) diameter threaded aluminum standoffs that attach to the bosses. The standoffs maintain a spacing of 19.88 ± 0.02 in (50.4952 ± 0.0508 cm) between the top of the lower grid plate and the bottom of the upper grid plate. The standoffs are placed on a 28 in (71.12 cm) diameter circle centered on the center of the grid plates. Similar standoffs maintain a 7.00 ± 0.02in (17.78 ± 0.0508 cm) spacing between the top of the upper grid plate and the bottom of the guide plate.

A set of three grid plates – lower, upper, and guide – was fabricated for the experiments. These plates have provisions for 2025 fuel rods in the 45 × 45 square-pitched critical array. The array has a pitch of 0.3150 in (0.8001 cm). The tolerance on the absolute location of each fuel rod position in the grid is 0.005 in (0.0127 cm). The lower grid plate has 2013 0.5 in (1.27 cm) deep holes bored in it to support and locate the bottom of the fuel rods. The upper grid plate and guide plate have matching through holes in them to locate the top of the fuel rods. The diameter of the grid plate holes is 0.260 +0.005/–0.000 in (0.6604 + 0.0127/–0.0000 cm). All three plates have three through holes – square in shape with rounded corners – machined in them to allow for passage of the four-rod control/safety elements. An excerpt from the design drawing for the upper grid plate is shown in Figure 6.

The rows and columns of holes in the guide plate are marked for identification. The guide plate and the upper grid plate are anodized in a checkerboard pattern to assist in identifying the grid locations.

Table 1 shows the axial locations of the grid/guide plates under the assumption that the origin is at the top of the lower grid plate.

Table 1. Axial Locations of the Grid and Guide Plate Surfaces as Installed in the Critical Assembly.

Part	Location	Axial Position Relative to the Top of the Lower Grid Plate	
		Position (in)	Position (cm)
Lower Grid Plate	Bottom of the lower grid plate	-1	-2.54
	Bottom of the fuel rod support holes	-0.5	-1.27
	Top of the lower grid plate	0	0
Upper Grid Plate	Bottom of the upper grid plate	19.88	50.4952
	Top of the upper grid plate	20.88	53.0352
Guide Plate	Bottom of the guide plate	27.88	70.8152
	Top of the guide plate	28.255	71.7677

1.2.5 Radiation Detectors – Two cylindrical fission chambers that are part of the facility plant protection system were used to obtain count-rate data during the experiments. These detectors were placed in dry wells outside the fuel array. The dry wells were fabricated from aluminum 6061-T6511 tubing 2.50 in (6.35 cm) OD with 0.125 in (0.3175 cm) wall. The bottom of the tube was closed with a 0.250 in (0.635 cm) thick welded aluminum 6061-T6 or –T651 plate. The bottom of the tube was in contact with the top of the lower grid plate. The detector tubes were surrounded by an annulus of polyethylene 11.82 in (30.0228 cm) tall with an inner diameter of 2.603 in (6.61162 cm) and an outer diameter of 4.535 in (11.5189 cm). The bottom of the polyethylene was 0.3 in (0.762 cm) above the top surface of the lower grid plate. The mass of each of the polyethylene annuli was measured on a balance with the following specifications given by the manufacturer: repeatability 0.01 g, linearity 0.02 g, readability 0.01 g. The average mass of the two annuli was 2017.28 g. The vertical axis of one detector tube, using the orientation of the upper grid plate shown in Figure 6, was 32.385 cm to the right of and 6.4 cm above the center of the grid plate. The second detector was 32.385 cm to the left of and 6.4 cm below the center of the grid plate, as shown in the figure. The detectors were placed axially at the bottom of the dry wells with the axes of the detectors parallel to the axis of the tank. A third fission chamber, located below and immediately adjacent to the bottom of the core tank, was used in some of the experiments.

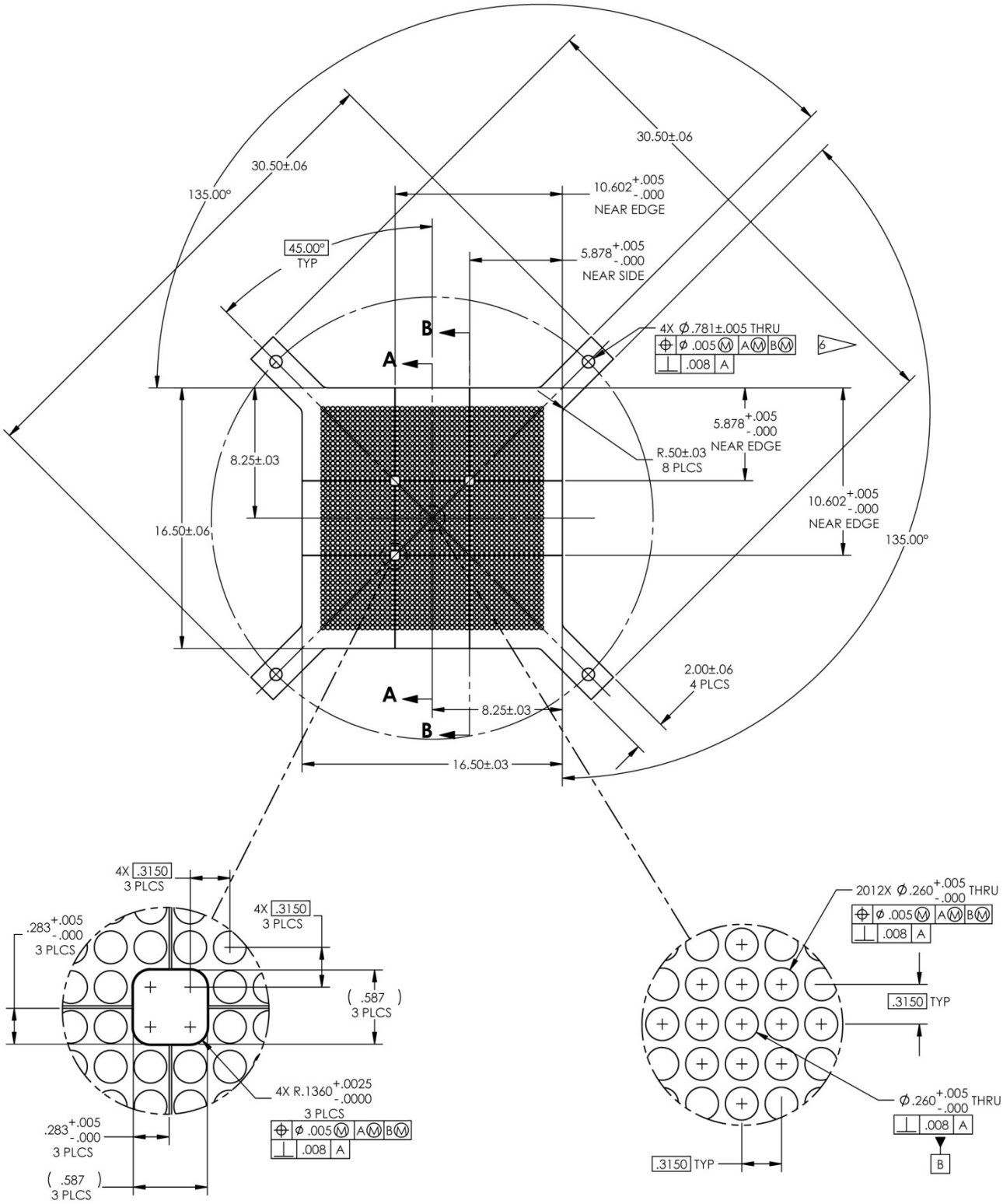

Figure 6. Excerpt from the Design Drawing for the Upper Grid Plate.

1.2.6 Water Moderator and Reflector – As noted above, the lower grid plate was supported in the core tank so that the core was reflected on the bottom by a 6.5 in (16.51 cm) thick layer of water. The bottom surface of the water in the core tank is 7.5 in (19.05 cm) below the upper surface of the lower grid plate. The level of the water in the core tank was controlled by the fixed overflow standpipe. It was adjusted so that the surface of the water in the core tank was 6 in (15.24 cm) above the upper grid plate. At this level, the moderator surface is 26.88 in (68.2752 cm) above the top of the lower grid plate. The remotely-adjustable standpipe was set at a level above the fixed standpipe. The diameter of the core tank was sufficient that the core was reflected radially by more than 6 in (15.24 cm) of water for all cores. There was nothing that is not described above within 6 in (15.24 cm) of the fuel rods.

Water can be pumped from the dump tank to the core tank through two pumps of differing capacity. When the core tank is being filled initially, water is pumped through the "fast" fill pump. This pump is active until the level of the water in the core tank reaches a predetermined level at which a float switch is activated. When the float switch is first activated, the fast-fill pump is disabled by an interlock in the assembly control system. From that point, water may only be added to the core tank through the "slow" fill pump. The volumetric capacity of the slow-fill pump is set to limit the maximum reactivity addition rate. The slow-fill pump runs continuously through the rest of the operation. The outlet of the line from the slow pump is set so the continuous flow of water mixes the water in the core tank to promote temperature homogenization of the water in the tank The level of the water in the core tank is limited by overflow into the lower of the two overflow standpipes.

The temperature of the water in the core tank is monitored by three thermocouples mounted in the assembly reflector at three different levels near the outer wall of the core tank. Another thermocouple in the dump tank monitors the temperature of the water there. The dump tank has an electrically-operated heater. The dump tank thermocouple signal is provided to a controller that switches the power to the heater on and off to maintain a constant water temperature in the dump tank.

1.2.7 Fuel Rods – With the exception of the fueled sections of the control and safety elements, the fuel rods in the critical assembly were all of the same design. The design of the fuel rods is shown in Figure 7. The fuel rods were fabricated in 2004 at Sandia National Laboratories from existing UO_2 fuel pellets removed from "Pathfinder" fuel assemblies obtained from The Pennsylvania State University. The fuel rods in the Pathfinder fuel assemblies were separated from the assemblies and the fuel pellets were removed from the original cladding tubes and fabricated into new fuel rods using 3003 aluminum tubing welded to end plugs of the same aluminum alloy.

The cladding tubes are welded to the lower caps and the weld was checked for leaks. Passing the leak check assured that the water moderator would not enter the fuel rods. The material stack in the fuel rods, starting at the bottom, is as follows: a 0.500 in (1.270 cm) aluminum 3003 lower cap; a nominal 19.257 in (48.91278 cm) stack of fuel pellets; a corrosion-resistant steel compression spring 0.180 in (0.4572 cm) outside diameter, 0.138 in (0.35052 cm) inside diameter, 0.875 in (2.2225 cm) uncompressed length whose length adjusts according to the actual length of the fuel stack; a 1.000 in (2.540 cm) aluminum 6061 spacer 0.207 ± 0.010 in (0.52578 ± 0.02540 cm) diameter, an 8.38 ± 0.02 in (21.2852 ± 0.0508 cm) long high-density polyethylene spacer also 0.207 ± 0.010 in (0.52578 ± 0.02540 cm) diameter, and a 1.000 inch (2.540 cm) aluminum 3003 top cap. Table 2 lists the axial locations of the interfaces between the fuel rod components when the fuel rods are installed in the critical assembly.

Table 2. Axial Locations of the Interfaces in the Fuel Rods as Installed in the Critical Assembly.

Location	Axial Position Relative to the Top of the Lower Grid Plate	
	Position (in)	Position (cm)
Bottom of the lower grid plate	-1.00	-2.54
Bottom of the fuel rod	-0.50	-1.27
Bottom of the fuel pellet stack	0.00	0.00
Top of the fuel pellet stack (measured)	19.2045	48.780 [(a)]
Bottom of the aluminum spacer	19.894	50.53076
Top of the aluminum spacer	20.894	53.07076
Top of the polyethylene spacer	29.274	74.35596
Top of the fuel rod	30.274	76.89596

(a) This is the mean measured fuel column length, different from the 19.257 in (48.91278 cm) nominal length. The measured length in inches is this value (48.780) divided by 2.54.

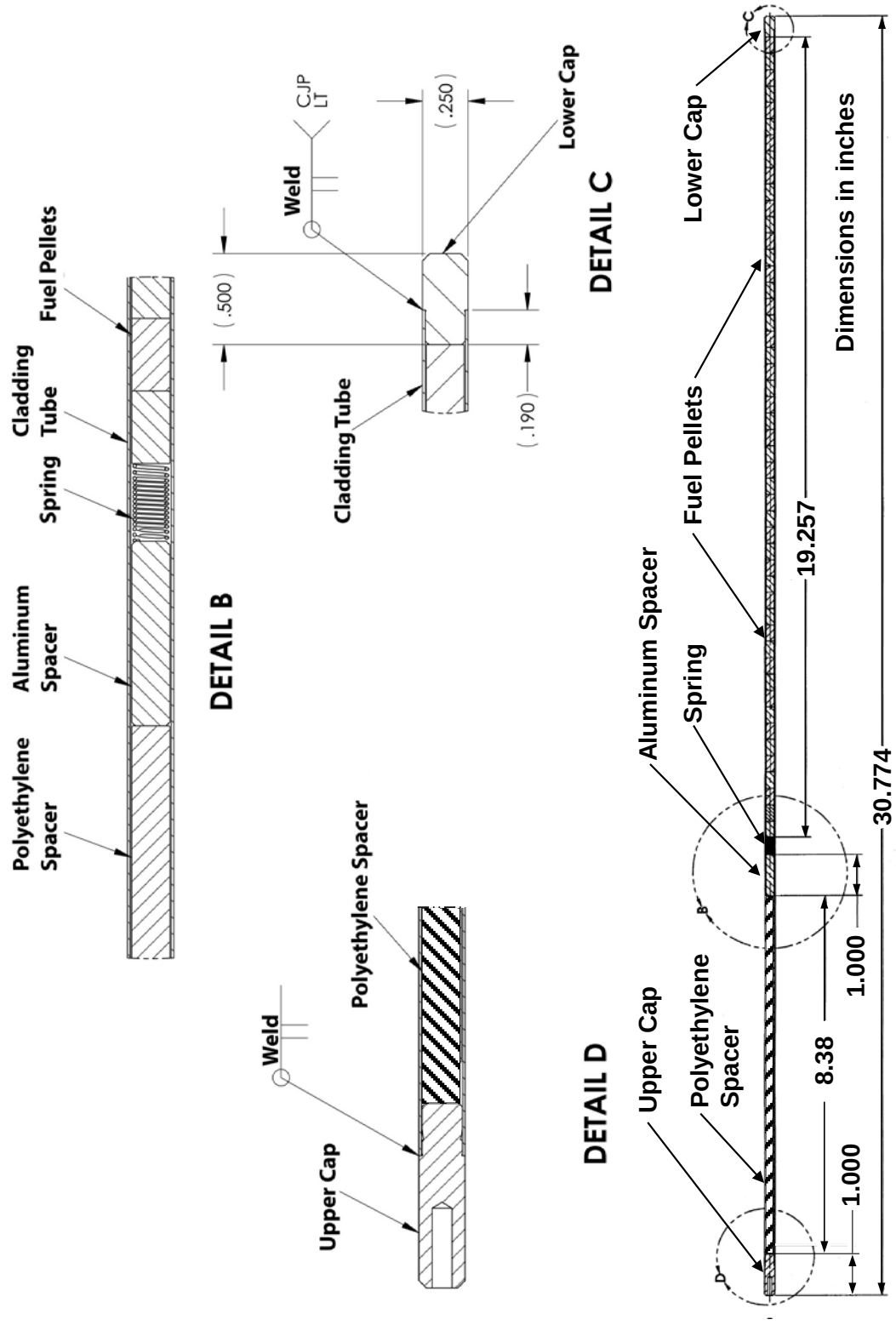

Figure 7. Design of the Fuel Rod.

The cladding tubes used in the fuel rods have a nominal outer diameter of 0.250 in (0.635 cm) with a nominal 0.014 in (0.03556 cm) wall. The lower cap of the fuel rods is 0.500 in (1.270 cm) long.

Before the fuel rods were fabricated, the masses of 100 of each non-fuel components of the fuel rods were measured. The mass measurements were made on a balance with the following specifications given by the manufacturer: repeatability 0.01 g, linearity 0.02 g, readability 0.01 g. The results of the mass measurements are summarized in Table 3. The sixth row in the table gives the results for 100 sets of all five parts. It can be seen that the variability in the mass sum is dominated by the variability in the mass of the polyethylene spacer. The variability is attributed to the manufacturing process used to fabricate the polyethylene spacers. The last (seventh) row in the table gives the results for 100 sets of parts without the polyethylene spacers.

Table 3. Measured Mass Data for the Fuel Rod Components.

Component	Average Mass (g)	Standard Deviation (g)
Cladding Tube/Lower Cap Assembly	13.824	0.027
Corrosion-Resistant Steel Springs	0.1923	0.0095
Aluminum Spacer	1.4368	0.0043
Polyethylene Spacer	4.524 [(a)]	0.094
Upper Cap	1.8350	0.0052
Sum of Five Parts for 100 Sets	21.813	0.094
Sum Without Polyethylene Spacer	17.289	0.027

(a) Note that the average mass of the 100 polyethylene spacers given here is different from the population average of the spacer mass for all polyethylene spacers used in the fuel rods given below.

During the fabrication of the 2199 fuel rods available for the experiments, the following quantities were measured for each fuel rod: total rod mass, polyethylene spacer mass, and fuel pellet column length. The mass measurements were made on a balance with the following specifications given by the manufacturer: repeatability 0.01 g, linearity 0.02 g, readability 0.01 g. The length measurements were made to the nearest 0.1 cm. The values of the measured masses and lengths were preserved for each fuel rod. The mass of the fuel pellets in each rod was obtained by subtracting the measured mass of the polyethylene spacer plus the 17.289 g average mass of the remaining hardware given in Table 3 from the total mass of the fuel rod. Table 4 lists average values of UO_2 fuel mass and fuel pellet stack length for the entire population of 2199 fuel rods. The linear fuel mass in each fuel rod was obtained from the UO_2 mass and the fuel pellet stack length for each fuel rod. The average value of the linear fuel mass is also listed in the table as is the average polyethylene spacer mass.

Table 4. Population Averages for the 2199 Fuel Rods.

Characteristic	Average Value	Standard Deviation
UO_2 Mass (g)	108.7165	0.323
Fuel Pellet Stack Length (cm)	48.780	0.125
Linear Fuel Mass (g/cm)	2.2287	0.0050
Polyethylene Spacer Mass (g)	4.454	0.102

After the fuel rods were fabricated, the outer diameter of each fuel rod was measured using a high-precision laser micrometer system. The system consisted of three micrometer heads and the hardware required to position the fuel rods in the micrometer heads. The micrometer heads were located to measure the fuel rod outside diameter at 6.4 in (16.256 cm), 10.15 in (25.781 cm), and 13.9 in (35.306 cm) above the bottom end of the fuel rod. This gave a fuel rod outer diameter measurement at about the midplane of the fuel pellet stack and 3.75 in (9.525 cm) above and below the midplane. Each micrometer made two simultaneous orthogonal diameter measurements. For each fuel rod, a measurement was taken, the fuel rod was rotated by 45°, and another measurement was taken. Thus, the outer diameter of each fuel rod was measured at three axial locations in four azimuthal orientations. The manufacturer's specifications indicated that the laser micrometers had a resolution of 0.000001 in (0.00000254 cm) and a repeatability of 0.000005 in (0.0000127 cm). The bias in the micrometer measurements was established using a pin gage standard with a calibration traceable to the US National Institute of Standards and Technology. The diameter measurements had a systematic uncertainty of 0.000022 in (0.00005588 cm) which is the sum in quadrature of the 0.000015 in (0.0000381 cm) uncertainty in the pin gage standard with the maximum in the random variations in the measurement of the standard on any axis for the three micrometers. The fuel rod diameter measurements were made in a number of sessions over the course of several months. The stability of the measurement system was monitored by repeatedly measuring two 12 in (30.48 cm) long pin gages during each of the sessions. These measurements also showed that the diameter measurements had a random reproducibility uncertainty of about 0.000030 in (0.0000762 cm). Of the 2199 fuel rods fabricated for the experiment, five were removed from service and not used. The average measured fuel rod diameter for the remaining population of 2194 fuel rods is 0.249980 in (0.634948 cm as rounded from the original data) with a standard deviation of 0.000086 in (0.000218 cm).

The design documents for the fuel elements from which the fuel pellets were removed specified the diameter of the fuel pellets as 0.207 in (0.52578 cm). The outer diameter of a sample of 123 fuel pellets, drawn randomly from the fuel pellet stock used in the fuel rods, was measured using one of the laser micrometers described above. The average measured diameter was 0.20694 in (0.52563 cm) with a standard deviation of the 123 measurements of 0.00019 in (0.00048 cm).

The fuel rods were designed to be supported by the two 1 in (2.54 cm) thick grid plates. The lower cap fits in a 0.5 in (1.27 cm) deep blind hole in the lower grid plate. The top of the lower cap is then aligned with the top of the grid plate to make the combination appear as a solid sheet of metal. With the appropriate grid plate spacing, the top and bottom of the aluminum spacers in the fuel rods are nearly aligned with the top and bottom of the upper grid plate.

1.2.8 Control and Safety Elements - The critical assembly has three identical fuel-followed control/safety elements, two operated as safety elements and one operated as a control element. Each control/safety element occupies four adjacent fuel rod positions in the critical assembly. Each element consists of four B_4C-loaded absorber sections followed by four polyethylene-filled decoupler sections followed by four fueled rod sections. These sections are joined into four-rod bundles by 6061 aluminum bundle plates. The three sections use the same 3003 aluminum tubing as the fuel rods. Each section has 3003 aluminum end caps at the top and bottom of identical design. When a control/safety element is fully withdrawn from the assembly, the fueled rod sections are in the core and are nearly identical neutronically to

the other fueled positions in the critical assembly. The design of the control and safety elements is shown in Figure 8. The design of the lower bundle plate is shown in Figure 9. The design of the middle bundle plate, of which there are two in each control or safety element, is shown in Figure 10. The design of the upper bundle plate is shown in Figure 11. All of the bundle plates were fabricated from 6061 aluminum.

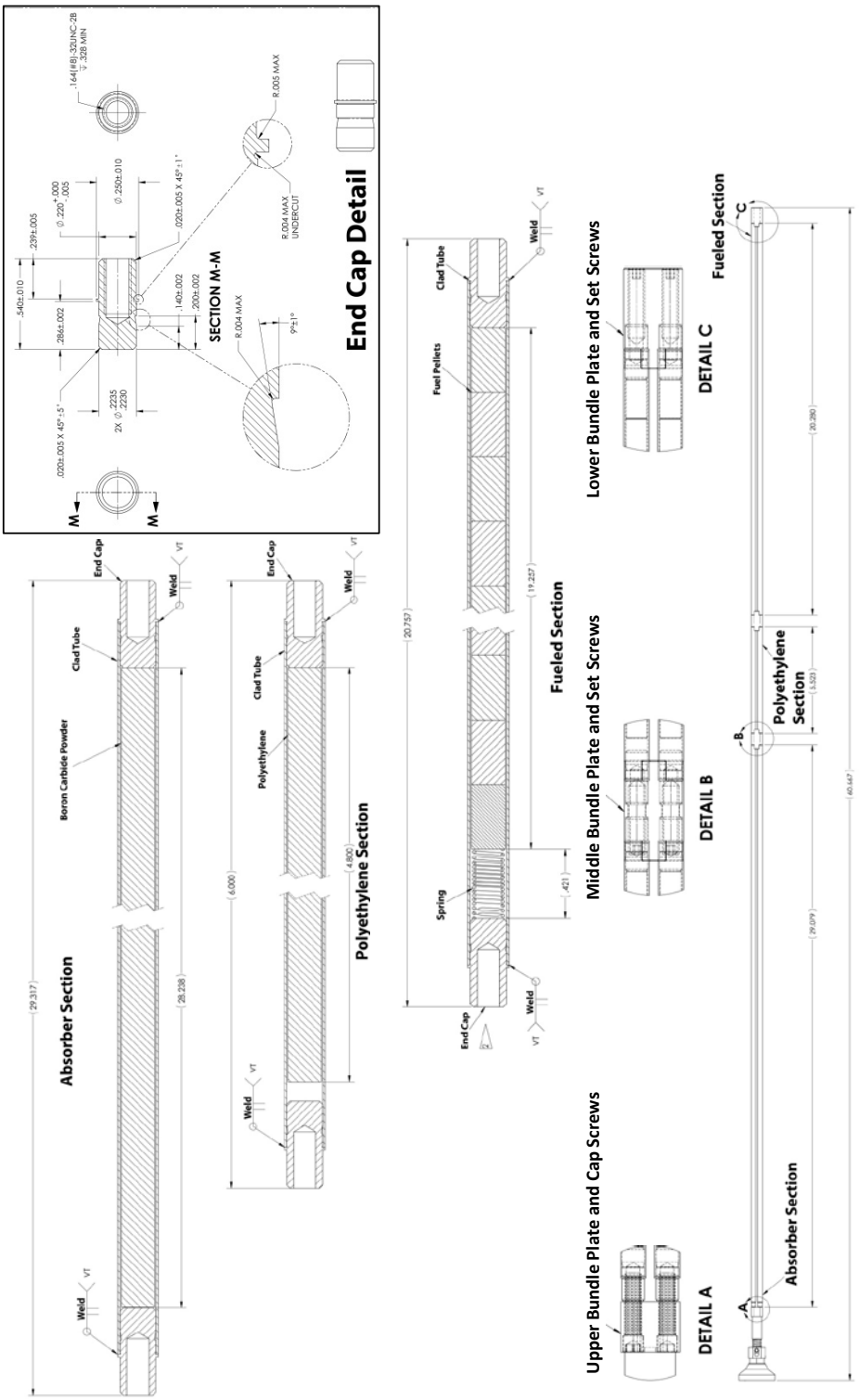

Figure 8. Design of the Control and Safety Elements.

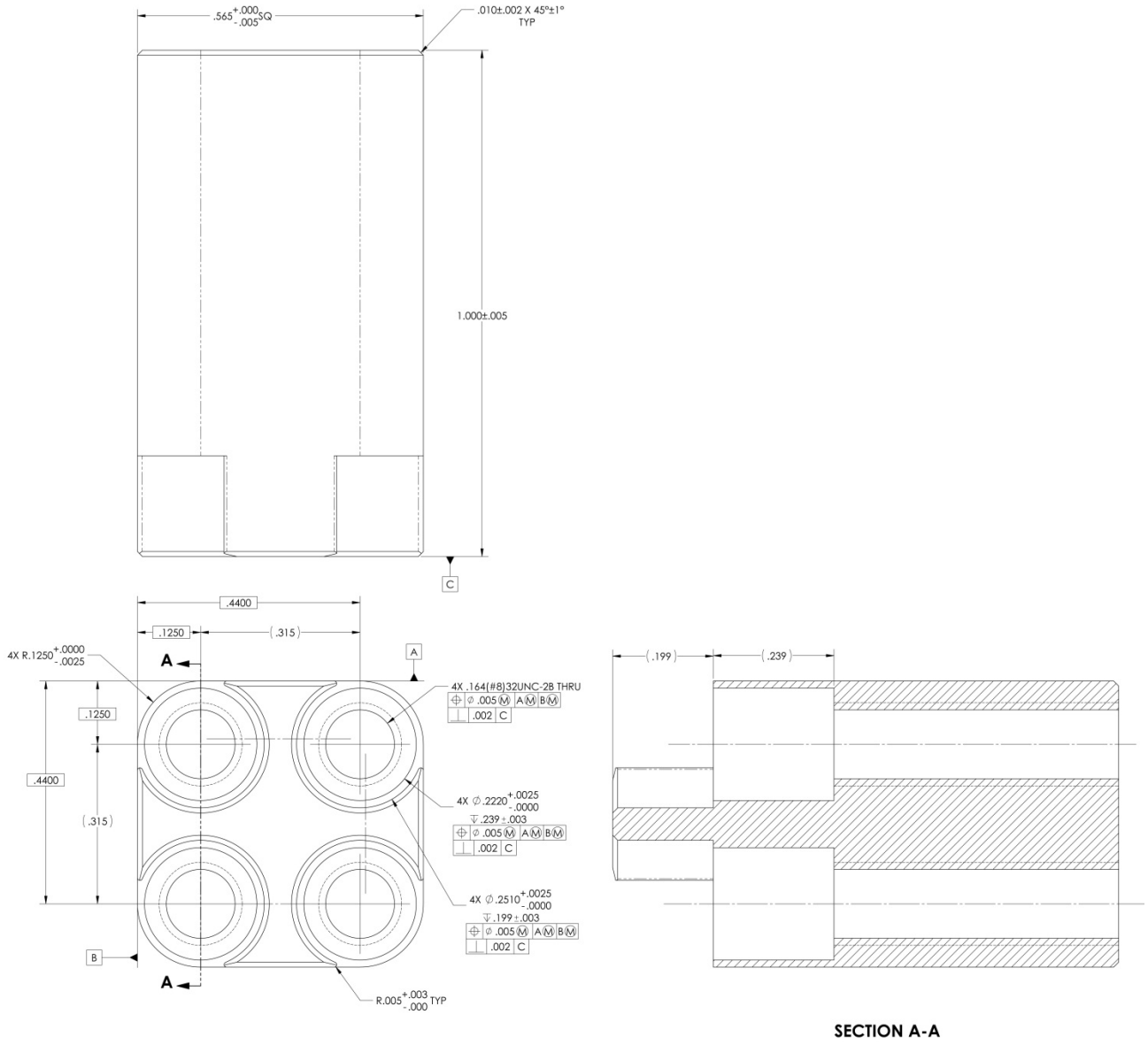

Figure 9. Excerpt from the Design Drawing for the Lower Bundle Plate.

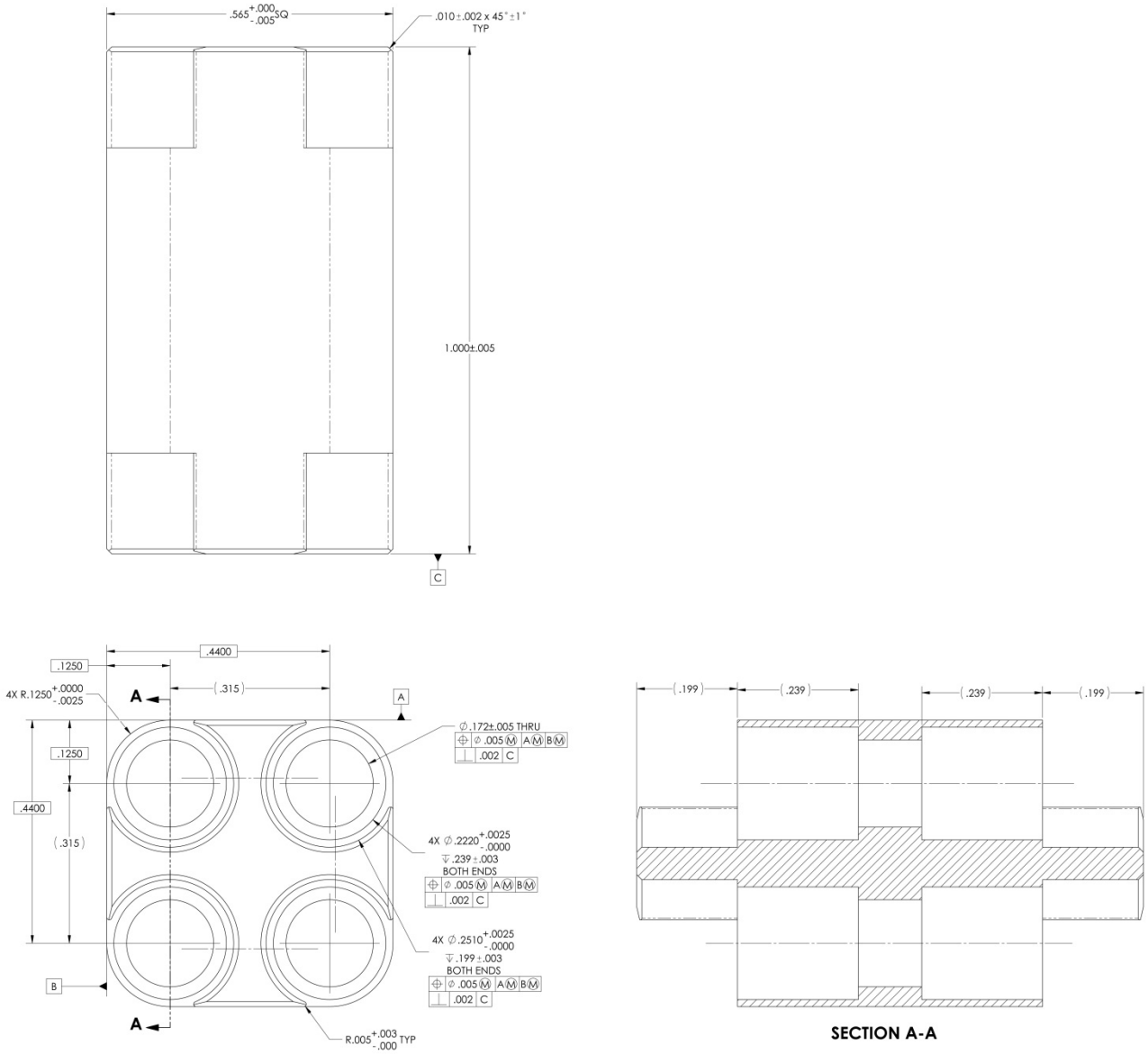

Figure 10. Excerpt from the Design Drawing for the Middle Bundle Plate.

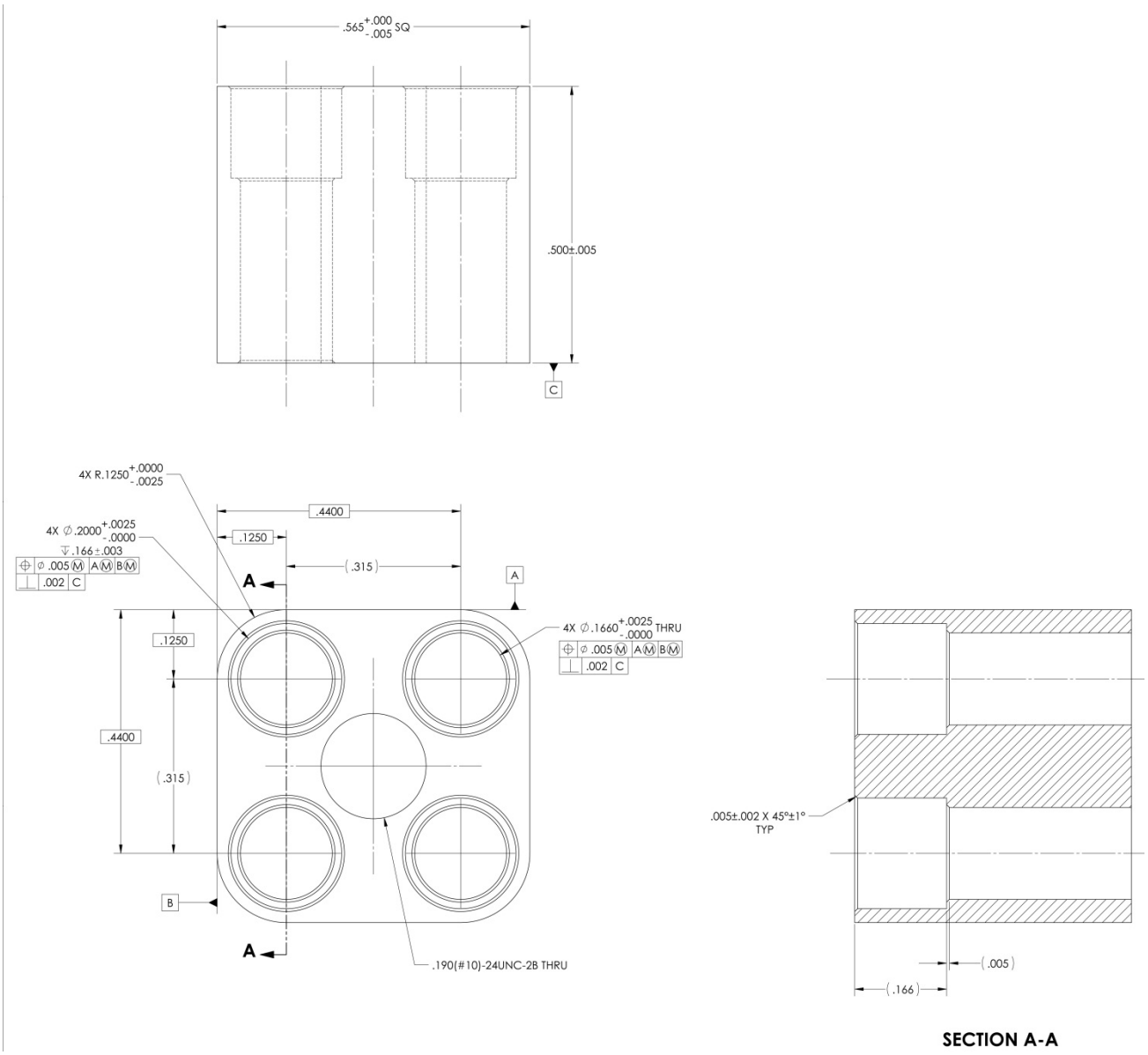

Figure 11. Excerpt from the Design Drawing for the Upper Bundle Plate.

The fueled section of the control/safety elements is similar to the fueled section of a fuel rod. The 3003 aluminum cladding tubes and end cap material are the same as were used in the fuel rods. In order to allow the elements to be lowered from the assembly, the lower grid plate has four-position through holes at the control/safety element positions as described above. The end caps on the fueled sections of the control/safety elements mate with a 6061 aluminum lower bundle plate that fills the hole in the lower grid plate. An 8-32 corrosion-resistant steel set screw 0.750 in (1.905 cm) long joins each fueled section to the bundle plate. Above the bottom end cap is a stack of fuel pellets and a spring similar to those in a fuel rod. The length and mass of the fuel pellet stack is known for each of the 23 fueled sections that were fabricated to the same precision as for the fuel rods. The relevant data on the fuel pellet stack for the population of 23 fueled sections is given in Table 5. The total mass of the UO_2 in the twelve fueled sections used in the experiments reported here is 1303.07 g and the total stack length is 584.7 cm.

Table 5. Population Averages for the 23 Control/Safety Element Fueled Sections.

Characteristic	Average Value	Standard Deviation
UO_2 Mass (g)	108.62	0.13
Fuel Pellet Stack Length (cm)	48.717	0.049
Linear Fuel Mass (g/cm)	2.2295	0.0020

The top end caps of the fueled sections are joined to the bottom end caps of the polyethylene-filled decoupler sections through a middle bundle plate using the same set screws as in the lower bundle plates. The length of the fueled sections is set so that, when the lower bundle plate upper and lower surfaces are in line with the surfaces of the lower grid plate, the upper and lower surfaces of the middle bundle plate are nearly in line with the upper and lower surfaces of the upper grid plate.

The decoupler sections contain 4.800 in (12.192 cm) long 0.207 in (0.52578 cm) diameter polyethylene rods inside the same 3003 aluminum tubes used for the fuel rod cladding. The average polyethylene mass in the population of 24 decoupler sections is 2.531 g with a standard deviation of 0.037 g. The end caps on the decoupler sections are identical to those on the fueled section.

The bottoms of the absorber sections are joined to the tops of the decoupler sections through a middle bundle plate. The same corrosion-resistant set screws are used. The absorber sections are filled with boron carbide powder. Two lots of boron carbide powder, each with a different average particle size, were mixed in equal parts prior to loading into the absorber sections. During loading, the powder was compacted by vibrating the tubes. The loading procedure specified that the absorber sections be filled to within about 0.3 in of the top of the tube. The top caps of the sections extend 0.286 in into the tubes. Thus the gap between the bottom of the cap and the top of the powder was small. The average boron carbide mass in the population of 23 absorber sections that were fabricated is 26.37 g with a standard deviation of 0.22 g. After filling, the top caps were welded to the absorber section tubes.

The top of each absorber section is joined to the upper bundle plate by a modified 8-32 socket head cap screw 1.125 in (2.8575 cm) tall. Table 6 lists the axial positions of the interfaces in the control and safety elements when the elements are fully withdrawn from the assembly to the positions in which the measurements reported here were made.

Table 6. Axial Locations of the Interfaces in the Control and Safety Elements when the Elements are Fully Withdrawn from the Critical Assembly.

Part	Location	Axial Position Relative to the Top of the Lower Grid Plate	
		Position (in)	Position (cm)
Lower Bundle Plate	Bottom of the lower bundle plate	-1	-2.54
	Bottom of the 0.222 in ID hole	-0.438	-1.11252
	Bottom of the 0.251 in ID hole	-0.199	-0.50546
	Top of the lower bundle plate	0	0
Fueled Section	Bottom of the fueled section	-0.438	-1.11252
	Bottom of the full-diameter clad	-0.199	-0.50546
	Bottom of the fuel pellet stack	0.102	0.25908
	Top of the fuel pellet stack	19.282	48.97608
	Bottom of the top end cap	19.78	50.2412
	Top of the full-diameter clad	20.081	51.00574
	Top of the fueled section	20.32	51.6128
Middle Bundle Plate 1	Bottom of the middle bundle plate 1	19.882	50.50028
	Top of the lower 0.251 in ID hole	20.081	51.00574
	Top of the lower 0.222 in ID hole	20.32	51.6128
	Bottom of the upper 0.222 in ID hole	20.444	51.92776
	Bottom of the upper 0.251 in ID hole	20.683	52.53482
	Top of the middle bundle plate 1	20.882	53.04028
Polyethylene Decoupler Section	Bottom of the decoupler section	20.444	51.92776
	Bottom of the full-diameter clad	20.683	52.53482
	Bottom of the polyethylene	20.984	53.29936
	Top of the polyethylene	25.784	65.49136
	Bottom of the top end cap	25.905	65.7987
	Top of the full-diameter clad	26.206	66.56324
	Top of the decoupler section	26.445	67.1703
Middle Bundle Plate 2	Bottom of the middle bundle plate 2	26.007	66.05778
	Top of the lower 0.251 in ID hole	26.206	66.56324
	Top of the lower 0.222 in ID hole	26.445	67.1703
	Bottom of the upper 0.222 in ID hole	26.569	67.48526
	Bottom of the upper 0.251 in ID hole	26.808	68.09232
	Top of the middle bundle plate 2	27.007	68.59778
Absorber Section	Bottom of the absorber section	26.569	67.48526
	Bottom of the full-diameter clad	26.808	68.09232
	Bottom of the absorber	27.109	68.85686
	Bottom of the top end cap	55.347	140.58138
	Top of the full-diameter clad	55.648	141.34592
	Top of the absorber section	55.887	141.95298
Upper Bundle Plate	Bottom of the upper bundle plate	55.887	141.95298
	Bottom of the 0.200 in ID hole	56.221	142.80134
	Top of the upper bundle plate	56.387	143.22298

Whenever moderator is present in the core tank during the execution of a critical experiment, the safety elements are held at their most reactive position with the absorber above the surface of the water and the fueled sections in the assembly core. In this position, a large negative reactivity is available to quickly shut down the assembly should the need arise. The absorber section in the elements is also well away from the

assembly core and does not significantly affect the reactivity of the system. The control element is used during critical assembly operations to make fine adjustments in the reactivity of the assembly. When data are taken during an approach-to-critical experiment, the control element is also fully withdrawn to its most reactive position so the absorber does not affect the system neutronically.

1.2.9 Experiment Rods – Experiment rods fabricated from either Commercially Pure Grade 2 titanium or 6061-T6 aluminum were placed near the center of the fuel array in several of the measured configurations. Figure 12 shows an excerpt from the design drawing for the experiment rods. These rods were fabricated from round stock with a specified diameter of 0.250 ± 0.005 in (0.635 ± 0.0127 cm). The experiment rods were 31.28 ± 0.02 in (79.4512 ± 0.0508 cm) long. The top of each rod had a 0.025 ± 0.005 in (0.0635 ± 0.0127 cm) 45° chamfer. The bottom of each rod had a similar 45° chamfer with a height of 0.040 ± 0.005 in (0.1016 ± 0.0127 cm). Table 7 lists the axial positions of the interfaces in the experiment rods as installed in the critical assembly. After fabrication, each of the experiment rods was laser-scribed with a unique serial number.

Table 7. Axial Locations of the Interfaces in the Experiment Rods as Installed in the Critical Assembly and Designed Diameter at Each Axial Location.

Location	Axial Position Relative to the Top of the Lower Grid Plate		Designed Diameter	
	Position (in)	Position (cm)	Diameter (in)	Diameter (cm)
Bottom of the experiment rod	-0.50	-1.27	0.170	0.4318
Top of the lower 45° chamfer	-0.46	-1.1684	0.250	0.635
Bottom of the upper 45° chamfer	30.755	78.1177	0.250	0.635
Top of the experiment rod	30.78	78.1812	0.200	0.508

Thirty six rods of each type were fabricated for the experiments. Each rod was uniquely marked with a serial number. The outside diameter of each of the experiment rods was measured using the same laser micrometer system that was used to measure the outside diameter of the fuel rods. The length of each experiment rod was measured using a digital caliper with an accuracy of 0.003 in (0.00762 cm) and a resolution of 0.0005 in (0.00127 cm). The mass of each aluminum rod was measured on a calibrated balance with the following specifications given by the manufacturer: reproducibility 0.015 mg, linearity 0.1 mg, readability 0.01 mg. The results of the diameter, length, and mass measurements were recorded for each experiment rod. Table 8 lists the measured diameters, lengths, and masses for each of the titanium and aluminum rods.

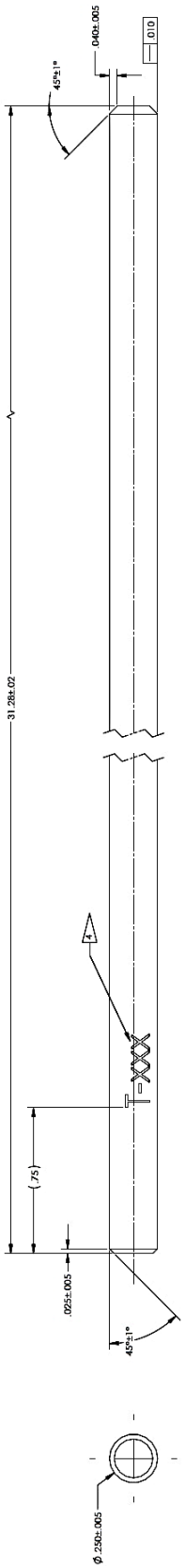

Figure 12. Excerpt from the Design Drawing for the Experiment Rods.

Table 8. Measured Diameters, Lengths, and Masses of the Experiment Rods.

Rod Number	Titanium Rods			Aluminum Rods		
	Diameter (in)	Length (in)	Mass (g)	Diameter (in)	Length (in)	Mass (g)
1	0.249580	31.2830	113.0201	0.250787	31.2805	68.2803
2	0.250447	31.2835	113.8712	0.250807	31.2850	68.3102
3	0.251627	31.2800	114.9350	0.250807	31.2815	68.6130
4	0.250566	31.2830	113.9104	0.250817	31.2810	68.3210
5	0.250478	31.2820	113.8657	0.250817	31.2790	68.2938
6	0.251087	31.2835	114.3266	0.250804	31.2840	68.3203
7	0.250487	31.2820	113.8893	0.251864	31.2845	68.8737
8	0.250606	31.2810	113.9170	0.251866	31.2785	68.8702
9	0.251161	31.2830	114.3276	0.252214	31.2795	69.0408
10	0.250719	31.2830	113.8817	0.251969	31.2825	68.9664
11	0.249578	31.2805	112.9756	0.251250	31.2795	68.5019
12	0.250123	31.2780	113.2541	0.251184	31.2835	68.4881
13	0.250343	31.2800	113.6875	0.251956	31.2835	68.9502
14	0.251553	31.2860	114.8348	0.252041	31.2865	68.9879
15	0.251912	31.2855	115.1445	0.251311	31.2825	68.5685
16	0.251031	31.2810	114.3008	0.251229	31.2870	68.5433
17	0.250897	31.2800	114.2498	0.252256	31.2835	68.9677
18	0.251702	31.2870	115.0418	0.251999	31.2780	68.9400
19	0.250719	31.2820	114.2576	0.250903	31.2795	68.3393
20	0.249324	31.2815	112.8267	0.250915	31.2780	68.3336
21	0.250935	31.2800	114.2699	0.251072	31.2810	68.4315
22	0.251136	31.2875	114.3777	0.251031	31.2855	68.4124
23	0.250938	31.2785	114.1983	0.252222	31.2805	69.0834
24	0.251410	31.2855	114.6602	0.252068	31.2850	69.0279
25	0.251414	31.2810	114.6667	0.251381	31.2835	68.6112
26	0.251005	31.2860	114.4562	0.251370	31.2810	68.5963
27	0.250715	31.2850	113.9848	0.251833	31.2805	68.8478
28	0.250165	31.2805	113.5633	0.251874	31.2795	68.8890
29	0.250900	31.2810	114.2761	0.250966	31.2780	68.3401
30	0.250201	31.2810	113.4869	0.251102	31.2825	68.4398
31	0.250930	31.2815	114.2261	0.252091	31.2815	68.9910
32	0.250796	31.2835	114.1413	0.251893	31.2780	68.8778
33	0.250139	31.2800	113.7600	0.251517	31.2845	68.6518
34	0.250966	31.2795	114.3114	0.251590	31.2775	68.7253
35	0.251061	31.2840	114.4037	0.251535	31.2780	68.6721
36	0.251076	31.2775	114.4283	0.251600	31.2755	68.7958
Average	0.250771	31.2822	114.1036	0.251471	31.2814	68.6556
Standard Deviation	0.00058	0.0025	0.54	0.00049	0.0028	0.27

With the exception of Cases 1 and 18, the experiments included various combinations of titanium experiment rods and/or aluminum experiment rods. Table 9 lists the rod number ranges of each type of experiment rod for each case.

Table 9. Combinations of Experiment Rods in the Various Cases.

Case	Serial Number Range	
	Titanium Rods	Aluminum Rods
1	–	–
2	1 – 4	–
3	1 – 9	–
4	1 – 16	–
5	1 – 25	–
6	1 – 36	–
7	1 – 36	–
8	1 – 36	–
9	1 – 36	–
10	–	1 – 4
11	–	1 – 9
12	–	1 – 16
13	–	1 – 25
14	–	1 – 36
15	–	1 – 36
16	–	1 – 36
17	–	1 – 36
18	–	–
19	–	1 – 36
20	1 – 4	5 – 36
21	1 – 4, 11-15	5 – 10, 16 – 36
22	1 – 16	17 – 36
23	1 – 16, 27 – 35	17 – 26, 36
24	1 – 36	–

1.2.10 Neutron Source – The neutron source in the assembly is a small double-sealed 316L stainless steel capsule containing a ^{252}Cf spontaneous fission source. The source is attached to a fixture designed to be placed in a fuel rod location in the assembly grid structure or in a mounting location outside the grid plates. The source and fixture are shown in Figure 13. The bottom (source) end of the fixture is the bottom end cap, essentially a cylinder of aluminum 3003 0.540 in (1.3716 cm) long and 0.220 in (0.5588 cm) diameter that is drilled and tapped to accommodate a 3-48 steel set screw that is 0.313 in (0.79502 cm) long. The bottom of the source fixture and top of the source capsule are 5.099 in (12.95146 cm) above the top of the lower grid plate. An aluminum 3003 tube identical to the fuel rod cladding tubes (nominally 0.250 in outer diameter, 0.0014 in wall) covers the top 0.254 in (0.64516 cm) of the bottom end cap and extends above the moderator where it connects to a handle that rests on the guide plate. The tube is slotted at the ends so that it fills with moderator when the critical assembly is filled.

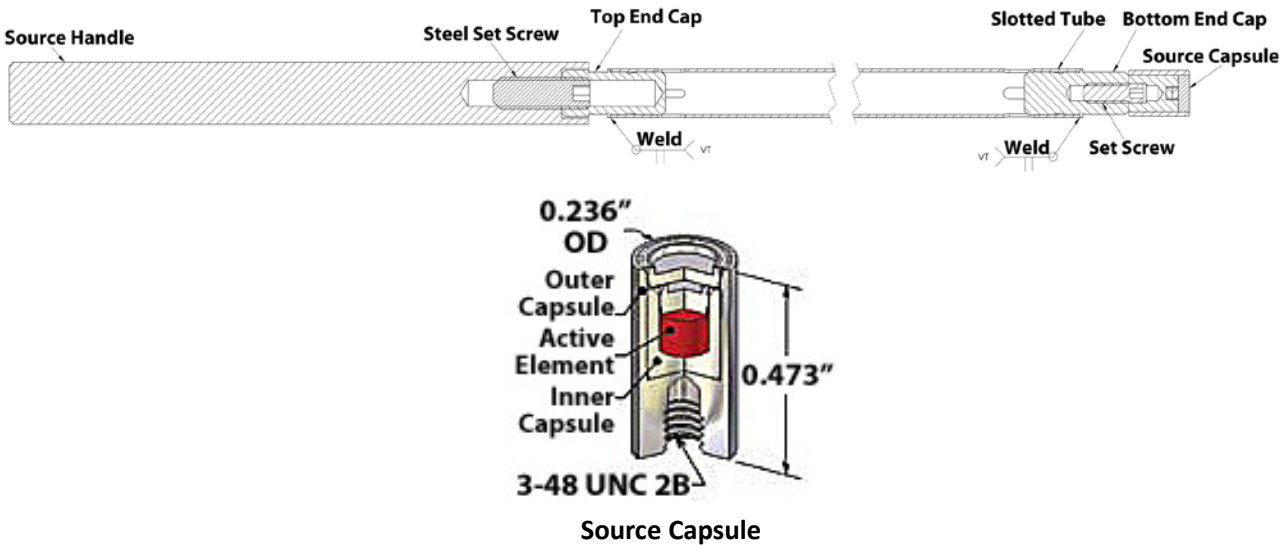

Figure 13. The Neutron Source and Supporting Fixture.

Table 10 shows the axial locations of the surfaces of the neutron source under the assumption that the origin is at the top of the lower grid plate.

Table 10. Axial Locations of the Interfaces in the Neutron Source as Installed in the Critical Assembly.

Part	Location	Axial Position Relative to the Top of the Lower Grid Plate	
		Position (in)	Position (cm)
Source Capsule	Bottom of the source capsule	4.626	11.75004
	Bottom of the set screw hole	5.016	12.74064
	Top of the source capsule	5.099	12.95146
Lower Set Screw	Bottom of the set screw	5.016	12.74064
	Top of the set screw	5.329	13.53566
Bottom End Cap	Bottom of the bottom end cap	5.099	12.95146
	Top of the set screw hole	5.586	14.18844
	Top of the bottom end cap	5.94	15.0876
Slotted Tube	Bottom of the slotted tube	5.382	13.67028
	Top of the slotted tube	28.156	71.51624
Top End Cap	Bottom of the top end cap	27.855	70.7517
	Bottom of the hole in the top end cap	27.908	70.88632
	Top of the top end cap	28.395	72.1233
Upper Set Screw	Bottom of the upper set screw	28.255	71.7677
	Top of the upper set screw	28.755	73.0377
Handle	Bottom of the handle	28.255	71.7677
	Top of the end cap hole in the handle	28.395	72.1233
	Top of the set screw hole in the handle	28.885	73.3679
	Top of the handle	32.255	81.9277

1.2.11 Experimental Method – The focus of these critical experiments was to measure the effects of titanium and aluminum rod replacements in the fuel array on the critical array size. Every experiment with titanium experiment rods has a corresponding experiment with aluminum experiment rods in the same configuration though the numbers of fuel rods in the array differ because of the differing effects of titanium and aluminum.

The critical array size for each configuration was determined in an approach-to-critical experiment with the number of fuel rods in the array as a free parameter. The inverse count rate at successive fuel configurations for two or three detectors as a function of number of fuel rods was extrapolated to zero to obtain an estimate of the critical array size. During all measurements the control and safety elements were in their fully withdrawn or most reactive positions. Because the assembly tank was full of moderator during the measurements, the fuel rod array was fully reflected as described in Section 1.2.6.

The square-pitched arrays were loaded from the center toward the outside while maintaining a roughly cylindrical cross section of the array. The loading order was identical for each experiment. Each fuel rod was in the same array location in every configuration that included that fuel rod.

Four of the configurations, Cases 1, 18, 19, and 24, were each addressed with a full approach-to-critical experiment. The initial array in these configurations had a calculated effective multiplication factor of about 0.9 and the second array had a calculated effective multiplication factor of about 0.95. Subsequent measurements were guided by the count rate results. Early in each approach, the fuel increments were many fuel rods. The fuel increments decreased in size during the approach until the last few count rate measurements were made at increments of a small number of fuel rods.

Cases 2 through 17 are variants of the configuration in Case 1 with the differences being in the number and position of experiment rods in the array. These configurations were addressed by unloading several fuel rods from the outside of the final configuration of a similar experiment and performing an approach-to-critical experiment while projecting inverse count rates as a function of number of rods in the core to zero. The difference for these configurations was that the approach-to-critical experiment covered a much narrower range of fuel loadings near delayed critical. A similar method was used for Cases 20 through 23 which were variants of the configuration of Case 19.

For all configurations, a final approach-to-critical experiment was performed in which count rate measurements were taken for specific symmetrical fuel arrays. In an orderly loading process, these arrays occur at intervals of four or eight fuel rods. Some of the experiments split an interval of eight rods into two four-rod intervals. The measured count rates were inverted. A linear fit to the inverse count rate as a function of number of fuel rods in the array was extrapolated to zero inverse count rate to estimate the critical configuration of the experiment. The extrapolated critical array sizes reported below were developed from inverse count rate data measured during these final experiments. It should be noted that the extrapolated critical array sizes apply only to the specific configurations in which the count rates were measured. The extrapolations only give the actual critical array size if all the fuel rods have the same reactivity worth in the interval from the smaller measured array size to the actual critical array size. Because the reactivity worth of the fuel rods depends on position in the array, sometimes strongly, no claim is made that the array will be exactly critical with the extrapolated number of fuel rods.

Based on the k_{eff} values derived in Section 2.3, all of the final configurations had subcritical multiplications that significantly exceeded 100.

1.2.12 Experiment Arrays – During the approach-to-critical experiments, detailed records were kept of the location and identity of each fuel rod in each core. A given fuel rod was placed in the same grid location in each core in which it was used. The total number of fuel rod positions occupied, the mass of UO_2 in the core, and the total length of the fuel columns in all the fuel rods for the largest array measured in each of the twenty-four configurations are listed in Table 11. Also listed in the table is previous array size that is used for extrapolation to delayed critical, the extrapolated array size at delayed critical, and the temperature at which the experimental measurements were made. Table 12 lists the average fuel rod diameter with standard deviation for the set of fuel rods used in each benchmark experiment. The fuel rod arrangement in the largest array measured for each of the twenty-four cores is shown in Figures 14 through 37. The locations of all fuel rods, control and safety elements, experiment rods, and the neutron source are indicated in the 45×45 array of holes in the grid plates. The locations of the fuel rods that make up the difference of the two array sizes listed in Table 11 are shown in the figures as incremental fuel rods.

Table 11. Measured and Extrapolated Array Sizes, Total UO_2 Mass and Column Length, and Assembly Temperature for the Twenty-Four Cases.

Case	Largest Array			Previous Array Size (rods) [a]	Extrapolated Critical Array Size (rods) [a] [d]	Temperature (ºC)
	Array Size (rods) [a]	UO_2 Mass (g) [b]	Fuel Column Length (cm) [c]			
1	1457	158478.41	71066.8	1453	1462.28 ± 0.02	25.0
2	1473	160214.80	71846.1	1465	1477.19 ± 0.01	24.8
3	1492	162274.98	72772.0	1484	1497.63 ± 0.01	25.4
4	1521	165420.97	74187.3	1517	1525.52 ± 0.01	25.5
5	1560	169659.69	76093.8	1556	1564.88 ± 0.01	25.2
6	1609	174973.80	78481.1	1605	1612.23 ± 0.01	25.0
7	1585	172373.63	77314.3	1581	1589.49 ± 0.01	25.6
8	1573	171072.67	76729.1	1569	1575.88 ± 0.01	25.0
9	1557	169329.99	75946.9	1553	1561.46 ± 0.01	25.3
10	1453	158042.41	70871.9	1449	1461.22 ± 0.03	25.3
11	1448	157498.24	70628.2	1444	1456.47 ± 0.03	25.2
12	1445	157171.81	70482.0	1437	1451.74 ± 0.02	25.1
13	1444	157061.52	70433.0	1436	1449.78 ± 0.02	25.2
14	1441	156734.46	70286.3	1433	1445.49 ± 0.01	25.3
15	1429	155432.28	69702.1	1425	1433.14 ± 0.01	25.4
16	1429	155430.24	69701.0	1425	1430.85 ± 0.01	25.4
17	1425	154992.99	69506.2	1417	1430.15 ± 0.01	25.4
18	1037	112795.71	50581.4	1029	1039.36 ± 0.01	24.9
19	1097	119322.08	53509.3	1093	1101.82 ± 0.01	25.5
20	1153	125411.32	56239.6	1149	1155.94 ± 0.01	25.3
21	1213	131935.29	59163.6	1209	1214.32 ± 0.01	25.4
22	1285	139762.09	62678.8	1281	1290.13 ± 0.01	25.3
23	1377	149747.95	67165.4	1369	1380.58 ± 0.01	25.4
24	1485	161478.75	72433.3	1477	1488.69 ± 0.01	25.5

(a) Includes the twelve fueled sections in the control element and the two safety elements.
(b) Sum of the UO_2 masses in the rods included in the configuration.
(c) Sum of the fuel column lengths in the rods included in the configuration.
(d) The critical array size determined from count-rate measurements made at the two array sizes given. The uncertainties listed are those attributed only to the stochastic nature of the radiation detection process.

Table 12. Average Fuel Rod Diameter and Standard Deviation of the Distribution for the Fuel Rods in Each Case.

Case	Array Size (rods)	Average Fuel Rod Outside Diameter (in)	Standard Deviation (in)	Number of Fuel Rods [(a)]
1	1457	0.249993	0.000085	1445
2	1473	0.249993	0.000085	1461
3	1492	0.249992	0.000085	1480
4	1521	0.249991	0.000085	1509
5	1560	0.249991	0.000084	1548
6	1609	0.249990	0.000085	1597
7	1585	0.249989	0.000085	1573
8	1573	0.249989	0.000085	1561
9	1557	0.249989	0.000085	1545
10	1453	0.249989	0.000085	1441
11	1448	0.249993	0.000085	1436
12	1445	0.249993	0.000085	1433
13	1444	0.249993	0.000085	1432
14	1441	0.249993	0.000085	1429
15	1429	0.249993	0.000085	1417
16	1429	0.249993	0.000085	1417
17	1425	0.249992	0.000085	1413
18	1037	0.249998	0.000084	1025
19	1097	0.249993	0.000085	1085
20	1153	0.249995	0.000085	1141
21	1213	0.249993	0.000085	1201
22	1285	0.249994	0.000085	1273
23	1377	0.249989	0.000084	1365
24	1485	0.249992	0.000085	1473

(a) Each configuration also included 12 fueled sections in the control and safety elements.

During the course of the critical experiments, reproducibility data were taken for two of the configurations investigated (Cases 1 and 2). The maximum deviation from the mean extrapolated array size was about 1.5 rods for these measurements with a standard deviation of about 0.9 rods.

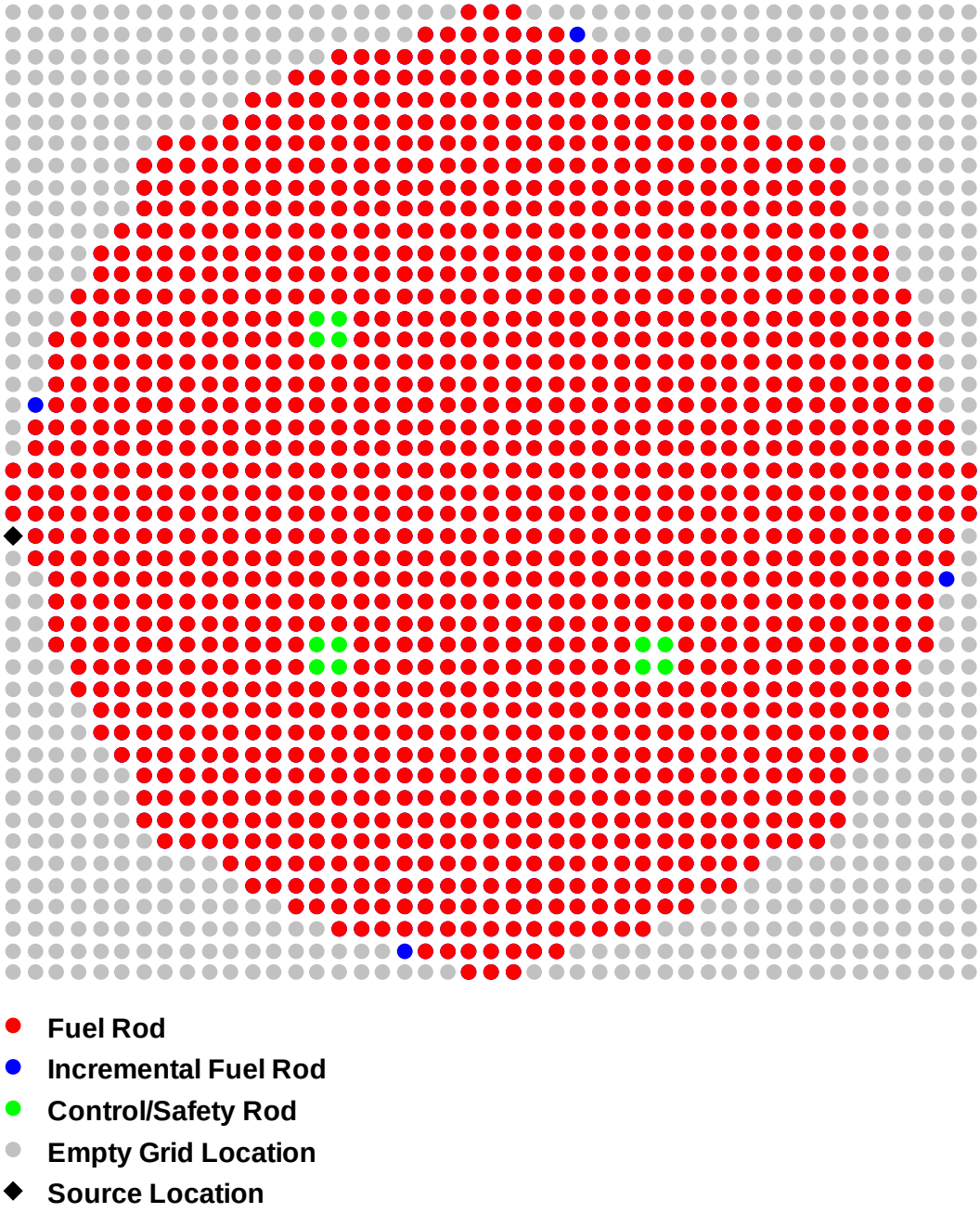

Figure 14. Fuel Rod Layout of the Largest Array Measured for Case 1.

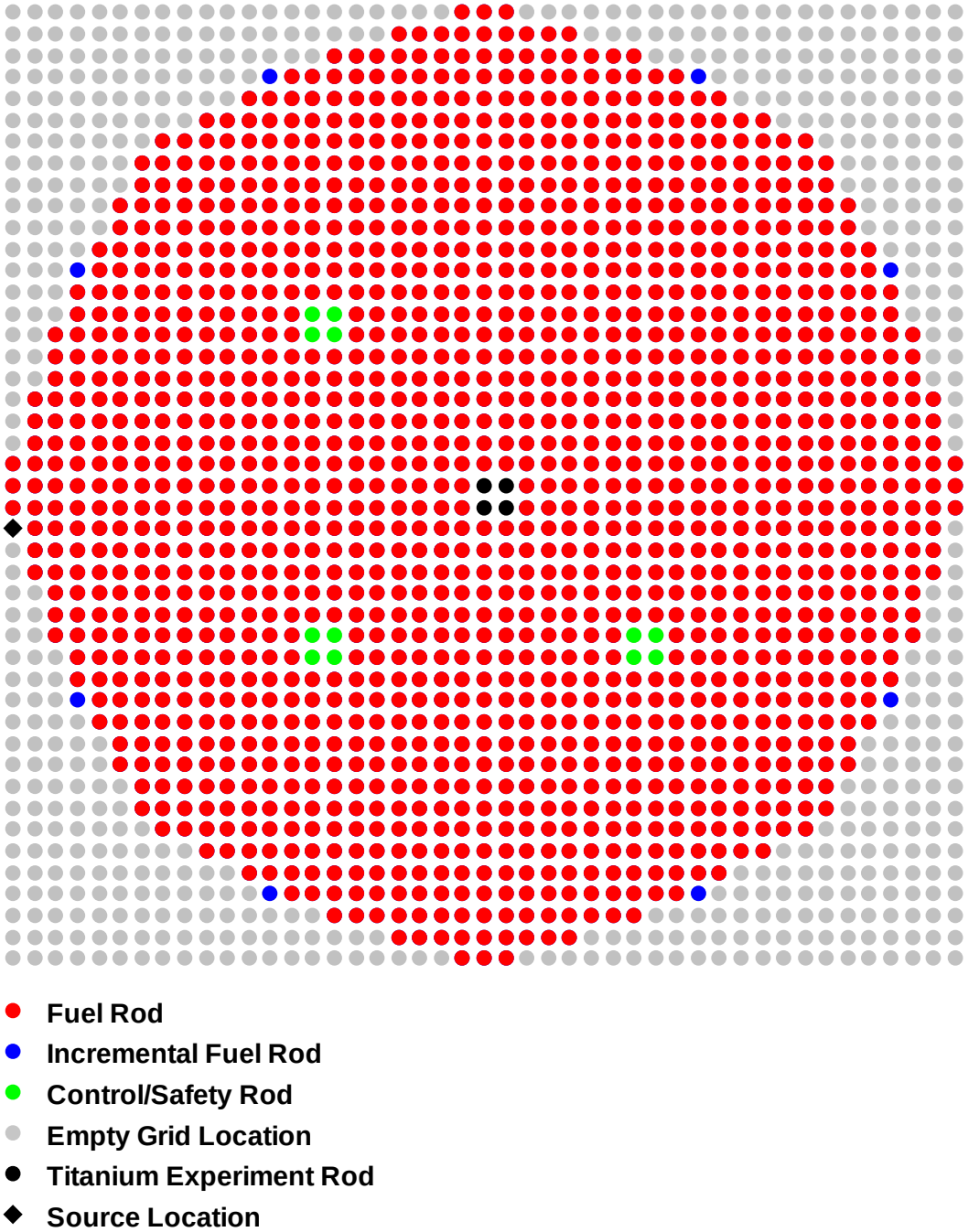

Figure 15. Fuel Rod Layout of the Largest Array Measured for Case 2.

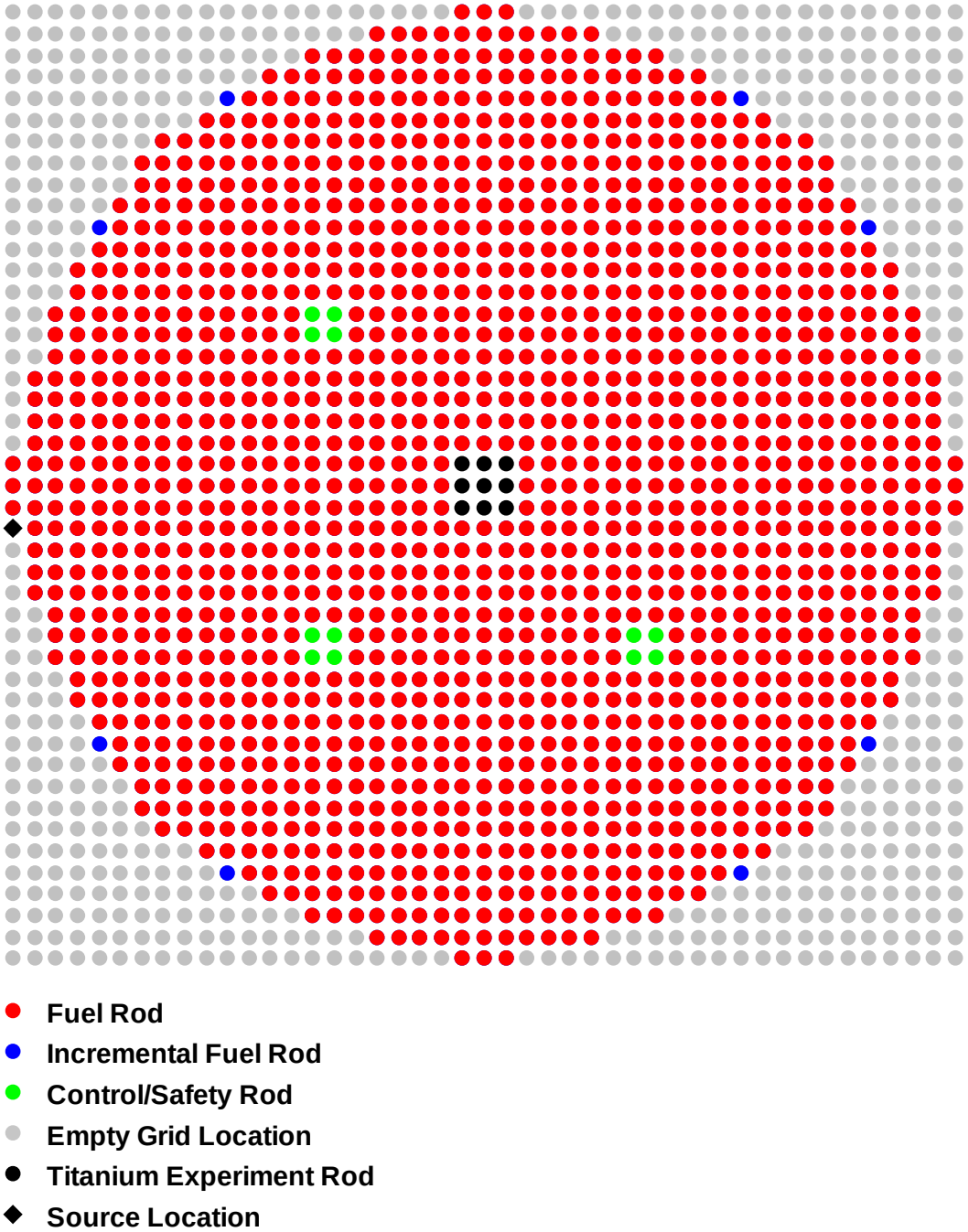

Figure 16. Fuel Rod Layout of the Largest Array Measured for Case 3.

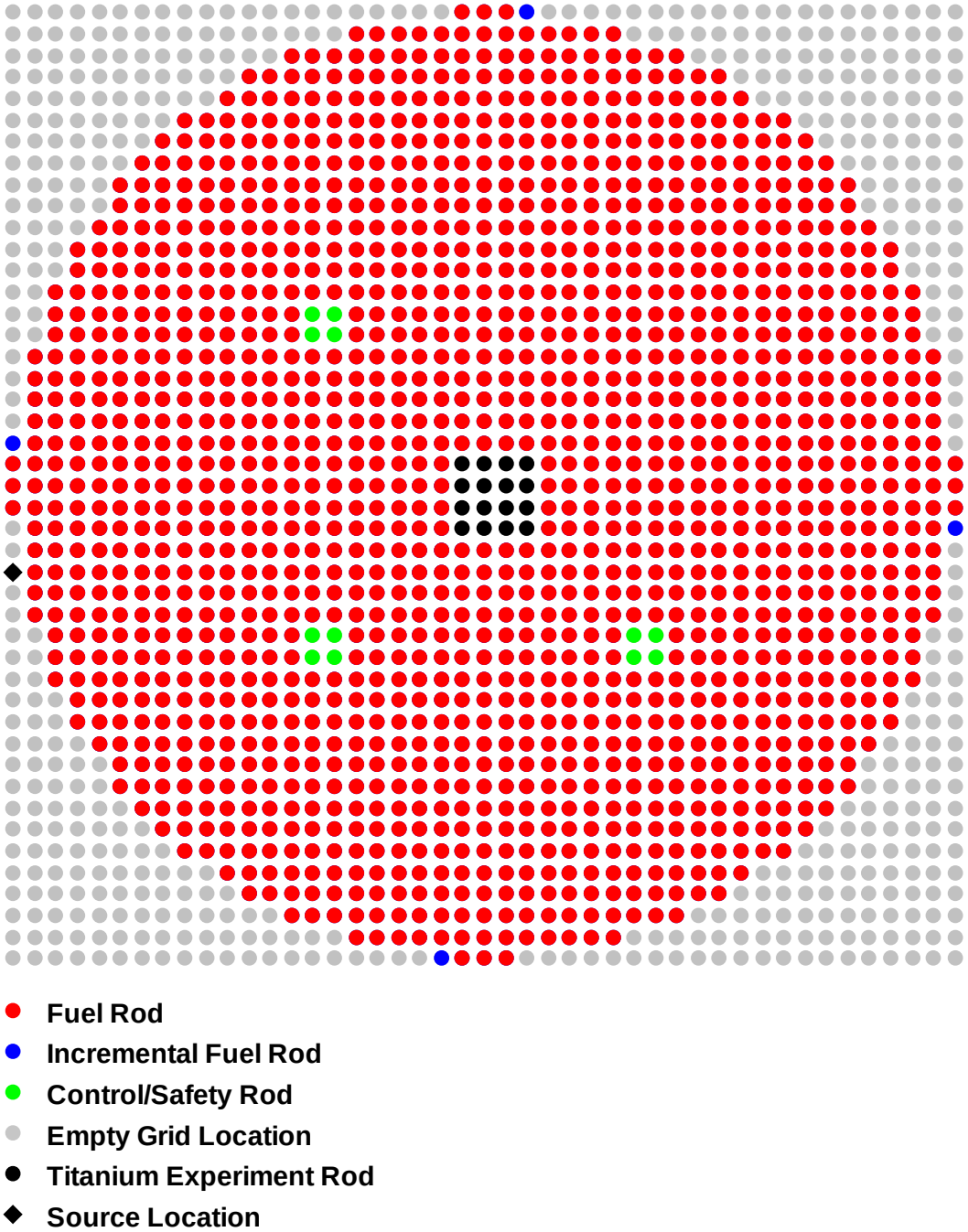

Figure 17. Fuel Rod Layout of the Largest Array Measured for Case 4.

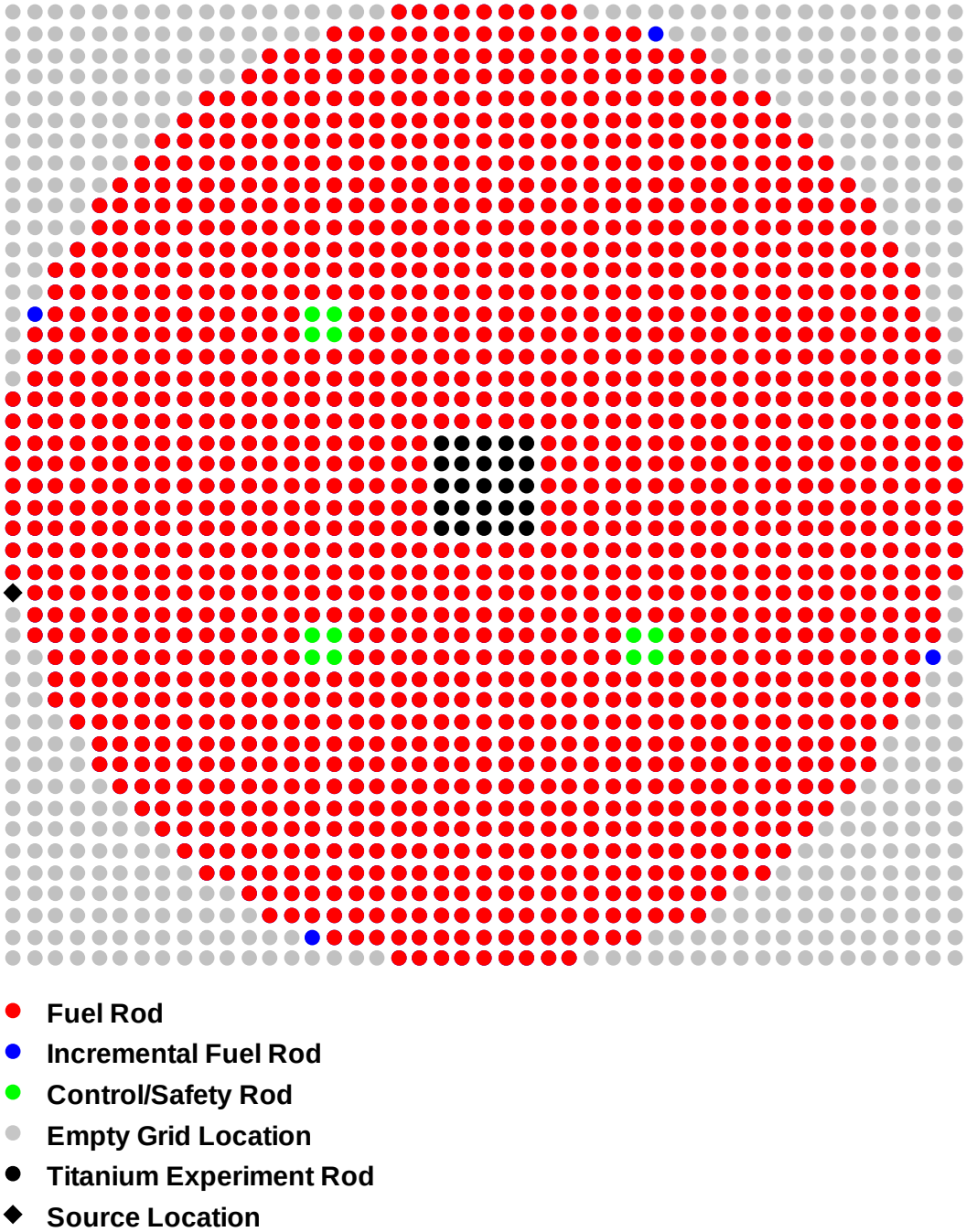

Figure 18. Fuel Rod Layout of the Largest Array Measured for Case 5.

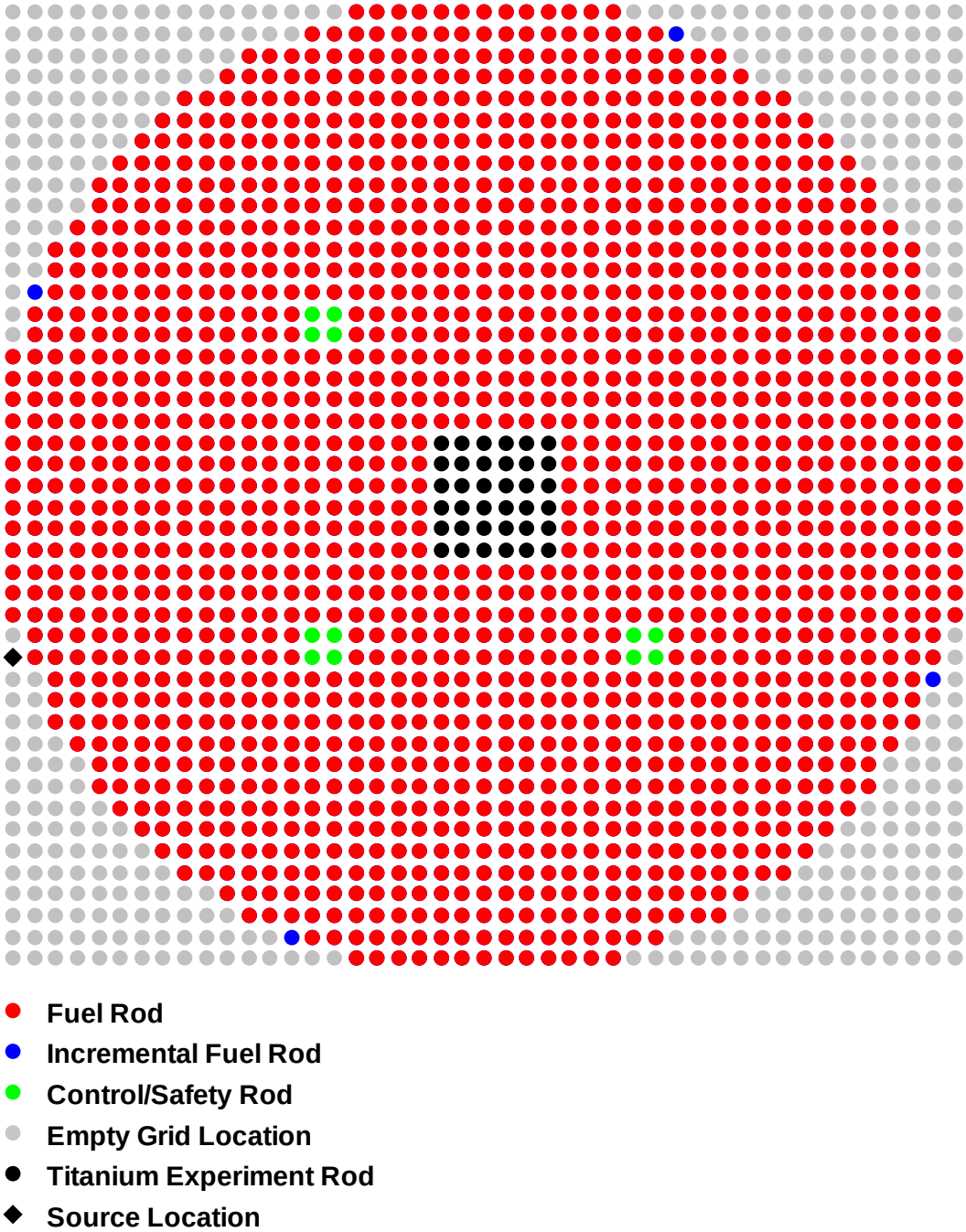

Figure 19. Fuel Rod Layout of the Largest Array Measured for Case 6.

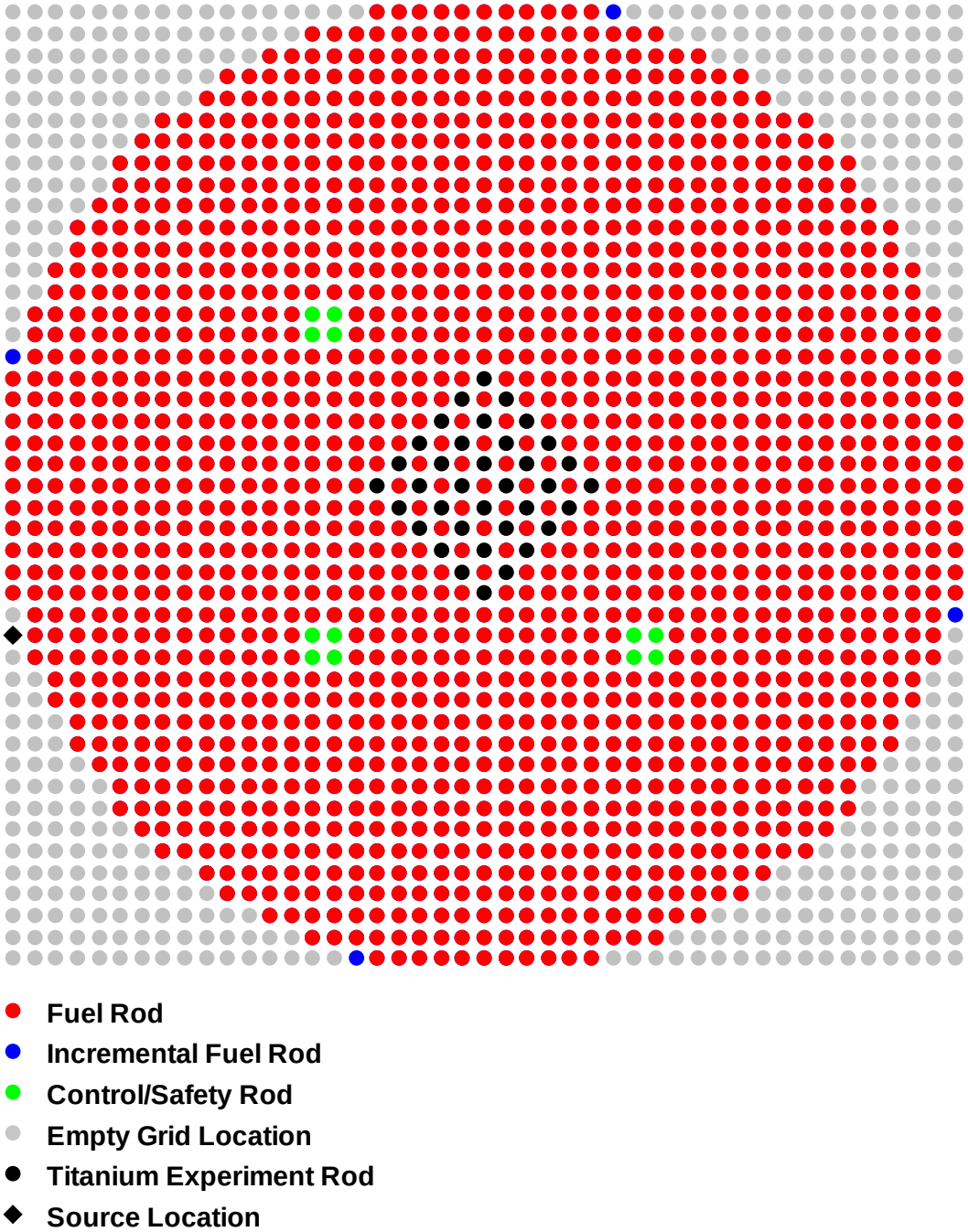

Figure 20. Fuel Rod Layout of the Largest Array Measured for Case 7.

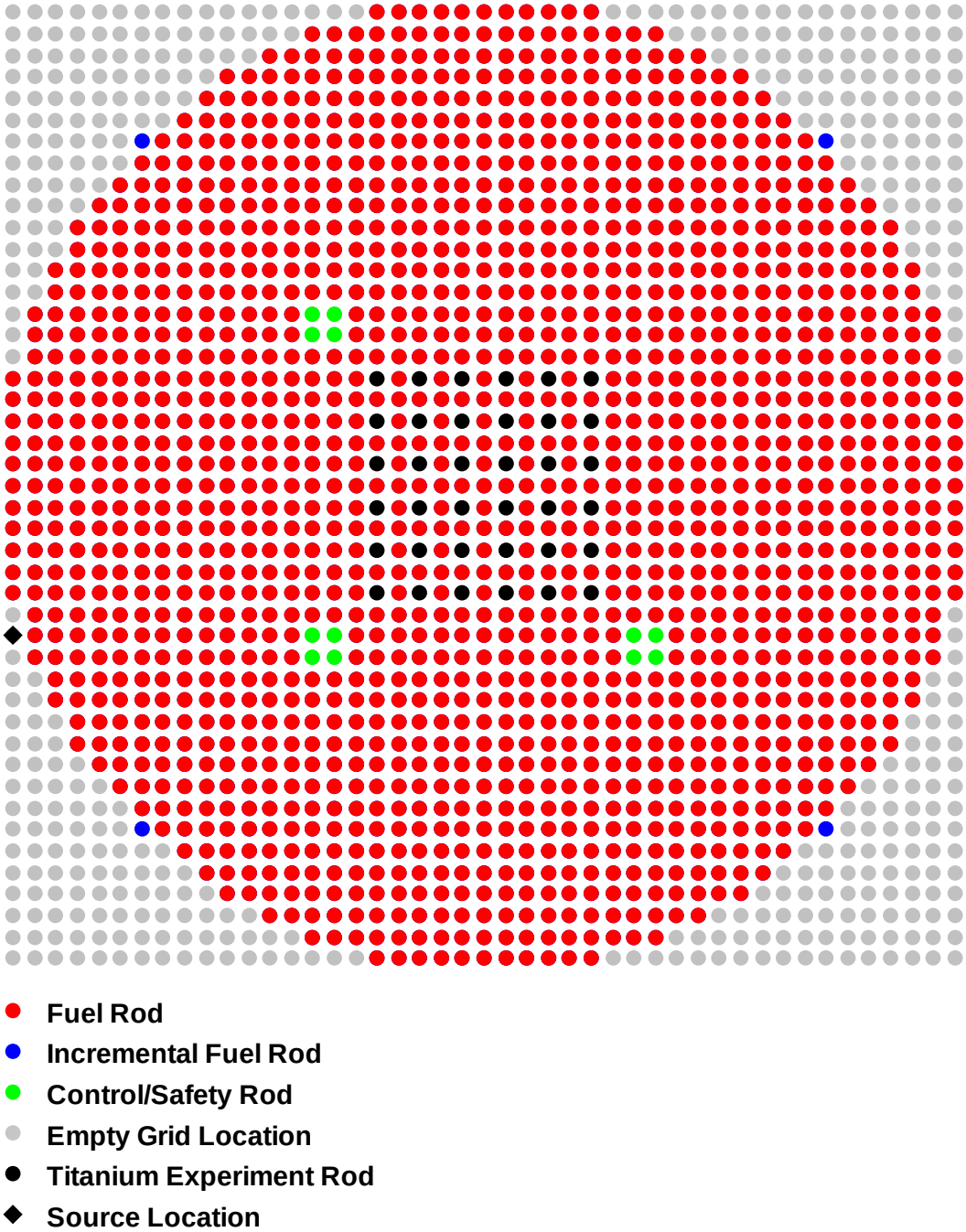

Figure 21. Fuel Rod Layout of the Largest Array Measured for Case 8.

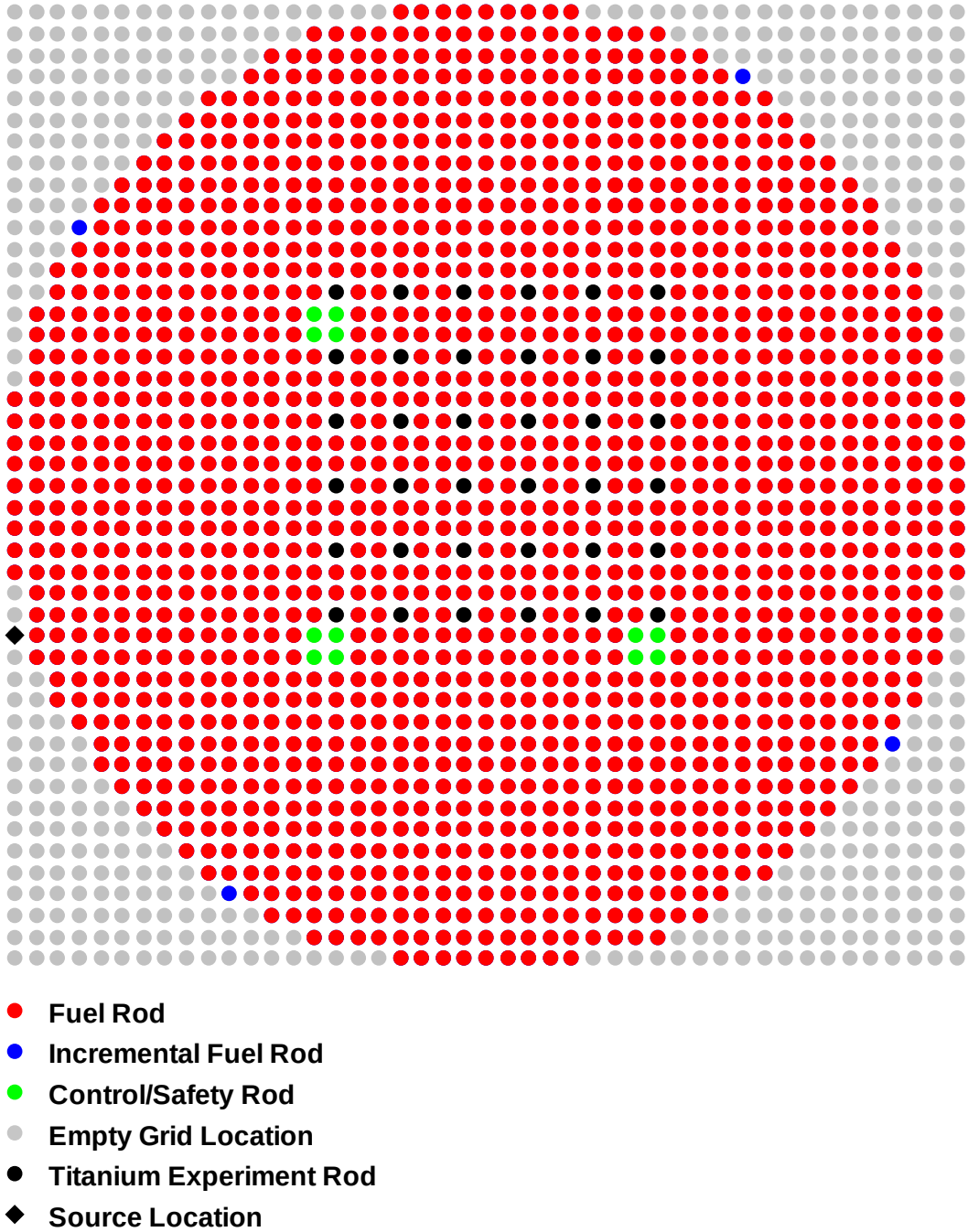

Figure 22. Fuel Rod Layout of the Largest Array Measured for Case 9.

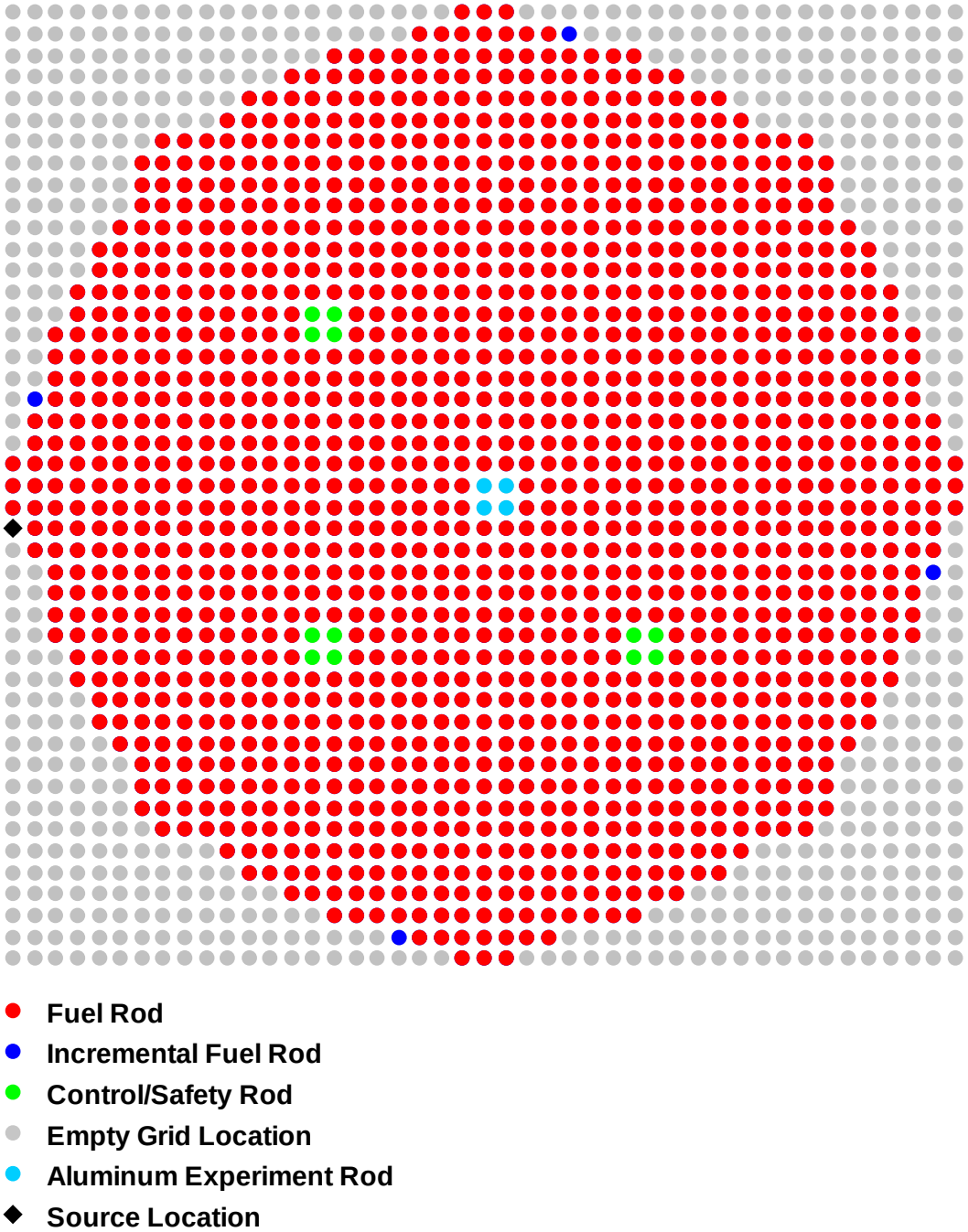

Figure 23. Fuel Rod Layout of the Largest Array Measured for Case 10.

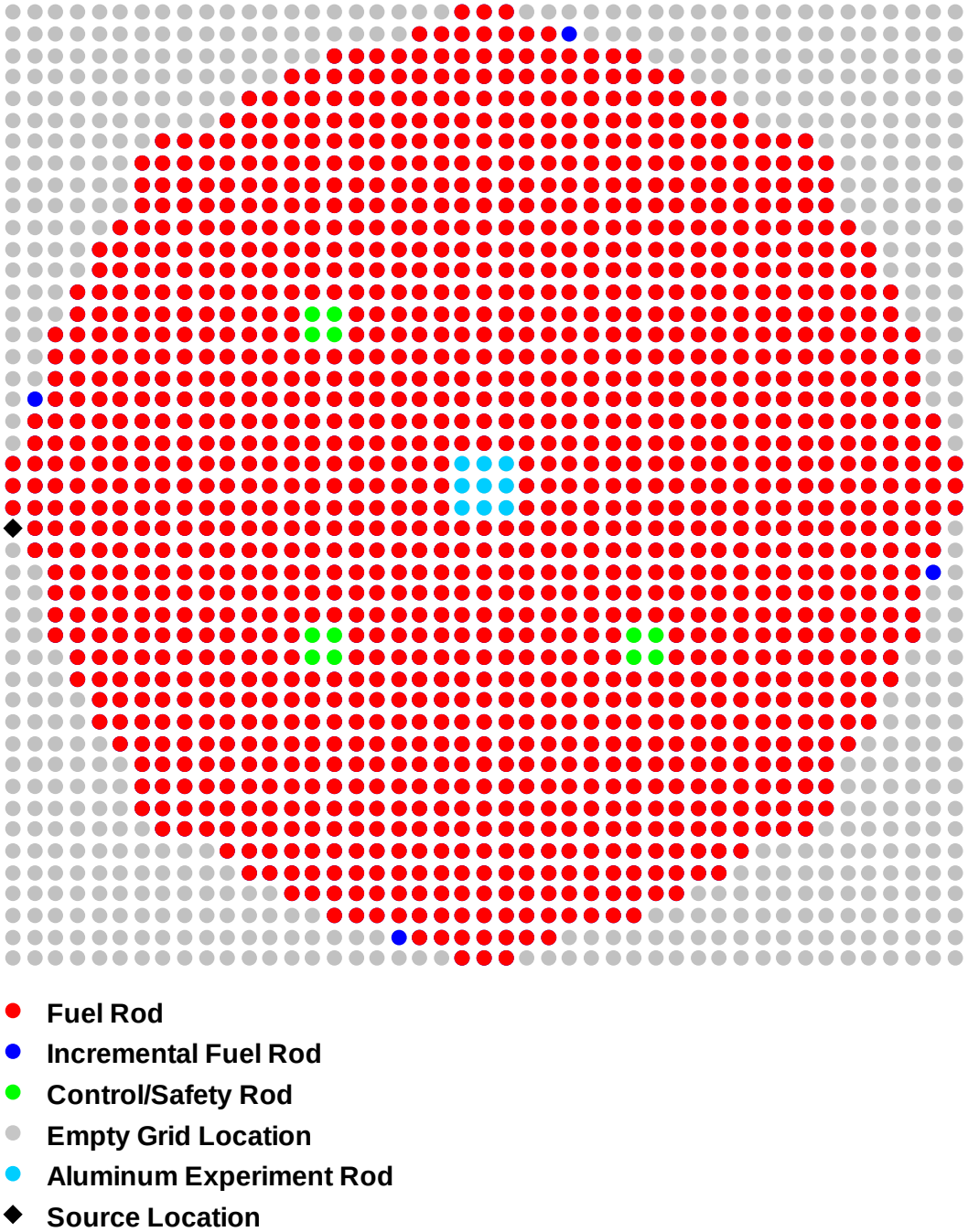

Figure 24. Fuel Element Layout of the Largest Array Measured for Case 11.

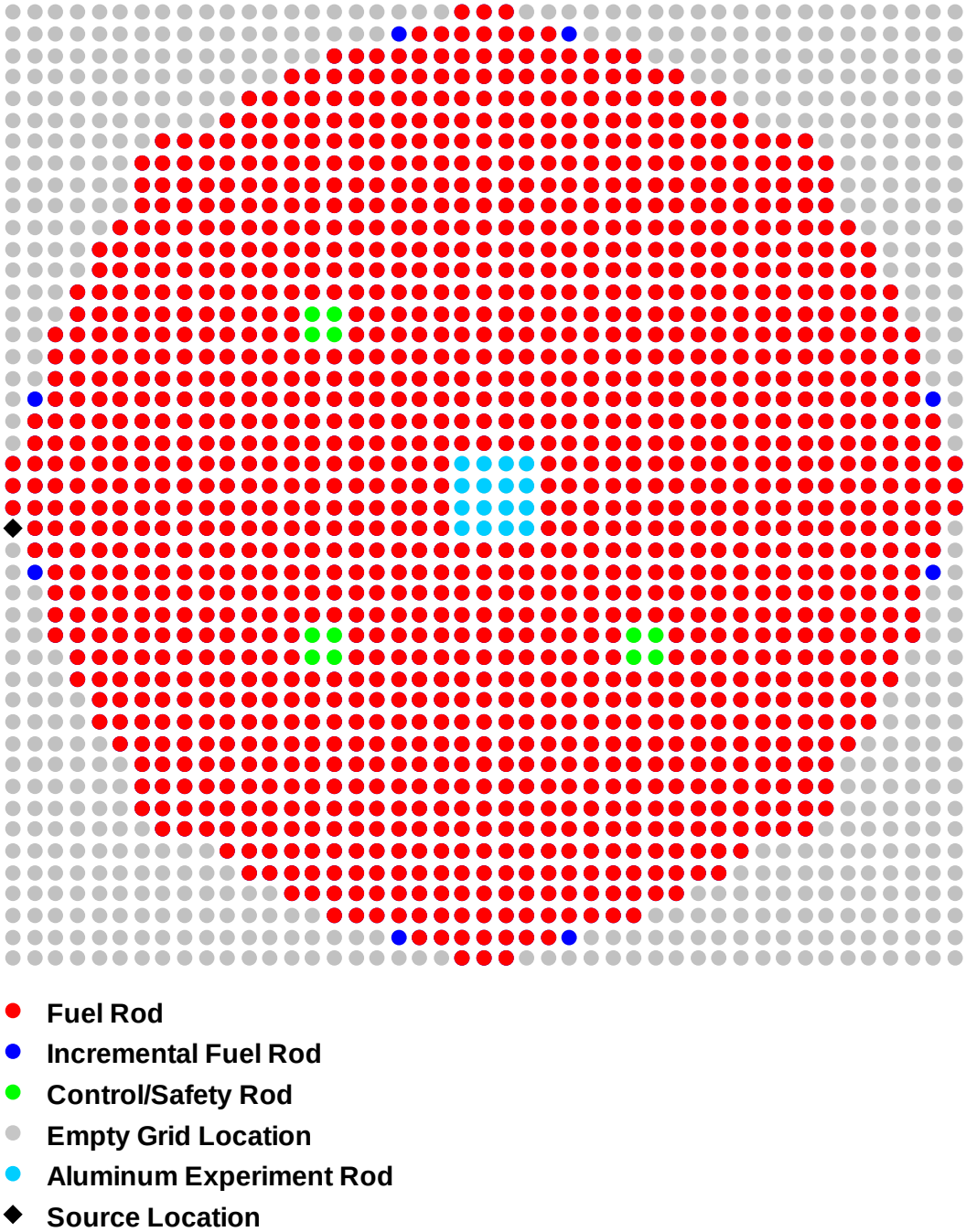

Figure 25. Fuel Element Layout of the Largest Array Measured for Case 12.

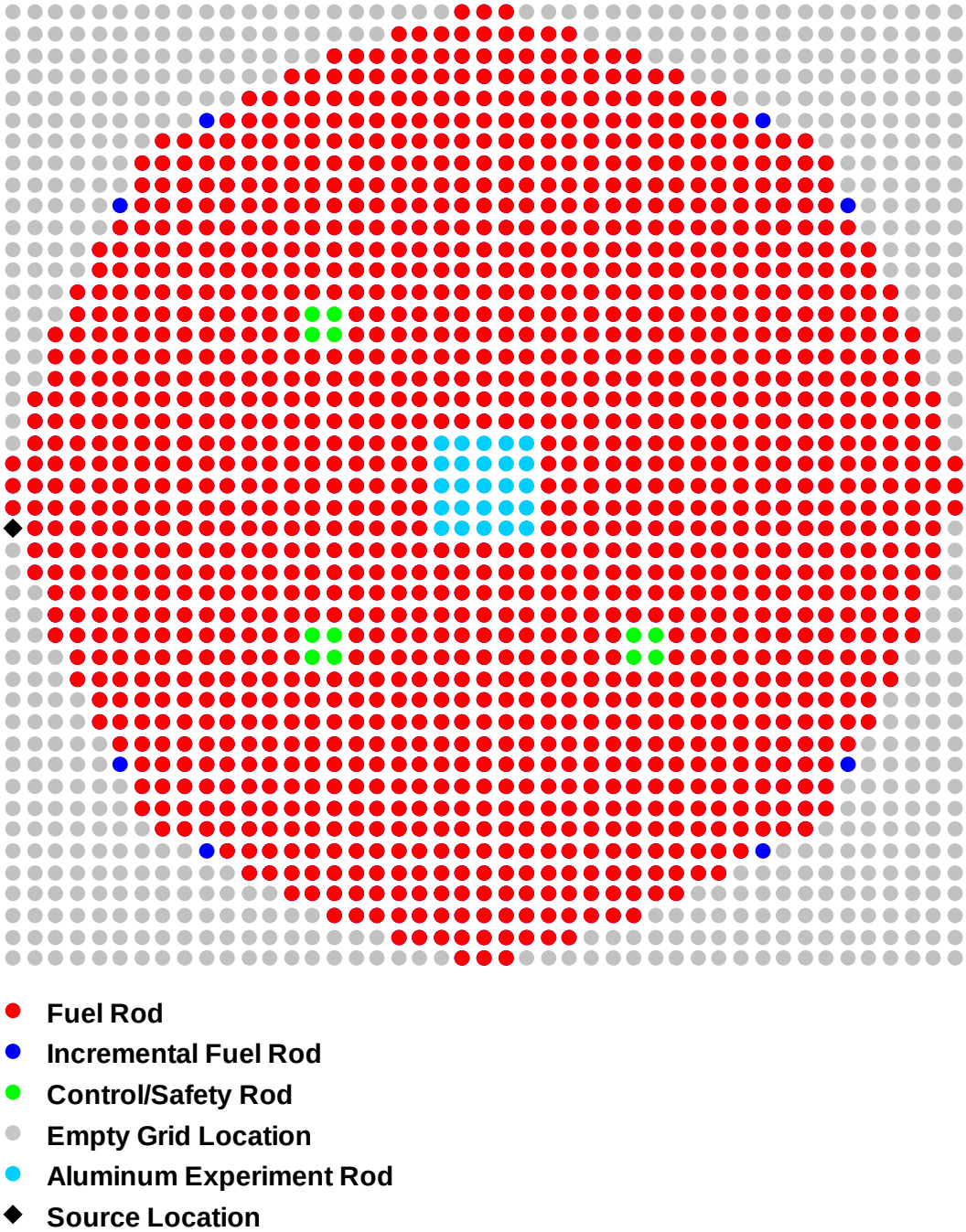

Figure 26. Fuel Element Layout of the Largest Array Measured for Case 13.

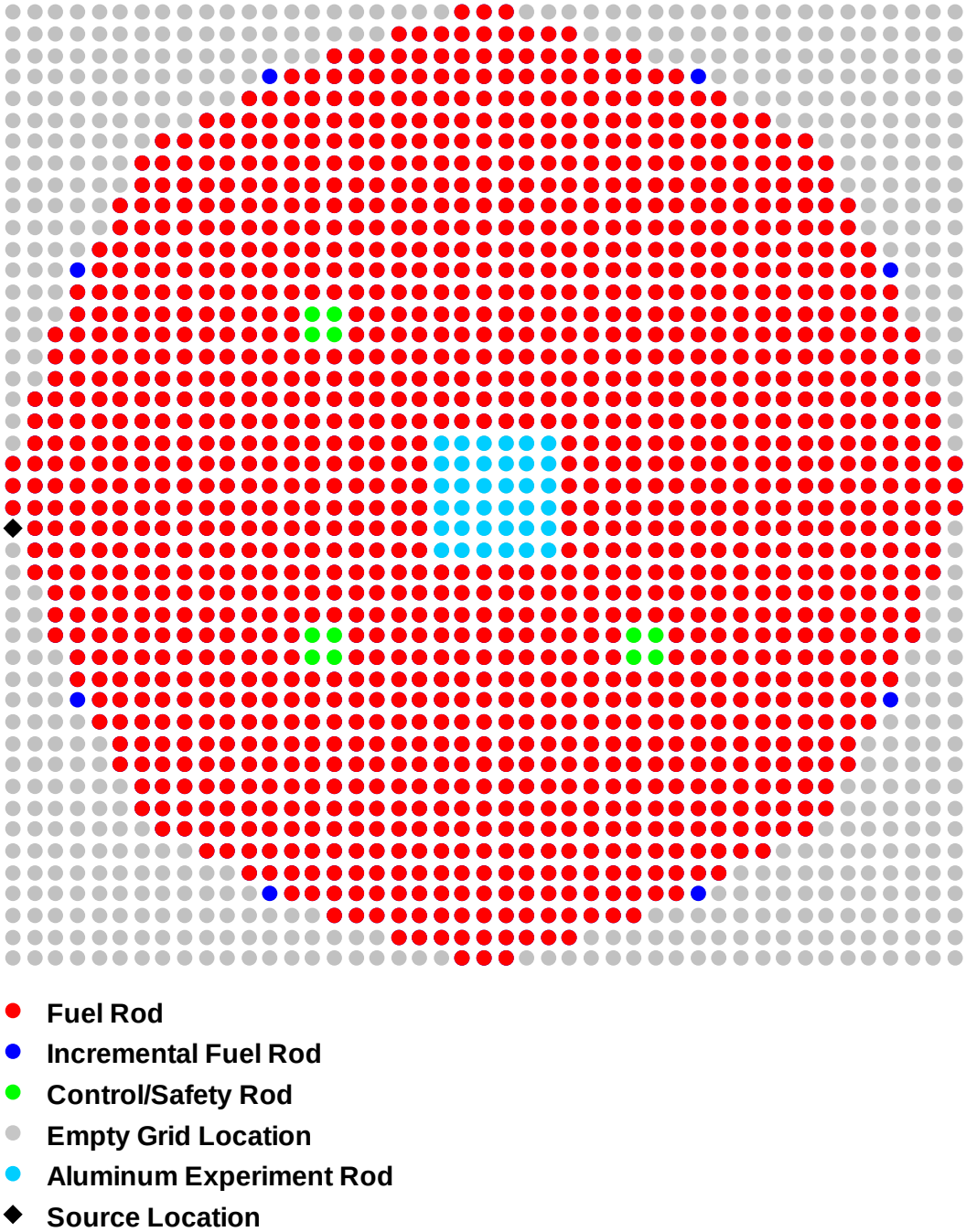

Figure 27. Fuel Element Layout of the Largest Array Measured for Case 14.

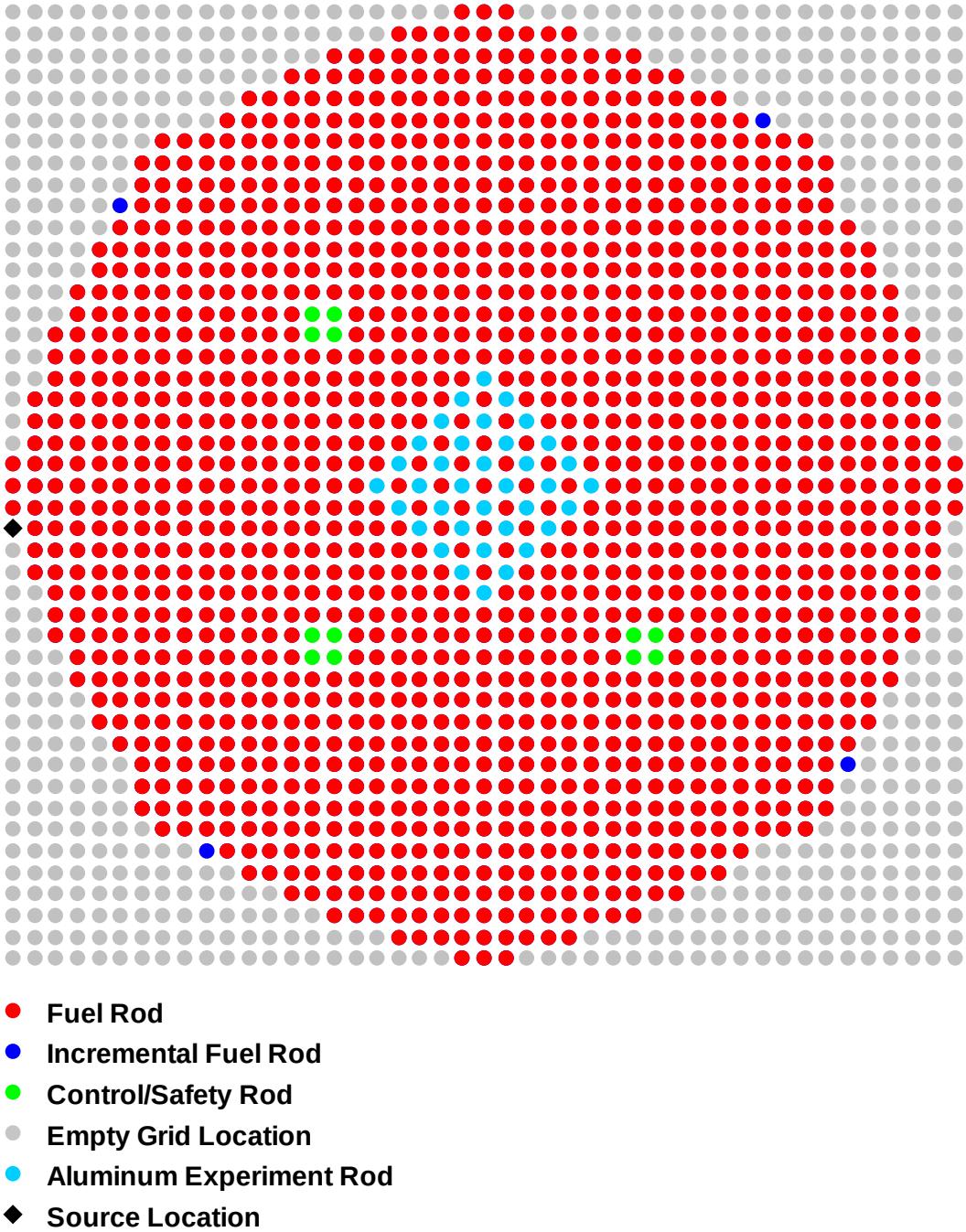

Figure 28. Fuel Element Layout of the Largest Array Measured for Case 15.

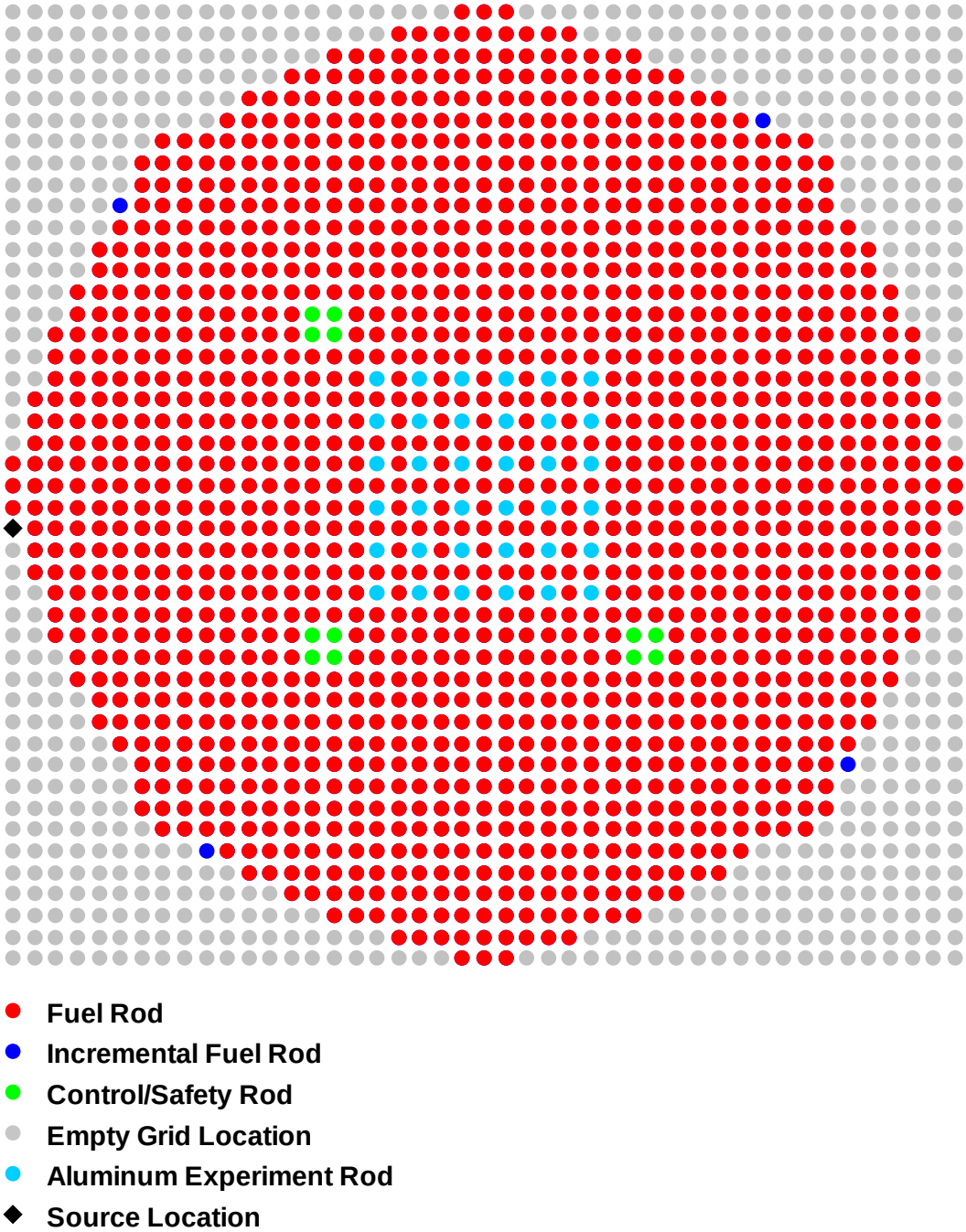

Figure 29. Fuel Element Layout of the Largest Array Measured for Case 16.

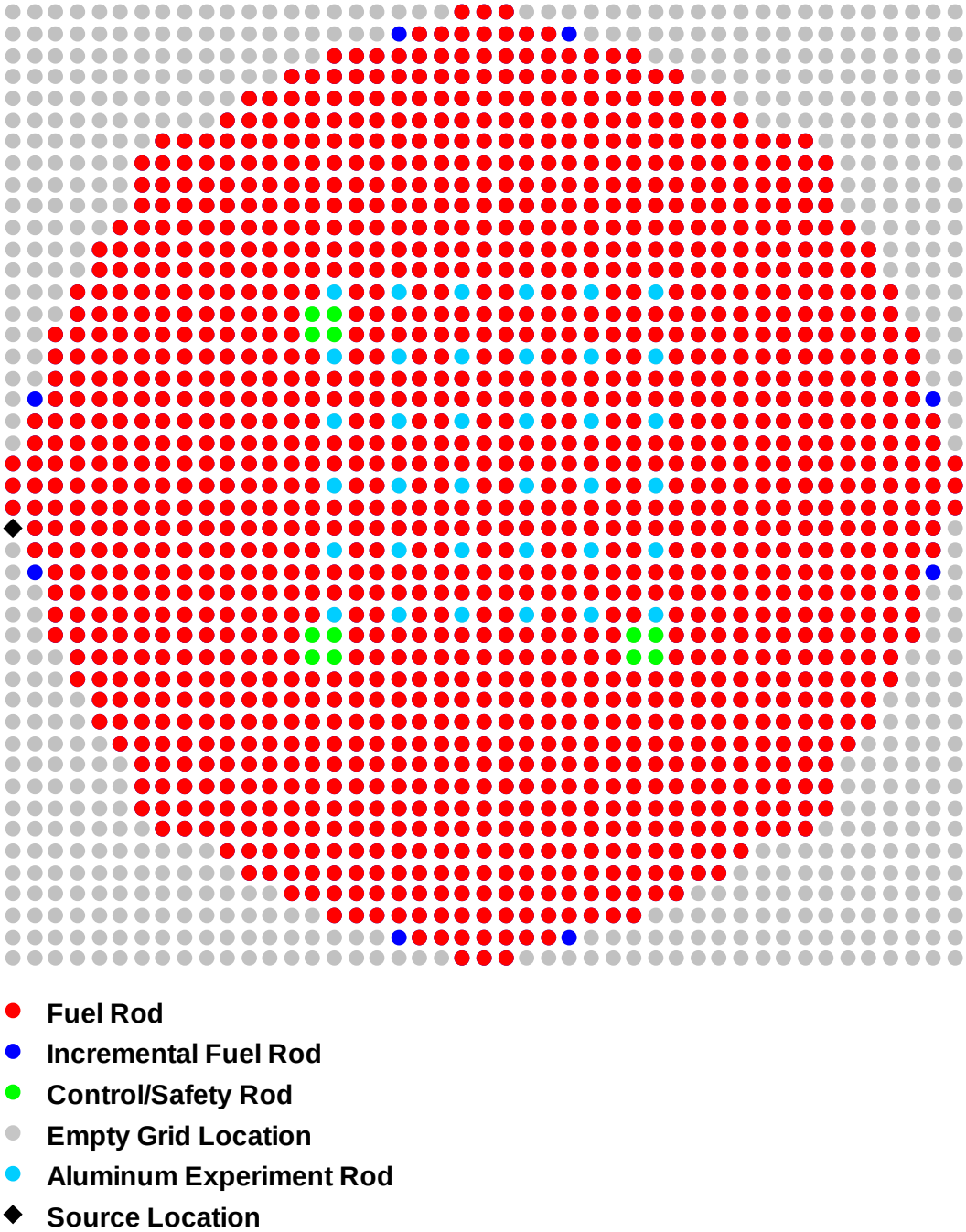

Figure 30. Fuel Element Layout of the Largest Array Measured for Case 17.

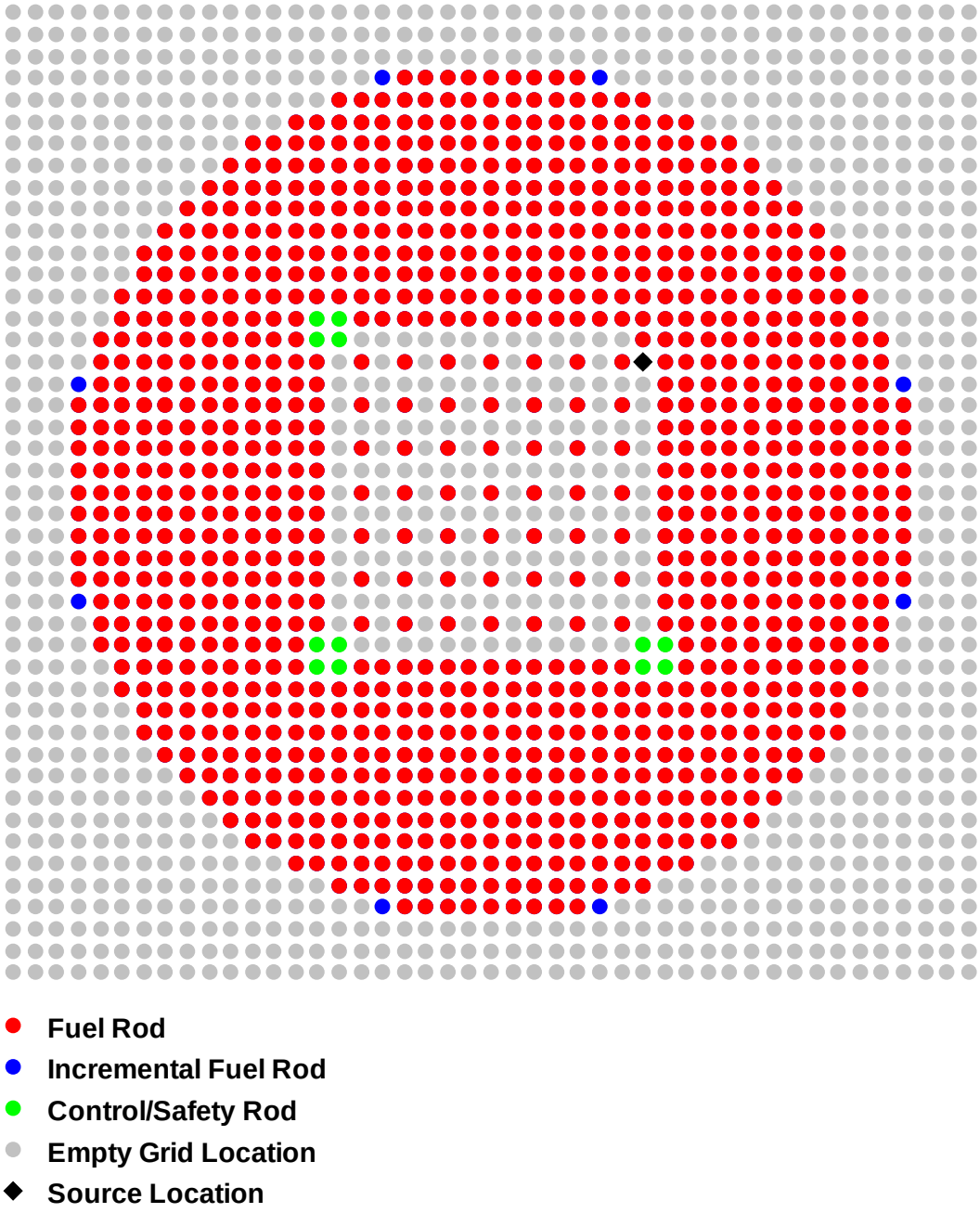

Figure 31. Fuel Element Layout of the Largest Array Measured for Case 18.

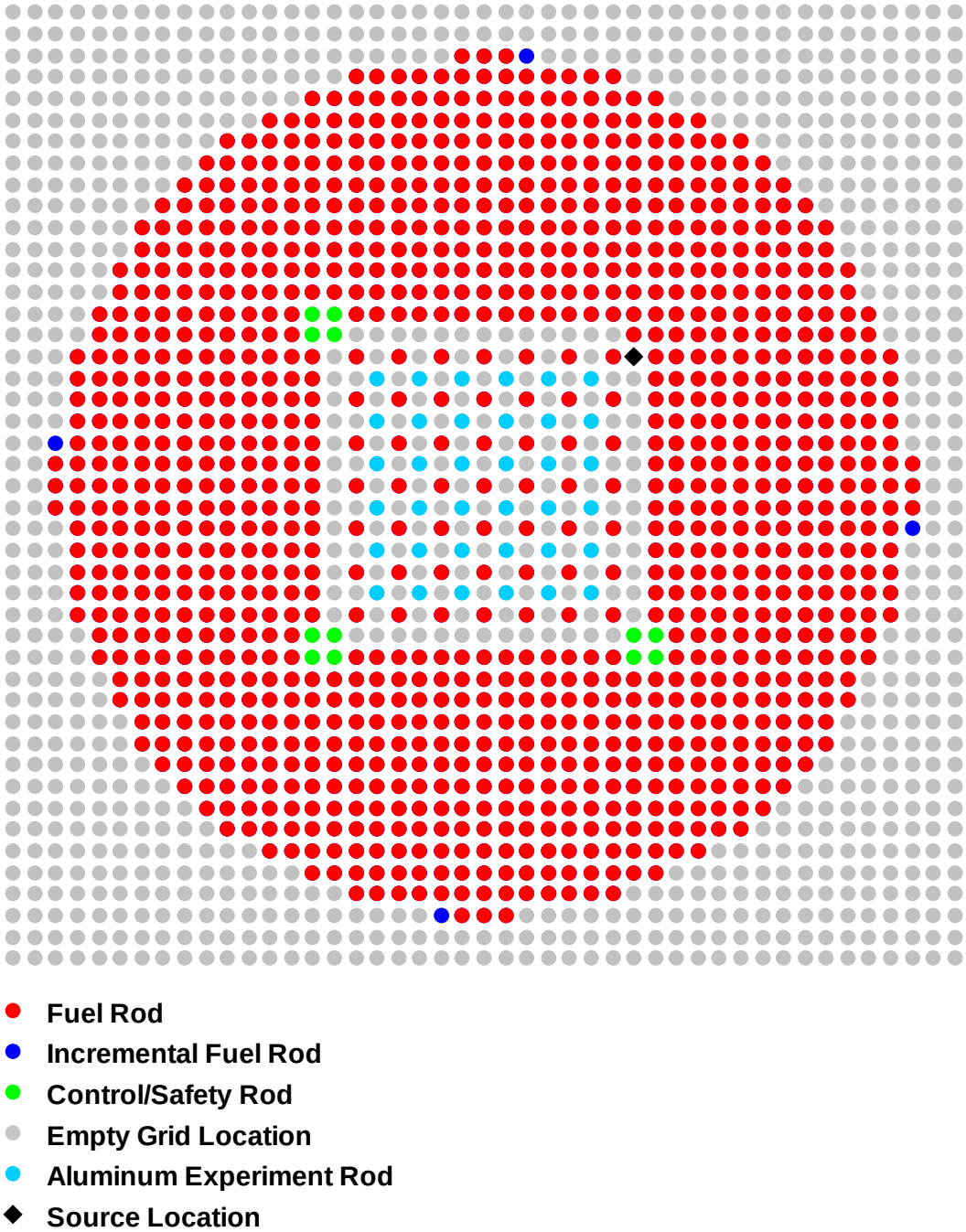

Figure 32. Fuel Element Layout of the Largest Array Measured for Case 19.

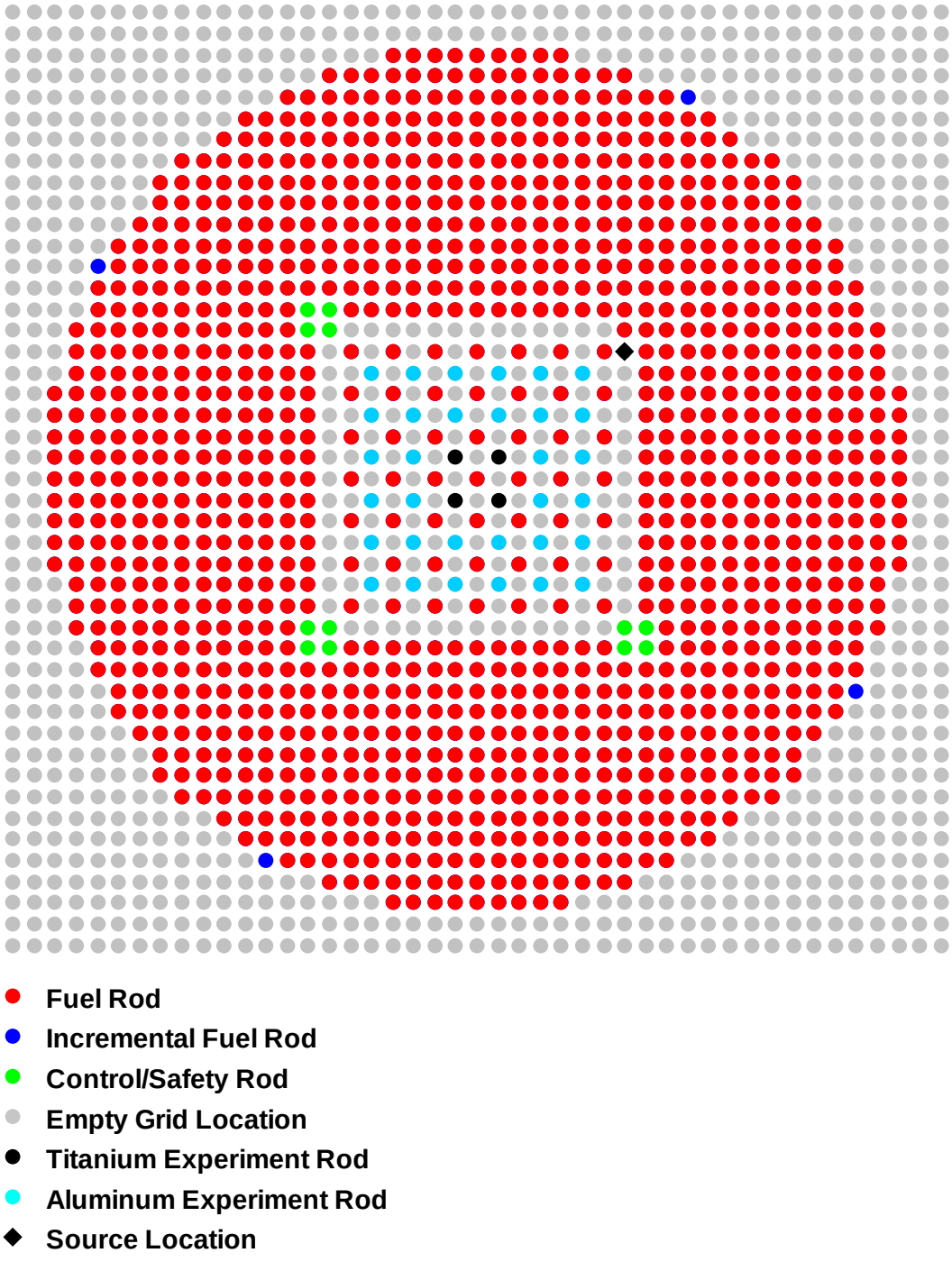

Figure 33. Fuel Element Layout of the Largest Array Measured for Case 20.

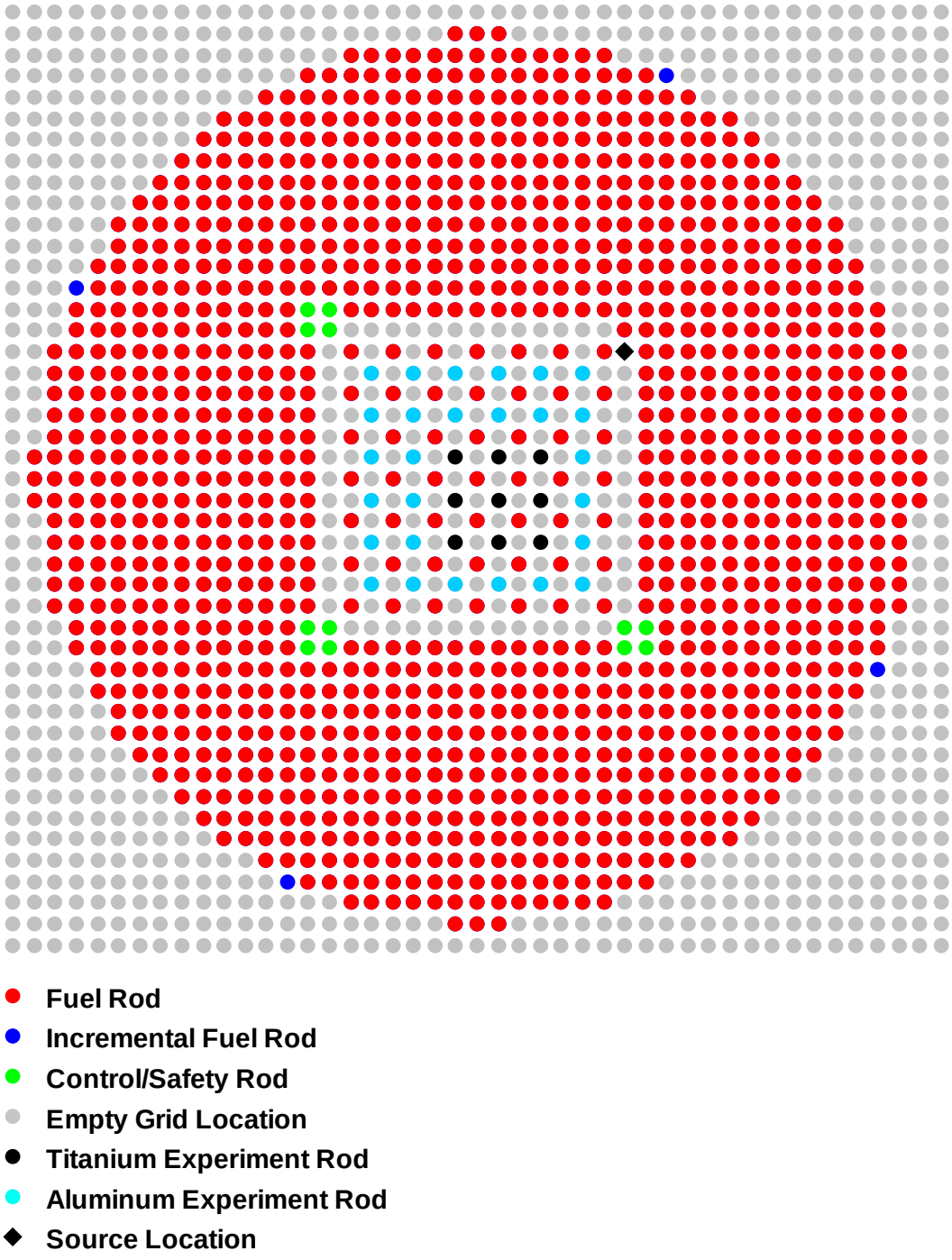

Figure 34. Fuel Element Layout of the Largest Array Measured for Case 21.

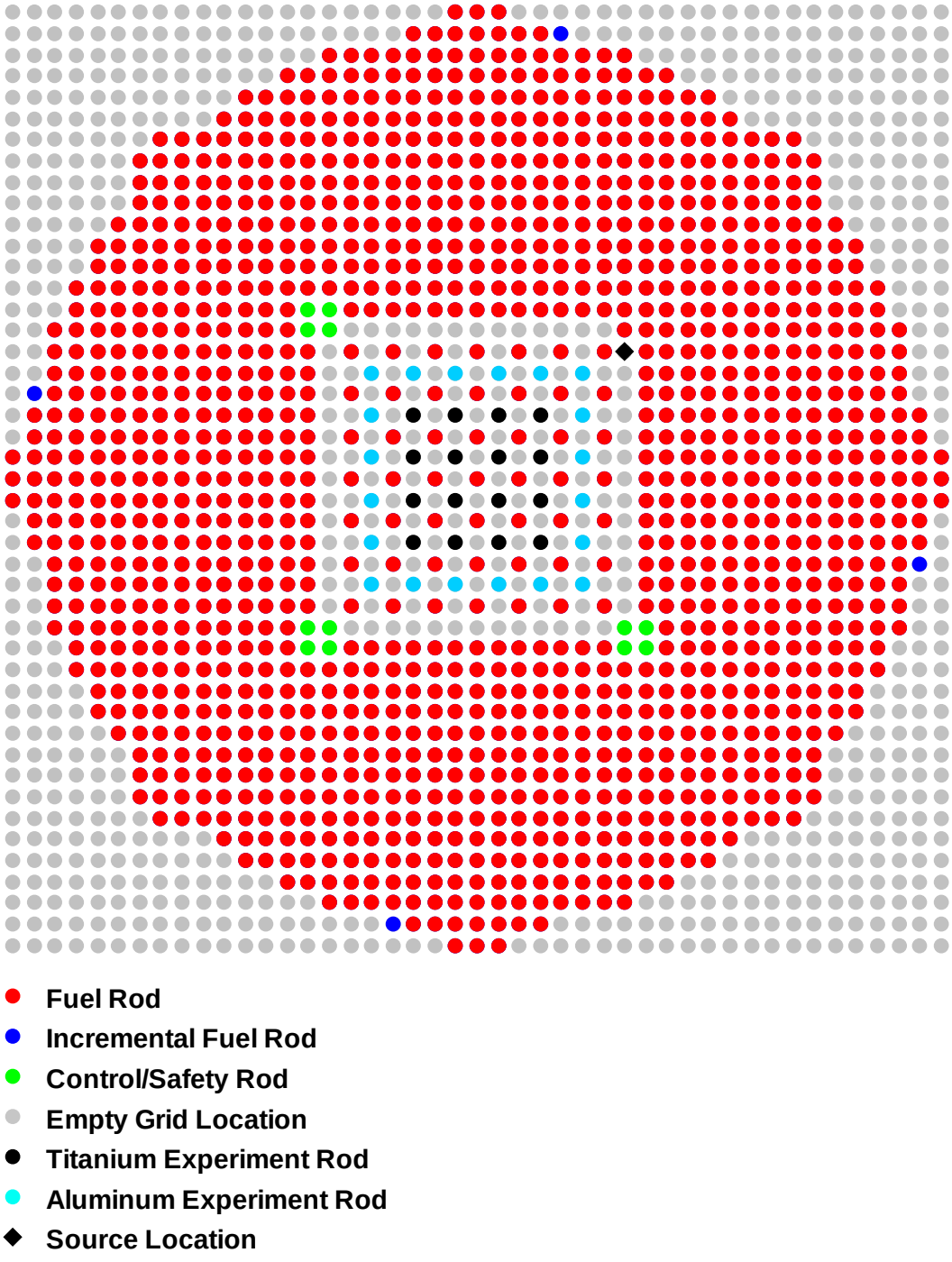

Figure 35. Fuel Element Layout of the Largest Array Measured for Case 22.

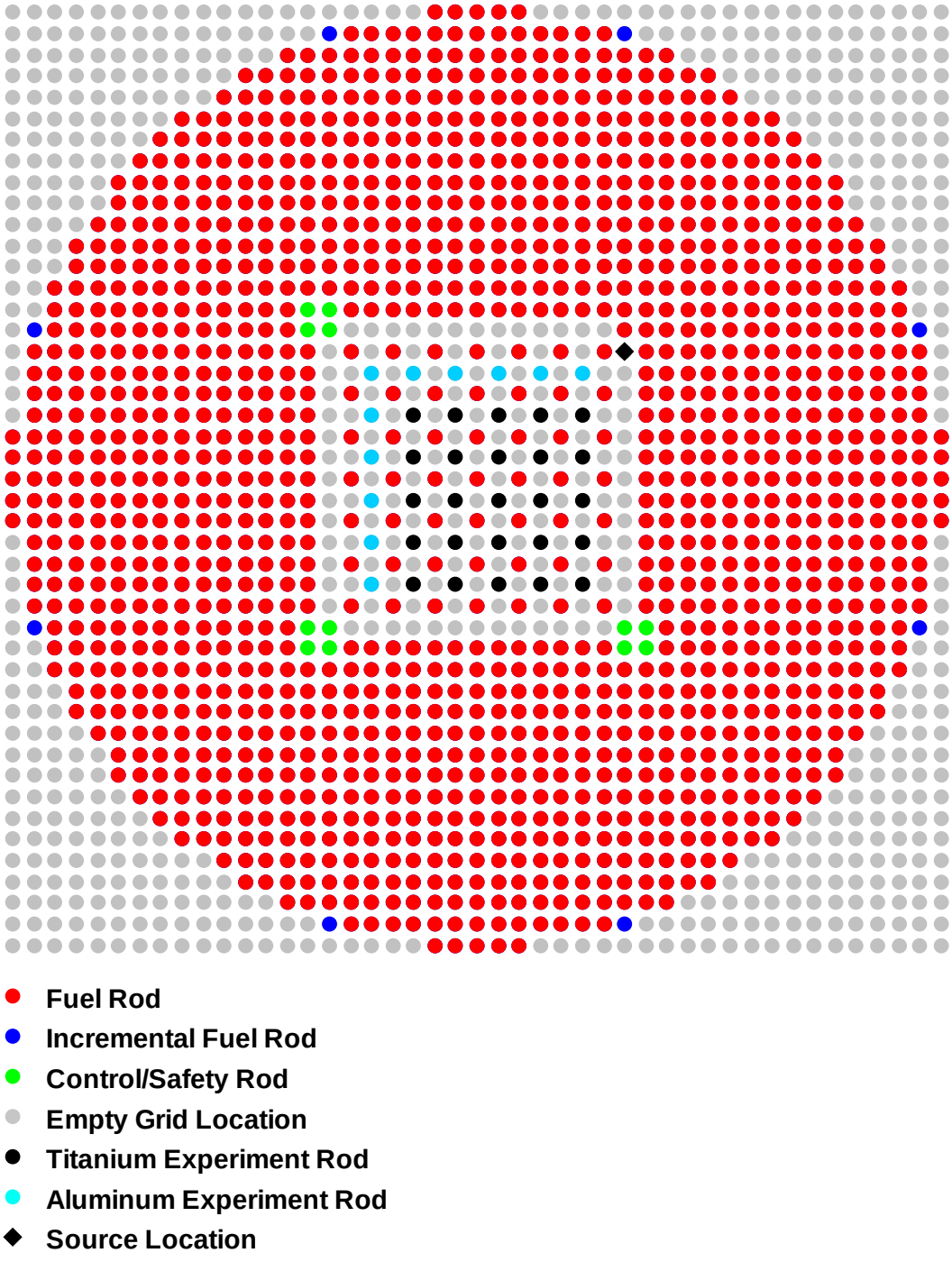

Figure 36. Fuel Element Layout of the Largest Array Measured for Case 23.

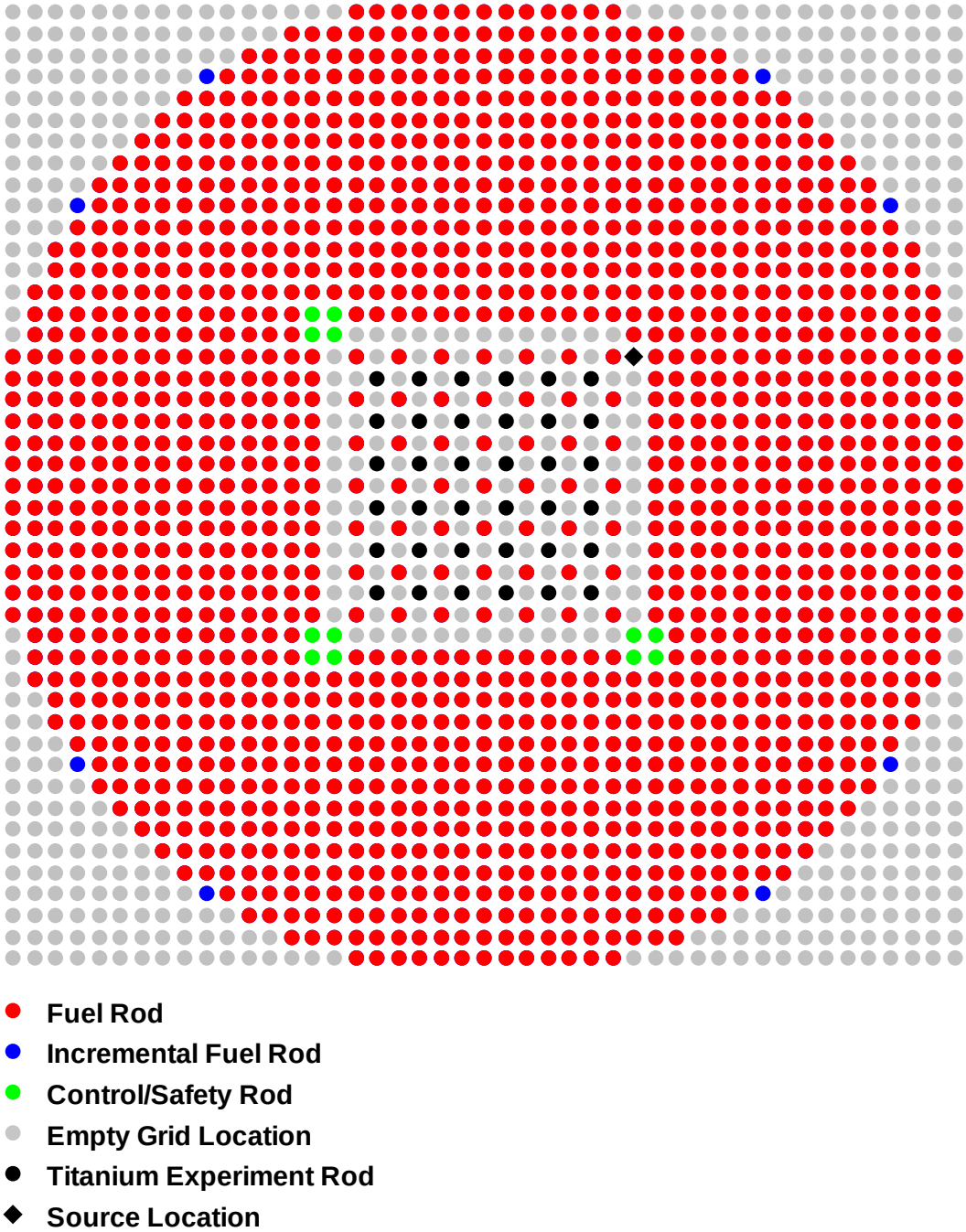

Figure 37. Fuel Element Layout of the Largest Array Measured for Case 24.

1.3 Description of Material Data

1.3.1 UO_2 Fuel – The fuel pellets used in the fuel rods were drawn from the fuel stock that was removed from fuel elements obtained from The Pennsylvania State University. The uranium isotopic data were measured for ten randomly-selected fuel pellets from the pool of fuel pellets used in the fuel rod fabrication using a high-resolution multi-collector inductively coupled plasma mass spectrometer (ICP-MS). The measured uranium isotopic data are given in Table 13. The uncertainties shown with the mass fractions are the standard deviations for the ten measurements. The systematic uncertainties were estimated by the laboratory that made the isotopic measurements.

Table 13. Isotopic Composition of Uranium in the UO_2 Fuel Pellets.

Uranium Isotope	Wt.%[(a)]	Systematic Uncertainty (Wt.%)[(b)]
^{234}U	0.02814 ± 0.00008	0.00013
^{235}U	6.9034 ± 0.0046	0.0069
^{236}U	0.06336 ± 0.00012	0.00063
^{238}U	93.0051 ± 0.0046	-
Total	100.000	-

(a) The uncertainties given are the standard deviations for ten measurements.
(b) The systematic uncertainties are given at the one-standard-deviation level.

The oxygen to uranium ratio was not measured.

Metallic impurities were also obtained during the ICP-MS measurements of the ten fuel pellets. The results of the impurity measurements are shown in Table 14.

Table 14. Results of the Fuel Impurity Measurements.

Element	Average [(a)] (g/g)	Standard Deviation [(a)] (g/g)	Maximum [(b)] (g/g)	Minimum [(c)] (g/g)	Reported Detection Limit [(d)] (g/g)	Measurements Above Detection Limit
Ag	1.61E-07	2.19E-07	6.67E-07	2.24E-08	2.24E-08	9
B	4.17E-07	4.73E-07	1.56E-06	2.24E-08	2.24E-08	9
Cd	2.25E-07	3.98E-07	9.36E-07	2.21E-08	2.27E-08	5
Co	2.06E-07	5.67E-08	3.13E-07	1.27E-07	-	10
Cr	2.11E-05	1.06E-05	4.03E-05	1.31E-05	-	10
Cu	2.19E-06	1.59E-06	4.95E-06	2.26E-07	2.26E-07	9
Fe	9.31E-05	4.31E-05	1.79E-04	5.27E-05	-	10
Mn	2.52E-06	1.04E-06	4.51E-06	1.50E-06	-	10
Mo	1.93E-06	1.85E-06	5.19E-06	6.34E-07	-	10
Ni	3.32E-05	1.13E-05	5.73E-05	2.31E-05	-	10
V	1.22E-07	2.33E-08	1.56E-07	9.71E-08	-	10
W	1.07E-07	1.14E-08	1.23E-07	8.53E-08	-	10
Sm	5.31E-08	-	5.31E-08	2.21E-08	2.27E-08	1
Dy	-	-	-	-	2.27E-08	0
Eu	-	-	-	-	2.27E-08	0
Gd	-	-	-	-	2.27E-08	0

(a) The impurities were reported as mass of impurity per unit UO_2 fuel pellet mass. Averages and standard deviations are reported for the measurements that were above the detection limit for the element. Measurements at the detection limits were not included in the averages or the calculation of the standard deviations. Because only one measurement was above the detection limit for Sm, no value is reported for the standard deviation.

(b) Reported maximum measured value. No value is included when all measurements were at the detection limit.

(c) Reported minimum measured value when all ten measurements were above the detection limit. Minimum of the reported detection limits when one or more measurements were below the detection limit. No value is included when all measurements were at the detection limit.

(d) The detection limit varied slightly from sample to sample. The maximum detection limit is recorded. Where all measurements were above the detection limit, no value is entered.

1.3.2 Fuel Rod Cladding – The fabrication drawings for the fuel rods specify the material for the clad tubing and end plugs as aluminum alloy 3003. The composition of the material used was not measured. The specification for the composition of aluminum alloy 3003 is given in Table 15. The density of the cladding material was not measured.

Table 15. Chemical Composition Limits of Aluminum Alloy 3003.

Element	Weight % [(a)]
Si	0.6 max
Fe	0.7 max
Cu	0.05 – 0.20
Mn	1.0 – 1.5
Zn	0.10 max
Other Elements Each	0.05 max
Other Elements Total	0.15 max
Al	Remainder

(a) From ASTM B210-04

1.3.3 Aluminum Grid Plates – The upper and lower grid plates were fabricated from 1.00 in (2.54 cm) thick plates of aluminum alloy 6061-T651. The measured composition of the grid plates is compared with the 6061 aluminum specification in Table 16. The density of the grid plate material was not measured.

Table 16. Chemical Composition Limits of Aluminum Alloy 6061 Compared to the Measured Composition of the Grid Plates.

Element	Weight %	
	6061 spec.[(a)]	Measured
Si	0.40 – 0.8	0.72
Fe	0.7 max	0.62
Cu	0.15 – 0.40	0.31
Mn	0.15 max	0.09
Mg	0.8 – 1.2	1.04
Cr	0.04 – 0.35	0.20
Zn	0.25 max	0.12
Ti	0.15 max	0.02
V	–	0.01
Zr	–	0.00
Other Elements Each	0.05 max	–
Other Elements Total	0.15 max	0.06
Al	Remainder	Remainder

(a) From ASTM B209-10

1.3.4 Aluminum Guide Plate – The composition of the aluminum tooling plate used in the guide plate was also measured. That composition is given Table 17. The density of the guide plate material was not measured.

Table 17. Chemical Composition of the Aluminum Tooling Plate used in the Guide Plate.

Element	Weight %
Si	0.50
Fe	0.60
Cu	1.2
Mn	0.75
Mg	1.6
Cr	0.06
Zn	3.00
Other Elements Total	0.06
Al	Remainder

1.3.5 Experiment Rods – The titanium experiment rods were fabricated from 0.250 in round Grade 2 rod stock. The Manufacturer's Mechanical Mill Certificate specified various measured properties of the material including the elemental composition. Table 18 lists the composition requirements for Grade 2 material from ASTM B348-13, "Standard Specification for Titanium and Titanium Alloy Bars and Billets," and the measured values for the supplied material.

Table 18. ASTM B348-13 Composition Limits for Grade 2 Titanium and the Measured Composition of the Titanium in the Rod Stock Used for the Titanium Experiment Rods.

Element	ASTM B348-13 Grade 2 (% by mass)	Manufacturer's Mechanical Mill Certificate Composition (% by mass)
C	0.08 max	0.01 – 0.01
O	0.25 max	0.09 – 0.11
N	0.03 max	0.02 – 0.02
H	0.015 max	0.004 – 0.004
Fe	0.30 max	0.19 – 0.22
Other (each)	0.1 max	< 0.1
Other (total)	0.4 max	< 0.4
Ti	Remainder	Remainder

The aluminum experiment rods were fabricated from 0.250 in round 6061-T651 rod stock. The Certified Inspection Report that was supplied by the fabricator specified that the alloy was 6061. A chemical analysis of a sample of the material was ordered by the fabricator. The composition requirements for alloy 6061 from ASTM B211-12, "Standard Specification for Aluminum and Aluminum-Alloy Rolled or Cold Finished Bar, Rod, and Wire," are shown in Table 19. Also shown in the table are the results of the composition analysis.

Table 19. ASTM B211-12 Composition Limits for 6061 Aluminum and the Measured Composition of the Aluminum in the Rod Stock Used for the Aluminum Experiment Rods.

Element	ASTM B211-12 Alloy 6061 (% by mass)	Chemical Analysis (% by mass)
Si	0.40 – 0.8	0.58
Fe	0.7 max	0.19
Cu	0.15 – 0.40	0.16
Mn	0.15 max	0.05
Mg	0.8 – 1.2	0.81
Cr	0.04 – 0.35	0.05
Zn	0.25 max	<0.01
Ti	0.15 max	0.02
Ga	–	0.01
V	–	0.01
Other (each)	0.05 max	–
Other (total)	0.15 max	–
Al	Remainder	Remainder

1.3.6 Water – The water moderator in the assembly was taken from the de-ionized water supply in the facility. Samples of the moderator were taken during the experiment and archived. No chemical analysis was done on the water samples.

The facility water is taken from the Albuquerque municipal water supply. The deionizer is fed from that source. The Albuquerque municipal water system is divided into nineteen distribution regions. The water quality is monitored in each distribution region. Table 20 lists the impurities detected in the water for the year 2014. Both the city-wide average and the maximum level across the system are listed in the table. Table 21 lists the elements for which testing was done but that were not detected in the system along with the detection limit for those elements.

Table 20. Impurities Measured in the Albuquerque Municipal Water Supply in the Year 2014.

Element	Units[a]	City-Wide Average[b]	Maximum Detected in the Water System[b]
As	PPB	3	8
Ba	PPM	ND[c]	0.2
Cr	PPB	ND[c]	8
U	PPB	3	6
Fe	PPM	0.022	0.941
Mn	PPM	0.004	0.123
Ca	PPM	48	68
Cl	PPM	31	47
Mg	PPM	5.8	7.3
K	PPM	3.9	8
Na	PPM	32	70

(a) Parts Per Million (PPM) or Parts Per Billion (PPB) by mass.
(b) Data obtained from http://www.abcwua.org/Water_Quality_by_Distribution_Zone.aspx on June 5, 2015.
(c) ND: Not Detected

Table 21. Impurities Tested but not Detected in the Albuquerque Municipal Water Supply in the Year 2014.

Element	Units[a]	Detection Limit[b]
Sb	PPB	1
Be	PPB	1
Cd	PPB	1
Hg	PPB	0.2
Se	PPB	5
Tl	PPB	1

(a) Parts Per Billion (PPB) by mass.
(b) Data obtained from http://www.abcwua.org/Substances_Not_Found.aspx on June 5, 2015.

1.3.7 Stainless Steel – The source capsule was fabricated from 316L stainless steel. The specific composition of the material used in the source was not measured. The specification for the composition 316L stainless steel is listed in Table 22. The density of the stainless steel was not measured.

Table 22. Composition of 316L Stainless Steel.

Element	Weight % [(a)]
C	0.030 max
Mn	2.00 max
P	0.045 max
S	0.030 max
Si	1.00 max
Cr	16.0 – 18.0
Ni	10.0 – 14.0
Mo	2.00 – 3.00
Fe	Remainder

(a) From ASTM A276-10

The composition of the corrosion-resistant steel springs in the fuel rods is listed in the manufacturer's catalog as "stainless steel." No further composition data were available on the springs.

1.3.8 Polyethylene – The fuel rods included polyethylene in the part of the rod that was in the reflector. The annuli surrounding the radiation detector dry wells were also polyethylene. Polyethylene has the basic molecular formula CH_2.

1.3.9 Boron Carbide – The boron carbide powder used to fill the absorber sections of the control and safety elements was mixed from two lots of powder mixed equally before loading into the absorber sections. The composition data for the two lots of boron carbide are given in Table 23.

Table 23. Composition and Particle Size Data for the Boron Carbide.

Quantity		Lot 1	Lot 2
Boron Mass Fraction (%) [(a)]		77.0	77.0
Carbon Mass Fraction (%)		21.7	21.6
B_2O_3 Mass Fraction (%)		0.1	0.1
Silicon Mass Fraction (%)		<0.010	<0.010
Iron Mass Fraction (%)		0.10	0.10
Nitrogen Mass Fraction (%)		0.04	0.07
^{10}B Isotopic Abundance (atom %)		20.02	20.01
Particle Size Distribution (micron) [(b)]	3%	11.23	158.2
	50%	7.251	80.13
	94%	3.140	40.47

(a) The mass fractions do not sum to 100%. The remainder is unknown and is treated as void.
(b) The particle size above which the specified fraction of the material falls.

1.4 Temperature Data

The water temperature in the experiment was measured at three different heights in the reflector of the assembly with thermocouples. The average measured temperature for each case is shown in Table 11.

1.5 Supplemental Experimental Measurements

Additional experimental measurements were not performed.

2.0 EVALUATION OF EXPERIMENTAL DATA

This section provides interpretation of some of the experiment material data, translates the experiment projections to delayed critical into k_{eff} for the benchmark experiment configurations, details adjustments to the k_{eff} data to a common temperature of 25ºC, and provides an analysis of the uncertainties in the experimental configurations. The uncertainties associated with all these factors are small.

2.1 Material Data

2.1.1 Fuel Rod UO_2 Mass – The UO_2 fuel pellet mass in each fuel rod (2199 total) and control/safety element fueled section (23 total) was measured. Records were kept of these data as well as the location and identity of every rod in all configurations. As a result, the fuel mass in each configuration was available. The average fuel mass in the entire population of 2222 fuel rods and control/safety element fueled sections was 108.7165 g with a standard deviation of 0.32 g. The average UO_2 mass for the fuel rods in each configuration is listed in Table 24.

Table 24. Average UO_2 Mass in Each Configuration.

Case	Number of Fuel Rods and Control/Safety Rod Sections	Average UO_2 Mass (g)	
		Value	Standard Deviation
1	1457	108.7706	0.30
2	1473	108.7677	0.30
3	1492	108.7634	0.30
4	1521	108.7580	0.30
5	1560	108.7562	0.30
6	1609	108.7469	0.30
7	1585	108.7531	0.30
8	1573	108.7557	0.30
9	1557	108.7540	0.30
10	1453	108.7697	0.30
11	1448	108.7695	0.30
12	1445	108.7694	0.30
13	1444	108.7684	0.30
14	1441	108.7678	0.30
15	1429	108.7700	0.30
16	1429	108.7685	0.30
17	1425	108.7670	0.30
18	1037	108.7712	0.31
19	1097	108.7713	0.31
20	1153	108.7696	0.31
21	1213	108.7678	0.30
22	1285	108.7643	0.30
23	1377	108.7494	0.30
24	1485	108.7399	0.30

2.1.2 Fuel Impurities – The fuel pellets were fresh UO_2 with measured enrichment and impurity content for ten randomly-chosen fuel pellets. Twelve impurity elements were measured above the detection limit in at least five of the measurements. The measured impurity content and standard deviation of the ten measurements is shown in Table 25. The standard deviations shown for three of the listed elements are larger than the average mass fraction for three impurities – Ag, B, and Cd. This is because each of these species had one measurement that was much higher than the others. Also shown in the table are the thermal absorption cross section for each impurity species and the fraction of the impurity thermal macroscopic absorption cross section contributed by each species. The uncertainty in the impurity macroscopic cross section is dominated by the contribution from boron which is in turn dominated by the fact that one of the measurements is an outlier compared to the rest of the measurements.

Table 25. Fuel Impurity Analysis.

Species	Mass Fraction[(a)]	Standard Deviation[(b)]	Thermal Absorption Cross Section[(c)] (barns)	Fractional Macroscopic Absorption Cross Section[(d)]	Fractional Contribution to the Macroscopic Absorption Cross Section Uncertainty[(e)]
Ag	1.61E-07	2.19E-07	63	0.0022	0.0037
B	4.17E-07	4.73E-07	760	0.6744	0.9789
Cd	2.25E-07	3.98E-07	2520	0.1160	0.1928
Co	2.06E-07	5.67E-08	37.2	0.0030	0.0011
Cr	2.11E-05	1.06E-05	3.1	0.0289	0.0190
Cu	2.19E-06	1.59E-06	3.8	0.0030	0.0029
Fe	9.31E-05	4.31E-05	2.56	0.0982	0.0594
Mn	2.52E-06	1.04E-06	13.3	0.0140	0.0076
Mo	1.93E-06	1.85E-06	2.5	0.0012	0.0014
Ni	3.32E-05	1.13E-05	4.5	0.0586	0.0261
V	1.22E-07	2.33E-08	5.0	0.0003	6.9E-05
W	1.07E-07	1.14E-08	18.2	0.0002	3.4E-05
Sum	1.55E-04[(f)]	–	–	1.0000[(f)]	1.0000[(g)]

(a) The average of the measured impurity mass fractions that were above the detection limit.
(b) The standard deviation of the measured impurity mass fractions that were above the detection limit.
(c) Thermal neutron (2200 m/s) absorption cross section from E. M. Baum, et al., Nuclides and Isotopes Sixteenth Edition, KAPL, Inc., 2002.
(d) The impurity macroscopic absorption cross section is the sum of the [product of the species atom density and the species absorption cross section] having a value of 0.00024 cm^{-1}.
(e) The uncertainty in the impurity macroscopic absorption cross section is the sum in quadrature of the [product of the uncertainty in the species atom density and the species absorption cross section] and has a value of 0.00021 cm^{-1}.
(f) Arithmetic sum.
(g) Sum in quadrature.

2.1.3 Fuel Rod Cladding – The clad tubes and end caps for the fuel rods were fabricated from 3003 aluminum. The elemental composition of the 3003 aluminum was not measured. For the work documented here, the composition of the tubes and end caps is assumed to be at the mid-range value where an elemental content is specified as a range and as half of the maximum value where one is given for an element. The composition specification for 3003 aluminum and the composition chosen here are shown in Table 26. The density of the 3003 aluminum was taken as 2.73 g/cm^3.[a]

[a] From http://matweb.com/search/DataSheet.aspx?MatGUID=fd4a40f87d3f4912925e5e6eab1fbc40 accessed on May 29, 2012. From http://matweb.com search for key word "3003" and choose the "Aluminum 3003-O" option.

Table 26. Elemental Composition Specification for Aluminum Alloy 3003 and the Composition Used for the Fuel Rod Cladding in the Analyses.

Element	Specification Composition (Weight %) [(a)]	Assumed Composition (Weight %)
Si	0.6 max	0.3
Fe	0.7 max	0.35
Cu	0.05 – 0.20	0.125
Mn	1.0 – 1.5	1.25
Zn	0.10 max	0.05
Other Elements Each	0.05 max	0
Other Elements Total	0.15 max	0
Al	Remainder	97.925

(a) From ASTM B210-04

2.1.4 Source Capsule Composition – The material in the source capsule was specified as 316L stainless steel. The elemental composition was not measured. The composition for the 316L stainless steel is assumed to be at the mid-range value where an elemental content is specified as a range and as half of the maximum value where one is given for an element. The composition specification for 316L stainless steel and the derived composition used here are shown in Table 27. The density of the 316L stainless steel was taken as 8.0 g/cm^3.[a]

Table 27. Elemental Composition Specification for 316L Stainless Steel and the Composition Used for the Source Capsule in the Analyses.

Element	Specification Composition (Weight %) [(a)]	Assumed Composition (Weight %)
C	0.030 max	0.015
Mn	2.00 max	1.00
P	0.045 max	0.0225
S	0.030 max	0.015
Si	1.00 max	0.50
Cr	16.0 – 18.0	17.0
Ni	10.0 – 14.0	12.0
Mo	2.00 – 3.00	2.50
Fe	Remainder	66.9475

(a) From ASTM A276-10

2.1.5 Fuel Rod Spring Composition – The composition of the springs in the fuel rods and control/safety rod fueled sections was specified in the manufacturer's catalog as stainless steel. The composition of 304 stainless steel, treated as described above, will be used. Table 28 lists the composition specification for 304 stainless steel spring wire with the derived composition. The springs, as manufactured, had an specified inner

[a] From http://matweb.com/search/DataSheet.aspx?MatGUID=a2d0107bf958442e9f8db6dc9933fe31 accessed on May 29, 2012. From http://matweb.com search for key word "316L" and choose the "AISI Type 316L Stainless Steel, annealed bar" option.

diameter of 0.138 in (0.35052 cm) and outer diameter of 0.180 in (0.4572 cm). Where they were included, the springs were modeled as annuli of inner diameter 0.35052 cm and outer diameter 0.4572 cm. The average spring mass was measured as 0.1923 ± 0.0095 g. As used in the fuel rods, the springs are compressed to a length of 1.75076 cm. The density of the springs in each model was obtained from the dimensions of the annulus and the average spring mass.

Table 28. Elemental Composition Specification for 304 Stainless Steel Spring Wire and the Composition Used for the Fuel Rod Springs in the Analyses.

Element	Specification Composition (Weight %) [(a)]	Assumed Composition (Weight %)
C	0.08 max	0.04
Mn	2.00 max	1.00
P	0.045 max	0.0225
S	0.030 max	0.015
Si	1.00 max	0.50
Cr	18.0 – 20.0	19.0
Ni	8.0 – 10.5	9.25
N	0.10 max	0.05
Fe	Remainder	70.1225

(a) From ASTM A313-10. Note that the composition differs slightly from the composition for bars and shapes given in ASTM A276-10.

2.1.6 Boron Carbide Composition – The boron carbide used in the absorber sections of the control and safety elements was mixed from two batches of boron carbide powder with slightly different compositions. The two batches were mixed equally so the appropriate composition to use is the average of the values for the two batches. The specifications for the two batches included mass fractions for boron and for B_2O_3. It is assumed that the boron included in the B_2O_3 is included in the given boron mass fraction leaving the oxygen at a mass fraction of 0.069% rounded to two significant figures. Because a maximum value is specified for silicon, half that value is assumed to be present. The elemental mass fractions in the boron carbide powder are shown in Table 29. The ^{10}B isotopic atom fraction in the boron is 20.015%.

Table 29. Composition Data for the Boron Carbide Powder.

Quantity	Value
Boron Mass Fraction (%)	77.0
Carbon Mass Fraction (%)	21.65
Oxygen Mass Fraction (%)	0.069
Silicon Mass Fraction (%)	0.005
Iron Mass Fraction (%)	0.10
Nitrogen Mass Fraction (%)	0.055
Sum (%) [(a)]	98.879

(a) The mass fractions do not sum to 100%. The remainder (1.121%) is unknown and is treated as void.

2.1.7 Experiment Rod Composition – The titanium experiment rods were fabricated from Grade 2 titanium rod stock. The elemental composition of the titanium was reported in the Manufacturer's Mechanical Mill Certificate supplied with the fabricated rods. The content for each measured element was specified as maximum and minimum values. The values were identical for three elements (C, N, and H) and differed for two (O and Fe). Where the maximum and minimum values differed, the value retained was the average of the two values. The measured composition values for titanium experiment rods and the composition values chosen here are shown in Table 30. The titanium content was set at 100% less the sum of the chosen values for each other element.

Table 30. Measured Composition of the Titanium Used in the Experiment Rods and the Composition Values Chosen.

Element	Manufacturer's Mechanical Mill Certificate Composition (% by mass)	Chosen Composition (% by mass)
C	0.01 – 0.01	0.01
O	0.09 – 0.11	0.10
N	0.02 – 0.02	0.02
H	0.004 – 0.004	0.004
Fe	0.19 – 0.22	0.205
Other (each)	< 0.1	0
Other (total)	< 0.4	0
Ti	Remainder	99.661

The aluminum experiment rods were fabricated from aluminum alloy 6061 rod stock. The elemental composition of the aluminum was reported in a laboratory analysis of a sample of the rod stock material. The measured values are shown in Table 31. In one case (Zn), the content was reported as less than a value. That element was assumed to be absent from the alloy. In the remaining cases, the reported value was retained. The aluminum content was set at 100% less the sum of the chosen values for each other element.

Table 31. Measured Composition of the Aluminum Used in the Experiment Rods and the Composition Values Chosen.

Element	Chemical Analysis (% by mass)	Composition Chosen (% by mass)
Si	0.58	0.58
Fe	0.19	0.19
Cu	0.16	0.16
Mn	0.05	0.05
Mg	0.81	0.81
Cr	0.05	0.05
Zn	<0.01	0.00
Ti	0.02	0.02
Ga	0.01	0.01
V	0.01	0.01
Al	Remainder	98.12

2.2 Geometric Data

2.2.1 Fuel Rod Pellet Stack Height – The fuel pellet stack height in each fuel rod and control/safety element fueled section was also measured during fabrication. The average fuel pellet stack length for the entire population of 2222 fuel rods and control/safety element fueled sections was 48.7789 cm with a standard deviation of 0.125 cm. The average fuel pellet stack height for the specific fuel rods included in the benchmark experiment configurations is listed in Table 32.

Table 32. Average Fuel Pellet Stack Height in Each Configuration.

Case	Number of Fuel Rods and Control/Safety Rod Sections	Average Fuel Pellet Stack Height (cm)	
		Value	Standard Deviation
1	1457	48.7754	0.115
2	1473	48.7748	0.115
3	1492	48.7753	0.115
4	1521	48.7781	0.115
5	1560	48.7763	0.116
6	1609	48.7787	0.116
7	1585	48.7788	0.115
8	1573	48.7777	0.115
9	1557	48.7763	0.116
10	1453	48.7764	0.116
11	1448	48.7765	0.116
12	1445	48.7763	0.116
13	1444	48.7761	0.116
14	1441	48.7768	0.116
15	1429	48.7761	0.116
16	1429	48.7763	0.116
17	1425	48.7778	0.119
18	1037	48.7767	0.119
19	1097	48.7768	0.118
20	1153	48.7773	0.116
21	1213	48.7746	0.116
22	1285	48.7766	0.116
23	1377	48.7766	0.115
24	1485	48.7754	0.115

2.2.2 Fuel Rod Diameter – The outer diameter of each fuel rod was measured. The average for the population of 2199 fuel rods was 0.634948 cm with a standard deviation of 0.000218 cm. The average outer diameter of the fuel rods for the specific fuel rods included in the benchmark experiment configurations is listed in Table 33.

Table 33. Average Fuel Rod Outer Diameter in Each Configuration.

Case	Number of Fuel Rods	Average Fuel Rod Outer Diameter (cm)	
		Value	Standard Deviation
1	1445	0.634983	0.000215
2	1461	0.634980	0.000216
3	1480	0.634978	0.000216
4	1509	0.634977	0.000214
5	1548	0.634975	0.000215
6	1597	0.634972	0.000215
7	1573	0.634972	0.000215
8	1561	0.634971	0.000216
9	1545	0.634973	0.000216
10	1441	0.634982	0.000216
11	1436	0.634982	0.000216
12	1433	0.634982	0.000216
13	1432	0.634983	0.000215
14	1429	0.634982	0.000215
15	1417	0.634981	0.000216
16	1417	0.634980	0.000216
17	1413	0.634981	0.000216
18	1025	0.634995	0.000213
19	1085	0.634987	0.000215
20	1141	0.634985	0.000215
21	1201	0.634982	0.000215
22	1273	0.634979	0.000216
23	1377	0.634972	0.000215
24	1473	0.634966	0.000214

2.2.3 Fuel Rod Cladding Inner Diameter – The mass of the assembled clad tube and lower end cap was measured for 100 samples during the fabrication of the fuel rods. The average mass was 13.824 g with a standard deviation of 0.027 g. The volume of the lower end cap was calculated from the dimensions given in the design drawings as 0.354 cm^3. Using the tolerances given on the drawing, the uncertainty in the volume is 0.010 cm^3. Using a density for 3003 aluminum of 2.73 g/cm^3, the calculated mass of the lower end cap is 0.967 g with a one-standard-deviation uncertainty based on drawing tolerances of 0.027 g. The mass of the 29.75 in (75.565 cm) long clad tube is then 12.857 g with an uncertainty of 0.027 g. The average measured outside diameter of the fuel rods is 0.249980 in (0.634948 cm as rounded from the original data) with standard deviation for 2194 measurements of 0.000086 in (0.000218 cm) and an overall uncertainty of 0.000023 in (0.000058 cm) including systematic uncertainties. From these data and using a density of 2.73 g/cm^3, an inner diameter of 0.569038 cm (0.224031 in) is obtained with an uncertainty of 0.000065 in (0.000164 cm).

2.2.4 Polyethylene Density – The average mass of the polyethylene spacers in the 2199 fuel rods is 4.454 g. The polyethylene spacer is designed as a cylinder 0.207 in (0.52578 cm) diameter and 8.38 in (21.2852) cm long. This gives an average density of the polyethylene in the spacer of 0.96377 g/cm^3.

The average mass of the polyethylene annuli on the radiation detector dry wells is 2017.28 g. The annuli are 11.82 in (30.0228 cm) tall and have inner diameters of 2.603 in (6.61162 cm) and outer diameters of 4.535 in (11.5189 cm). The average mass and dimensions of the annuli give a polyethylene density of about 0.9612 g/cm^3. Because this density is nearly the same as the density obtained for the polyethylene spacers in the fuel rods, the same density will be used for both.

2.2.5 Boron Carbide Powder Density – The average mass of boron carbide powder in the 23 absorber sections that were fabricated is 26.37 g. With an inner diameter of the cladding of 0.569038 cm (0.224031 in) and a height for the absorber of 28.238 in (71.72452 cm), the average density of the boron carbide power is 1.4457 g/cm^3 as loaded.

2.2.6 Experiment Rod Dimensions and Density – The design drawing for the experiment rods shows the designed rod length to be 31.28 ± 0.020 in (79.4512 ± 0.0508 cm) and the diameter to be 0.250 ± 0.005 in (0.635 ± 0.0127 cm). The top and bottom edges of the rods were broken by a 45° chamfer. The height of the bottom chamfer was 0.040 ± 0.005 in (0.1016 ± 0.0127 cm) and of the top chamfer was 0.025 ± 0.005 in (0.0635 ± 0.0127 cm). Thus, the experiment rods consist of a right cylindrical volume 31.215 in tall joined at the bottom to a 45° right conic frustum 0.040 in long and at the top to a 45° right conic frustum 0.025 in long.

The volume of a 45° right conic frustum V_f with larger base radius R and height H is given by

$$V_f = \frac{\pi H}{3}\left[R^2 + R(R-H) + (R-H)^2\right]$$

while the volume of a right circular cylinder V_c with radius R and length L is given by

$$V_c = \pi R^2 L \ .$$

Using these formulas and the nominal as-designed dimensions of the experiment rods – 79.4512 cm overall length, 0.3175 cm radius, 0.1016 cm lower 45° chamfer, and 0.0635 cm upper 45° chamfer – the rounded nominal volume of an experiment rod is 25.14862 cm^3.

For a given collection of experiment rods, the volume-weighted average radius of the rods in the collection can be obtained by calculating the volume of each rod in the collection using the measured diameter and length of each rod and the as-designed values for the frusta dimensions; summing the volumes of the rods in the collection, dividing the sum by the number of rods in the collection to obtain the average rod volume, and finding the radius that yields the average volume using the appropriate measured and as-designed dimensions. Table 34 lists volume-weighted average values of the radius of the rods in the collection of experiment rods used in the experiments. Also listed is the sum of the measured masses of the experiment rods in each collection. The average material density for each set of experiment rods can be obtained from the quotient of the sum of the measured masses of the rods divided by the sum of the volumes of the rods in each collection. These average densities are also listed in the table. Table 35 lists the radius and density data for the experiment rods included in each case.

Table 34. Volume-Weighted Average Radii, Total Masses, and Average Densities for the Experiment Rods in Several Serial Number Ranges.

Rod Number Range	Titanium Rods			Aluminum Rods		
	Average Radius (cm)	Total Mass (g)	Average Density (g/cm^3)	Average Radius (cm)	Total Mass (g)	Average Density (g/cm^3)
1 – 4	0.318206	455.7367	4.51000	0.318522	273.2235	2.69851
1 – 9	0.318353	1026.0629	4.50873	0.319022	616.6223	2.69827
1 – 16	0.318398	1824.1419	4.50755	0.319225	1097.6286	2.69824
1 – 25	0.318506	2852.6906	4.50838	0.319308	1715.7756	2.69802
1 – 36	0.318479	4107.7287	4.50900	0.319368	2471.6024	2.69802
5 – 36	0.318513	3651.9920	4.50888	0.319474	2198.3789	2.69796
17 – 36	0.318544	2283.5868	4.51016	0.319483	1373.9738	2.69785
1 – 4, 11-15	0.318310	1025.6332	4.50808	–	–	–
1 – 16, 27 – 35	0.318373	2850.2955	4.50839	–	–	–
5 – 10, 16 – 36	–	–	–	0.319475	1854.8823	2.69797
17 – 26, 36	–	–	–	0.319442	755.5391	2.69797

Table 35. Average Radius and Density for the Experiment Rods in Each Case.

Case	Titanium Experiment Rods			Aluminum Experiment Rods		
	Serial Numbers	Average Radius (cm)	Average Density (g/cm^2)	Serial Numbers	Average Radius (cm)	Average Density (g/cm^2)
1	–	–	–	–	–	–
2	1 – 4	0.318206	4.51000	–	–	–
3	1 – 9	0.318353	4.50873	–	–	–
4	1 – 16	0.318398	4.50755	–	–	–
5	1 – 25	0.318506	4.50838	–	–	–
6	1 – 36	0.318479	4.50900	–	–	–
7	1 – 36	0.318479	4.50900	–	–	–
8	1 – 36	0.318479	4.50900	–	–	–
9	1 – 36	0.318479	4.50900	–	–	–
10	–	–	–	1 – 4	0.318522	2.69851
11	–	–	–	1 – 9	0.319022	2.69827
12	–	–	–	1 – 16	0.319225	2.69824
13	–	–	–	1 – 25	0.319308	2.69802
14	–	–	–	1 – 36	0.319368	2.69802
15	–	–	–	1 – 36	0.319368	2.69802
16	–	–	–	1 – 36	0.319368	2.69802
17	–	–	–	1 – 36	0.319368	2.69802
18	–	–	–	–	–	–
19	–	–	–	1 – 36	0.319368	2.69802
20	1 – 4	0.318206	4.51000	5 – 36	0.319474	2.69796
21	1 – 4, 11-15	0.318310	4.50808	5 – 10, 16 – 36	0.319475	2.69797
22	1 – 16	0.318398	4.50755	17 – 36	0.319483	2.69785
23	1 – 16, 27 – 35	0.318373	4.50839	17 – 26, 36	0.319442	2.69797
24	1 – 36	0.318479	4.50900	–	–	–

2.3 Derivation of the Experimental k_{eff}

The approach-to-critical experiments reported here were done with the number of fuel rods in the critical assembly as the approach variable. Once the critical configuration had been measured, the high-multiplication part of the approach-to-critical was repeated using closely-spaced fuel arrays. For square pitched arrays, symmetrical configurations occur at four or eight fuel rod intervals. During the experiments, measurements were made with arrays that were either these symmetrical configurations or fell at the midpoint of an eight-rod interval between symmetrical configurations. Figure 38 shows an inverse multiplication plot for Case 1 as represented by the inverse detector count rates. A projection from the inverse count rate pairs to zero inverse count rate gives the estimated critical array size for each pair. Note that in this case the last measurement was made at the midpoint between two symmetrical configurations.

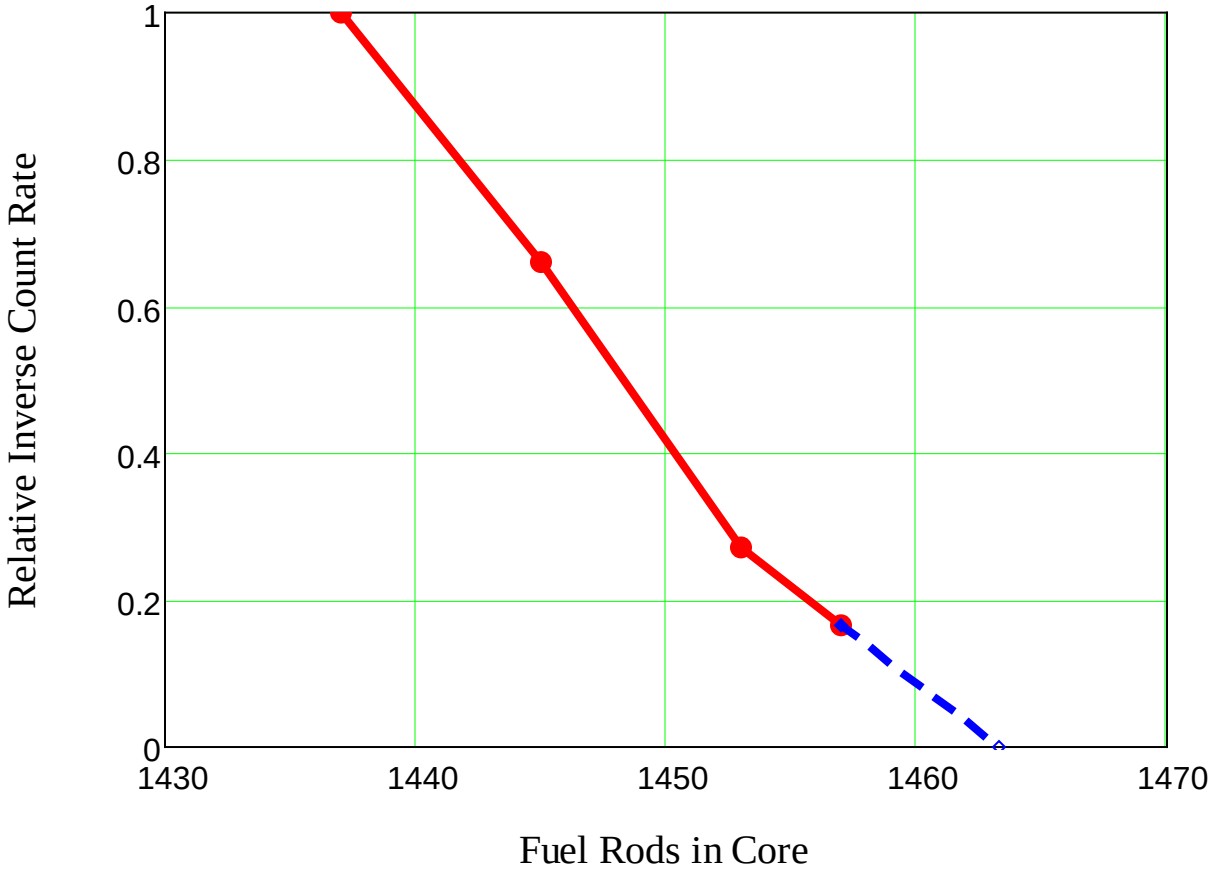

Figure 38. Measured Relative Inverse Count Rate for Case 1.

Inverse multiplication measurements were made on a series of roughly cylindrical pure-water-moderated 7uPCX cores as a function of the fuel loading of the core. The arrays are differentiated by the number and arrangement of experiment rods included in the array. Measurements were made for symmetrical fuel arrays as described above. For each pair of symmetrical fuel arrays, a projection of the measured relative inverse multiplication values was made to zero inverse multiplication or infinite multiplication, the equivalent of the delayed critical condition. From the projection, the number of fuel rods necessary to reach delayed critical could be determined under the assumption that all the remaining fuel rods had identical reactivity worth to the fuel rods in the last measured increment.

In each core configuration, the measured arrays were analyzed using SCALE 6.1.3 with multigroup ENDF/B-VII.0 cross sections and MCNP6.1 with continuous-energy ENDF/B-VII.1 cross sections. The calculated incremental reactivity worth $\Delta\rho$ of each fuel rod in a symmetrical fuel increment (described above) of ΔN rods was determined from

$$\Delta\rho = \frac{k_1 - k_0}{k_1 k_0 \Delta N}$$

where k_1 is the calculated k_{eff} for the system with N_1 fuel rods and k_0 is the calculated k_{eff} for the system with N_0 fuel rods with

$$\Delta N = N_1 - N_0 \ .$$

The values of the incremental fuel rod reactivity worth used here were derived from the variance-weighted average of the values of the incremental fuel rod reactivity worth obtained for each code/cross-section combination described above. Figure 39 shows the calculated incremental fuel rod reactivity worth in several fuel increments for Case 1. Using this incremental reactivity worth and the difference between the number of fuel rods in the array and the number of rods projected at delayed critical, the k_{eff} for each array could be determined.

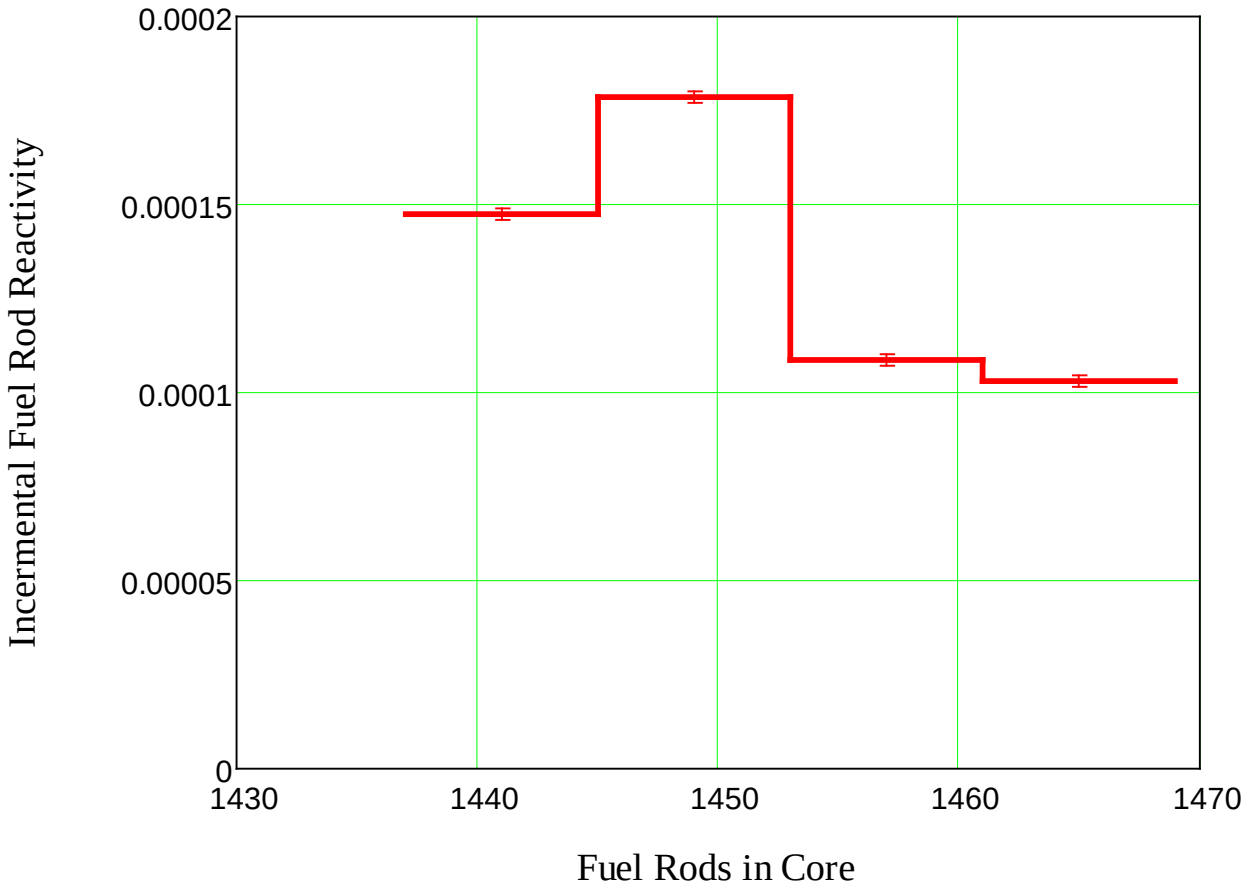

Figure 39. Calculated Fuel Rod Worth Near Delayed Critical for Case 1.

For example, consider that the projection between the inverse multiplication values at 1453 and 1457 rods in Figure 38 terminates at a value on the axis defined here as N_p. Note that, because the reactivity worth of the fuel rods varies by interval, the projected critical loading based on the inverse multiplication data at 1453 and 1457 rods, N_p, does not necessarily yield an array that is exactly at delayed critical since N_p falls outside the given interval and the fuel rods in the interval from 1461 to N_p have a different reactivity worth. The incremental fuel rod worth in the interval, defined here as $\Delta\rho$ (about 0.00011 for rods in the increment between 1453 and 1457), is obtained from Figure 39. The reactivity difference ρ_{1457} between the array with 1457 rods and the projected critical array at N_p is given by

$$\rho_{1457} = (1457 - N_p)\Delta\rho \ .$$

Knowing that the k_{eff} for an array with N_p rods is 1, the k_{eff} for the array with 1457 fuel rods, k_{1457}, is obtained by inverting the definition of the reactivity as

$$k_{1457} = \frac{1}{(1-\rho_{1457})} = \frac{1}{1-(1457 - N_p)\Delta\rho} \ .$$

The k_{eff} for the array with 1453 rods is obtained similarly.

Table 36 lists the results of the approach-to-critical experiments for the symmetrical benchmark experiment arrays evaluated here. For the square-pitched arrays used, symmetrical arrays are separated by sets of four incremental fuel rods if the incremental rods are on the principal axes or the diagonals of the array. Otherwise, symmetrical arrays are separated by sets of eight incremental fuel rods. Included in the table are the calculated incremental fuel rod reactivity worths for the fuel rods in the appropriate intervals. These data were used as described above to derive the k_{eff} for the benchmark experiment arrays. Many of the larger measured arrays fell at the midpoint between symmetrical arrays. The derived k_{eff} values for the measured arrays are shown in Table 37.

Table 36. Data Used in the Derivation of the Array k_{eff} for each Case.

Case	Fuel Rods in Larger Symmetrical Array[(a)]	Fuel Rods in Smaller Symmetrical Array[(a)]	Projected Fuel Rods at Delayed Critical[(b)]		Calculated Incremental Fuel Rod Reactivity	Uncertainty
			Value	Unc.		
1	1461	1453	1462.28	0.02	0.0001134	0.0000021
2	1473	1465	1477.19	0.01	0.0001376	0.0000019
3	1492	1484	1497.63	0.01	0.0001184	0.0000020
4	1525	1517	1525.52	0.01	0.0001178	0.0000016
5	1564	1556	1564.88	0.01	0.0001206	0.0000015
6	1613	1605	1612.23	0.01	0.0001109	0.0000016
7	1589	1581	1589.49	0.01	0.0001193	0.0000018
8	1573	1569	1575.88	0.01	0.0001528	0.0000032
9	1561	1553	1561.46	0.01	0.0001165	0.0000018
10	1457	1449	1461.22	0.03	0.0001060	0.0000021
11	1452	1444	1456.47	0.03	0.0001053	0.0000021
12	1445	1437	1451.74	0.02	0.0001107	0.0000021
13	1444	1436	1449.78	0.02	0.0001020	0.0000021
14	1441	1433	1445.49	0.01	0.0001422	0.0000021
15	1433	1425	1433.14	0.01	0.0000993	0.0000021
16	1433	1425	1430.85	0.01	0.0001041	0.0000021
17	1425	1417	1430.15	0.01	0.0001088	0.0000021
18	1037	1029	1039.36	0.01	0.0001384	0.0000018
19	1101	1093	1101.82	0.01	0.0001290	0.0000018
20	1157	1149	1155.94	0.01	0.0001447	0.0000022
21	1217	1209	1214.32	0.01	0.0001369	0.0000022
22	1289	1281	1290.13	0.01	0.0001062	0.0000018
23	1377	1369	1380.58	0.01	0.0001167	0.0000022
24	1485	1477	1488.69	0.01	0.0001059	0.0000018

(a) The number of incremental fuel rods between adjacent symmetrical fuel arrays is eight for all cases except Case 8 where the difference is four fuel rods. For Case 8 the incremental fuel rods are on the diagonal of the fuel array.

(b) The uncertainties listed are those attributed only to the stochastic nature of the radiation detection process

Table 37. k_{eff} Values Derived from the Projections to Delayed Critical.

Case	Larger Measured Array[a]			Smaller Measured Array		
	Fuel Rods	k_{eff}	Uncertainty[b]	Fuel Rods	k_{eff}	Uncertainty[b]
1	1457	0.99940	0.00010	1453	0.99895	0.00010
2	1473	0.99942	0.00012	1465	0.99833	0.00013
3	1492	0.99933	0.00011	1484	0.99839	0.00011
4	1521	0.99947	0.00011	1517	0.99900	0.00011
5	1560	0.99941	0.00011	1556	0.99893	0.00011
6	1609	0.99964	0.00010	1605	0.99920	0.00010
7	1585	0.99946	0.00011	1581	0.99899	0.00011
8	1573	0.99956	0.00014	1569	0.99895	0.00014
9	1557	0.99948	0.00011	1553	0.99902	0.00011
10	1453	0.99913	0.00010	1449	0.99871	0.00010
11	1448	0.99911	0.00010	1444	0.99869	0.00010
12	1445	0.99925	0.00010	1437	0.99837	0.00010
13	1444	0.99941	0.00009	1436	0.99860	0.00010
14	1441	0.99936	0.00013	1433	0.99823	0.00013
15	1429	0.99959	0.00009	1425	0.99919	0.00009
16	1429	0.99981	0.00009	1425	0.99939	0.00009
17	1425	0.99944	0.00010	1417	0.99857	0.00010
18	1037	0.99967	0.00012	1029	0.99857	0.00013
19	1097	0.99938	0.00012	1093	0.99886	0.00012
20	1153	0.99957	0.00013	1149	0.99900	0.00013
21	1213	0.99982	0.00012	1209	0.99927	0.00012
22	1285	0.99946	0.00010	1281	0.99903	0.00010
23	1377	0.99958	0.00011	1369	0.99865	0.00011
24	1485	0.99961	0.00010	1477	0.99876	0.00010

(a) Many of the larger measured arrays fell at the midpoint between the symmetrical arrays listed in Table 36. This occurred for the larger measured arrays in Cases 1, 4, 5, 6, 7, 9, 10, 11, 15, 16, 19, 20, 21, and 22.
(b) The uncertainties account for the stochastic nature of the radiation detection process, the uncertainty in the reproducibility of the projections to delayed critical, and the uncertainties in the calculation of the incremental fuel rod reactivity worth.

2.4 Uncertainty Analyses

A number of uncertainty analyses were done. The direct perturbation analyses in sections 2.4.1 through 2.4.8 were done with KENO V.a using the 238-group ENDF/B-VII.0 cross section set from SCALE 6.1.3. The sensitivity analysis done in Sections 2.4.9 through 2.4.17 were done using TSUNAMI-3D with 238-group ENDF/B-VII.0 cross sections from SCALE6.1.3. The temperature sensitivity analysis in Section 2.4.18 was done with MCNP6.1.1 using continuous-energy cross sections from ENDF/B-VII.1.

Where uncertainties are given below, the method of handling the uncertainties by type as defined in the *ICSBEP Guide to the Expression of Uncertainties* is followed. Where the uncertainty is given at the one-standard-deviation level, the uncertainty is used as-is. Where an uncertainty is given as a tolerance or a bounding value, it is assumed to specify an outer limit with a constant probability distribution between the limits. The value of the tolerance is divided by the square root of 3 to get the one-standard-deviation uncertainty in the nominal value. This treatment is used in the determination of the uncertainty of the fuel rod pitch and in the uncertainty of the composition of the fuel rod cladding.

In each of the following cases using direct perturbations, the sensitivity of the assembly to a given uncertainty was determined by analyzing arrays in which the parameter varied over a range. A least-squares fit of the k_{eff} data to a line was done. The stochastic uncertainties from the Monte Carlo calculations were propagated through the least-squares equations used in the fit. The sensitivity of the array to the parameter was the slope of the line. The uncertainty in the sensitivity was the uncertainty in the slope. The relative uncertainty in the sensitivity gives a measure of the statistical significance of the fit.

2.4.1 Fuel Rod Pitch – The uncertainty in the fuel rod pitch contributes to the uncertainty in the amount of water moderator in the core. This uncertainty is related to the uncertainty in the placement of the holes in the grid plates during fabrication, to the width of the nominal gap between the outside of the fuel rods and the inside of the grid plate holes, to the uncertainty in the diameter of the holes in the grid plates, to the uncertainty in the outside diameter of the fuel rods, and to the number of rows of fuel rods in the core. The fabrication tolerance in the placement of each hole is that it be within ±0.005 in (0.0127 cm) of its intended location relative to the center of the grid plate. The nominal gap between the outside of the fuel rods and the inside of the grid plate holes is 0.00631 in (0.0160 cm). The uncertainty in the diameter of the grid plate holes is one-sided (+0.005/–0.000 in). Assuming that the nominal value of hole diameter falls at the center of this range, the tolerance is then ±0.0025 in (0.00635 cm). The outer diameters of the fuel rods were measured. The uncertainty in the average value for the configuration with the fewest rods (Case 18 with 1037 total rods) is 0.0000026 in (0.000084 divided by the square root of 1037) added in quadrature to the systematic uncertainty in the diameter measurements of 0.000022 in resulting in a one-standard-deviation uncertainty of 0.000022 in (0.000056 cm). Multiplying this value by the square root of 3 to get 0.000038 in (0.000097 cm) maintains the level of significance associated with the tolerances. Summing these four values in quadrature yields

$$\sqrt{0.005^2 + 0.00631^2 + 0.0025^2 + 0.000038^2} = 0.00843 \text{ in (0.02141 cm).}$$

The tolerance in the fuel rod pitch is twice this value divided by [the diameter of the core divided by the fuel rod pitch]. Note that this last factor reduces to one less than the number of fuel rods on a chord across the core.

For Cases 1 through 17, 22, 23, and 24 there were 45 fuel rods on a chord across the core. In this case, the diameter of the core divided by the fuel rod pitch is 44. By the above method, the tolerance in the pitch is

(2 × 0.00843 in)/44 = 0.000383 in (0.000973 cm).

For Case 21, there were 43 fuel rods on a chord across the core. In this case, the diameter of the core divided by the fuel rod pitch is 42. The tolerance on the pitch is then

(2 × 0.00843 in)/42 = 0.000401 in (0.001020 cm).

For Cases 19 and 20, there were 41 fuel rods on a chord across the core. In this case, the diameter of the core divided by the fuel rod pitch is 40. The tolerance on the pitch is then

(2 × 0.00843 in)/40 = 0.000422 in (0.001071 cm).

For Case 18, there were 39 fuel rods on a chord across the core. In this case, the diameter of the core divided by the fuel rod pitch is 38. The tolerance on the pitch is then

(2 × 0.00843 in)/38 = 0.000444 in (0.001127 cm).

Dividing the above tolerances by the square root of three gives the one-standard-deviation value for the uncertainty in the fuel rod pitch. The values so obtained are 0.000221 in (0.000562 cm) for Cases 1 through 17, 22, 23, and 24; is 0.000232 (0.000589 cm) for Case 21; is 0.000243 in (0.000618 cm) for Cases 19 and 20; and is 0.000256 (0.000651 cm) for Case 18.

Arrays with fuel rod pitch up to 0.01 cm on either side of the nominal value in 0.005 cm increments were analyzed to obtain the effect of pitch on k_{eff}. The results were used in a least-squares linear fit to determine the sensitivity of the experiment to the fuel rod pitch. The sensitivity was combined with the pitch uncertainty to obtain the uncertainty in the benchmark experiment k_{eff}.

2.4.2 Clad Outer Diameter – The outer diameter of the fuel rod clad tubes was measured for the 2194 rods available for the experiments. The population average for the measurements was 0.249980 in (0.634948 cm as rounded from the original data) with a standard deviation of 0.000086 in (0.000218 cm). The uncertainty in the mean value is 0.0000026 in (0.0000065 cm), the standard deviation divided by the square root of 1085, the lowest number of fuel rods in any of the benchmark experiment configurations. Because the outside diameter was known for each fuel rod and the identity of each fuel rod in every configuration was known, the distribution of the fuel rod diameters does not contribute to the uncertainty in the experiments. The systematic uncertainty in the measurements was 0.000022 in (0.000056 cm). The resolution of the instruments used was 0.000001 in (0.00000254 cm) and the repeatability was 0.000005 in (0.0000127 cm). The random uncertainty in the diameter measurements was 0.000030 in (0.0000762 cm) and will be treated as a systematic uncertainty. The sum in quadrature of the systematic uncertainties (0.000022 in, 0.000001 in, 0.000005 in, and 0.000030 in) is 0.0000375 in (0.0000954 cm). Arrays with fuel rod clad diameters up to 0.00508 cm on either side of the nominal value were analyzed to determine the sensitivity of the experiments to the clad tube diameter. The mass of the clad tube was kept constant during these variations.

2.4.3 Clad Inner Diameter – The method of obtaining the inside diameter of the fuel clad tubes based on the tube outer diameter and the measured mass of the assembly of the clad tube and the lower end cap is described above. Using that method, the uncertainty in the inner diameter of the clad tube is 0.000065 in (0.000164 cm). Arrays with fuel rod clad inside diameters up to 0.04 cm on either side of the nominal value were analyzed. The outside diameter of the fuel rod clad tubes was held constant for these calculations.

2.4.4 Fuel Outer Diameter – The outer diameter of 123 randomly-selected fuel pellets was measured. The average diameter was 0.20694 in (0.52563 cm) with a standard deviation of 0.00019 in (0.00048 cm). The systematic uncertainties in the fuel pellet outer diameter measurements are 0.000001 in resolution, 0.000005 in repeatability, 0.000022 in absolute uncertainty, and 0.000030 in reproducibility. Considering the number of measurements and the systematic uncertainties in the measurements, the uncertainty in the average diameter is 0.000041 in (0.000105 cm). Arrays with fuel pellet diameters up to 0.004 in on either side of nominal were analyzed. The density of the fuel was modified in the analysis to keep the fuel mass in the fuel rods constant.

2.4.5 Upper Reflector Thickness – The depth of the water in the core tank is set by an overflow standpipe. A bounding value on the 1-σ uncertainty in the depth of the water in the core tank is estimated to be 0.5 cm. Arrays with water levels from 1.45 cm above to 3.55 cm below the nominal value were analyzed using MCNP5 with ENDF/B-VII.0 cross sections to determine the sensitivity of the experiments to the thickness of the upper reflector.

2.4.6 Fuel Rod UO_2 Mass – The UO_2 fuel mass in the driver fuel rods was measured giving a standard deviation for 2222 measurements of 0.322 g. Because the fuel mass was known for each fuel rod and the identity of each fuel rod in every configuration was known, the distribution of the fuel rod UO_2 mass does not contribute to the uncertainty in the experiments. The fuel mass measurements were made using an instrument with a repeatability of 0.01 g, linearity of 0.02 g, and readability of 0.01 g. The uncertainty in the fuel mass is the sum in quadrature of the systematic uncertainties in the mass measurements (0.01 g, 0.02 g, and 0.01 g)

and is 0.024 g. Arrays with the fuel rod UO_2 mass varying from 1 g below to 1 g above the nominal value were analyzed to determine the sensitivity of the experiments to this uncertainty. The variations were done by changing the fuel density while keeping the fuel dimensions constant.

2.4.7 Fuel Rod Pellet Stack Height – The fuel pellet stack height was measured during fabrication for all fuel rods to the nearest millimeter. The systematic uncertainty in this measurement is estimated to be 0.5 mm. The standard deviation for 2222 fuel columns was 0.125 cm. Because the pellet stack height was known for each fuel rod and the identity of each fuel rod in every configuration was known, the distribution of the fuel rod UO_2 column height does not contribute to the uncertainty in the experiments. The uncertainty in the average fuel pellet stack height is the estimated systematic uncertainty in the measurement or 0.05 cm. Arrays with fuel pellet stack heights 1 cm on either side of the nominal value were analyzed to determine the sensitivity of the experiments to the uncertainty in the pellet stack height. The mass of fuel in the fuel rods was held constant by varying the fuel density to compensate for pellet stack height changes.

2.4.8 Experiment Rod Outer Diameter – The outer diameter of every experiment rod was measured. The average outer diameter outer of the titanium experiment rods was 0.250771 in (0.636956 cm) with a standard deviation of 0.000581 in (0.001476 cm). Because every experiment rod was measured, the uncertainty in the average experiment outside diameter could be set to the measuring instrument uncertainty. However, for conservatism, the uncertainty was set at the standard deviation for each set of experiment rods. Arrays with experiment rod diameters up to 0.014 cm on either side of nominal were analyzed. The density of the experiment rod material was modified in the analysis to keep the material mass in the experiment rods constant.

2.4.9 Fuel Enrichment – The fuel isotopics were measured on ten randomly-selected fuel pellet samples drawn from the pellet stock used in the experiment fuel rods. The standard deviation of the ^{235}U enrichment measurements was 0.0046 wt.%. The systematic uncertainty was 0.0069 wt.%. Considering the random uncertainty and the number of measurements and adding in quadrature to the systematic uncertainty, the uncertainty in the ^{235}U enrichment of the fuel is 0.0071 wt.%.

The TSUNAMI-3D module of the SCALE6.1.3 code package was used to calculate the k_{eff} sensitivities to the materials in a detailed model of several of the experiment configurations. When appropriately combined, these sensitivities can be used to assess uncertainties in the benchmark k_{eff} that result from uncertainties of different material properties of the system in question. For example, the sensitivity of k_{eff} to the enrichment of the fuel S_E can be obtained by combining the sensitivities of k_{eff} to the ^{235}U and ^{238}U in the fuel by

$$S_E = \frac{A_U N_U}{A_{235} N_{235}} S_{235} - \frac{A_U N_U}{A_{238} N_{238}} S_{238}$$

where A_U, A_{235}, and A_{238} are the atomic masses for the fuel uranium, ^{235}U, and ^{238}U; the N_U, N_{235}, and N_{238} are the atom densities for uranium, ^{235}U, and ^{238}U in the fuel; and S_{235} and S_{238} are the sensitivities of the system k_{eff} to the fuel ^{235}U and ^{238}U. This formulation is based on the assumption that changes in ^{235}U mass are compensated by equivalent but opposite changes in ^{238}U mass in the fuel, holding the overall fuel mass and volume constant. The sensitivity S_E can be combined with the uncertainty in the fuel enrichment to obtain the contribution to the benchmark uncertainty due to uncertainties in the fuel enrichment.

2.4.10 Fuel ^{234}U Content – The ^{234}U content of the fuel was also measured. The standard deviation of the ten ^{234}U measurements was 0.00008 wt.%. The systematic uncertainty was 0.00013 wt.%. Considering the random uncertainty and the number of measurements and adding in quadrature to the systematic uncertainty, the uncertainty in the ^{234}U content of the fuel is 0.00013 wt.%.

Similar techniques to those described above for the fuel enrichment can be used to obtain the sensitivity of the benchmark k_{eff} to uncertainties in the ^{234}U content of the fuel. In the equation for the sensitivity above, the data for ^{234}U would replace that for ^{235}U. The sensitivity so obtained can be combined with the uncertainty in the ^{234}U content of the fuel to obtain the k_{eff} uncertainty due to the ^{234}U content uncertainty.

2.4.11 Fuel ^{236}U Content – The ^{236}U content of the fuel was also measured. The standard deviation of the ten ^{236}U measurements was 0.00012 wt.%. The systematic uncertainty was 0.00063 wt.%. Considering the random uncertainty and the number of measurements and adding in quadrature to the systematic uncertainty, the uncertainty in the ^{236}U content of the fuel is 0.00063 wt.%.

As for the ^{234}U uncertainties, the techniques described above for the fuel enrichment can be used to obtain the sensitivity of the benchmark k_{eff} to uncertainties in the ^{236}U content of the fuel. In the equation for the sensitivity above, the data for ^{236}U would replace that for ^{235}U. The sensitivity so obtained can be combined with the uncertainty in the ^{236}U content of the fuel to obtain the k_{eff} uncertainty due to the ^{236}U content uncertainty.

2.4.12 Fuel Stoichiometry – The oxygen-to-uranium ratio in the fuel was not measured and was assumed to be 2.00. A range of 0.1 was assumed to bound the uncertainty in the oxygen-to-uranium ratio.

Under the assumption that the fuel mass and volume are held constant, the sensitivity of the system k_{eff} to the oxygen-to-uranium ratio in the fuel S_S can be obtained from the sensitivities of the system k_{eff} to the constituents of the fuel by

$$S_S = \frac{N_U (A_O N_O S_U - A_U N_U S_O)}{N_O (A_O N_O + A_U N_U)}$$

with the variables A, N, and S indicating similar quantities as described above and the subscript O referring to the oxygen in the fuel and the subscript U referring to the uranium content of the fuel. As before, this sensitivity is combined with the uncertainty in the oxygen-to-uranium ratio in the fuel to obtain the uncertainty in the system k_{eff} introduced by the uncertainty in the fuel oxygen-to-uranium ratio.

2.4.13 Impurities in the UO_2 Fuel – The impurities in the fuel fell into two classes – those for which a definite value was measured and those that were determined to be less than the detection limit for the analysis system. For the impurities that were detected, an uncertainty at the one-standard-deviation level of 50% of the detected value was assumed. For the impurities that were below a detection limit, the uncertainty at one standard deviation was assumed to be equal to the detection limit.

Under the assumption that the fuel mass and volume are held constant, the sensitivity of the system k_{eff} S_C due to the uncertainty in any given impurity can be obtained from

$$S_C = \frac{S_I}{N_I} - \frac{A_I S_{UO2}}{M_{UO2} N_{UO2}}$$

where the symbols *S*, *N*, and *A* indicate the same quantities as above; the subscript *I* refers to the impurity species and the subscript *UO2* refers to the UO_2 in the fuel; and M_{UO2} is the molecular weight of the UO_2 in the fuel. The uncertainty in S_C is obtained by propagating the uncertainties in S_I and S_{UO2} through the definition of S_C. Tables 38 through 42 list the uncertainty in the atom density of each fuel impurity, the sensitivity of the system k_{eff} to the atom density uncertainties, and the k_{eff} uncertainty that results from the

uncertainty in each impurity. The k_{eff} uncertainties for the individual impurities are summed in quadrature to obtain the overall contribution to the uncertainty in the system k_{eff}.

Table 38. Atom Density Uncertainty and k_{eff} Sensitivity for the Fuel Impurities for Case 1.

Impurity	Uncertainty ($b^{-1}cm^{-1}$)	Sensitivity (b cm)		Δk_{eff}
		Value	Unc.	
Ag	4.616E-09	-2.386E+02	3.56E-01	-0.000001
B	1.193E-07	-5.906E+02	2.44E-01	-0.000070
Cd	6.190E-09	-3.460E+03	1.71E+00	-0.000021
Co	1.081E-08	-4.643E+01	1.07E-01	-0.000001
Cr	1.255E-06	-2.146E+00	5.60E-03	-0.000003
Cu	1.066E-07	-3.492E+00	5.74E-03	0.000000
Fe	5.156E-06	-1.963E+00	7.62E-03	-0.000010
Mn	1.419E-07	-1.118E+01	5.21E-02	-0.000002
Mo	6.222E-08	-9.013E+00	2.50E-02	-0.000001
Ni	1.749E-06	-3.378E+00	1.03E-02	-0.000006
V	7.407E-09	-3.092E+00	1.43E-02	0.000000
W	1.798E-09	-9.802E+01	3.91E-01	0.000000
Sm	1.053E-09	-7.677E+03	1.44E-02	-0.000008
Dy	8.564E-10	-9.547E+02	1.21E-02	-0.000001
Eu	9.158E-10	-3.826E+03	1.17E-02	-0.000004
Gd	8.850E-10	-2.047E+04	5.45E-01	-0.000018
			Sum in Quadrature	0.000077

Table 39. Atom Density Uncertainty and k_{eff} Sensitivity for the Fuel Impurities for Case 6.

Impurity	Uncertainty ($b^{-1}cm^{-1}$)	Sensitivity (b cm)		Δk_{eff}
		Value	Unc.	
Ag	4.616E-09	-2.353E+02	3.53E-01	-0.000001
B	1.193E-07	-5.873E+02	2.44E-01	-0.000070
Cd	6.190E-09	-3.444E+03	1.71E+00	-0.000021
Co	1.081E-08	-4.608E+01	1.06E-01	0.000000
Cr	1.255E-06	-2.218E+00	5.49E-03	-0.000003
Cu	1.066E-07	-3.561E+00	5.69E-03	0.000000
Fe	5.156E-06	-2.040E+00	7.60E-03	-0.000011
Mn	1.419E-07	-1.126E+01	5.20E-02	-0.000002
Mo	6.222E-08	-8.964E+00	2.47E-02	-0.000001
Ni	1.749E-06	-3.477E+00	1.02E-02	-0.000006
V	7.407E-09	-3.223E+00	4.29E-03	0.000000
W	1.798E-09	-9.651E+01	3.88E-01	0.000000
Sm	1.053E-09	-7.643E+03	1.43E-02	-0.000008
Dy	8.564E-10	-9.464E+02	1.20E-02	-0.000001
Eu	9.158E-10	-3.799E+03	1.16E-02	-0.000003
Gd	8.850E-10	-2.042E+04	5.44E-01	-0.000018
			Sum in Quadrature	0.000077

Table 40. Atom Density Uncertainty and k_{eff} Sensitivity for the Fuel Impurities for Case 14.

Impurity	Uncertainty ($b^{-1}cm^{-1}$)	Sensitivity (b cm)		Δk_{eff}
		Value	Unc.	
Ag	4.616E-09	-2.330E+02	3.52E-01	-0.000001
B	1.193E-07	-5.937E+02	2.53E-01	-0.000071
Cd	6.190E-09	-3.477E+03	1.74E+00	-0.000022
Co	1.081E-08	-4.595E+01	1.05E-01	0.000000
Cr	1.255E-06	-2.166E+00	5.62E-03	-0.000003
Cu	1.066E-07	-3.486E+00	5.81E-03	0.000000
Fe	5.156E-06	-1.978E+00	7.68E-03	-0.000010
Mn	1.419E-07	-1.115E+01	5.19E-02	-0.000002
Mo	6.222E-08	-8.754E+00	2.46E-02	-0.000001
Ni	1.749E-06	-3.396E+00	1.04E-02	-0.000006
V	7.407E-09	-3.135E+00	1.41E-02	0.000000
W	1.798E-09	-9.514E+01	3.88E-01	0.000000
Sm	1.053E-09	-7.758E+03	1.44E-02	-0.000008
Dy	8.564E-10	-9.509E+02	1.23E-02	-0.000001
Eu	9.158E-10	-3.821E+03	1.19E-02	-0.000003
Gd	8.850E-10	-2.088E+04	5.49E-01	-0.000018
			Sum in Quadrature	0.000078

Table 41. Atom Density Uncertainty and k_{eff} Sensitivity for the Fuel Impurities for Case 19.

Impurity	Uncertainty ($b^{-1}cm^{-1}$)	Sensitivity (b cm)		Δk_{eff}
		Value	Unc.	
Ag	4.616E-09	-2.020E+02	3.07E-01	-0.000001
B	1.193E-07	-5.786E+02	2.81E-01	-0.000069
Cd	6.190E-09	-3.342E+03	1.75E+00	-0.000021
Co	1.081E-08	-4.243E+01	9.12E-02	0.000000
Cr	1.255E-06	-2.502E+00	5.39E-03	-0.000003
Cu	1.066E-07	-3.759E+00	5.90E-03	0.000000
Fe	5.156E-06	-2.322E+00	7.47E-03	-0.000012
Mn	1.419E-07	-1.110E+01	4.46E-02	-0.000002
Mo	6.222E-08	-8.196E+00	2.18E-02	-0.000001
Ni	1.749E-06	-3.742E+00	9.91E-03	-0.000007
V	7.407E-09	-3.531E+00	4.74E-03	0.000000
W	1.798E-09	-8.242E+01	3.40E-01	0.000000
Sm	1.053E-09	-7.656E+03	1.42E-02	-0.000008
Dy	8.564E-10	-8.952E+02	1.27E-02	-0.000001
Eu	9.158E-10	-3.639E+03	1.23E-02	-0.000003
Gd	8.850E-10	-2.163E+04	5.58E-01	-0.000019
			Sum in Quadrature	0.000076

Table 42. Atom Density Uncertainty and k_{eff} Sensitivity for the Fuel Impurities for Case 24.

Impurity	Uncertainty ($b^{-1}cm^{-1}$)	Sensitivity (b cm)		Δk_{eff}
		Value	Unc.	
Ag	4.616E-09	-1.837E+02	2.89E-01	-0.000001
B	1.193E-07	-5.870E+02	3.40E-01	-0.000070
Cd	6.190E-09	-3.348E+03	1.93E+00	-0.000021
Co	1.081E-08	-4.054E+01	8.53E-02	0.000000
Cr	1.255E-06	-2.525E+00	5.79E-03	-0.000003
Cu	1.066E-07	-3.699E+00	6.68E-03	0.000000
Fe	5.156E-06	-2.319E+00	8.07E-03	-0.000012
Mn	1.419E-07	-1.092E+01	4.15E-02	-0.000002
Mo	6.222E-08	-7.478E+00	2.09E-02	0.000000
Ni	1.750E-06	-3.702E+00	1.07E-02	-0.000006
V	7.405E-09	-3.519E+00	1.21E-02	0.000000
W	1.798E-09	-7.409E+01	3.18E-01	0.000000
Sm	1.053E-09	-7.866E+03	1.56E-02	-0.000008
Dy	8.564E-10	-8.812E+02	1.45E-02	-0.000001
Eu	9.158E-10	-3.616E+03	1.41E-02	-0.000003
Gd	8.850E-10	-2.304E+04	5.97E-01	-0.000020
			Sum in Quadrature	0.000078

2.4.14 Fuel Clad Composition – The composition range for 3003 aluminum tubing is shown in Table 26 above. The composition is specified as limits either as two bounding values giving minimum and maximum content of a given element or as a single bounding value giving the maximum allowed content of a given element. The assumption was made that any level of content between the limiting values is equally probable. Therefore, the probability distribution between the limits is constant. As a result, one standard deviation is the width of the interval divided by $\sqrt{3}$.

Under the assumption that the mass and volume of the cladding material are held constant and that changes in a constituent are counterbalanced by changes in the aluminum content, the sensitivity of the system k_{eff} S_C due to the uncertainty in any given constituent of the alloy can be obtained from

$$S_C = \frac{S_I}{N_I} - \frac{A_I S_{Al}}{A_{Al} N_{Al}}$$

where the symbols *S*, *N*, and *A* indicate the same quantities as above; the subscript *I* refers to the constituent species and the subscript *Al* refers to the aluminum in the cladding material. The uncertainty in S_C is obtained by propagating the uncertainties in S_I and S_{Al} through the definition of S_C. Tables 43 through 47 list the uncertainty in the atom density of each fuel clad constituent, the sensitivity of the system k_{eff} to the atom density uncertainties, and the k_{eff} uncertainty that results from the uncertainty in each fuel clad constituent. The k_{eff} uncertainties for the individual constituents are summed in quadrature to obtain the overall contribution to the uncertainty in the system k_{eff}.

Table 43. Atom Density Uncertainty and k_{eff} Sensitivity for the Fuel Clad Constituents for Case 1.

Constituent	Uncertainty ($b^{-1}cm^{-1}$)	Sensitivity (b cm)		Δk_{eff}
		Value	Unc.	
Si	1.013E-04	-6.979E-03	1.94E-03	-0.000001
Fe	5.945E-05	-7.530E-01	3.92E-03	-0.000045
Cu	1.120E-05	-1.286E+00	3.87E-03	-0.000014
Mn	4.317E-05	-3.742E+00	1.83E-02	-0.000162
Zn	7.251E-06	-5.512E-01	5.00E-03	-0.000004
			Sum in Quadrature	0.000168

Table 44. Atom Density Uncertainty and k_{eff} Sensitivity for the Fuel Clad Constituents for Case 6.

Constituent	Uncertainty ($b^{-1}cm^{-1}$)	Sensitivity (b cm)		Δk_{eff}
		Value	Unc.	
Si	1.013E-04	-5.786E-03	1.89E-03	-0.000001
Fe	5.945E-05	-7.375E-01	3.82E-03	-0.000044
Cu	1.120E-05	-1.261E+00	3.78E-03	-0.000014
Mn	4.317E-05	-3.713E+00	1.80E-02	-0.000160
Zn	7.251E-06	-5.343E-01	4.85E-03	-0.000004
			Sum in Quadrature	0.000167

Table 45. Atom Density Uncertainty and k_{eff} Sensitivity for the Fuel Clad Constituents for Case 14.

Constituent	Uncertainty ($b^{-1}cm^{-1}$)	Sensitivity (b cm)		Δk_{eff}
		Value	Unc.	
Si	1.013E-04	-6.446E-03	1.90E-03	-0.000001
Fe	5.945E-05	-7.551E-01	3.88E-03	-0.000045
Cu	1.120E-05	-1.282E+00	3.82E-03	-0.000014
Mn	4.317E-05	-3.770E+00	1.80E-02	-0.000163
Zn	7.251E-06	-5.403E-01	4.89E-03	-0.000004
			Sum in Quadrature	0.000170

Table 46. Atom Density Uncertainty and k_{eff} Sensitivity for the Fuel Clad Constituents for Case 19.

Constituent	Uncertainty ($b^{-1}cm^{-1}$)	Sensitivity (b cm)		Δk_{eff}
		Value	Unc.	
Si	1.013E-04	-1.929E-03	1.60E-03	0.000000
Fe	5.945E-05	-7.014E-01	3.56E-03	-0.000042
Cu	1.120E-05	-1.159E+00	3.32E-03	-0.000013
Mn	4.317E-05	-3.539E+00	1.46E-02	-0.000153
Zn	7.251E-06	-4.490E-01	4.03E-03	-0.000003
			Sum in Quadrature	0.000159

Table 47. Atom Density Uncertainty and k_{eff} Sensitivity for the Fuel Clad Constituents for Case 24.

Constituent	Uncertainty ($b^{-1}cm^{-1}$)	Sensitivity (b cm)		Δk_{eff}
		Value	Unc.	
Si	1.013E-04	-2.873E-03	1.64E-03	0.000000
Fe	5.945E-05	-7.010E-01	3.47E-03	-0.000042
Cu	1.120E-05	-1.177E+00	3.33E-03	-0.000013
Mn	4.317E-05	-3.566E+00	1.54E-02	-0.000154
Zn	7.251E-06	-4.693E-01	4.17E-03	-0.000003
			Sum in Quadrature	0.000160

2.4.15 Aluminum Grid Plate Composition – The elemental composition of the 6061 aluminum grid plates was measured and reported by the supplier of the grid plates. No uncertainties were given for the measurements. The measured composition for the aluminum grid plates is shown in Table 16 above. The aluminum was treated in a manner similar to the 3003 aluminum cladding. Because the composition was measured, the uncertainty in any given value is assumed to be 25% of that value.

The sensitivity of the system k_{eff} to any given constituent of the grid plates and its uncertainty is obtained in the same manner as described above for the constituents of the cladding material. Tables 48 through 52 list the uncertainty in the atom density of each grid plate constituent, the sensitivity of the system k_{eff} to the atom density uncertainties, and the k_{eff} uncertainty that results from the uncertainty in each grid plate constituent. The k_{eff} uncertainties for the individual constituents are summed in quadrature to obtain the overall contribution to the uncertainty in the system k_{eff}.

Table 48. Atom Density Uncertainty and k_{eff} Sensitivity for the Grid Plate Constituents for Case 1.

Constituent	Uncertainty ($b^{-1}cm^{-1}$)	Sensitivity (b cm)		Δk_{eff}
		Value	Unc.	
Si	1.042E-04	1.827E-02	1.03E-03	0.000002
Fe	4.513E-05	-2.332E-01	3.30E-03	-0.000011
Cu	1.983E-05	-3.756E-01	2.59E-03	-0.000007
Mn	6.659E-06	-1.258E+00	8.98E-03	-0.000008
Mg	1.739E-04	7.461E-02	1.30E-03	0.000013
Cr	1.564E-05	-2.843E-01	1.82E-03	-0.000004
Zn	7.458E-06	-8.451E-02	2.55E-03	-0.000001
Ti	1.698E-06	-5.285E-01	3.52E-03	-0.000001
V	7.980E-07	-2.969E-01	5.41E-03	0.000000
			Sum in Quadrature	0.000021

Table 49. Atom Density Uncertainty and k_{eff} Sensitivity for the Grid Plate Constituents for Case 6.

Constituent	Uncertainty ($b^{-1}cm^{-1}$)	Sensitivity (b cm)		Δk_{eff}
		Value	Unc.	
Si	1.042E-04	1.812E-02	1.05E-03	0.000002
Fe	4.513E-05	-2.292E-01	3.35E-03	-0.000010
Cu	1.983E-05	-3.695E-01	2.63E-03	-0.000007
Mn	6.659E-06	-1.227E+00	9.20E-03	-0.000008
Mg	1.739E-04	7.388E-02	1.32E-03	0.000013
Cr	1.564E-05	-2.796E-01	1.85E-03	-0.000004
Zn	7.458E-06	-8.376E-02	2.59E-03	-0.000001
Ti	1.698E-06	-5.148E-01	3.57E-03	-0.000001
V	7.980E-07	-2.918E-01	5.49E-03	0.000000
			Sum in Quadrature	0.000020

Table 50. Atom Density Uncertainty and k_{eff} Sensitivity for the Grid Plate Constituents for Case 14.

Constituent	Uncertainty ($b^{-1}cm^{-1}$)	Sensitivity (b cm)		Δk_{eff}
		Value	Unc.	
Si	1.042E-04	1.917E-02	1.06E-03	0.000002
Fe	4.513E-05	-2.421E-01	3.40E-03	-0.000011
Cu	1.983E-05	-3.918E-01	2.66E-03	-0.000008
Mn	6.659E-06	-1.324E+00	9.25E-03	-0.000009
Mg	1.739E-04	7.653E-02	1.33E-03	0.000013
Cr	1.564E-05	-2.980E-01	1.86E-03	-0.000005
Zn	7.458E-06	-8.677E-02	2.61E-03	-0.000001
Ti	1.698E-06	-5.518E-01	3.61E-03	-0.000001
V	7.980E-07	-3.142E-01	5.54E-03	0.000000
			Sum in Quadrature	0.000021

Table 51. Atom Density Uncertainty and k_{eff} Sensitivity for the Grid Plate Constituents for Case 19.

Constituent	Uncertainty ($b^{-1}cm^{-1}$)	Sensitivity (b cm)		Δk_{eff}
		Value	Unc.	
Si	1.042E-04	1.584E-02	8.41E-04	0.000002
Fe	4.513E-05	-2.044E-01	2.84E-03	-0.000009
Cu	1.983E-05	-3.341E-01	2.19E-03	-0.000007
Mn	6.659E-06	-1.148E+00	7.20E-03	-0.000008
Mg	1.739E-04	6.357E-02	1.05E-03	0.000011
Cr	1.564E-05	-2.570E-01	1.50E-03	-0.000004
Zn	7.458E-06	-7.450E-02	2.03E-03	-0.000001
Ti	1.698E-06	-4.860E-01	2.88E-03	-0.000001
V	7.980E-07	-2.901E-01	4.22E-03	0.000000
			Sum in Quadrature	0.000018

Table 52. Atom Density Uncertainty and k_{eff} Sensitivity for the Grid Plate Constituents for Case 24.

Constituent	Uncertainty ($b^{-1}cm^{-1}$)	Sensitivity (b cm)		Δk_{eff}
		Value	Unc.	
Si	1.042E-04	1.655E-02	9.12E-04	0.000002
Fe	4.513E-05	-2.101E-01	2.99E-03	-0.000009
Cu	1.983E-05	-3.407E-01	2.33E-03	-0.000007
Mn	6.659E-06	-1.145E+00	7.91E-03	-0.000008
Mg	1.739E-04	6.529E-02	1.14E-03	0.000011
Cr	1.564E-05	-2.595E-01	1.62E-03	-0.000004
Zn	7.458E-06	-7.920E-02	2.24E-03	-0.000001
Ti	1.698E-06	-4.850E-01	3.12E-03	-0.000001
V	7.980E-07	-2.836E-01	4.69E-03	0.000000
			Sum in Quadrature	0.000019

2.4.16 Experiment Rod Composition – The elemental compositions of the titanium and aluminum experiment rods were measured and reported by the suppliers of the experiment rods. No uncertainties were given for the measurements. The measured composition for the titanium experiment rods is shown in Table 30 above. The measured composition of the aluminum experiment rods is shown in Table 31 above. Both materials were treated in a manner similar to the 3003 aluminum cladding. Because the composition was measured, the uncertainty in any given value is assumed to be 25% of that value.

The sensitivity of the system k_{eff} to any given constituent of the experiment rod material and its uncertainty is obtained in the same manner as described above for the constituents of the cladding material.

Under the assumption that the mass and volume of the experiment rod material are held constant and that changes in a constituent are counterbalanced by changes in the parent material (titanium or aluminum) content, the sensitivity of the system k_{eff} S_C due to the uncertainty in any given constituent of the material can be obtained from

$$S_C = \frac{S_I}{N_I} - \frac{A_I S_P}{A_P N_P}$$

where the symbols *S*, *N*, and *A* indicate the same quantities as above; the subscript *I* refers to the constituent species and the subscript *P* refers to the parent species in the experiment rods. The uncertainty in S_C is obtained by propagating the uncertainties in S_I and S_P through the definition of S_C. Tables 53 through 56 list the uncertainty in the atom density of each experiment rod constituent, the sensitivity of the system k_{eff} to the atom density uncertainties, and the k_{eff} uncertainty that results from the uncertainty in each experiment rod constituent. The k_{eff} uncertainties for the individual constituents are summed in quadrature to obtain the overall contribution to the uncertainty in the system k_{eff}.

Table 53. Atom Density Uncertainty and k_{eff} Sensitivity for the Titanium Experiment Rods in Case 6.

Constituent	Uncertainty ($b^{-1}cm^{-1}$)	Sensitivity (b cm)		Δk_{eff}
		Value	Unc.	
C	5.608E-06	5.705E-02	1.17E-03	0.000000
O	4.243E-05	6.978E-02	1.43E-03	0.000003
N	9.694E-06	-1.903E-02	2.04E-03	0.000000
H	2.694E-05	-3.673E-02	6.44E-03	-0.000001
Fe	2.492E-05	1.370E-01	2.54E-03	0.000003
			Sum in Quadrature	0.000005

Table 54. Atom Density Uncertainty and k_{eff} Sensitivity for the Aluminum Experiment Rods in Case 14.

Constituent	Uncertainty ($b^{-1}cm^{-1}$)	Sensitivity (b cm)		Δk_{eff}
		Value	Unc.	
Si	8.388E-05	7.977E-03	1.60E-03	0.000001
Fe	1.382E-05	-2.813E-01	4.40E-03	-0.000004
Cu	1.023E-05	-4.715E-01	3.64E-03	-0.000005
Mn	3.697E-06	-1.709E+00	1.84E-02	-0.000006
Mg	1.354E-04	3.091E-02	2.24E-03	0.000004
Cr	3.906E-06	-3.430E-01	2.59E-03	-0.000001
Ti	1.697E-06	-7.220E-01	4.46E-03	-0.000001
Ga	5.826E-07	-7.873E-01	1.40E-02	0.000000
V	7.974E-07	-5.674E-01	7.01E-03	0.000000
			Sum in Quadrature	0.000010

Table 55. Atom Density Uncertainty and k_{eff} Sensitivity for the Aluminum Experiment Rods in Case 19.

Constituent	Uncertainty ($b^{-1}cm^{-1}$)	Sensitivity (b cm)		Δk_{eff}
		Value	Unc.	
Si	8.387E-05	1.563E-02	1.75E-03	0.000001
Fe	1.382E-05	-5.167E-01	6.13E-03	-0.000007
Cu	1.023E-05	-8.317E-01	4.67E-03	-0.000009
Mn	3.698E-06	-3.187E+00	1.98E-02	-0.000012
Mg	1.354E-04	4.960E-02	2.40E-03	0.000007
Cr	3.906E-06	-6.371E-01	3.10E-03	-0.000002
Ti	1.697E-06	-1.361E+00	5.78E-03	-0.000002
Ga	5.827E-07	-1.060E+00	1.36E-02	-0.000001
V	7.973E-07	-1.104E+00	8.09E-03	-0.000001
			Sum in Quadrature	0.000018

Table 56. Atom Density Uncertainty and k_{eff} Sensitivity for the Titanium Experiment Rods in Case 24.

Constituent	Uncertainty ($b^{-1}cm^{-1}$)	Sensitivity (b cm)		Δk_{eff}
		Value	Unc.	
C	5.608E-06	1.454E-01	1.45E-03	0.000001
O	4.243E-05	1.866E-01	1.56E-03	0.000008
N	9.694E-06	-2.664E-02	3.10E-03	0.000000
H	2.694E-05	-2.354E-02	9.74E-03	-0.000001
Fe	2.492E-05	3.974E-01	4.03E-03	0.000010
			Sum in Quadrature	0.000013

2.4.17 Water Composition – The impurities measured in the municipal water supply that feeds the facility in 2014 are listed in Table 20 above. For conservatism, the maximum impurity levels were assumed to be the 1-σ uncertainties. Table 21 lists several impurity species for which testing was done but that could not be detected. Also listed in the table is the minimum detection level for each species. For these impurities, the 1-σ uncertainties are assumed to be the minimum detection levels.

Under the assumption that the water mass and volume are held constant, the sensitivity of the system k_{eff} S_C due to the uncertainty in any given impurity in the water can be obtained from

$$S_C = \frac{S_I}{N_I} - \frac{A_I S_W}{M_W N_W}$$

where the symbols *S*, *N*, and *A* indicate the same quantities as above; the subscript *I* refers to the impurity species and the subscript *W* refers to the Water; and M_W is the molecular weight of water. The uncertainty in S_C is obtained by propagating the uncertainties in S_I and S_W through the definition of S_C. Tables 57 through 61 list the uncertainty in the atom density of each water impurity, the sensitivity of the system k_{eff} to the atom density uncertainties, and the k_{eff} uncertainty that results from the uncertainty in each impurity. The k_{eff} uncertainties for the individual impurities are summed in quadrature to obtain the overall contribution to the uncertainty in the system k_{eff}.

Table 57. Atom Density Uncertainty and k_{eff} Sensitivity for the Water Impurities for Case 1.

Impurity	Uncertainty ($b^{-1}cm^{-1}$)	Sensitivity (b cm)		Δk_{eff}
		Value	Unc.	
As	6.413E-11	-8.379E+01	2.69E-01	0.000000
Ba	8.746E-10	-9.467E+01	4.93E-01	0.000000
Cr	9.240E-11	-3.750E+01	1.87E-01	0.000000
U	1.514E-11	-2.168E+02	8.55E-01	0.000000
Fe	1.012E-08	-3.946E+01	2.01E-01	0.000000
Mn	1.345E-09	-5.457E+01	1.97E-01	0.000000
Ca	1.019E-06	-2.699E+01	1.44E-01	-0.000028
Cl	7.962E-07	-7.009E+01	1.27E-01	-0.000056
Mg	1.804E-07	-1.502E+01	8.73E-02	-0.000003
K	1.229E-07	-2.882E+01	1.40E-01	-0.000004
Na	1.829E-06	-1.460E+01	8.25E-02	-0.000027
Sb	4.932E-12	-1.498E+02	4.37E-01	0.000000
Be	6.664E-11	-4.213E+00	3.24E-02	0.000000
Cd	5.343E-12	-6.187E+03	4.04E-01	0.000000
Hg	5.988E-13	-5.988E+02	7.20E-01	0.000000
Se	3.803E-11	-7.090E+01	2.84E-01	0.000000
			Sum in Quadrature	0.000068

Table 58. Atom Density Uncertainty and k_{eff} Sensitivity for the Water Impurities for Case 6.

Impurity	Uncertainty ($b^{-1}cm^{-1}$)	Sensitivity (b cm)		Δk_{eff}
		Value	Unc.	
As	6.413E-11	-8.181E+01	2.64E-01	0.000000
Ba	8.746E-10	-9.010E+01	4.84E-01	0.000000
Cr	9.240E-11	-3.585E+01	1.83E-01	0.000000
U	1.514E-11	-2.112E+02	8.39E-01	0.000000
Fe	1.012E-08	-3.767E+01	1.97E-01	0.000000
Mn	1.345E-09	-5.309E+01	1.94E-01	0.000000
Ca	1.019E-06	-2.567E+01	1.41E-01	-0.000026
Cl	7.962E-07	-6.972E+01	1.25E-01	-0.000056
Mg	1.804E-07	-1.424E+01	8.57E-02	-0.000003
K	1.229E-07	-2.756E+01	1.38E-01	-0.000003
Na	1.829E-06	-1.390E+01	8.10E-02	-0.000025
Sb	4.932E-12	-1.472E+02	4.29E-01	0.000000
Be	6.664E-11	-3.969E+00	3.18E-02	0.000000
Cd	5.343E-12	-6.289E+03	3.96E-01	0.000000
Hg	5.988E-13	-5.998E+02	7.07E-01	0.000000
Se	3.803E-11	-6.863E+01	2.78E-01	0.000000
			Sum in Quadrature	0.000067

Table 59. Atom Density Uncertainty and k_{eff} Sensitivity for the Water Impurities for Case 14.

Impurity	Uncertainty ($b^{-1}cm^{-1}$)	Sensitivity (b cm)		Δk_{eff}
		Value	Unc.	
As	6.413E-11	-8.422E+01	2.82E-01	0.000000
Ba	8.746E-10	-9.397E+01	5.16E-01	0.000000
Cr	9.240E-11	-3.755E+01	1.95E-01	0.000000
U	1.514E-11	-2.188E+02	8.95E-01	0.000000
Fe	1.012E-08	-3.942E+01	2.10E-01	0.000000
Mn	1.345E-09	-5.581E+01	2.06E-01	0.000000
Ca	1.019E-06	-2.678E+01	1.51E-01	-0.000027
Cl	7.962E-07	-7.432E+01	1.33E-01	-0.000059
Mg	1.804E-07	-1.485E+01	9.13E-02	-0.000003
K	1.229E-07	-2.884E+01	1.47E-01	-0.000004
Na	1.829E-06	-1.448E+01	8.64E-02	-0.000026
Sb	4.932E-12	-1.512E+02	4.58E-01	0.000000
Be	6.664E-11	-4.133E+00	3.39E-02	0.000000
Cd	5.343E-12	-6.701E+03	4.22E-01	0.000000
Hg	5.988E-13	-6.452E+02	7.54E-01	0.000000
Se	3.803E-11	-7.200E+01	2.97E-01	0.000000
			Sum in Quadrature	0.000070

Table 60. Atom Density Uncertainty and k_{eff} Sensitivity for the Water Impurities for Case 19.

Impurity	Uncertainty ($b^{-1}cm^{-1}$)	Sensitivity (b cm)		Δk_{eff}
		Value	Unc.	
As	6.413E-11	-8.161E+01	3.90E-01	0.000000
Ba	8.746E-10	-8.014E+01	7.15E-01	0.000000
Cr	9.240E-11	-3.436E+01	2.71E-01	0.000000
U	1.514E-11	-2.081E+02	1.24E+00	0.000000
Fe	1.012E-08	-3.544E+01	2.91E-01	0.000000
Mn	1.345E-09	-6.122E+01	2.86E-01	0.000000
Ca	1.019E-06	-2.283E+01	2.09E-01	-0.000023
Cl	7.962E-07	-9.750E+01	1.85E-01	-0.000078
Mg	1.804E-07	-1.230E+01	1.27E-01	-0.000002
K	1.229E-07	-2.629E+01	2.04E-01	-0.000003
Na	1.829E-06	-1.251E+01	1.20E-01	-0.000023
Sb	4.932E-12	-1.495E+02	6.34E-01	0.000000
Be	6.664E-11	-3.204E+00	4.69E-02	0.000000
Cd	5.343E-12	-9.741E+03	5.85E-01	0.000000
Hg	5.988E-13	-9.124E+02	1.04E+00	0.000000
Se	3.803E-11	-7.340E+01	4.11E-01	0.000000
			Sum in Quadrature	0.000084

Table 61. Atom Density Uncertainty and k_{eff} Sensitivity for the Water Impurities for Case 24.

Impurity	Uncertainty ($b^{-1}cm^{-1}$)	Sensitivity (b cm)		Δk_{eff}
		Value	Unc.	
As	6.413E-11	-8.809E+01	4.12E-01	0.000000
Ba	8.746E-10	-8.560E+01	7.56E-01	0.000000
Cr	9.240E-11	-3.852E+01	2.86E-01	0.000000
U	1.514E-11	-2.253E+02	1.31E+00	0.000000
Fe	1.012E-08	-3.927E+01	3.07E-01	0.000000
Mn	1.345E-09	-7.419E+01	3.02E-01	0.000000
Ca	1.019E-06	-2.443E+01	2.21E-01	-0.000025
Cl	7.962E-07	-1.277E+02	1.95E-01	-0.000102
Mg	1.804E-07	-1.297E+01	1.34E-01	-0.000002
K	1.229E-07	-2.929E+01	2.15E-01	-0.000004
Na	1.829E-06	-1.350E+01	1.26E-01	-0.000025
Sb	4.932E-12	-1.607E+02	6.70E-01	0.000000
Be	6.664E-11	-3.264E+00	4.96E-02	0.000000
Cd	5.343E-12	-1.291E+04	6.18E-01	0.000000
Hg	5.988E-13	-1.235E+03	1.10E+00	0.000000
Se	3.803E-11	-8.622E+01	4.34E-01	0.000000
			Sum in Quadrature	0.000108

2.4.18 Temperature – The experiments were run near a temperature of 25 °C and the data were corrected to that temperature. A bounding estimate of the uncertainty in the measured experiment temperature is 1 °C. The sensitivity of the arrays to moderator/reflector temperature was determined by analyzing arrays at temperatures from 5 °C to 50 °C in 5 °C increments using MCNP6.1.1 and ENDF/B-VII.1 cross sections.

In the analysis, the water temperature was varied as well as the water density. Thermal scattering kernel data appropriate for each water temperature were used during the variations. The sensitivity of the arrays to fuel temperature was also computed with the same code/cross sections using the temperature-dependent uranium cross sections included with the code. The variations in the calculated k_{eff} data in both cases necessitated the use of a second-order polynomial fit. The sensitivity was taken as the slope of the polynomial at the experiment temperature. The stochastic uncertainties in the Monte Carlo calculations were propagated through the fit. The two sensitivities were combined to obtain the overall temperature sensitivity of the assemblies. The uncertainties in the two sensitivities were combined in quadrature.

2.4.19 Uncertainty Values – The results of the sensitivity studies were combined with the uncertainties in the various parameters to determine the contribution of each uncertainty source to the overall uncertainty in the experiments. The results are shown in Table 62 for Case 1, Table 63 for Case 6, Table 64 for Case14, Table 65 for Case 19, and Table 66 for Case 24. For each array, the uncertainty contribution from each source is listed. Also listed is the total uncertainty for each configuration which is the sum in quadrature of the various uncertainty components. This value represents the uncertainty in the experiments at the one-standard-deviation level.

Table 62. Results of the Uncertainty Analysis for Case 1.

Uncertainty Source	Uncertainty Value	Sensitivity		Δk_{eff}
		Value	Unc.[a]	
Pitch of Fuel Rods (cm) [b]	0.000562	1.3202	0.0027	0.00074
Clad OD (cm) [b]	0.0000954	-1.2484	0.0059	-0.00012
Clad ID (cm) [b]	0.000164	-0.09330	0.00095	-0.00002
Fuel Pellet OD (cm) [b]	0.000105	-0.0503	0.0021	-0.00001
Water Depth (mm) [b]	5	-0.0000014	0.0000017	-0.00001
Rod Fuel Mass (g) [b]	0.024	0.000660	0.000021	0.00002
Rod Fuel Length (cm) [b]	0.05	0.001065	0.000020	0.00005
Enrichment [c]	0.000071	1.6219	0.0050	0.00011
^{234}U [c]	0.0000013	-4.8273	0.0083	-0.00001
^{236}U [c]	0.0000063	-1.7377	0.0034	-0.00001
UO_2 Stoichiometry (O per U) [c]	0.1	-0.00743	0.00011	-0.00074
Fuel Impurities [c]		See Text		0.00008
Clad Composition [c]		See Text		0.00017
Grid Plate Composition [c]		See Text		0.00002
Water Composition [c]		See Text		0.00007
Temperature (K) [d]	1	-0.0000155	0.0000008	-0.00002
			Sum in Quadrature	0.00108

(a) 1-σ uncertainty due to the stochastic uncertainties contributed by the Monte Carlo calculations done for the sensitivity studies.
(b) The sensitivity analysis was done by direct perturbation with the code KENO V.a using the 238-group ENDF/B-VII.0 cross section set from SCALE6.1.3.
(c) The sensitivity analysis was done by combining material sensitivities calculated with the code TSUNAMI-3D using the 238-group ENDF/B-VII.0 cross section set from SCALE6.1.3.
(d) The temperature sensitivity analysis was done as described in the text with the code MCNP6.1 using the continuous-energy ENDF/B-VII.1 cross sections.

Table 63. Results of the Uncertainty Analysis for Case 6.

Uncertainty Source	Uncertainty Value	Sensitivity		Δk_{eff}
		Value	Unc. [a]	
Pitch of Fuel Rods (cm) [b]	0.000562	1.2372	0.0027	0.00070
Clad OD (cm) [b]	0.0000954	-1.1721	0.0054	-0.00011
Clad ID (cm) [b]	0.000164	-0.08519	0.00093	-0.00001
Fuel Pellet OD (cm) [b]	0.000105	-0.0493	0.0021	-0.00001
Water Depth (mm) [b]	5	0.0000018	0.0000017	0.00001
Rod Fuel Mass (g) [b]	0.024	0.000705	0.000021	0.00002
Rod Fuel Length (cm) [b]	0.05	0.001091	0.000019	0.00005
Experiment Rod OD (cm) [b]	0.000581	0.00498	0.00088	0.00000
Enrichment [c]	0.000071	1.7119	0.0050	0.00012
^{234}U [c]	0.0000013	-4.7638	0.0082	-0.00001
^{236}U [c]	0.0000063	-1.7071	0.0034	-0.00001
UO_2 Stoichiometry (O per U) [c]	0.1	-0.00635	0.00011	-0.00064
Fuel Impurities [c]		See Text		0.00008
Clad Composition [c]		See Text		0.00017
Grid Plate Composition [c]		See Text		0.00002
Experiment Rod Composition [c]		See Text		0.00000
Water Composition [c]		See Text		0.00007
Temperature (K) [d]	1	-0.0000077	0.0000011	-0.00001
			Sum in Quadrature	0.00098

(a) 1-σ uncertainty due to the stochastic uncertainties contributed by the Monte Carlo calculations done for the sensitivity studies.
(b) The sensitivity analysis was done by direct perturbation with the code KENO V.a using the 238-group ENDF/B-VII.0 cross section set from SCALE6.1.3.
(c) The sensitivity analysis was done by combining material sensitivities calculated with the code TSUNAMI-3D using the 238-group ENDF/B-VII.0 cross section set from SCALE6.1.3.
(d) The temperature sensitivity analysis was done as described in the text with the code MCNP6.1 using the continuous-energy ENDF/B-VII.1 cross sections.

Table 64. Results of the Uncertainty Analysis for Case 14.

Uncertainty Source	Uncertainty Value	Sensitivity		Δk_{eff}
		Value	Unc.[a]	
Pitch of Fuel Rods (cm) [b]	0.000562	1.2858	0.0028	0.00072
Clad OD (cm) [b]	0.0000954	-1.1862	0.0059	-0.00011
Clad ID (cm) [b]	0.000164	-0.09204	0.00095	-0.00002
Fuel Pellet OD (cm) [b]	0.000105	-0.0523	0.0021	-0.00001
Water Depth (mm) [b]	5	-0.0000014	0.0000017	-0.00001
Rod Fuel Mass (g) [b]	0.024	0.000727	0.000021	0.00002
Rod Fuel Length (cm) [b]	0.05	0.001065	0.000019	0.00005
Experiment Rod OD (cm) [b]	0.000490	-0.00912	0.00086	0.00000
Enrichment [c]	0.000071	1.6053	0.0052	0.00011
^{234}U [c]	0.0000013	-4.7382	0.0082	-0.00001
^{236}U [c]	0.0000063	-1.6865	0.0034	-0.00001
UO_2 Stoichiometry (O per U) [c]	0.1	-0.00735	0.00011	-0.00074
Fuel Impurities [c]		See Text		0.00008
Clad Composition [c]		See Text		0.00017
Grid Plate Composition [c]		See Text		0.00002
Experiment Rod Composition [c]		See Text		0.00001
Water Composition [c]		See Text		0.00007
Temperature (K) [d]	1	-0.0000104	0.0000013	0.00001
			Sum in Quadrature	0.00106

(a) 1-σ uncertainty due to the stochastic uncertainties contributed by the Monte Carlo calculations done for the sensitivity studies.
(b) The sensitivity analysis was done by direct perturbation with the code KENO V.a using the 238-group ENDF/B-VII.0 cross section set from SCALE6.1.3.
(c) The sensitivity analysis was done by combining material sensitivities calculated with the code TSUNAMI-3D using the 238-group ENDF/B-VII.0 cross section set from SCALE6.1.3.
(d) The temperature sensitivity analysis was done as described in the text with the code MCNP6.1 using the continuous-energy ENDF/B-VII.1 cross sections.

Table 65. Results of the Uncertainty Analysis for Case 19.

Uncertainty Source	Uncertainty Value	Sensitivity		Δk_{eff}
		Value	Unc.[a]	
Pitch of Fuel Rods (cm) [b]	0.000618	0.951	0.003	0.00059
Clad OD (cm) [b]	0.0000954	-0.9193	0.0047	-0.00009
Clad ID (cm) [b]	0.000164	-0.06974	0.00091	-0.00001
Fuel Pellet OD (cm) [b]	0.000105	-0.0171	0.0021	0.00000
Water Depth (mm) [b]	5	-0.0000012	0.0000017	-0.00001
Rod Fuel Mass (g) [b]	0.024	0.000999	0.000021	0.00002
Rod Fuel Length (cm) [b]	0.05	0.000396	0.000019	0.00002
Experiment Rod OD (cm) [b]	0.000490	-0.03696	0.00089	-0.00002
Enrichment [c]	0.000071	2.0077	0.0071	0.00014
^{234}U [c]	0.0000013	-3.9009	0.0068	-0.00001
^{236}U [c]	0.0000063	-1.238	0.0028	-0.00001
UO_2 Stoichiometry (O per U) [c]	0.1	-0.00426	0.00009	-0.00043
Fuel Impurities [c]		See Text		0.00008
Clad Composition [c]		See Text		0.00016
Grid Plate Composition [c]		See Text		0.00002
Experiment Rod Composition [c]		See Text		0.00002
Water Composition [c]		See Text		0.00008
Temperature (K) [d]	1	0.0000193	0.0000010	0.00002
			Sum in Quadrature	0.00077

(a) 1-σ uncertainty due to the stochastic uncertainties contributed by the Monte Carlo calculations done for the sensitivity studies.
(b) The sensitivity analysis was done by direct perturbation with the code KENO V.a using the 238-group ENDF/B-VII.0 cross section set from SCALE6.1.3.
(c) The sensitivity analysis was done by combining material sensitivities calculated with the code TSUNAMI-3D using the 238-group ENDF/B-VII.0 cross section set from SCALE6.1.3.
(d) The temperature sensitivity analysis was done as described in the text with the code MCNP6.1 using the continuous-energy ENDF/B-VII.1 cross sections.

Table 66. Results of the Uncertainty Analysis for Case 24.

Uncertainty Source	Uncertainty Value	Sensitivity		Δk_{eff}
		Value	Unc.[a]	
Pitch of Fuel Rods (cm) [b]	0.000562	0.8777	0.0027	0.00049
Clad OD (cm) [b]	0.0000954	-0.8318	0.0082	-0.00008
Clad ID (cm) [b]	0.000164	-0.07486	0.00093	-0.00001
Fuel Pellet OD (cm) [b]	0.000105	-0.0159	0.0022	0.00000
Water Depth (mm) [b]	5	-0.0000020	0.0000017	-0.00001
Rod Fuel Mass (g) [b]	0.024	0.001050	0.000021	0.00003
Rod Fuel Length (cm) [b]	0.05	0.0002055	0.000019	0.00001
Experiment Rod OD (cm) [b]	0.000581	-0.0240	0.0010	-0.00001
Enrichment [c]	0.000071	2.0671	0.0058	0.00015
^{234}U [c]	0.0000013	-4.1886	0.0072	-0.00001
^{236}U [c]	0.0000063	-1.4123	0.0030	-0.00001
UO_2 Stoichiometry (O per U) [c]	0.1	-0.00366	0.00010	-0.00037
Fuel Impurities [c]		See Text		0.00008
Clad Composition [c]		See Text		0.00016
Grid Plate Composition [c]		See Text		0.00002
Experiment Rod Composition [c]		See Text		0.00001
Water Composition [c]		See Text		0.00011
Temperature (K) [d]	1	0.0000199	0.0000008	-0.00002
			Sum in Quadrature	0.00067

(a) 1-σ uncertainty due to the stochastic uncertainties contributed by the Monte Carlo calculations done for the sensitivity studies.
(b) The sensitivity analysis was done by direct perturbation with the code KENO V.a using the 238-group ENDF/B-VII.0 cross section set from SCALE6.1.3.
(c) The sensitivity analysis was done by combining material sensitivities calculated with the code TSUNAMI-3D using the 238-group ENDF/B-VII.0 cross section set from SCALE6.1.3.
(d) The temperature sensitivity analysis was done as described in the text with the code MCNP6.1 using the continuous-energy ENDF/B-VII.1 cross sections.

The uncertainties estimated for Case 1 will be used for that case. The uncertainties estimated for Case 6 will be assumed to apply to all cases that have titanium experiment rods with no empty internal array positions (Cases 2 through 9). The uncertainties estimated for Case 14 will be assumed to apply to all cases that have aluminum experiment rods with no empty internal array positions (Cases 10 through 17). The uncertainties estimated for Case 19 will be assumed to apply to Cases 18 through 21. The uncertainties estimated for Case 24 will be assumed to apply to Cases 22 through 24.

2.5 Reactivity Worth of the Experiment Rods

This report evaluates a series of rod-replacement experiments with the goal of providing integral tests of titanium cross sections. Cases 1 and 18 contain no experiment rods. Cases 2 through 17 and 19 through 24 include various numbers and arrangements of titanium and/or aluminum experiment rods. The worth of the experiment rods in each configuration was evaluated by calculating the k_{eff} of a detailed model of each configuration with the experiment rods as described and with the material in the experiment rods voided. The analysis was done using MCNP6.1.1 with continuous-energy ENDF/B-VII.1 cross sections. The reactivity worth of the experiment rods, ρ_x, is given by

$$\rho_x = \frac{k_x - k_v}{k_x k_v}$$

Where k_x is the calculated k_{eff} with the experiment rods present and k_v is the calculated k_{eff} with the experiment rods voided. Table 67 lists the calculated worth of the experiment rods present in Cases 1 through 24.

Table 67. Calculated Reactivity Worth of the Experiment Rods in Each Configurations.

Case	Number of Experiment Rods		Experiment Rod Reactivity Worth (%)	Uncertainty
	Titanium	Aluminum		
1	0	0	0 [(a)]	-
2	4	0	-0.22	0.01
3	9	0	-0.50	0.01
4	16	0	-0.92	0.01
5	25	0	-1.42	0.01
6	36	0	-2.01	0.01
7	36	0	-1.84	0.01
8	36	0	-1.69	0.01
9	36	0	-1.52	0.01
10	0	4	0.02	0.01
11	0	9	0.01	0.01
12	0	16	-0.02	0.01
13	0	25	-0.03	0.01
14	0	36	-0.04	0.01
15	0	36	0.03	0.01
16	0	36	0.07	0.01
17	0	36	0.06	0.01
18	0	0	0 [(a)]	-
19	0	36	-0.16	0.01
20	4	32	-0.91	0.01
21	9	27	-1.66	0.01
22	16	20	-2.60	0.01
23	25	11	-3.56	0.01
24	36	0	-4.58	0.01

(a) Cases 1 and 18 have no experiment rods. The reactivity is set to 0 with no uncertainty.

3.0 BENCHMARK SPECIFICATIONS

3.1 Description of Model

The models of the experiments consist of nearly cylindrical square-pitched arrays of UO_2 fuel rods supported by aluminum grid plates and completely submerged in water. The arrays are centered in a 93.6752 cm diameter cylinder of water with 16.51 cm of water below the lower grid plate and 15.24 cm of water above the upper grid plate. This section describes the reactivity effects of several simplifications of the benchmark models.

The following modeling approximations were made:

- The population average value of the UO_2 fuel mass was used.
- The population average value of the UO_2 fuel pellet stack height was used.
- The population average value of the fuel rod outer diameter was used.
- The slight misalignment of the aluminum plugs above the fuel pellet stack with the upper grid plate was ignored.
- The parts of the critical assembly above the level of the water moderator were removed.
- The upper grid plate support bosses and posts were removed and replaced with water.
- The control and safety elements were each replaced with four fuel rods.
- The neutron source was replaced by an empty position in the fuel assembly.
- All materials outside of the water reflector were removed.
- The density of the polyethylene annuli around the detectors was set equal to the density of the polyethylene plugs in the fuel rods.

Each of these modeling approximations was investigated in one or more of evaluations LEU-COMP-THERM-080, LEU-COMP-THERM-078, and LEU-COMP-THERM-096 and were found to be small.

In the benchmark models of Cases 2 through 17 and 19 through 24, population average values for the experiment rod outer diameter and density were used. It is judged that the effects of these two approximations are small.

3.1.1 Integral Calculation of the Benchmark Model Bias – The k_{eff} for all cases was calculated using the detailed MCNP6.1.1 model and compared to the calculated k_{eff} for a model in which all the simplifications described above had been made. The ENDF/B-VII.1 cross sections were used. Table 68 lists the calculated biases attributable to the model simplifications. The bias associated with simplification of the benchmark model is small in all cases. The biases listed in the table will be applied to the benchmark model k_{eff}.

Table 68. Benchmark Model Bias and Uncertainty.

Case	Simplified Model Bias	Uncertainty in the Bias
1	0.00000	0.00004
2	0.00000	0.00004
3	0.00000	0.00004
4	0.00007	0.00004
5	0.00006	0.00004
6	0.00005	0.00004
7	0.00006	0.00004
8	0.00005	0.00004
9	-0.00002	0.00004
10	0.00000	0.00004
11	-0.00002	0.00004
12	0.00005	0.00004
13	0.00014	0.00004
14	0.00007	0.00004
15	0.00012	0.00004
16	-0.00004	0.00004
17	0.00001	0.00004
18	-0.00002	0.00004
19	0.00013	0.00004
20	0.00009	0.00004
21	-0.00005	0.00004
22	0.00000	0.00004
23	-0.00005	0.00004
24	0.00006	0.00004

3.1.2 Temperature Corrections to Experiment k_{eff} – The benchmark experiments were run near a temperature of 25°C and this temperature was chosen as the benchmark model temperature. The experiment k_{eff} for all cases was slightly less than 1 as detailed in section 2.3. A correction to the experiment k_{eff}, Δk_T, for a temperature difference ΔT between the benchmark model temperature and the experiment temperature is given by

$$\Delta k_T = \Delta T \bullet S_T$$

where S_T is the temperature sensitivity of the configuration involved and includes the effects of temperature on the fuel and moderator/reflector.

Detailed models of all cases were analyzed for moderator temperatures in 5 °C increments from 5 °C to 50 °C using MCNP6.1 with continuous-energy ENDF/B-VII.1 cross sections using thermal scattering data and water densities appropriate to each temperature. The moderator temperature sensitivity of each model was determined by fitting a second-order polynomial to the k_{eff} results as a function of moderator temperature and finding the slope of the fitting function at 25 °C.

Detailed models of all cases were analyzed at fuel temperatures of 250, 293, 600, 900, and 1200 K using MCNP6.1 with continuous-energy uranium cross sections at those temperatures. Thermal expansion of the

UO_2 was included in the analysis. As for the moderator, the temperature sensitivity of each model was determined by fitting a second-order polynomial to the k_{eff} result and finding the slope of the fitting function at 25 °C. The overall temperature sensitivity S_T was taken as the sum of the moderator and fuel sensitivities. The combined temperature sensitivity S_T, the experiment temperature, and the Δk_T correction to the experiment k_{eff} are shown in Table 69.

Table 69. Temperature Corrections to the Experiment k_{eff}.

Case	Temperature Sensitivity S_T ($\times 10^{-5}$ °C^{-1})		Experiment Temperature (°C)	Temperature Correction Δk_T to Experiment k_{eff}	
	Value	σ		Value	σ
1	-1.55	0.08	25.0	0.00000	0.00000
2	-1.56	0.10	24.8	0.00000	0.00000
3	-1.46	0.13	25.4	0.00001	0.00000
4	-1.21	0.10	25.5	0.00001	0.00000
5	-1.02	0.13	25.2	0.00000	0.00000
6	-0.77	0.11	25.0	0.00000	0.00000
7	-0.85	0.12	25.6	0.00001	0.00000
8	-1.32	0.12	25.0	0.00000	0.00000
9	-1.32	0.12	25.3	0.00000	0.00000
10	-1.30	0.12	25.3	0.00000	0.00000
11	-1.28	0.13	25.2	0.00000	0.00000
12	-1.04	0.12	25.1	0.00000	0.00000
13	-1.30	0.13	25.2	0.00000	0.00000
14	-1.04	0.13	25.3	0.00000	0.00000
15	-1.26	0.12	25.4	0.00001	0.00000
16	-1.35	0.12	25.4	0.00001	0.00000
17	-1.43	0.12	25.4	0.00001	0.00000
18	2.58	0.14	24.9	0.00000	0.00000
19	1.93	0.10	25.5	-0.00001	0.00000
20	2.02	0.13	25.3	-0.00001	0.00000
21	1.87	0.10	25.4	-0.00001	0.00000
22	1.75	0.13	25.3	-0.00001	0.00000
23	1.77	0.10	25.4	-0.00001	0.00000
24	1.99	0.08	25.5	-0.00001	0.00000

3.2 Dimensions

The critical assembly can be modeled as a cylinder of water with two grid plates in it supporting a 45×45 square-pitched array of fuel rods centered on the axis of the cylinder. Not all of the array positions are fueled – some have no fuel rod. The model includes two dry wells surrounded by polyethylene outside of the fuel array that were used for radiation detection instruments. A cut-away perspective view of the benchmark model for Case 6 is shown in Figure 40. A layout of the benchmark model for Case 19 is shown in Figure 41.

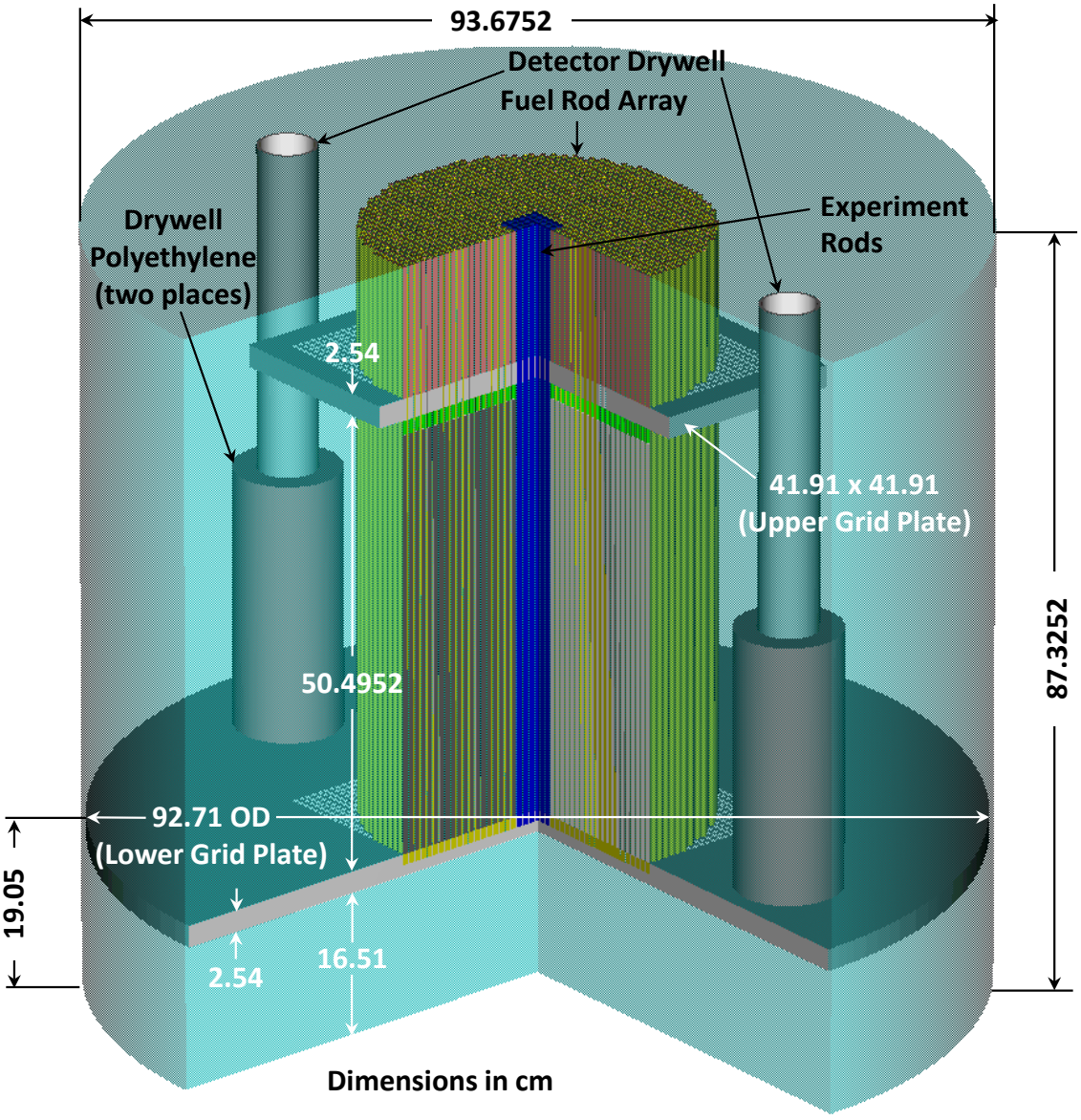

Figure 40. Cut-Away Perspective View of the Benchmark Model of Case 6.

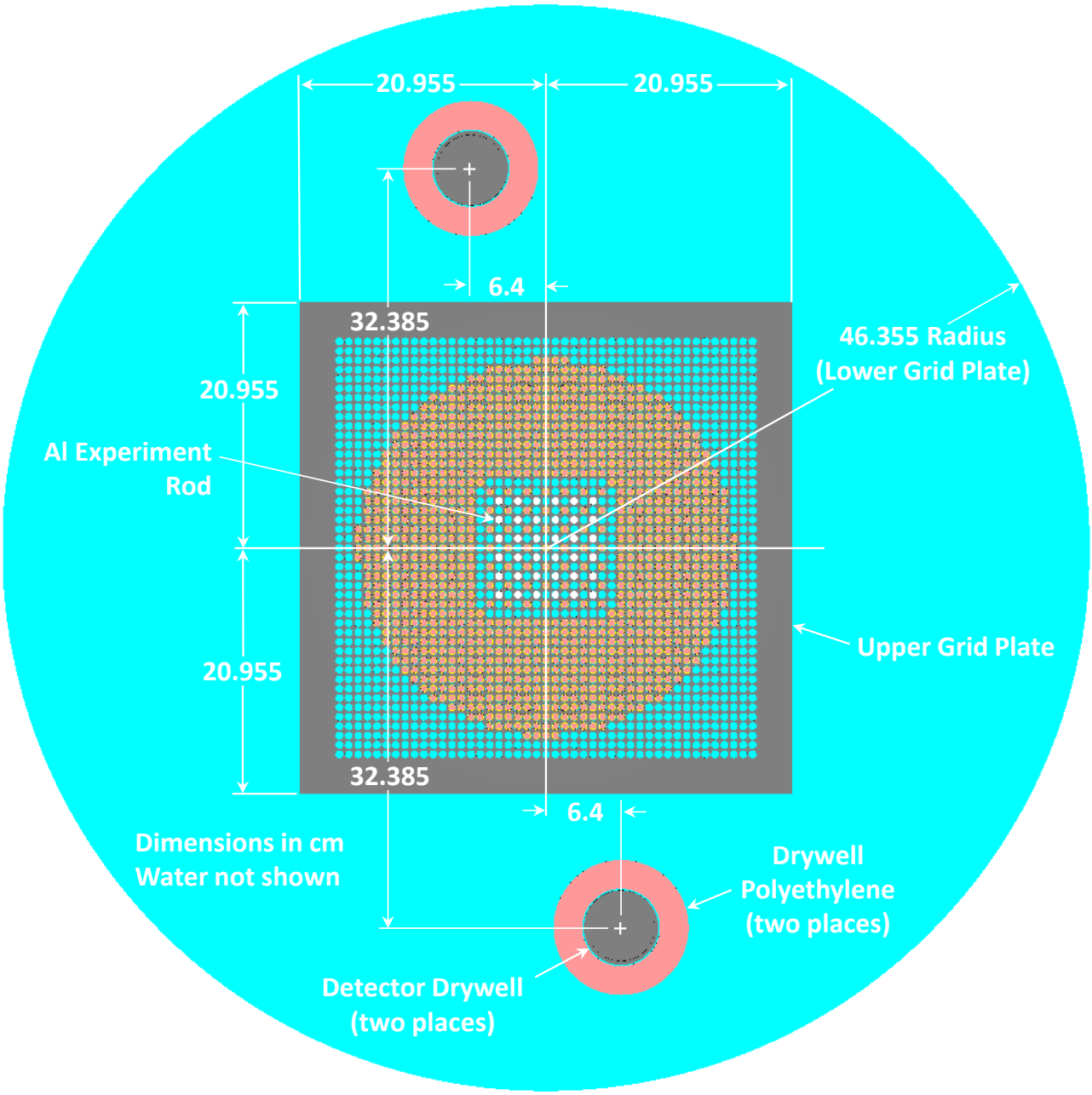

Figure 41. Layout of the Benchmark Model of Case 19.

The water moderator and reflector is a right circular cylinder 93.6752 cm in diameter and 87.3252 cm tall. The lower grid plate is a 6061 aluminum cylinder 92.71 cm diameter and 2.54 cm thick centered on the axis of the moderator cylinder. The top of the lower grid plate is 19.05 cm above the bottom of the water cylinder. The lower grid plate has a 45×45 square-pitched array of blind 0.333375 cm radius cylindrical holes bored from the top surface 1.27 cm deep that support the fuel rods from the bottom. The upper grid plate is a 41.91cm square 2.54 cm thick centered on the axis of the water cylinder. The bottom of the upper grid plate is 50.4952 cm above the top surface of the lower grid plate. The upper grid plate has a 45×45 square-pitched array of 0.333375 cm radius through holes bored in it to locate the fuel rods in the array. The pitch of the fuel rod array is 0.8001 cm.

The fuel rods in the model extend from the bottom of the holes in the lower grid plate to the surface of the water. In the description that follows, the upper surface of the lower grid plate, also the axial location of the bottom of the fuel in the fuel rods, is the origin of the axial coordinates. The fuel rods are 0.317474 cm radius right-circular cylinders. Figure 42 shows a schematic of several fuel rods in the model. Table 70 lists modeling information by axial interval for the fuel rods. Table 71 lists similar information for array positions that are unfueled.

Table 70. Axial and Radial Modeling Information for a Fuel Rod.

Position (cm)				Material
Axial[(a)]		Radial[(b)]		
From	To	From	To	
-2.54	-1.27	0.0	Cell[(c)]	Grid Plate 6061 Aluminum
-1.27	0.0	0.0	0.317474	Cladding 3003 Aluminum
		0.317474	0.333375	Water
		0.333375	Cell	Grid Plate 6061 Aluminum
0.0	48.780	0.0	0.262814	UO_2
		0.262814	0.284519	Void
		0.284519	0.317474	Cladding 3003 Aluminum
		0.317474	Cell	Water
48.780	50.4952	0.0	0.17526	Void
		0.17526	0.2286	Spring 304 Stainless Steel
		0.2286	0.284519	Void
		0.284519	0.317474	Cladding 3003 Aluminum
		0.317474	Cell	Water
50.4952	53.0352	0.0	0.26289	6061 Aluminum
		0.26289	0.284519	Void
		0.284519	0.317474	Cladding 3003 Aluminum
		0.317474	0.333375	Water
		0.333375	Cell	Grid Plate 6061 Aluminum
53.0352	68.2752	0.0	0.26289	Polyethylene
		0.26289	0.284519	Void
		0.284519	0.317474	Cladding 3003 Aluminum
		0.317474	Cell	Water

(a) The origin of the axial coordinates is the top of the lower grid plate.
(b) The origin of the radial coordinates is the axial center of the 0.8001×0.8001 cm square cell
(c) "Cell" refers to the boundary of the square cell in the array. Each surface of the cell is 0.40005 cm from the central axis of the cell.

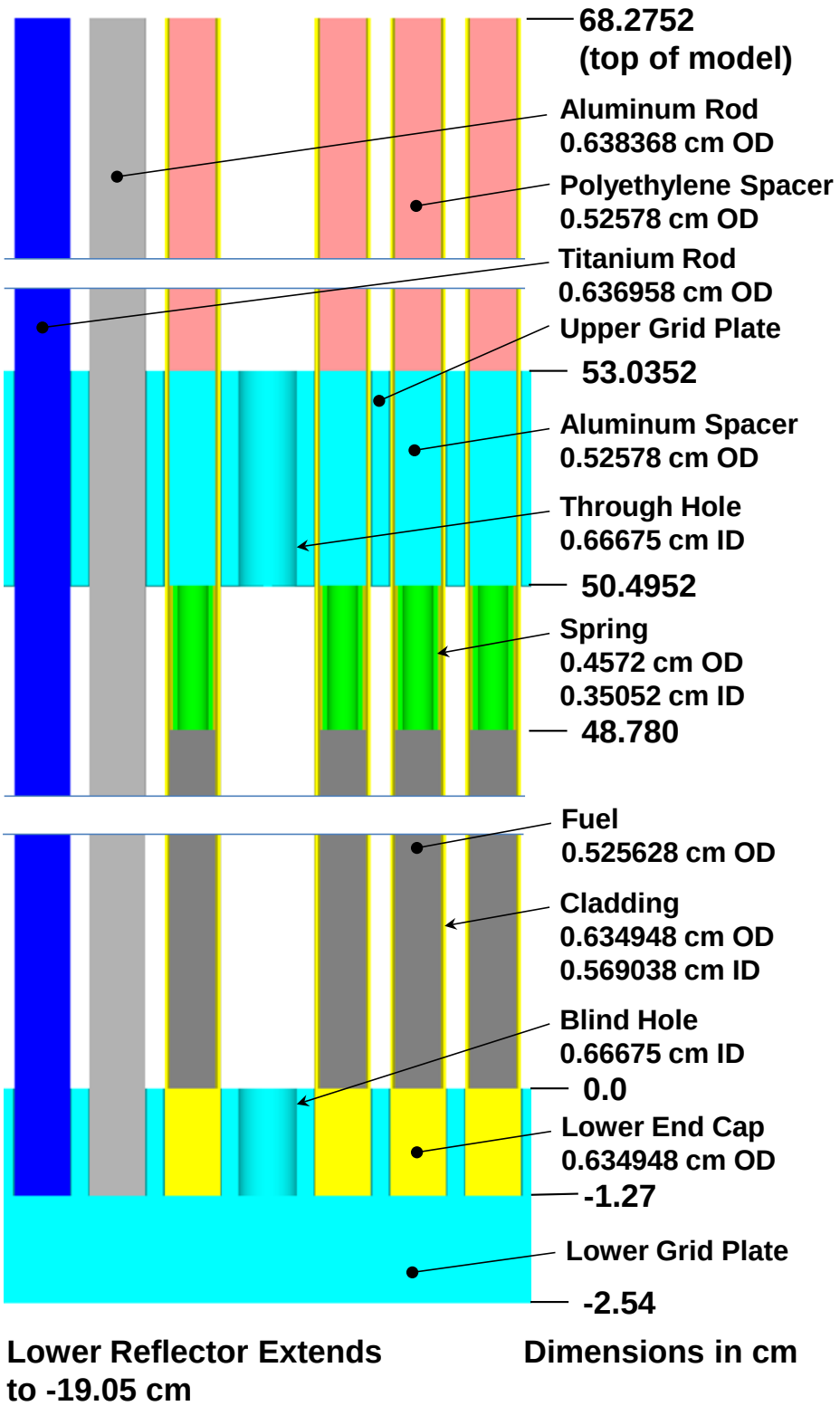

Figure 42. Schematic of the Fuel Rods in the Model.

Table 71. Axial and Radial Modeling Information for an Empty Grid Location

Position (cm)				Material
Axial[a]		Radial[b]		
From	To	From	To	
-2.54	-1.27	0.0	Cell[c]	Grid Plate 6061 Aluminum
-1.27	0.0	0.0	0.333375	Water
		0.333375	Cell	Grid Plate 6061 Aluminum
0.0	50.4952	0.0	Cell	Water
50.4952	53.0352	0.0	0.333375	Water
		0.333375	Cell	Grid Plate 6061 Aluminum
53.0352	68.2752	0.0	Cell	Water

(a) The origin of the axial coordinates is the top of the lower grid plate.
(b) The origin of the radial coordinates is the axial center of the 0.8001×0.8001 cm square cell
(c) "Cell" refers to the boundary of the square cell in the array. Each surface of the cell is 0.40005 cm from the central axis of the cell.

Table 72 lists modeling information by axial interval for the titanium experiment rods.

Table 72. Axial and Radial Modeling Information for a Titanium Experiment Rod.

Position (cm)				Material
Axial[a]		Radial[b]		
From	To	From	To	
-2.54	-1.27	0.0	Cell[c]	Grid Plate 6061 Aluminum
-1.27	0.0	0.0	0.318479	Titanium Experiment Rod
		0.318479	0.333375	Water
		0.333375	Cell	Grid Plate 6061 Aluminum
0.0	50.4952	0.0	0.318479	Titanium Experiment Rod
		0.318479	Cell	Water
50.4952	53.0352	0.0	0.318479	Titanium Experiment Rod
		0.318479	0.333375	Water
		0.333375	Cell	Grid Plate 6061 Aluminum
53.0352	68.2752	0.0	0.318479	Titanium Experiment Rod
		0.318479	Cell	Water

(a) The origin of the axial coordinates is the top of the lower grid plate.
(b) The origin of the radial coordinates is the axial center of the 0.8001×0.8001 cm square cell.
(c) "Cell" refers to the boundary of the square cell in the array. Each surface of the cell is 0.40005 cm from the central axis of the cell.

Table 73 lists modeling information by axial interval for the aluminum experiment rods.

Table 73. Axial and Radial Modeling Information for an Aluminum Experiment Rod.

Position (cm)				Material
Axial[a]		Radial[b]		
From	To	From	To	
-2.54	-1.27	0.0	Cell[c]	Grid Plate 6061 Aluminum
-1.27	0.0	0.0	0.319368	Aluminum Experiment Rod
		0.319368	0.333375	Water
		0.333375	Cell	Grid Plate 6061 Aluminum
0.0	50.4952	0.0	0.319368	Aluminum Experiment Rod
		0.319368	Cell	Water
50.4952	53.0352	0.0	0.319368	Aluminum Experiment Rod
		0.319368	0.333375	Water
		0.333375	Cell	Grid Plate 6061 Aluminum
53.0352	68.2752	0.0	0.319368	Aluminum Experiment Rod
		0.319368	Cell	Water

(a) The origin of the axial coordinates is the top of the lower grid plate.
(b) The origin of the radial coordinates is the axial center of the 0.8001×0.8001 cm square cell.
(c) "Cell" refers to the boundary of the square cell in the array. Each surface of the cell is 0.40005 cm from the central axis of the cell.

All configurations include two 6.35 cm outside diameter 6061 aluminum tubes surrounded by polyethylene that function as dry wells for the assembly instrumentation. With the origin of the coordinate system at the center of the top surface of the lower grid plate and the z-axis aligned with the axis of the water cylinder, the axis of one of the dry wells is located at x=-6.4 cm, y=32.385 cm while the axis of the other is located at x=6.4cm, y=-32.385 cm. Figure 43 shows an elevation view of the assembly with a cut-away view of one of the detector wells. Table 74 gives modeling details for the dry wells.

Table 74. Axial and Radial Modeling Information for a Dry Well.

Position (cm)				Material
Axial[(a)]		Radial[(b)]		
From	To	From	To	
0.0	0.635	0.0	3.175	6061 Aluminum
0.635	0.762	0.0	2.8575	Void
		2.8575	3.175	6061 Aluminum
0.762	30.7848	0.0	2.8575	Void
		2.8575	3.175	6061 Aluminum
		3.175	3.30581	Water
		3.30581	5.75945	Polyethylene
30.7848	68.2752	0.0	2.8575	Void
		2.8575	3.175	6061 Aluminum

(a) The origin of the axial coordinates is the top of the lower grid plate.
(b) The origin of the radial coordinates is the axial center of the dry well

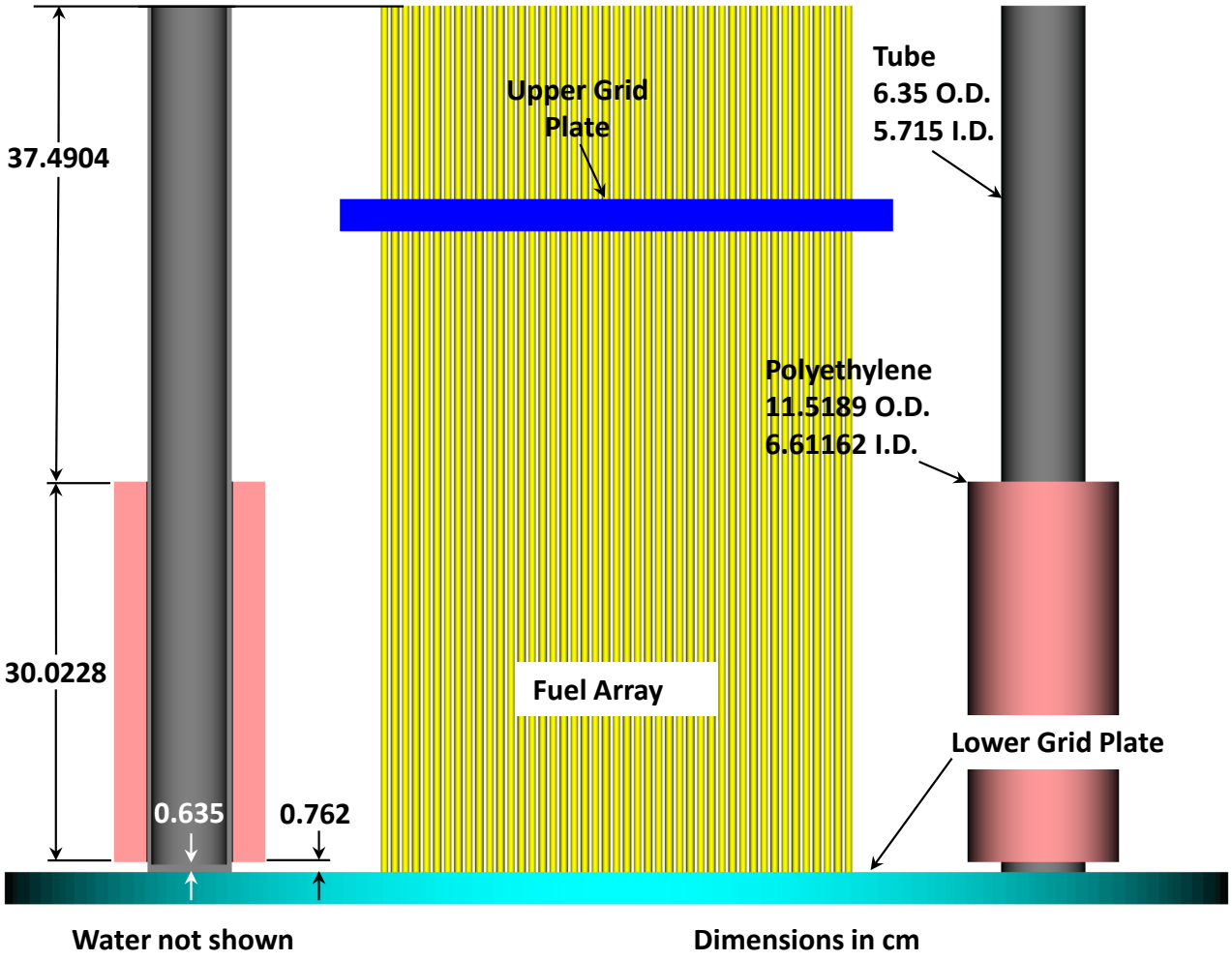

Figure 43. Elevation View of the Benchmark Model Showing a Cut-Away View of One of the Detector Wells.

The layout of the fuel rods in the 45×45 array in Cases 1 through 24 are shown in Figures 44 through 67.

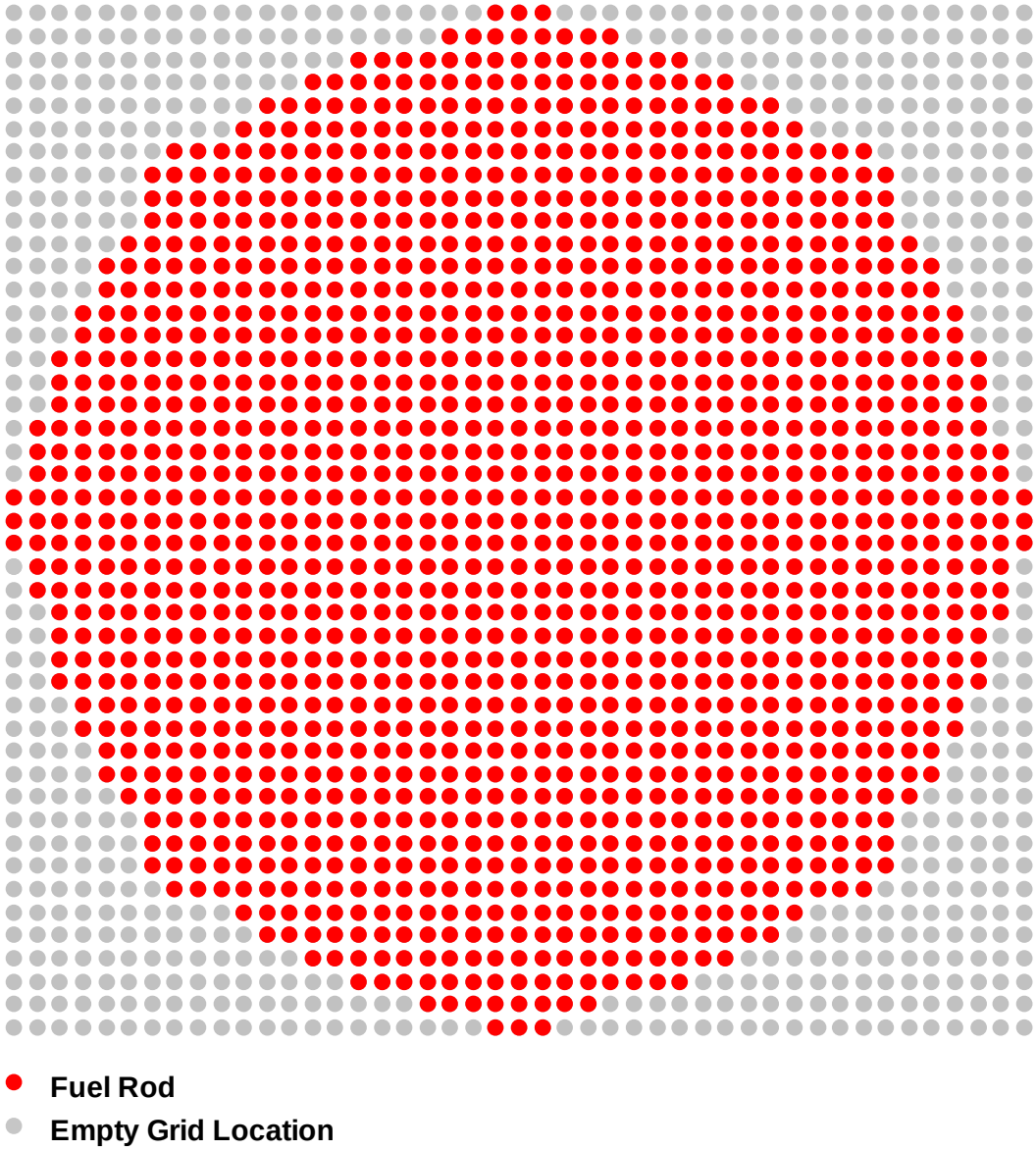

Figure 44. 1457 Fuel Rod Layout for Case 1.

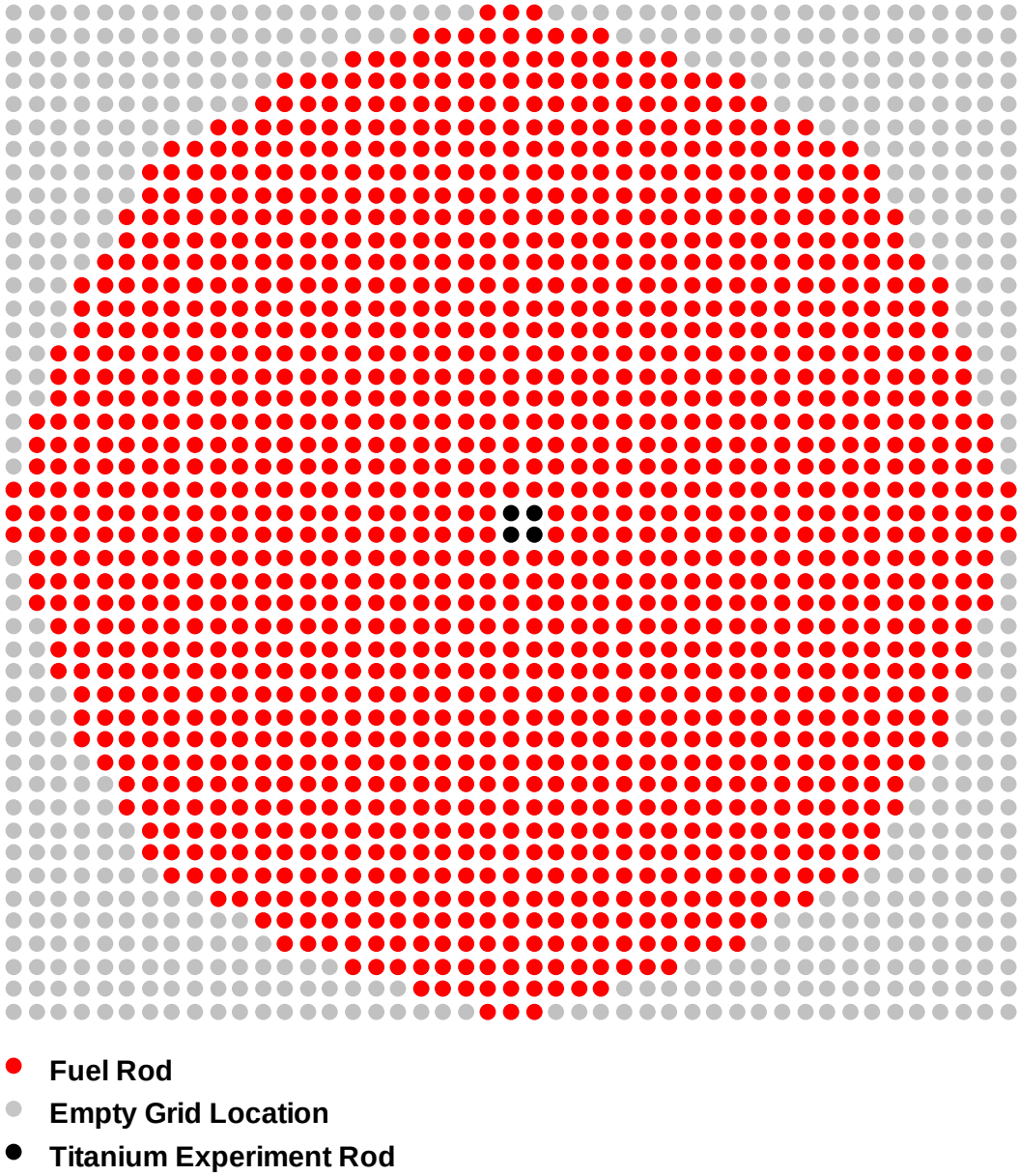

Figure 45. Array Layout for Case 2 (1473 Fuel Rods, 4 Titanium Experiment Rods).

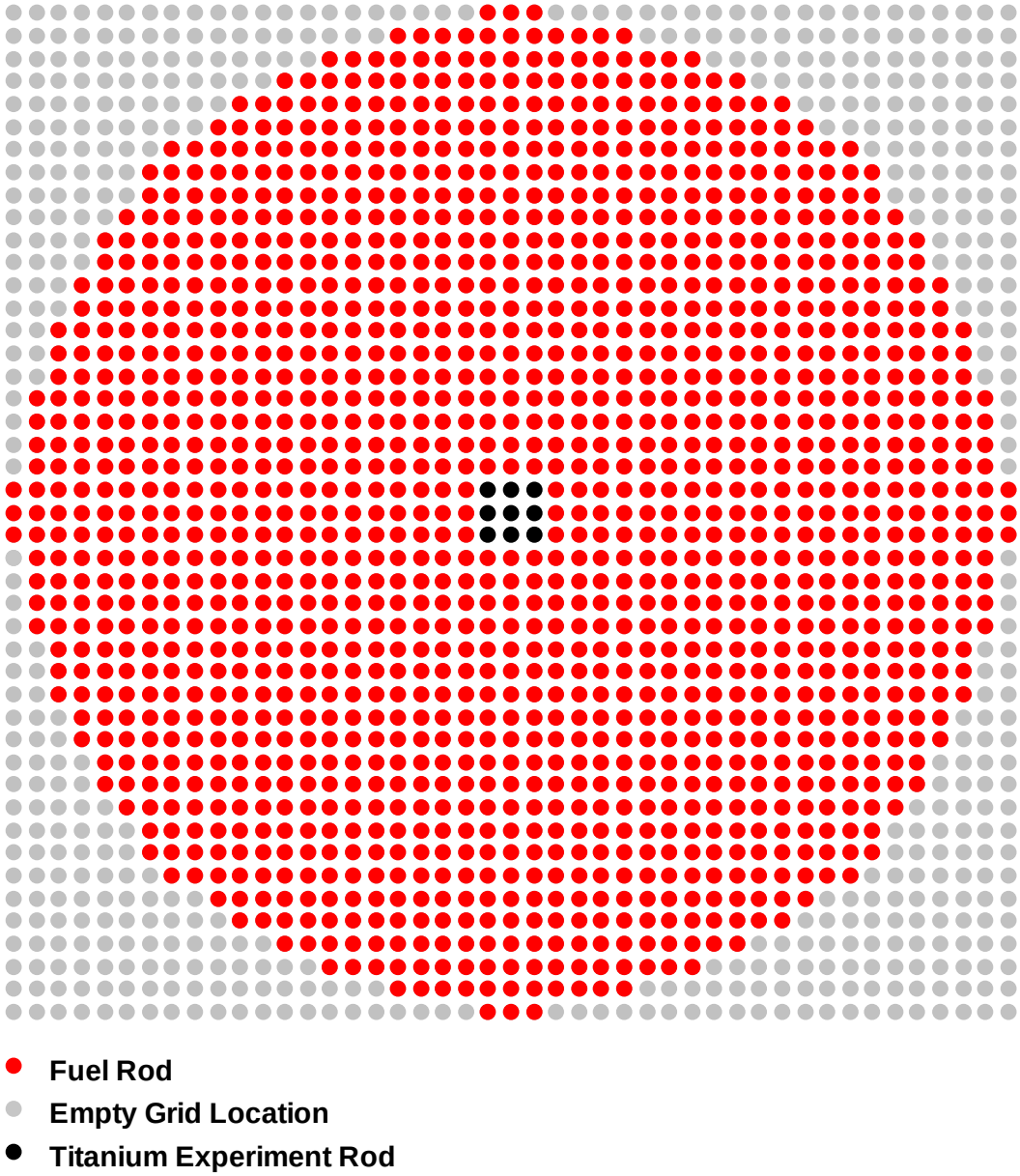

Figure 46. Array Layout for Case 3 (1492 Fuel Rods, 9 Titanium Experiment Rods).

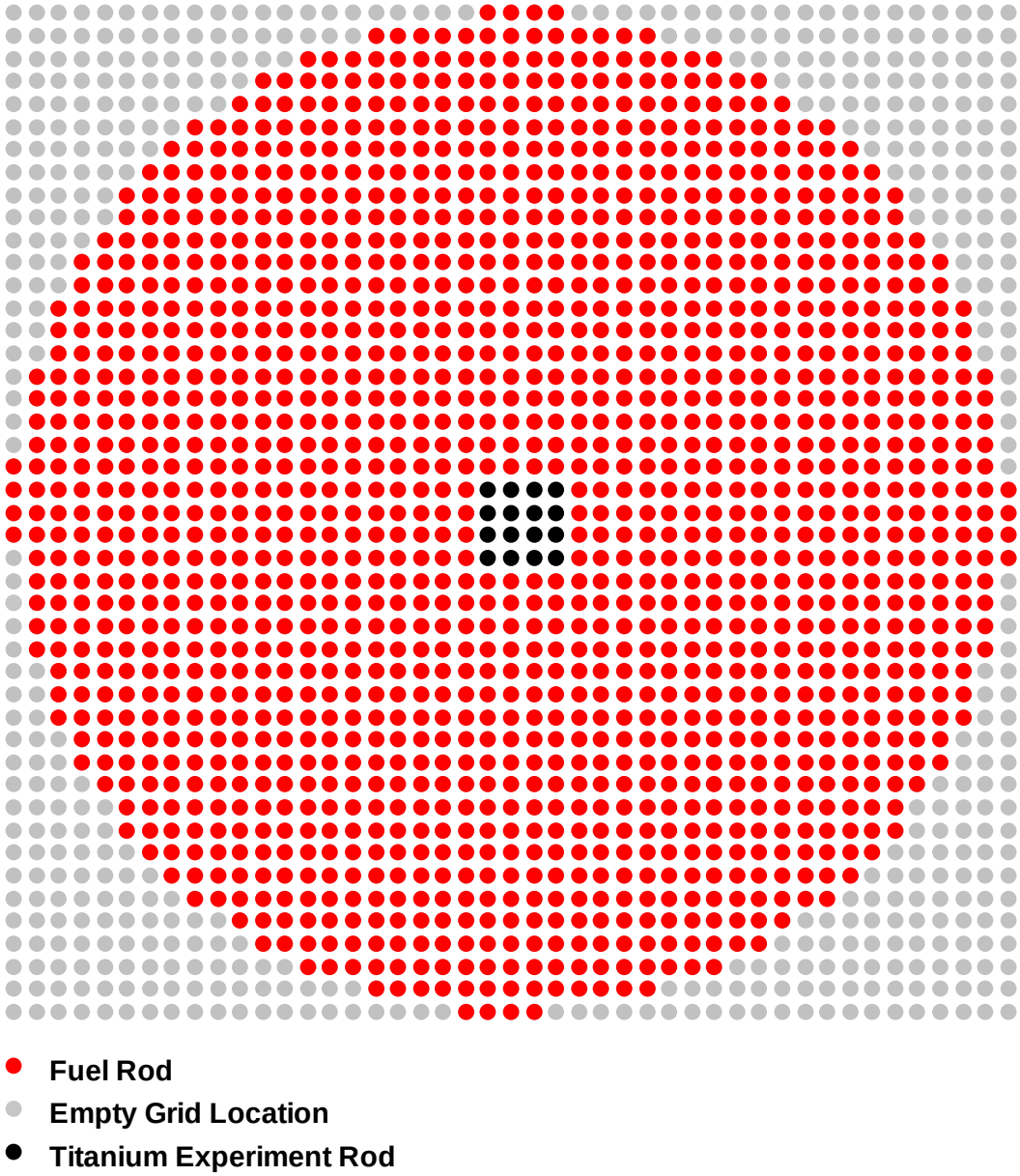

Figure 47. Array Layout for Case 4 (1521 Fuel Rods, 16 Titanium Experiment Rods).

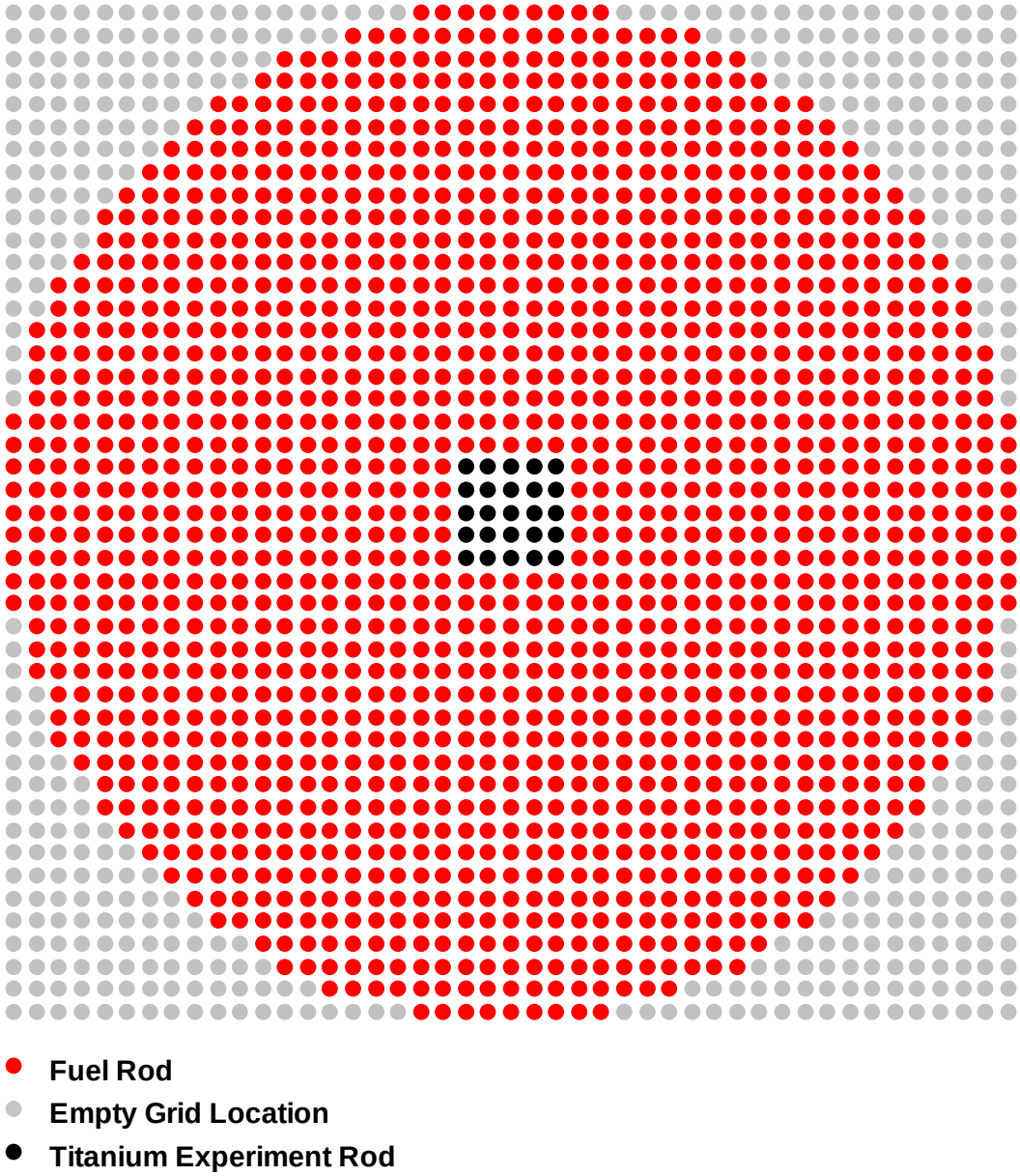

Figure 48. Array Layout for Case 5 (1560 Fuel Rods, 25 Titanium Experiment Rods).

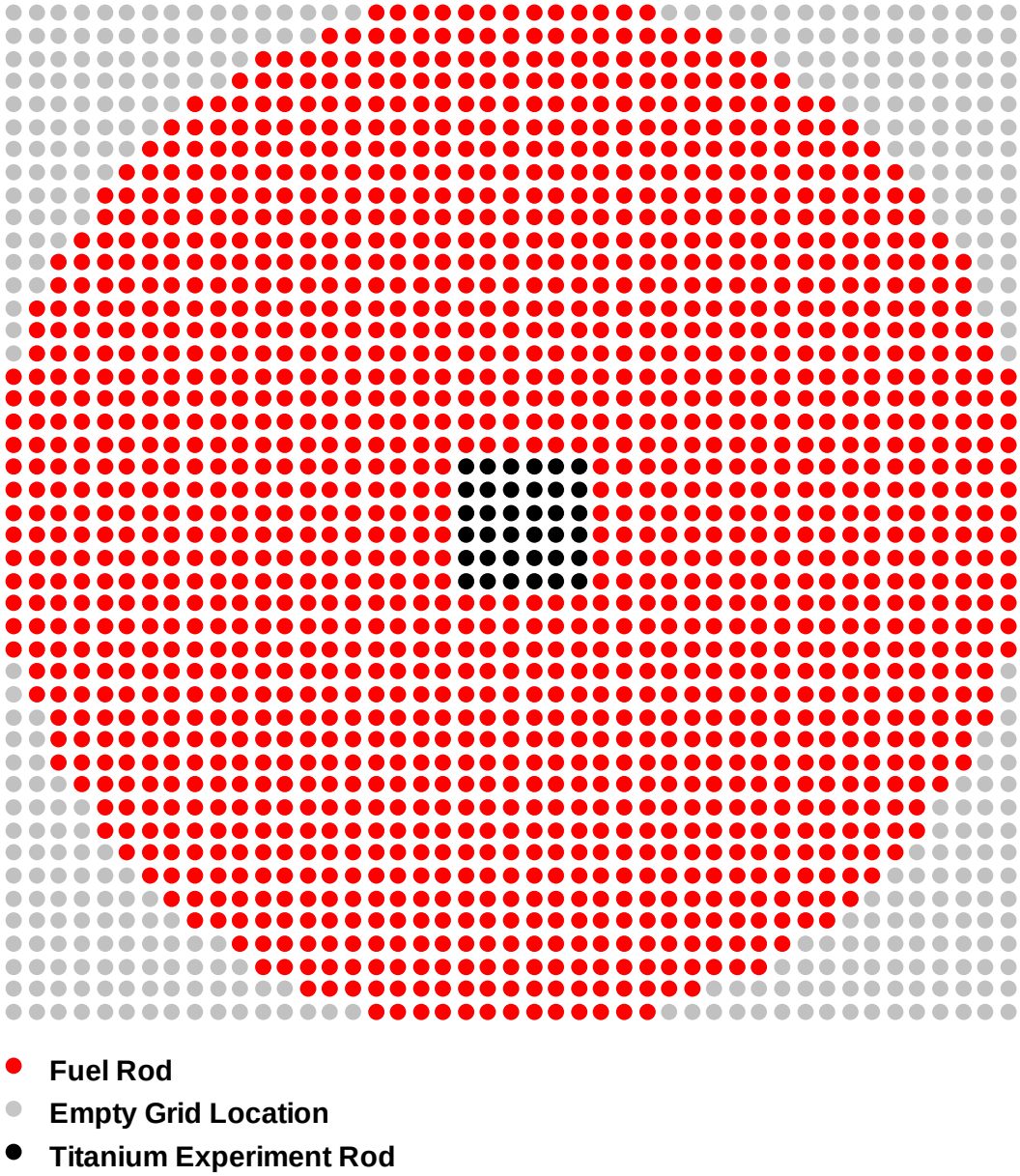

Figure 49. Array Layout for Case 6 (1609 Fuel Rods, 36 Titanium Experiment Rods).

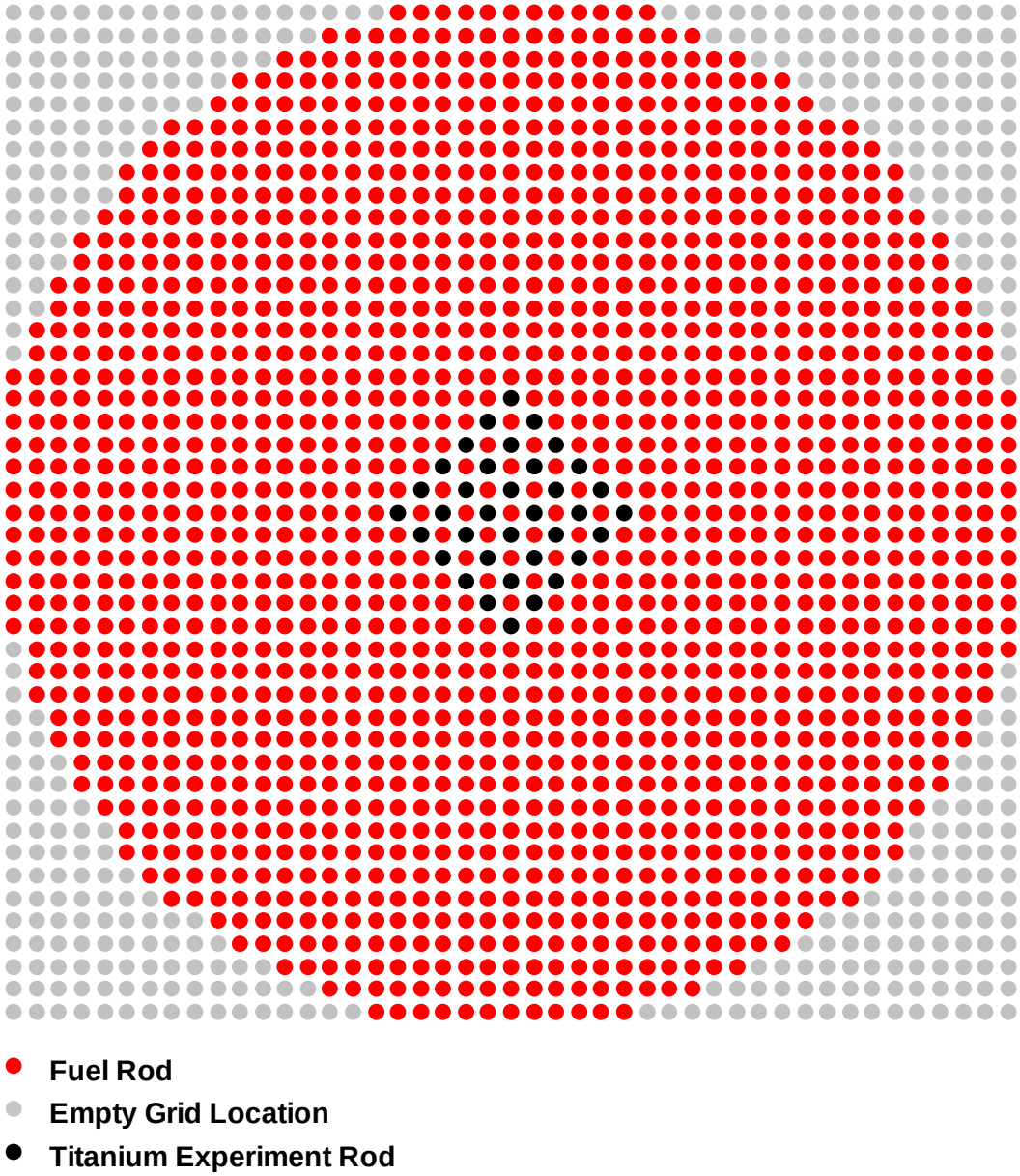

Figure 50. Array Layout for Case 7 (1585 Fuel Rods, 36 Titanium Experiment Rods).

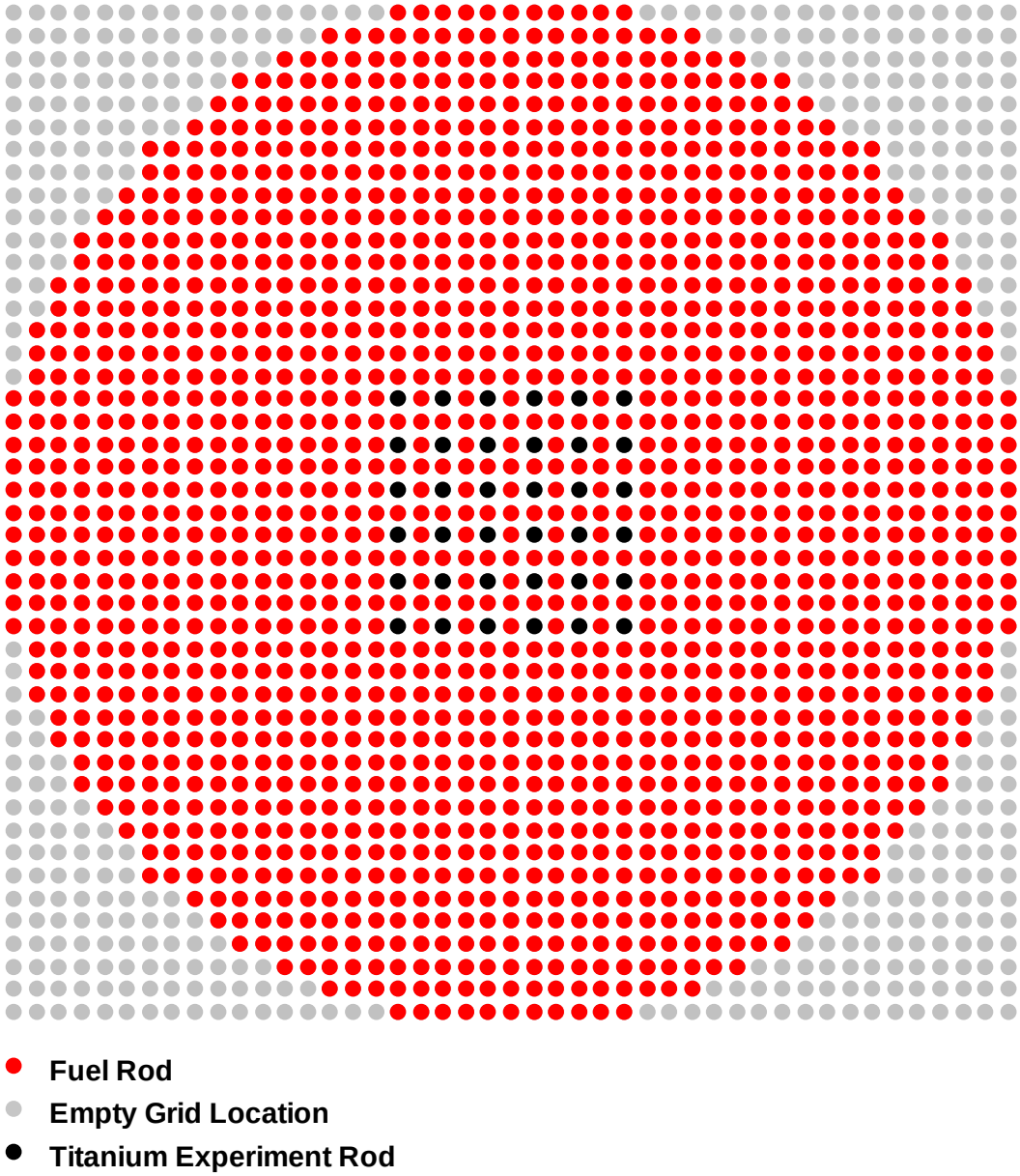

Figure 51. Array Layout for Case 8 (1573 Fuel Rods, 36 Titanium Experiment Rods).

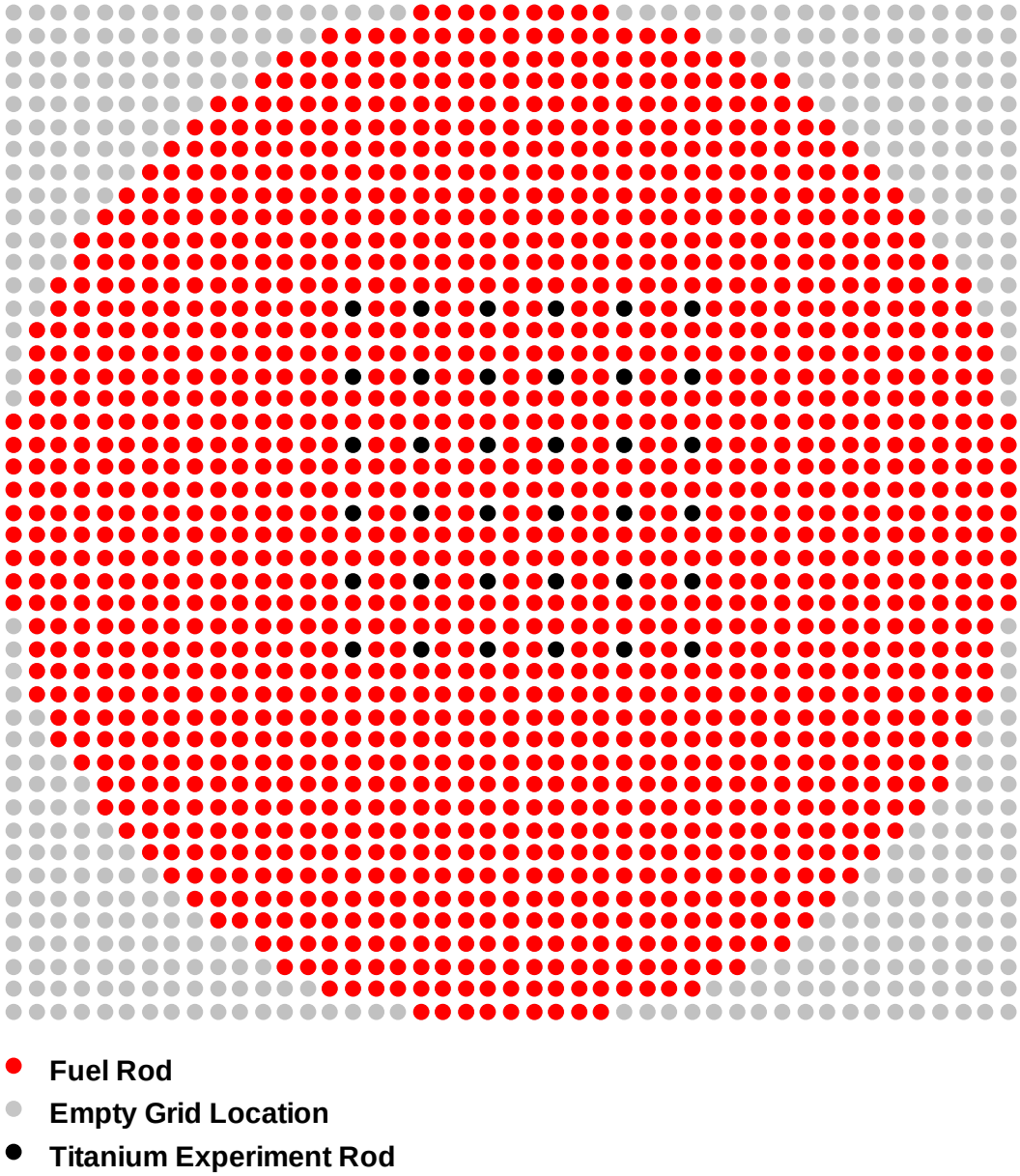

Figure 52. Array Layout for Case 9 (1557 Fuel Rods, 36 Titanium Experiment Rods).

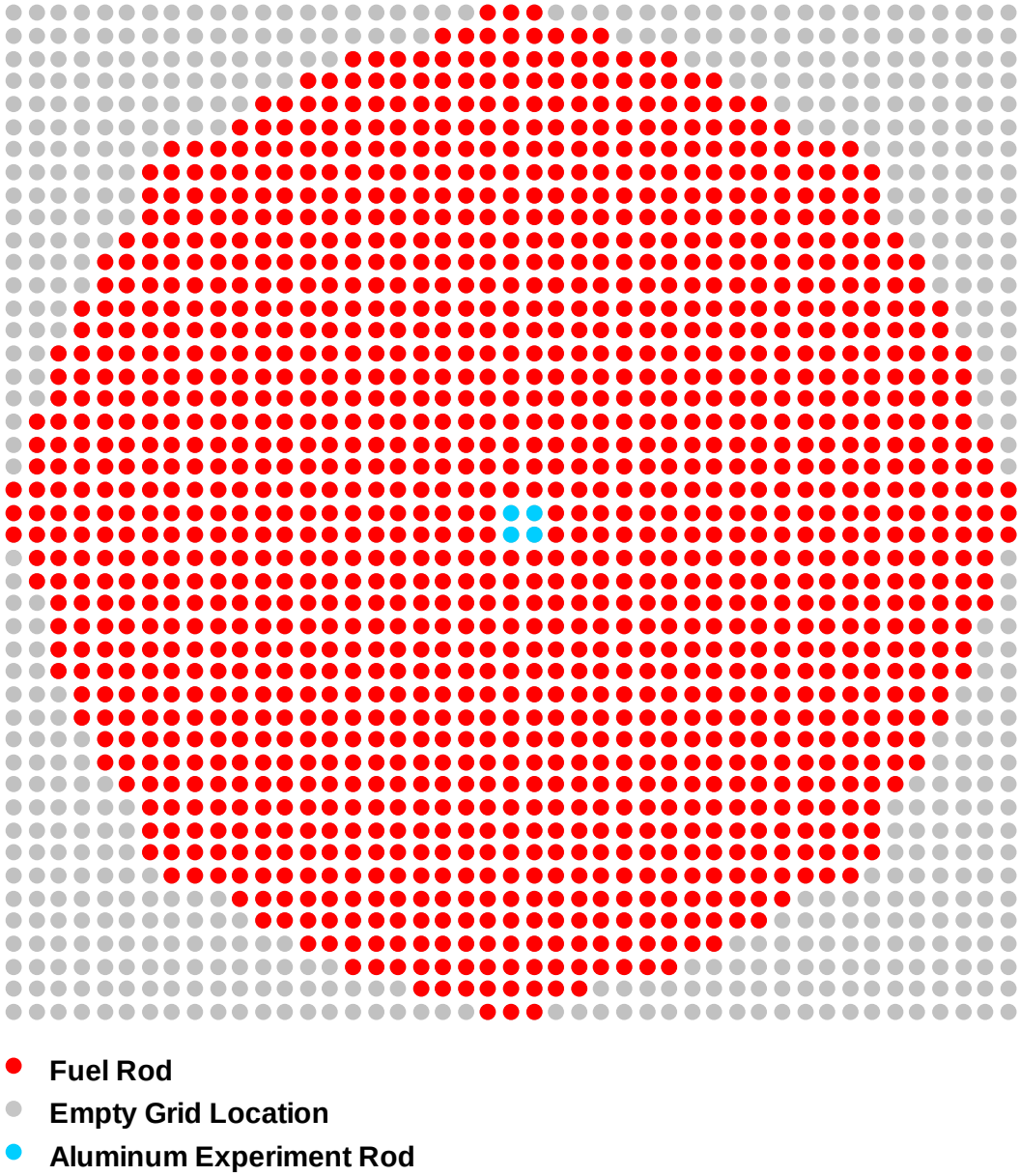

Figure 53. Array Layout for Case 10 (1453 Fuel Rods, 4 Aluminum Experiment Rods).

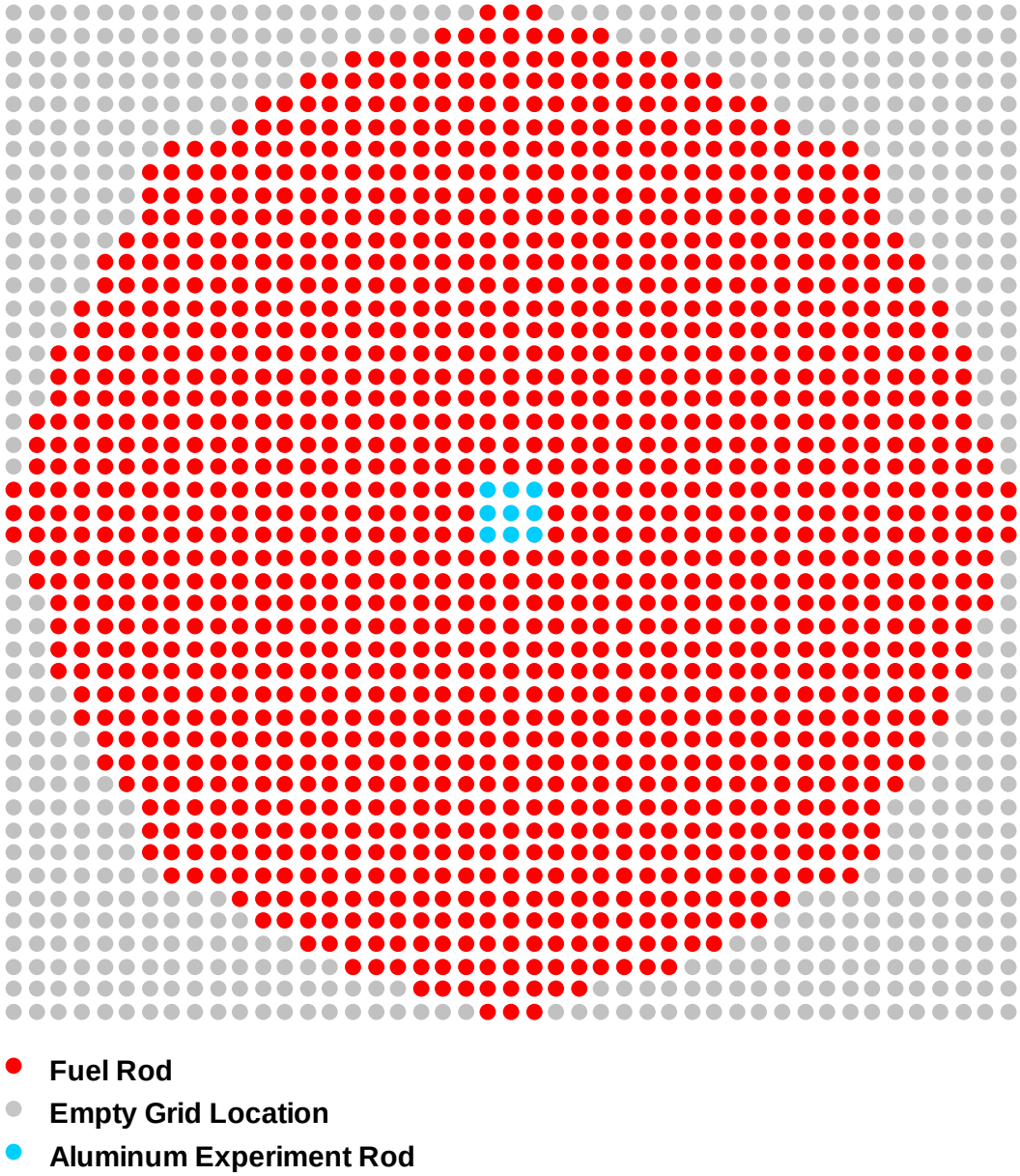

Figure 54. Array Layout for Case 11 (1448 Fuel Rods, 9 Aluminum Experiment Rods).

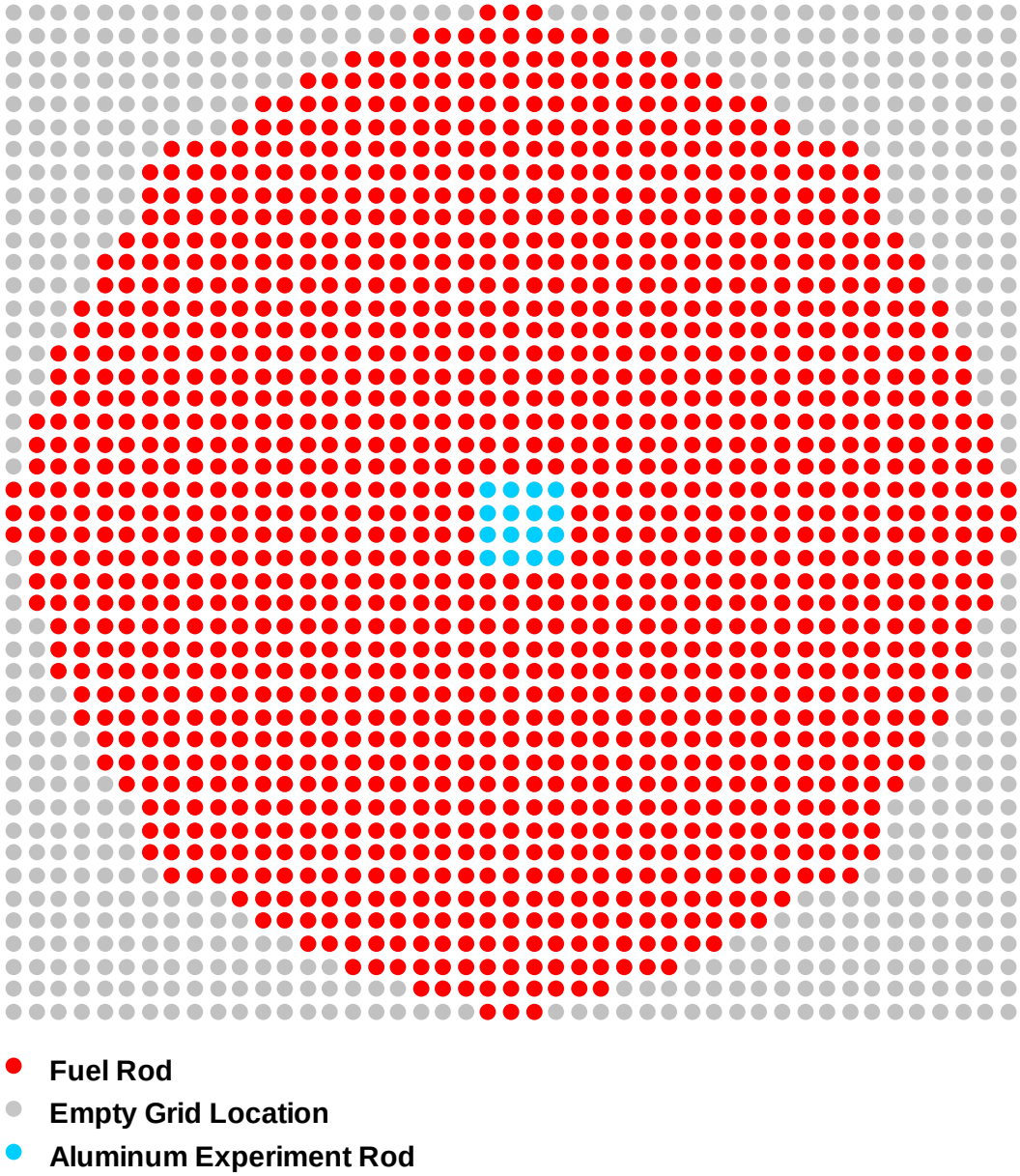

Figure 55. Array Layout for Case 12 (1445 Fuel Rods, 16 Aluminum Experiment Rods).

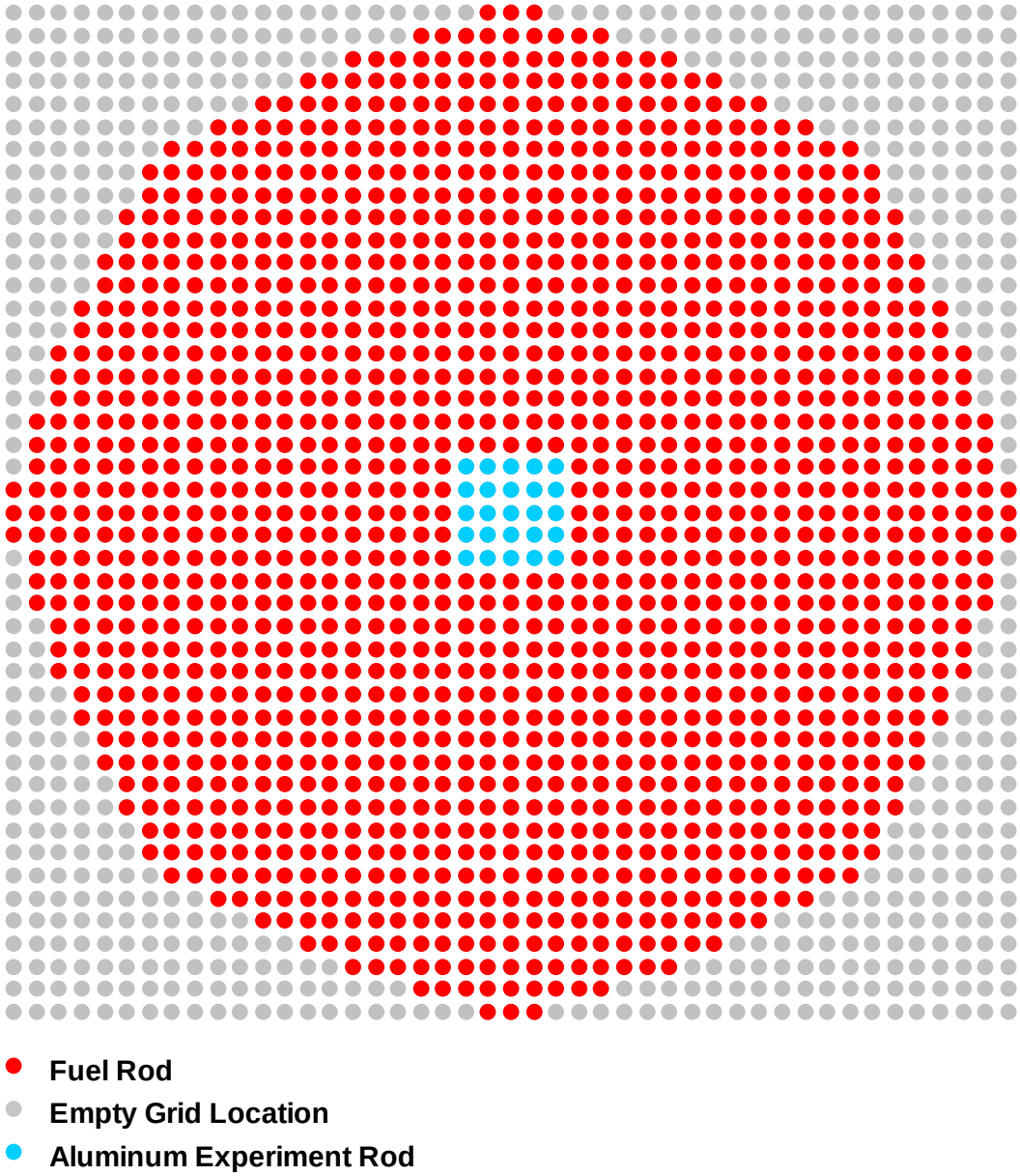

Figure 56. Array Layout for Case 13 (1444 Fuel Rods, 25 Aluminum Experiment Rods).

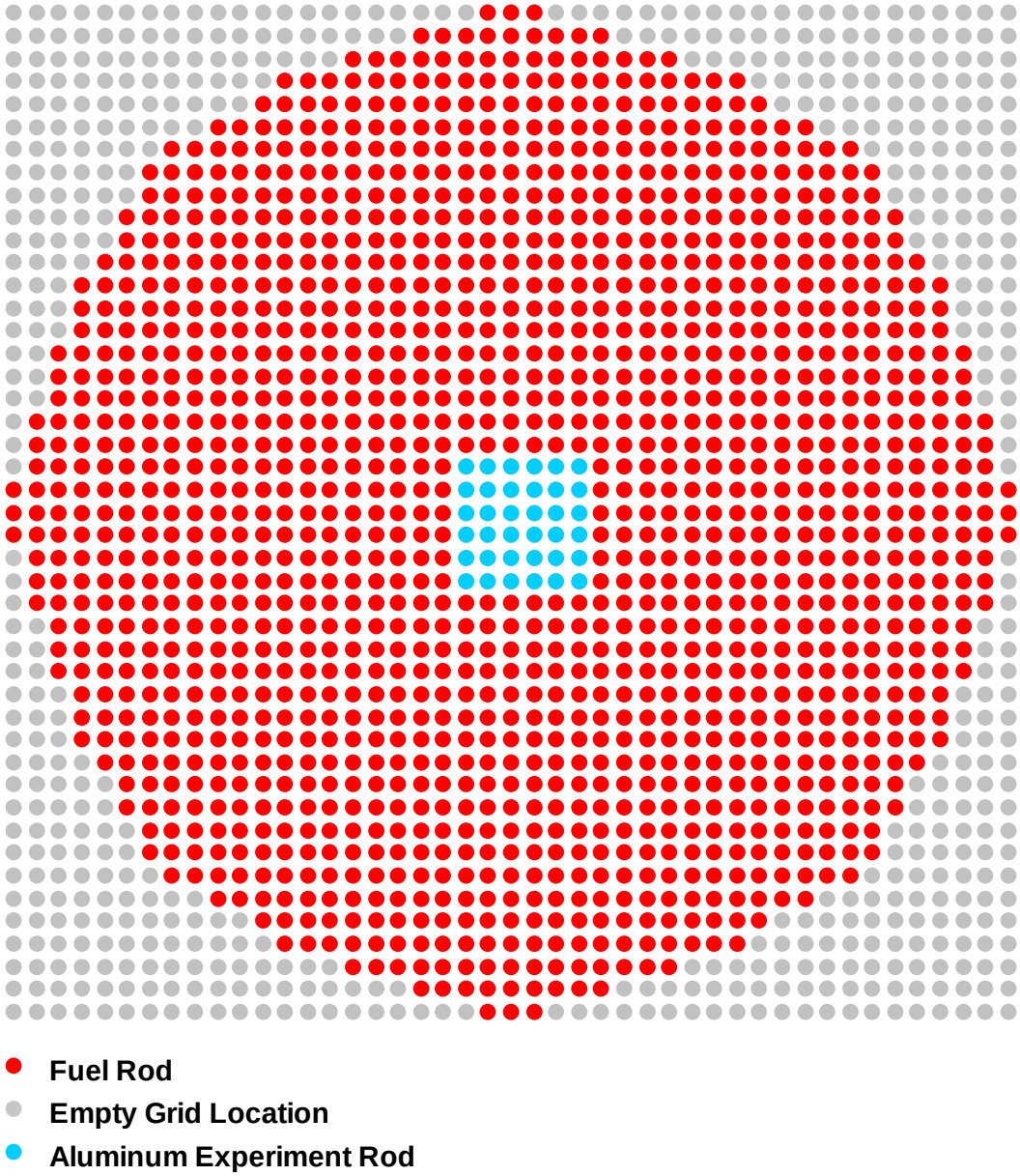

Figure 57. Array Layout for Case 14 (1441 Fuel Rods, 36 Aluminum Experiment Rods).

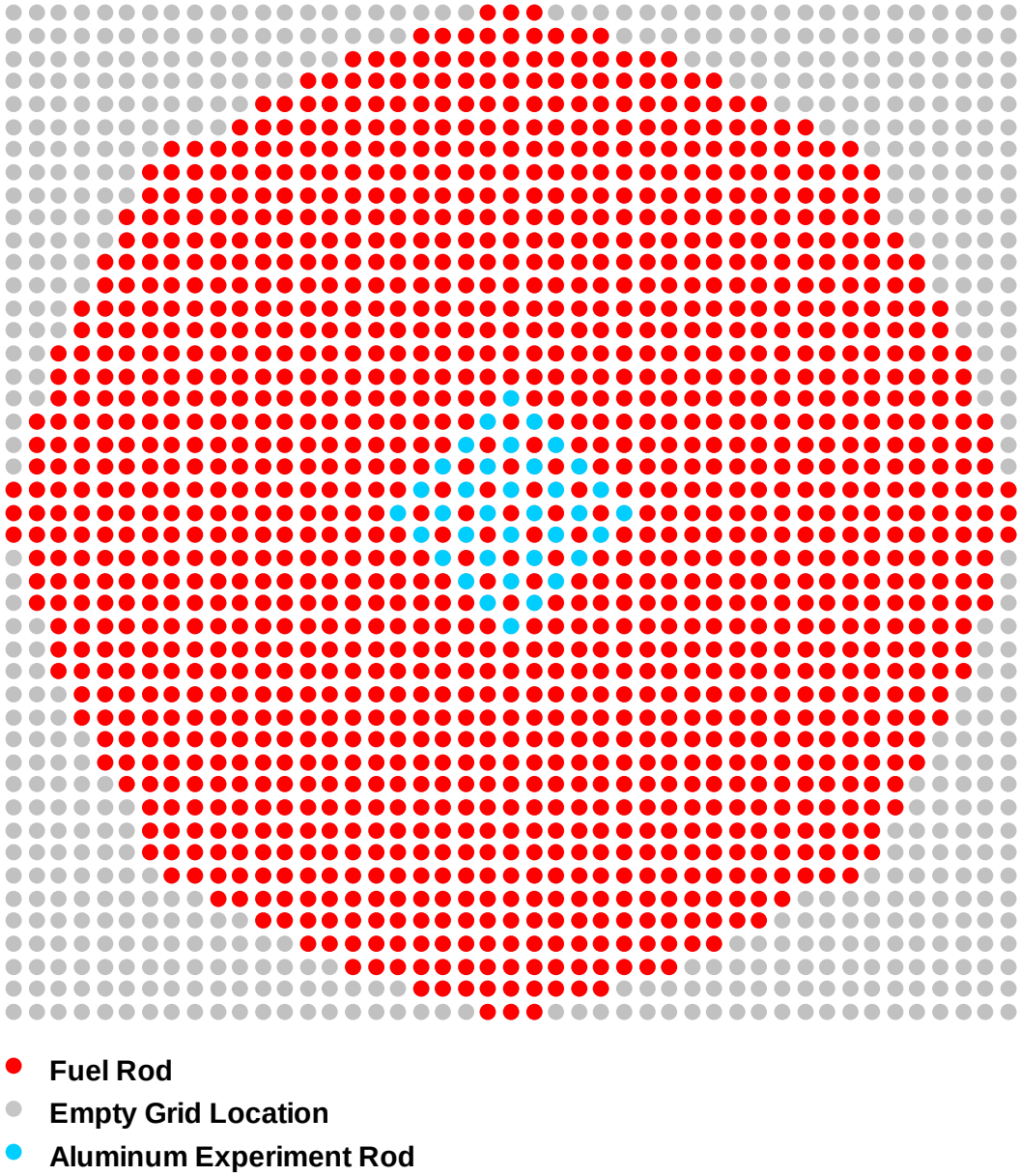

Figure 58. Array Layout for Case 15 (1429 Fuel Rods, 36 Aluminum Experiment Rods).

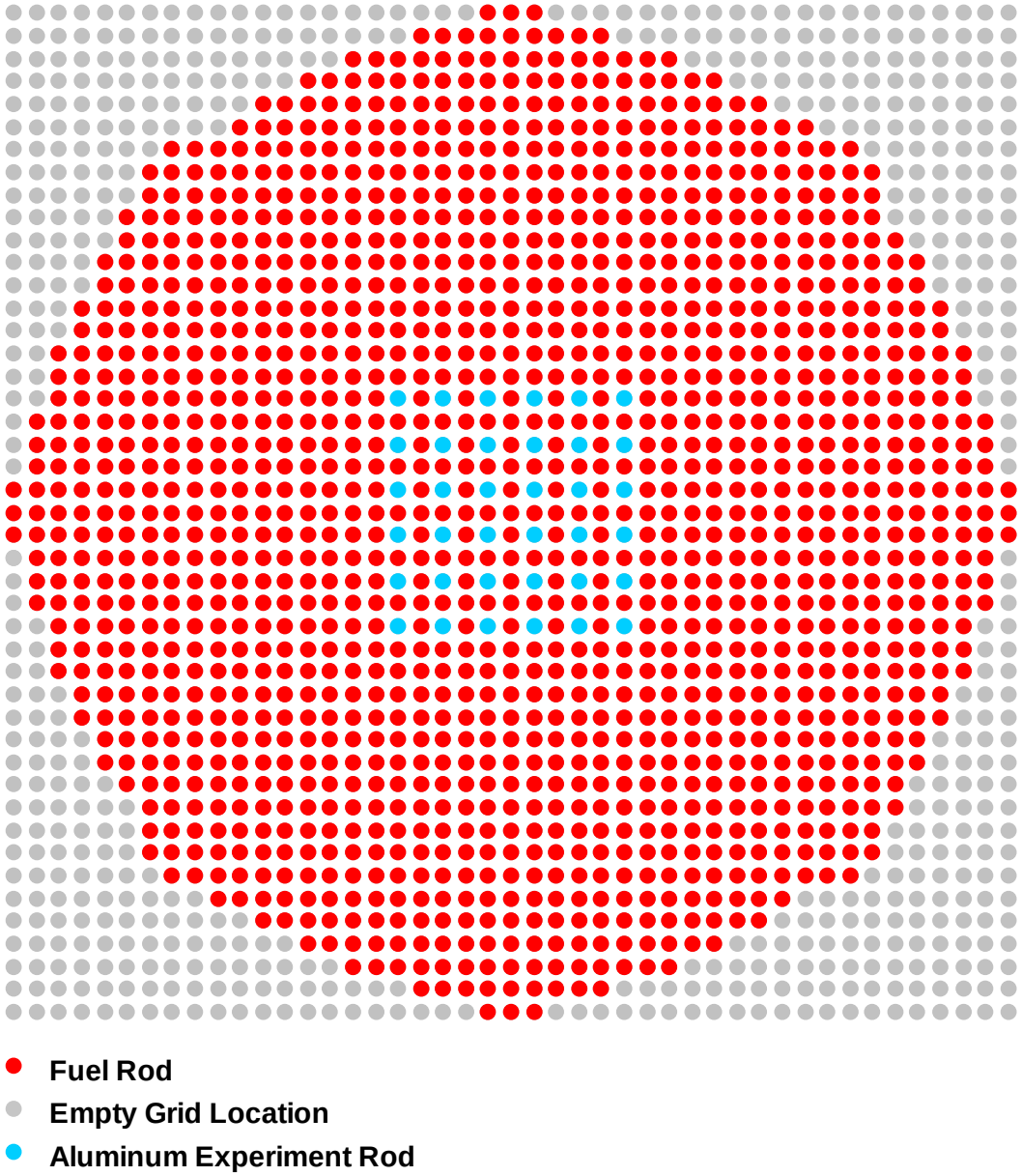

Figure 59. Array Layout for Case 16 (1429 Fuel Rods, 36 Aluminum Experiment Rods).

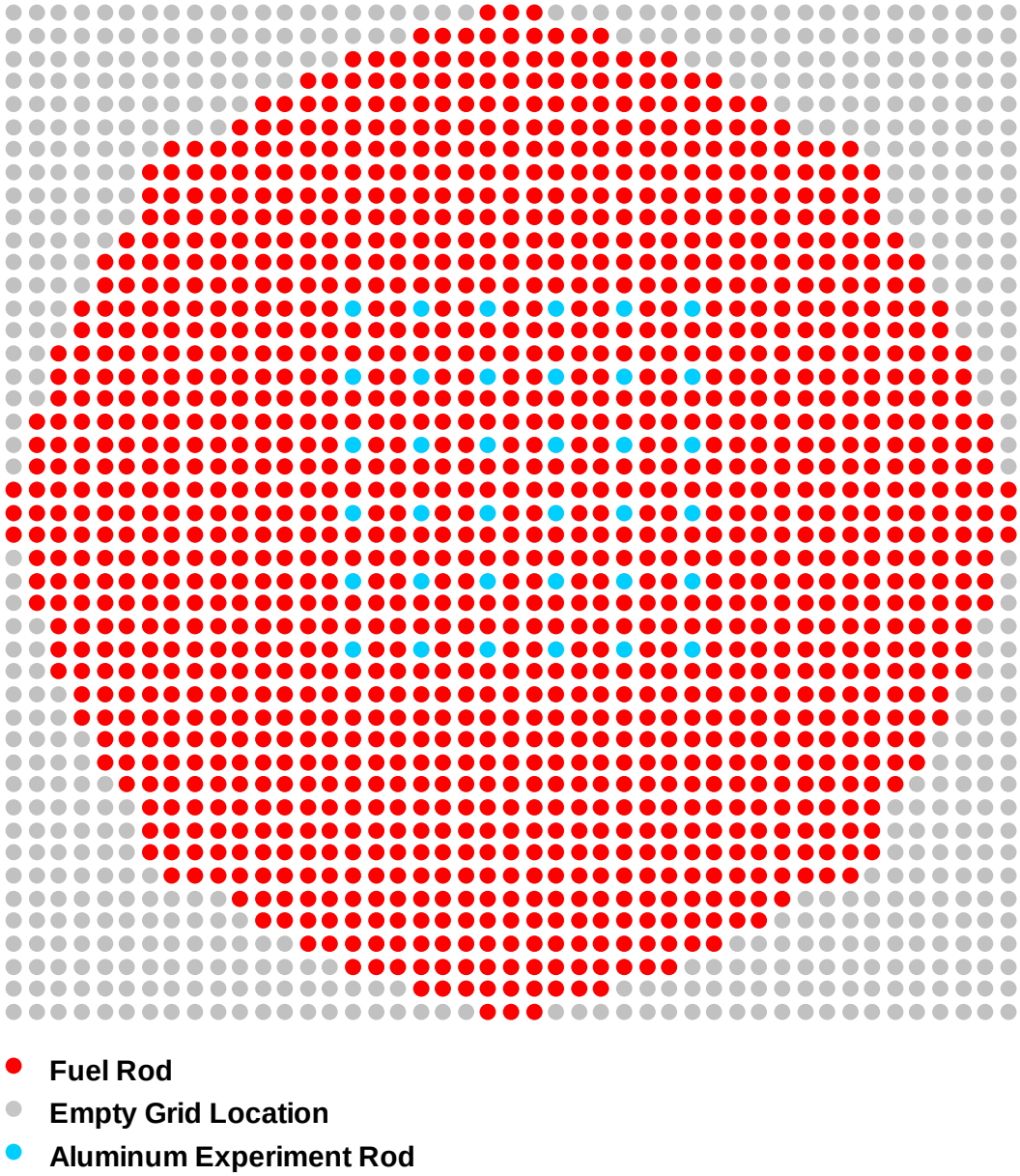

Figure 60. Array Layout for Case 17 (1425 Fuel Rods, 36 Aluminum Experiment Rods).

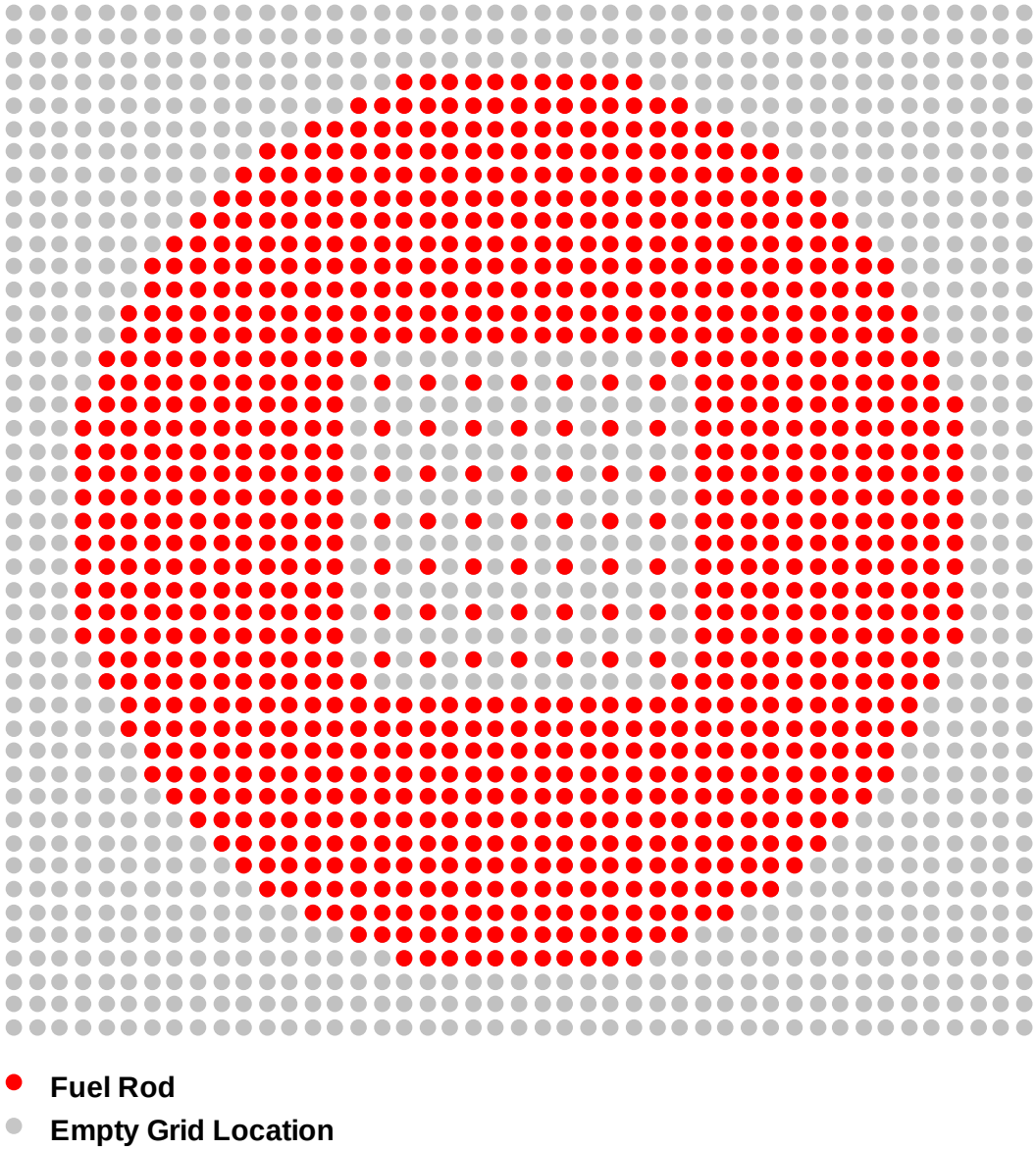

Figure 61. Array Layout for Case 18 (1037 Fuel Rods).

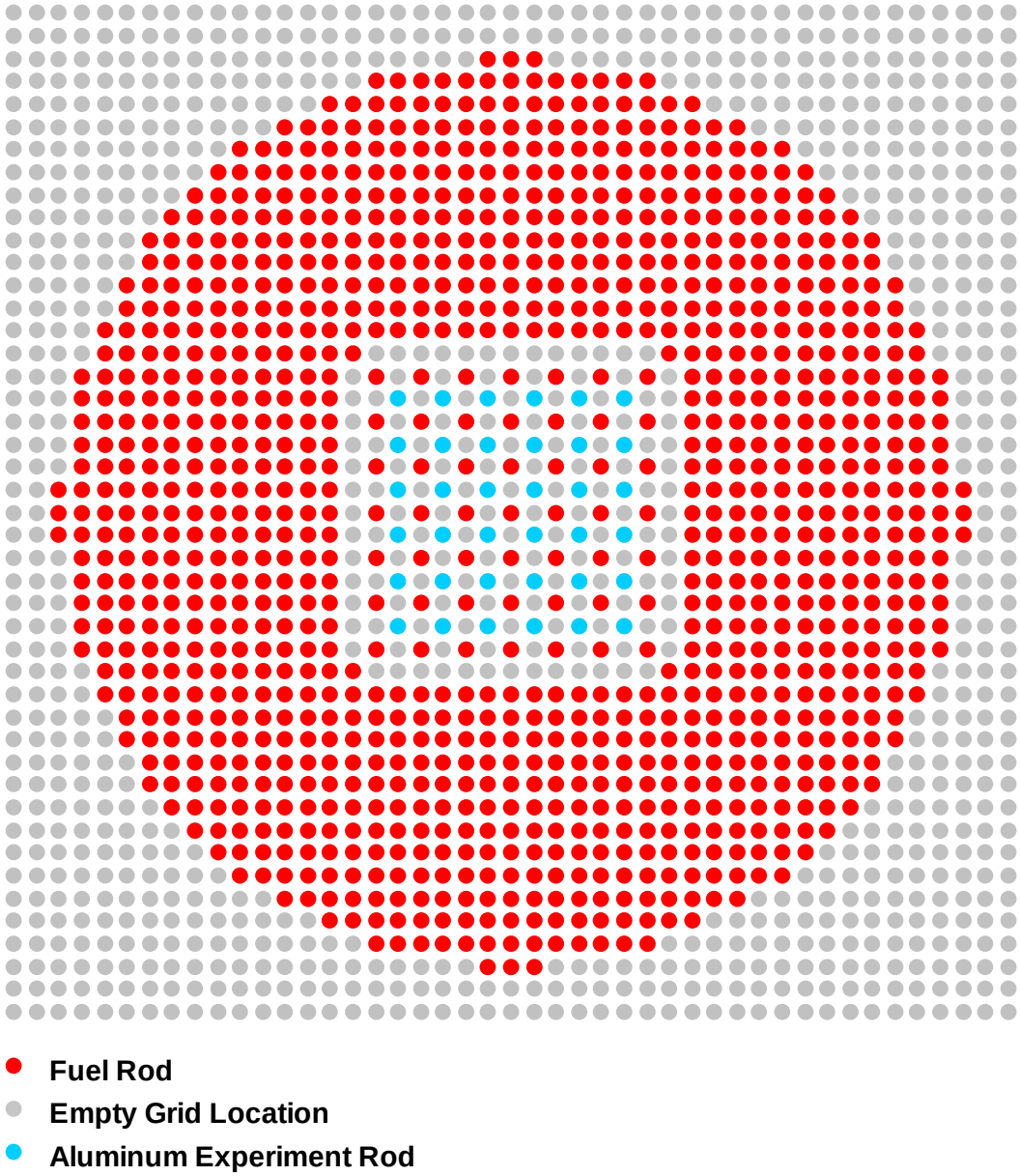

Figure 62. Array Layout for Case 19 (1097 Fuel Rods, 36 Aluminum Experiment Rods).

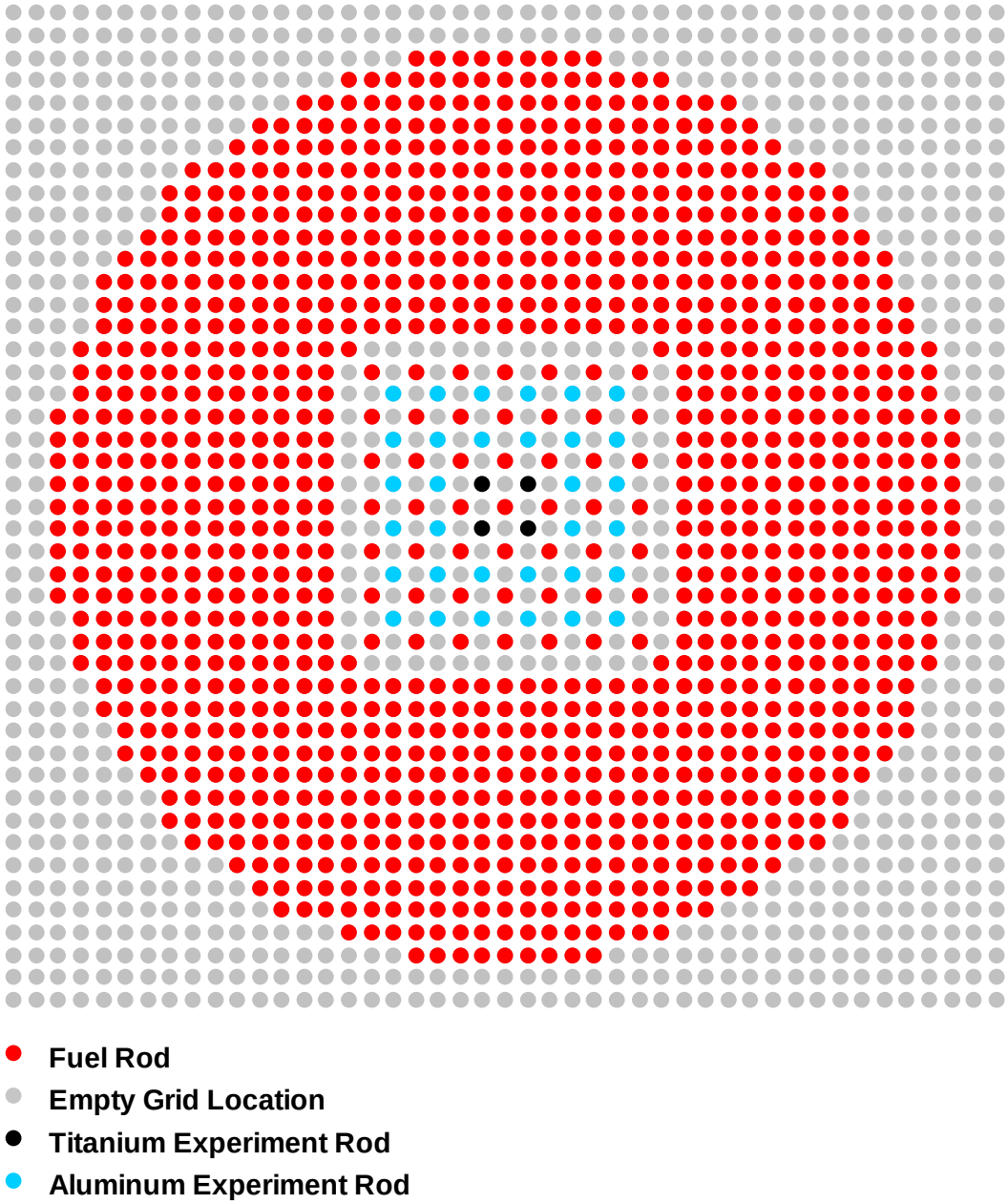

Figure 63. Array Layout for Case 20 (1153 Fuel Rods, 4 Titanium Experiment Rods, 32 Aluminum Experiment Rods).

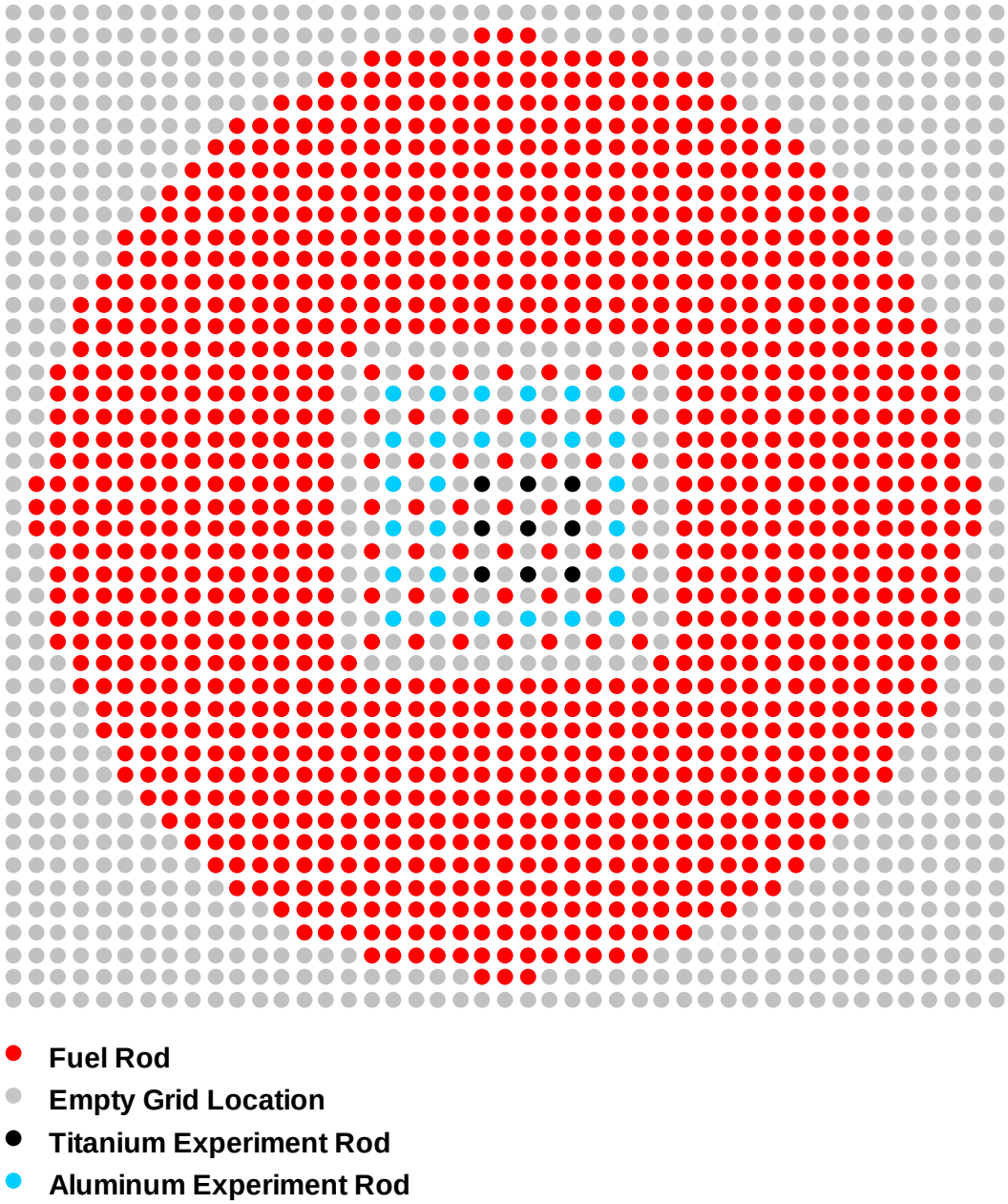

Figure 64. Array Layout for Case 21 (1213 Fuel Rods, 9 Titanium Experiment Rods, 27 Aluminum Experiment Rods).

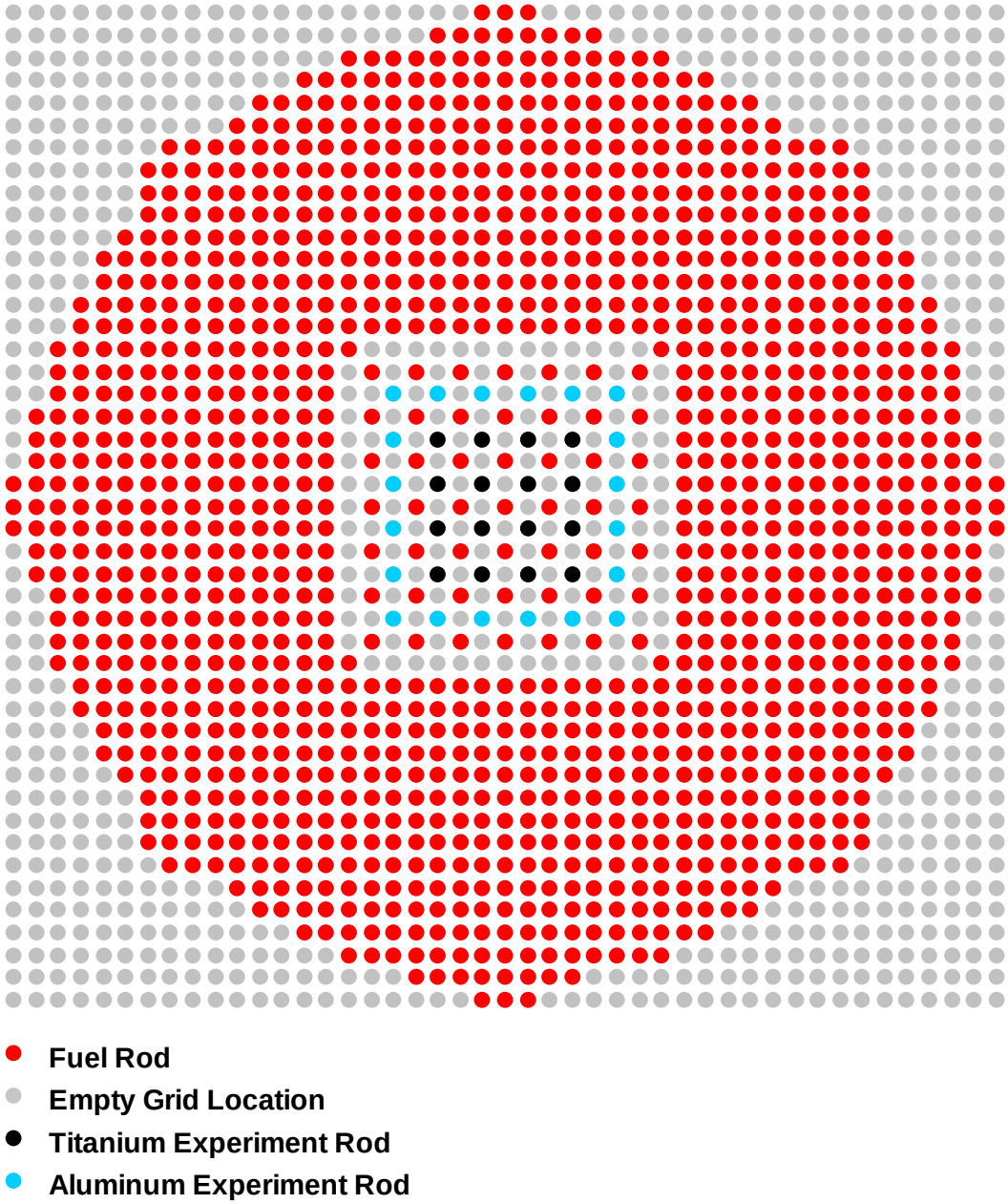

Figure 65. Array Layout for Case 22 (1285 Fuel Rods, 16 Titanium Experiment Rods, 20 Aluminum Experiment Rods).

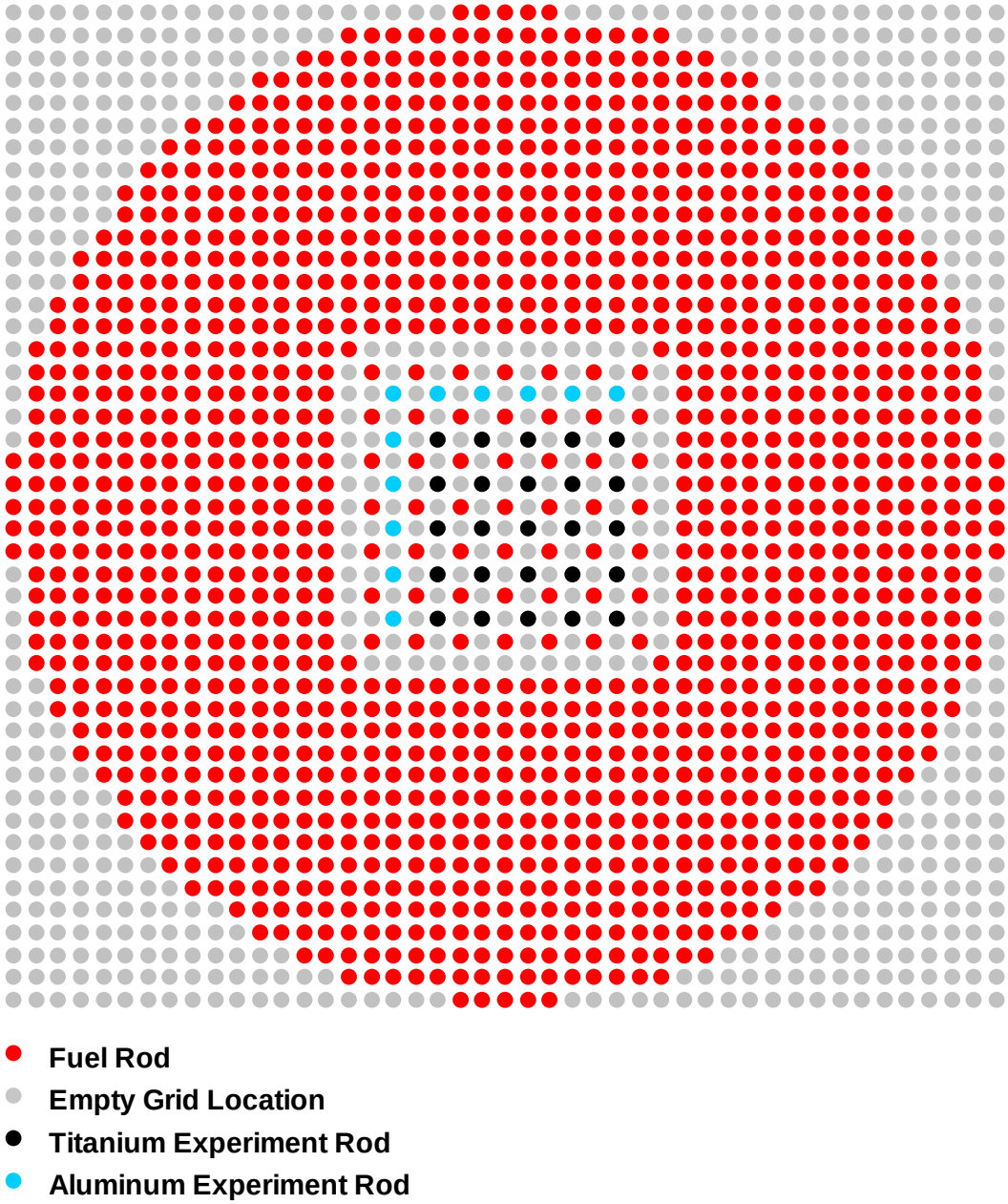

Figure 66. Array Layout for Case 23 (1377 Fuel Rods, 25 Titanium Experiment Rods, 11 Aluminum Experiment Rods).

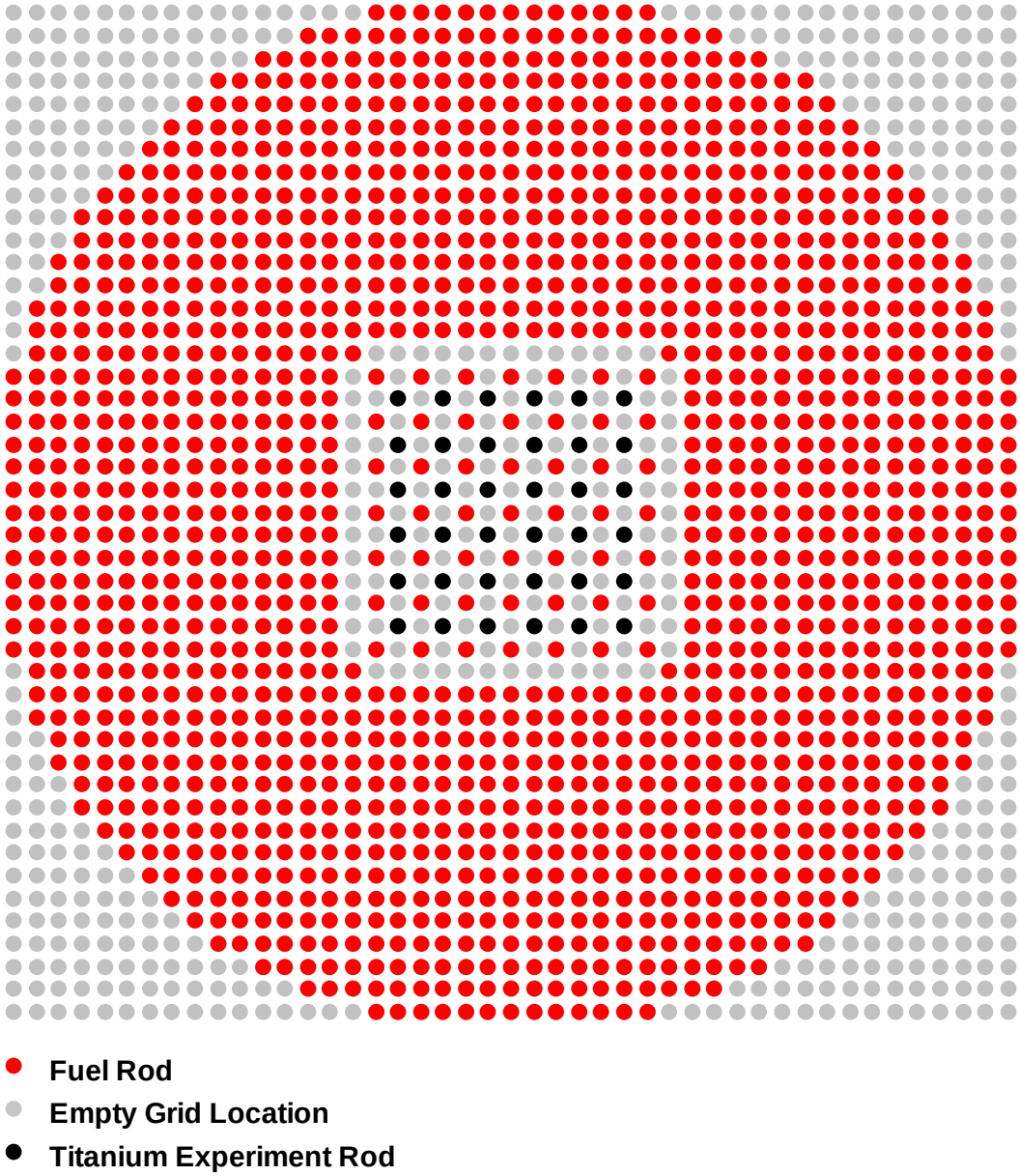

Figure 67. Array Layout for Case 24 (1485 Fuel Rods, 36 Titanium Experiment Rods).

3.3 Material Data

The atom densities for the materials in the critical experiment models are listed in Table 75.

Table 75. Atom Densities of the Materials in the Critical Experiment Models.

Material	Element or Nuclide	Atom Number Density ($barn^{-1}cm^{-1}$)
UO_2 Fuel (108.7165 g of fuel [$UO_{2.00}$ + impurities] in a cylinder 0.525628 cm diameter, 48.780 cm long)	^{234}U	6.5539E-06
	^{235}U	1.6010E-03
	^{236}U	1.4632E-05
	^{238}U	2.1296E-02
	O	4.5837E-02
	Ag	9.2319E-09
	B	2.3858E-07
	Cd	1.2380E-08
	Co	2.1620E-08
	Cr	2.5100E-06
	Cu	2.1316E-07
	Fe	1.0311E-05
	Mn	2.8372E-07
	Mo	1.2443E-07
	Ni	3.4989E-06
	V	1.4813E-08
	W	3.5998E-09
3003 Aluminum Cladding ($2.73\ g/cm^3$)[(a)]	Al	5.9668E-02
	Si	1.7561E-04
	Fe	1.0303E-04
	Cu	3.2339E-05
	Mn	3.7407E-04
	Zn	1.2571E-05
Water ($0.99705\ g/cm^3$)[(b)]	H	6.6659E-02
	O	3.3329E-02
6061 Aluminum Grid Plates ($2.70\ g/cm^3$)[(c)]	Al	5.8376E-02
	Si	4.1683E-04
	Fe	1.8051E-04
	Cu	7.9320E-05
	Mn	2.6637E-05
	Mg	6.9574E-04
	Cr	6.2542E-05
	Zn	2.9839E-05
	Ti	6.7918E-06
	V	3.1918E-06

(a) Density from http://matweb.com/search/DataSheet.aspx?MatGUID=fd4a40f87d3f4912925e5e6eab1fbc40 accessed on May 29, 2012.
(b) This density is from the National Institute of Standards and Technology Chemistry WebBook, http://webbook.nist.gov/chemistry/.
(c) Density from http://matweb.com/search/DataSheet.aspx?MatGUID=1b8c06d0ca7c456694c7777d9e10be5b accessed on May 29, 2012.

Table 75 (cont'd). Composition of the Materials in the Critical Experiment Models.

Material	Element or Nuclide	Atom Number Density ($barn^{-1}cm^{-1}$)
304 Stainless Steel Springs (0.1923 g in an annulus 0.35052 cm ID, 0.45720 cm OD and 1.7152 cm tall)	Fe	1.2527E-02
	Cr	3.6455E-03
	Ni	1.5724E-03
	Mn	1.8160E-04
	C	3.3225E-05
	P	7.2471E-06
	S	4.6663E-06
	Si	1.7761E-04
	N	3.5613E-05
Polyethylene (4.454 g in a cylinder 0.52578 cm OD and 21.2852 cm long)	H	8.2755E-02
	C	4.1377E-02
Titanium Experiment Rods (4.50900 g/cm^3)	Ti	5.6520E-02
	C	2.2423E-05
	O	1.6972E-04
	N	3.8773E-05
	H	1.0776E-04
	Fe	9.9675E-05
Aluminum Experiment Rods (2.69802 g/cm^3)	Al	5.9086E-02
	Si	3.3554E-04
	Fe	5.5278E-05
	Cu	4.0910E-05
	Mn	1.4787E-05
	Mg	5.4148E-04
	Cr	1.5624E-05
	Ti	6.7869E-06
	Ga	2.3303E-06
	V	3.1895E-06

3.4 Temperature Data

The temperature of the moderator was maintained near 25 °C. The critical data were corrected to 25 °C as noted above. The model temperature is therefore 25 °C.

3.5 Experimental and Benchmark-Model k_{eff}

The approach-to-critical experiments were done by varying the number of fuel rods in the assembly. The projected critical array size was determined by extrapolation of inverse detector count rates from two different fuel arrays to zero. The array k_{eff} was obtained using the extrapolations and the calculated incremental fuel rod worth for the fuel rods in the interval measured. The array k_{eff} was corrected to a temperature of 25 °C.

Several simplifications were made to the benchmark model. These simplifications resulted in a small bias that was applied to the temperature-corrected experiment k_{eff} to obtain the benchmark model k_{eff}. The experiment uncertainty was estimated by analyzing the effect on k_{eff} of a number of dimensional and material uncertainties in the experiments. The uncertainties in the temperature-corrected k_{eff}, the modeling biases, and the experiment were added in quadrature to determine the uncertainty in the benchmark model k_{eff}. Table 76 summarizes these data.

Table 76. Benchmark-Model k_{eff} and Uncertainty for the Twenty-Four Cases.

Case	Experiment		Simplification Bias		Temperature Correction		Experiment Uncertainty	Benchmark Model	
	k_{eff}	Unc.	Δk_{eff}	Unc.	Δk_{eff}	Unc.		k_{eff}	Unc.
1	0.99940	0.00010	0.00000	0.00004	0.00000	0.00000	0.00108	0.99940	0.00109
2	0.99942	0.00012	0.00000	0.00004	0.00000	0.00000	0.00098	0.99942	0.00099
3	0.99933	0.00011	0.00000	0.00004	0.00001	0.00000	0.00098	0.99934	0.00098
4	0.99947	0.00011	0.00007	0.00004	0.00001	0.00000	0.00098	0.99955	0.00098
5	0.99941	0.00011	0.00006	0.00004	0.00000	0.00000	0.00098	0.99947	0.00098
6	0.99964	0.00010	0.00005	0.00004	0.00000	0.00000	0.00098	0.99969	0.00098
7	0.99946	0.00011	0.00006	0.00004	0.00001	0.00000	0.00098	0.99953	0.00098
8	0.99956	0.00014	0.00005	0.00004	0.00000	0.00000	0.00098	0.99961	0.00099
9	0.99948	0.00011	-0.00002	0.00004	0.00000	0.00000	0.00098	0.99946	0.00098
10	0.99913	0.00010	0.00000	0.00004	0.00000	0.00000	0.00106	0.99913	0.00107
11	0.99911	0.00010	-0.00002	0.00004	0.00000	0.00000	0.00106	0.99909	0.00107
12	0.99925	0.00010	0.00005	0.00004	0.00000	0.00000	0.00106	0.99930	0.00107
13	0.99941	0.00009	0.00014	0.00004	0.00000	0.00000	0.00106	0.99955	0.00107
14	0.99936	0.00013	0.00007	0.00004	0.00000	0.00000	0.00106	0.99943	0.00107
15	0.99959	0.00009	0.00012	0.00004	0.00001	0.0000	0.00106	0.99972	0.00107
16	0.99981	0.00009	-0.00004	0.00004	0.00001	0.00000	0.00106	0.99978	0.00107
17	0.99944	0.00010	0.00001	0.00004	0.00001	0.00000	0.00106	0.99946	0.00107
18	0.99967	0.00012	-0.00002	0.00004	0.00000	0.00000	0.00077	0.99965	0.00078
19	0.99938	0.00012	0.00013	0.00004	-0.00001	0.00000	0.00077	0.99950	0.00078
20	0.99957	0.00013	0.00009	0.00004	-0.00001	0.00000	0.00077	0.99965	0.00078
21	0.99982	0.00012	-0.00005	0.00004	-0.00001	0.00000	0.00077	0.99976	0.00078
22	0.99946	0.00010	0.00000	0.00004	-0.00001	0.00000	0.00067	0.99945	0.00068
23	0.99958	0.00011	-0.00005	0.00004	-0.00001	0.00000	0.00067	0.99952	0.00068
24	0.99961	0.00010	0.00006	0.00004	-0.00001	0.00000	0.00067	0.99966	0.00068

4.0 RESULTS OF SAMPLE CALCULATIONS

The results of sample calculations using KENO V.a and MCNP6.1.1 for the twenty-four cases are shown in Tables 77 and 78. The input listings used in some of the calculations are shown in Appendix A.

Table 77. Sample Calculation Results Using ENDF/B-VII.0 Cross Sections (United States).

Code (Cross Section Set) →	KENO V.a (238-group ENDF/B-VII.0 SCALE6.2 Library)		KENO V.a (Continuous-Energy ENDF/B-VII.0 SCALE6.2 Library)		MCNP 6.1.1 (Continuous-Energy ENDF/B-VII.0)	
Case ↓	k_{eff}	σ	k_{eff}	σ	k_{eff}	σ
1	0.99695	0.00022	0.99792	0.00018	0.99807	0.00019
2	0.99760	0.00018	0.99842	0.00024	0.99849	0.00019
3	0.99756	0.00021	0.99850	0.00020	0.99864	0.00019
4	0.99775	0.00021	0.99846	0.00020	0.99898	0.00018
5	0.99757	0.00017	0.99877	0.00021	0.99887	0.00018
6	0.99817	0.00018	0.99911	0.00019	0.99930	0.00018
7	0.99820	0.00021	0.99891	0.00018	0.99919	0.00019
8	0.99865	0.00018	0.99974	0.00019	0.99944	0.00018
9	0.99820	0.00018	0.99930	0.00022	0.99960	0.00019
10	0.99712	0.00019	0.99792	0.00022	0.99822	0.00018
11	0.99711	0.00019	0.99837	0.00018	0.99836	0.00018
12	0.99752	0.00019	0.99810	0.00020	0.99845	0.00018
13	0.99772	0.00018	0.99894	0.00020	0.99901	0.00018
14	0.99749	0.00019	0.99845	0.00019	0.99895	0.00018
15	0.99782	0.00020	0.99875	0.00020	0.99874	0.00019
16	0.99838	0.00019	0.99890	0.00018	0.99875	0.00018
17	0.99779	0.00022	0.99874	0.00021	0.99872	0.00019
18	0.99921	0.00019	0.99904	0.00017	0.99906	0.00018
19	0.99914	0.00020	0.99886	0.00018	0.99879	0.00018
20	0.99937	0.00023	0.99938	0.00023	0.99952	0.00019
21	1.00014	0.00019	1.00007	0.00019	1.00002	0.00019
22	0.99999	0.00018	0.99948	0.00019	0.99980	0.00019
23	1.00019	0.00022	1.00003	0.00023	1.00019	0.00018
24	1.00020	0.00019	1.00045	0.00023	1.00070	0.00018

Table 78. Sample Calculation Results Using ENDF/B-VII.1 Cross Sections (United States).

Code (Cross Section Set) →	KENO V.a (252-group ENDF/B-VII.1 SCALE6.2 Library)		KENO V.a (Continuous-Energy ENDF/B-VII.1 SCALE6.2 Library)		MCNP 6.1.1 (Continuous-Energy ENDF/B-VII.1)	
Case ↓	k_{eff}	σ	k_{eff}	σ	k_{eff}	σ
1	0.99677	0.00020	0.99785	0.00021	0.99821	0.00019
2	0.99718	0.00019	0.99815	0.00020	0.99832	0.00019
3	0.99742	0.00020	0.99810	0.00019	0.99817	0.00018
4	0.99735	0.00018	0.99831	0.00018	0.99824	0.00018
5	0.99776	0.00019	0.99777	0.00019	0.99837	0.00019
6	0.99746	0.00021	0.99848	0.00023	0.99846	0.00019
7	0.99772	0.00019	0.99851	0.00022	0.99856	0.00018
8	0.99770	0.00021	0.99829	0.00021	0.99838	0.00020
9	0.99767	0.00018	0.99841	0.00020	0.99858	0.00018
10	0.99688	0.00022	0.99776	0.00021	0.99784	0.00018
11	0.99682	0.00025	0.99818	0.00021	0.99818	0.00018
12	0.99783	0.00019	0.99819	0.00019	0.99834	0.00017
13	0.99773	0.00020	0.99805	0.00021	0.99855	0.00018
14	0.99786	0.00018	0.99891	0.00019	0.99852	0.00018
15	0.99789	0.00017	0.99882	0.00020	0.99851	0.00018
16	0.99797	0.00018	0.99902	0.00020	0.99904	0.00018
17	0.99789	0.00020	0.99854	0.00019	0.99830	0.00018
18	0.99904	0.00018	0.99886	0.00020	0.99916	0.00019
19	0.99870	0.00020	0.99850	0.00017	0.99891	0.00018
20	0.99876	0.00022	0.99917	0.00020	0.99880	0.00017
21	0.99898	0.00017	0.99911	0.00020	0.99896	0.00019
22	0.99848	0.00018	0.99868	0.00018	0.99881	0.00018
23	0.99858	0.00020	0.99857	0.00019	0.99883	0.00018
24	0.99842	0.00019	0.99833	0.00020	0.99866	0.00017

Figure 68 shows the reactivity offset ρ of the multigroup KENO V.a calculations using ENDF/B-VII.0 cross sections, defined as

$$\rho = \frac{k_c - k_b}{k_c k_b} ,$$

where k_c is the calculated k_{eff} for the benchmark model of a given configuration and k_b is the evaluated benchmark model k_{eff} for the same configuration. The red error bars shown in the figure represent the uncertainty in the evaluated benchmark model k_{eff}. The smaller black error bars shown in the figure represent the stochastic uncertainties in the Monte Carlo calculations. The unweighted average reactivity offset for all cases is -0.0012.

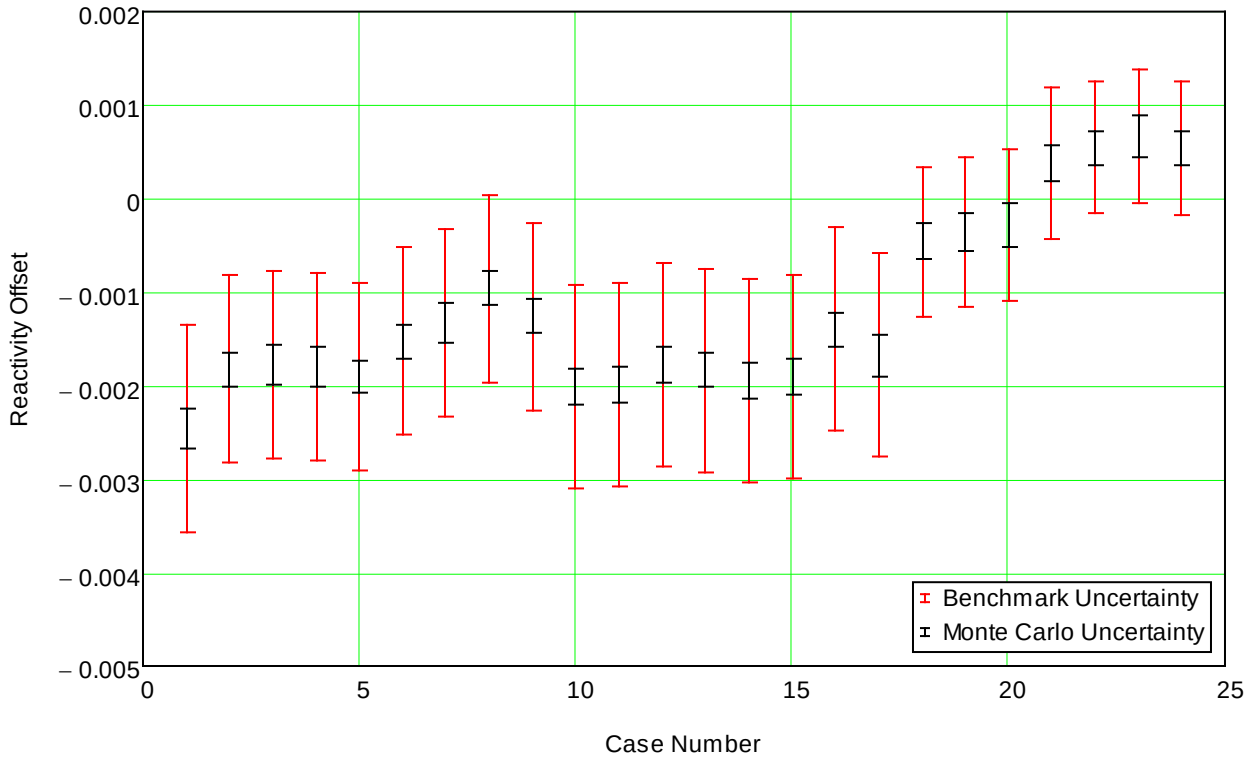

Figure 68. Reactivity Offset for KENO V.a Calculations using Cross Sections from the 238-Group ENDF/B-VII.0 SCALE6.2 Library.

Figure 69 shows the reactivity offset for the continuous-energy KENO V.a calculations using ENDF/B-VII.0 cross sections. The unweighted average reactivity offset for all cases is -0.0006.

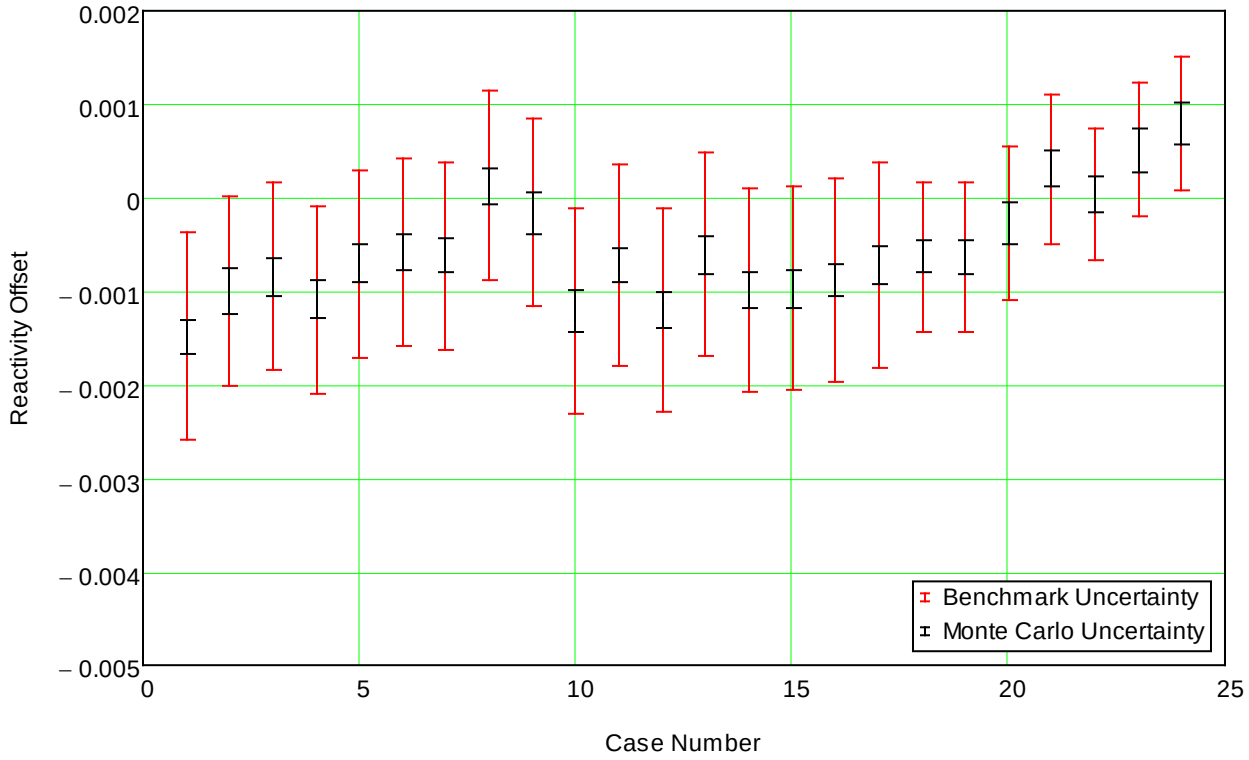

Figure 69. Reactivity Offset for KENO V.a Calculations using Continuous-Energy Cross Sections from the ENDF/B-VII.0 SCALE6.2 Library.

Figure 70 shows the reactivity offset for the continuous-energy MCNP6.1.1 calculations using continuous-energy ENDF/B-VII.0 cross sections. The unweighted average reactivity offset for all cases is -0.0004.

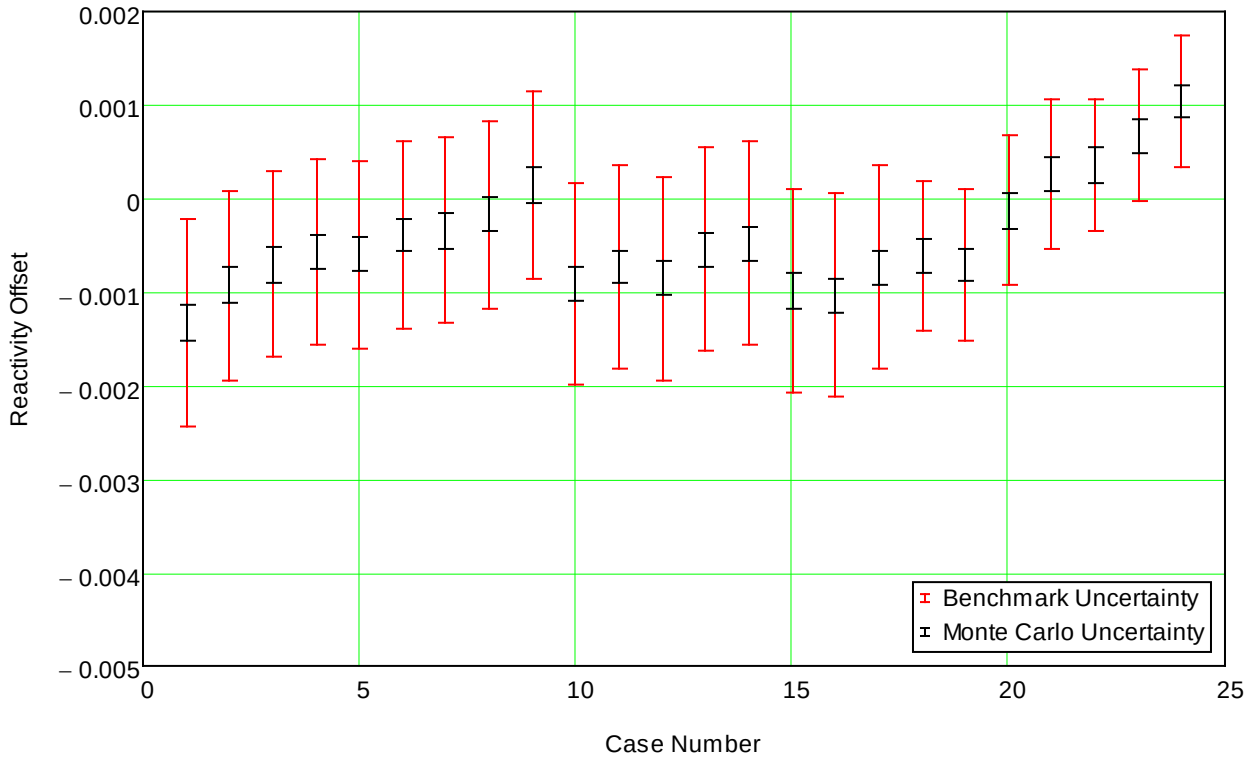

Figure 70. Reactivity Offset for MCNP6.1.1 Calculations using Continuous-Energy Cross Sections from the ENDF/B-VII.0 Library.

Figure 71 shows the reactivity offset for the multigroup KENO V.a calculations using ENDF/B-VII.1 cross sections. The unweighted average reactivity offset for all cases is -0.0016.

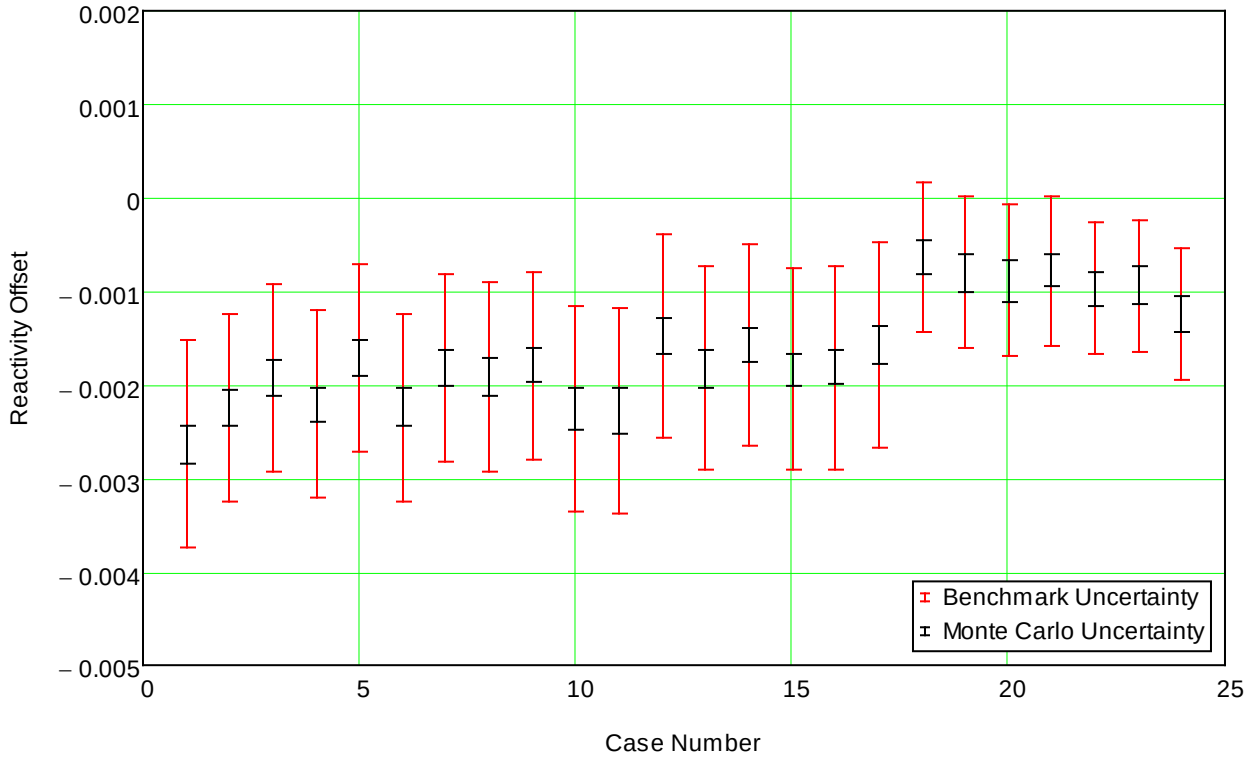

Figure 71. Reactivity Offset for KENO V.a Calculations using Cross Sections from the 252-Group ENDF/B-VII.1 SCALE6.2 Library.

Figure 72 shows the reactivity offset for the continuous-energy KENO V.a calculations using ENDF/B-VII.1 cross sections. The unweighted average reactivity offset for all cases is -0.0011.

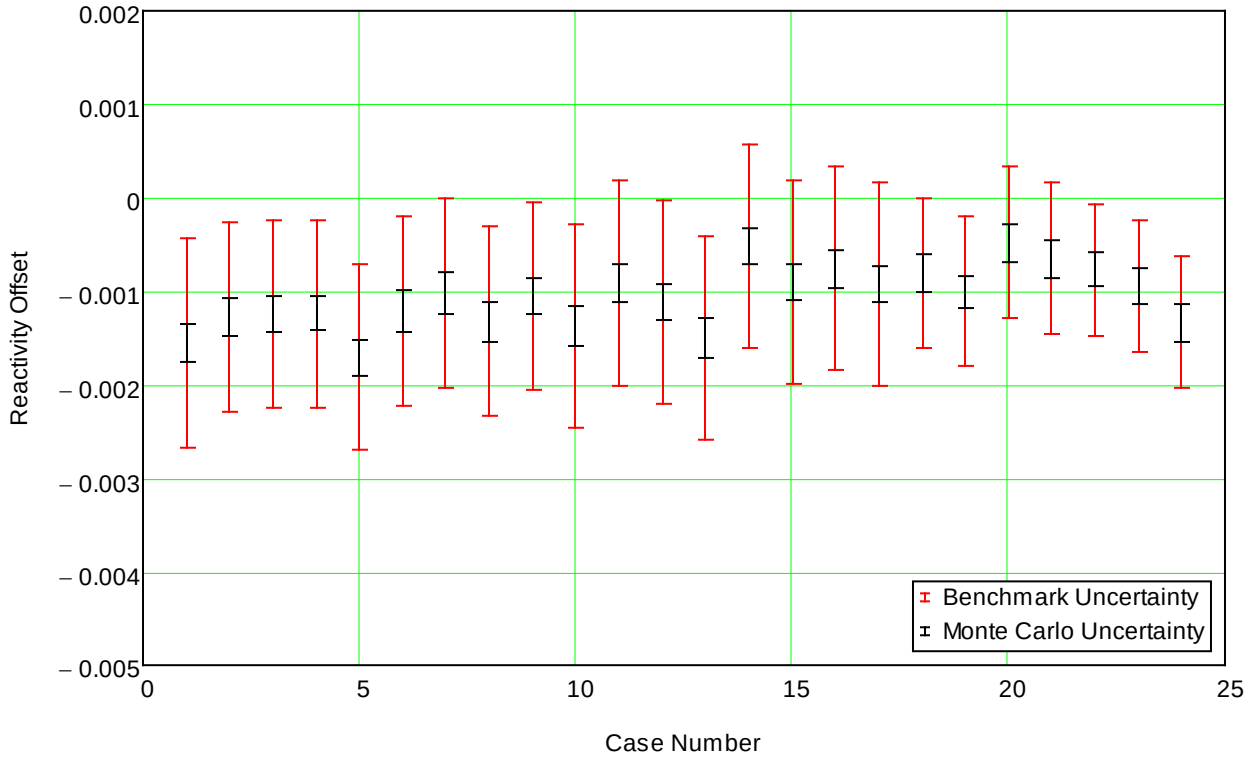

Figure 72. Reactivity Offset for KENO V.a Calculations using Continuous-Energy Cross Sections from the ENDF/B-VII.1 SCALE6.2 Library.

Figure 73 shows the reactivity offset for the continuous-energy MCNP6.1.1 calculations using continuous-energy ENDF/B-VII.1 cross sections. The unweighted average reactivity offset for all cases is -0.0010.

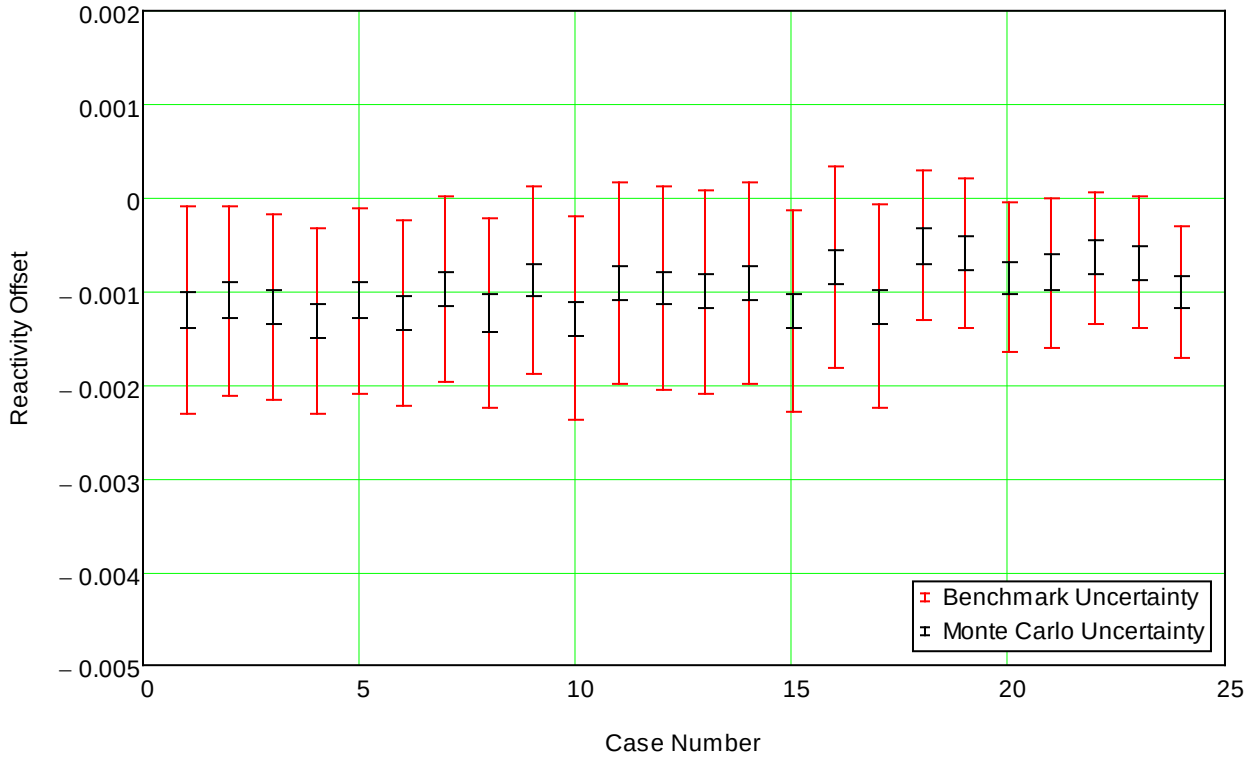

Figure 73. Reactivity Offset for MCNP6.1.1 Calculations using Continuous-Energy Cross Sections from the ENDF/B-VII.1 Library.

The results of MORET 5 calculations for the twenty-four cases are shown in Table 79. The MORET 5.C.1 calculations are run in one step. The input listings used in some of the calculations are shown in Appendix A.3 (MORET 5).

MORET 5 can be used in two calculation routes:

- Either coupled with the APOLLO2 deterministic code in a multi-group APOLLO2-MORET 5 route. It uses macroscopic cross sections from APOLLO2 and calculates k_{eff} through a 3D simulation.
- Or in a Monte Carlo MORET 5 continuous energy code. MORET uses cross sections at the ACE format based on the JEFF-3.1, JEFF-3.2, ENDF/B-VII.0 and ENDF/B-VII.1 evaluations and performs the 3D simulation to determine k_{eff}.

The reported results are run with the continuous energy MORET 5 code using various cross sections libraries. The calculations were run with a minimum of 150 batches and a targeted Monte Carlo standard deviation of 0.00050.

An example of input listing for Case 9 is provided below. The number of batches is 420 and the number of neutron per batch is 10125.

A general good agreement with the benchmark k_{eff} is obtained since no significant tendency can be identified given the amount of the experimental uncertainties. Similarly, no significant tendency versus cross sections library can be put forward.

Table 79. Sample Calculation Results (France)

Code (Cross Section Set) → Case ↓	Continuous Energy MORET 5.C.1 (ENDF/B-VII.0)[(a)]	Continuous Energy MORET 5.C.1 (ENDF/B-VII.1)[(a)]	Continuous Energy MORET 5.C.1 (JEFF-3.1)[(a)]	Continuous Energy MORET 5.C.1 (JEFF-3.2)[(a)]
1	0.99795	0.99857	0.99680	0.99676
2	0.99762	0.99794	0.99623	0.99776
3	0.99754	0.99785	0.99763	0.99658
4	0.99828	0.99726	0.99612	0.99731
5	0.99820	0.99740	0.99715	0.99732
6	0.99838	0.99688	0.99657	0.99788
7	0.99814	0.99779	0.99708	0.99791
8	0.99755	0.99757	0.99830	0.99756
9	0.99855	0.99698	0.99859	0.99807
10	0.99791	0.99659	0.99609	0.99720
11	0.99775	0.99706	0.99615	0.99627
12	0.99745	0.99670	0.99727	0.99615
13	0.99812	0.99664	0.99660	0.99665
14	0.99691	0.99718	0.99737	0.99707
15	0.99818	0.99667	0.99681	0.99674
16	0.99820	0.99786	0.99768	0.99688
17	0.99806	0.99763	0.99703	0.99707
18	0.99774	0.99823	0.99750	0.99678
19	0.99797	0.99894	0.99742	0.99674
20	0.99832	0.99802	0.99791	0.99786
21	0.99954	0.99815	0.99808	0.99872
22	0.99899	0.99879	0.99879	0.99770
23	0.99989	0.99818	0.99914	0.99807
24	0.99980	0.99889	0.99860	0.99890

(a) Results provided by Nicolas Leclaire and Mathieu Monestier (France).

Figure 74 shows the reactivity offset for the continuous-energy MORET 5.C.1 calculations using continuous-energy ENDF/B-VII.0 cross sections. The unweighted average reactivity offset for all cases is -0.0013.

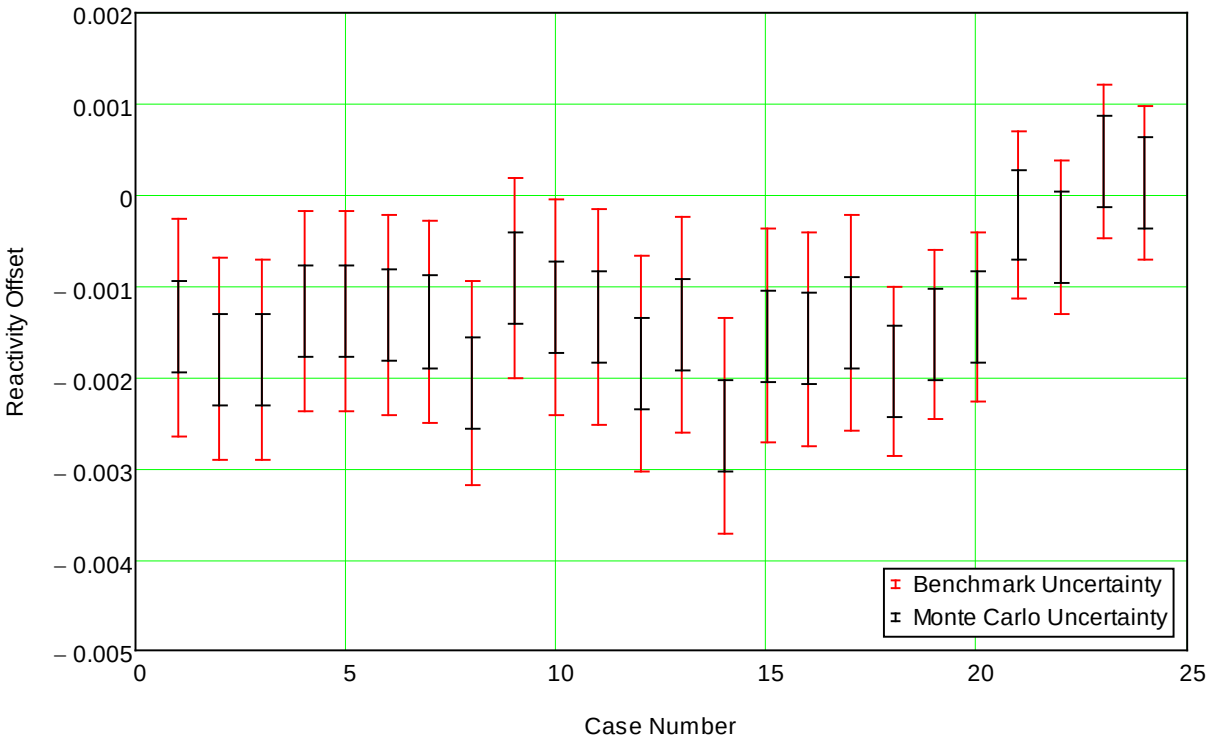

Figure 74. Reactivity Offset for MORET 5.C.1 Calculations using Continuous-Energy Cross Sections from the ENDF/B-VII.0 Library.

Figure 75 shows the reactivity offset for the continuous-energy MORET 5.C.1 calculations using continuous-energy ENDF/B-VII.1 cross sections. The unweighted average reactivity offset for all cases is -0.0019.

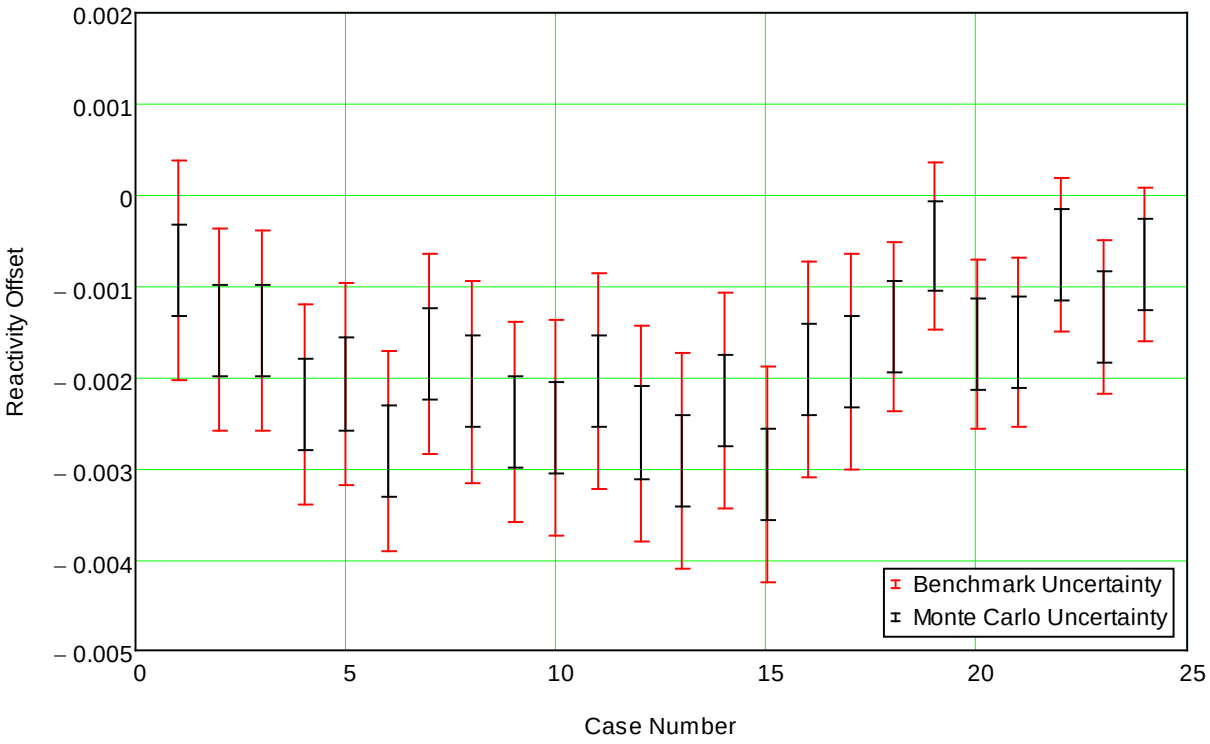

Figure 75. Reactivity Offset for MORET 5.C.1 Calculations using Continuous-Energy Cross Sections from the ENDF/B-VII.1 Library.

Figure 76 shows the reactivity offset for the continuous-energy MORET 5.C.1 calculations using continuous-energy JEFF-3.1 cross sections. The unweighted average reactivity offset for all cases is -0.0021.

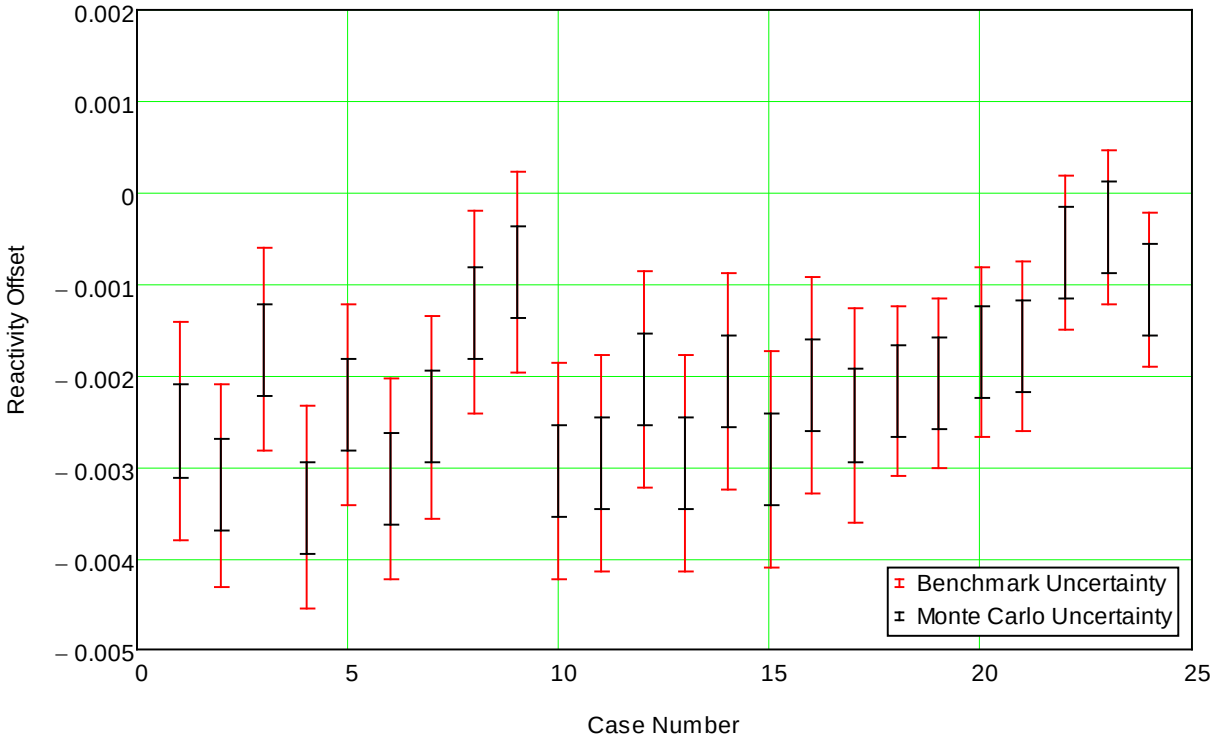

Figure 76. Reactivity Offset for MORET 5.C.1 Calculations Using Continuous-Energy Cross Sections from the JEFF-3.1 Library.

Figure 77 shows the reactivity offset for the continuous-energy MORET 5.C.1 calculations using continuous-energy JEFF-3.2 cross sections. The unweighted average reactivity offset for all cases is -0.0022.

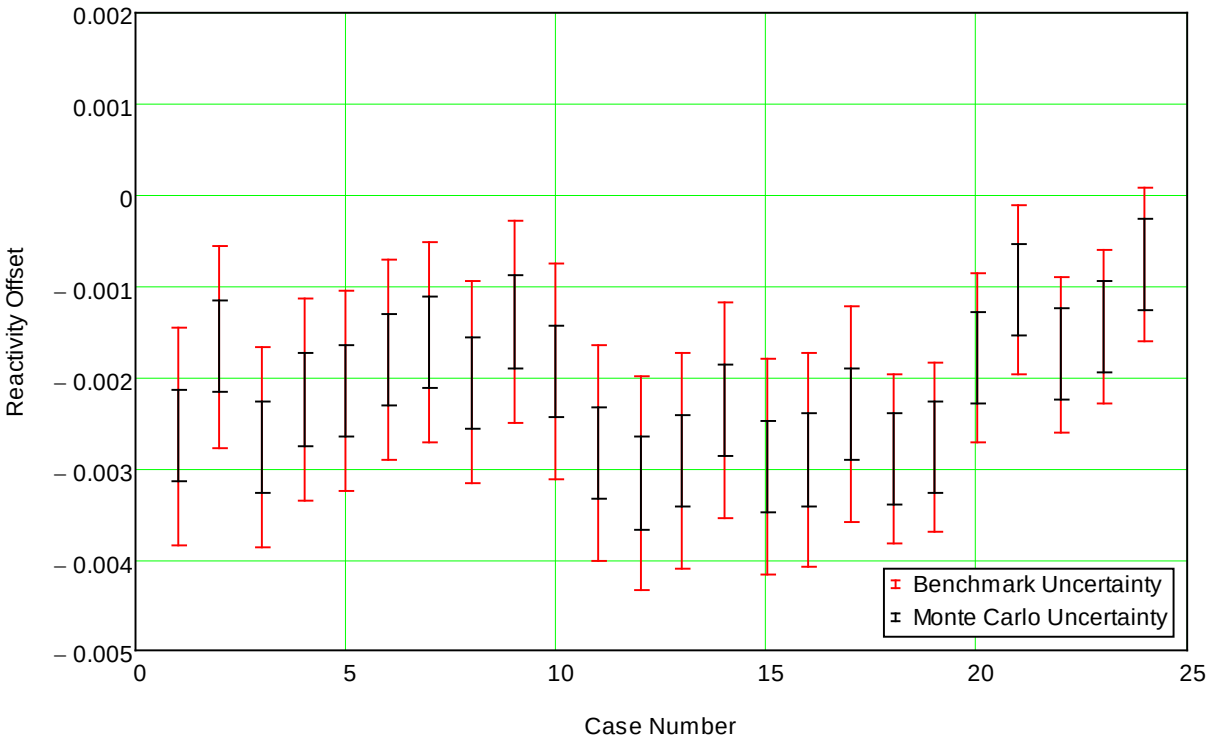

Figure 77. Reactivity Offset for MORET 5.C.1 Calculations using Continuous-Energy Cross Sections from the JEFF-3.2 Library.

5.0 REFERENCES

There are no published references.

APPENDIX A: TYPICAL INPUT LISTINGS

A.1 KENO INPUT LISTING

KENO V.a and the 252-group ENDF/B-VII.1 cross section set from SCALE 6.2 were used. A total of 550 batches of 40,000 neutrons were run. The first 50 batches were skipped.

```
KENO V.a input for Case 24

=csas25
LCT097 case 24 1485 fuel rods, 36 Ti experiment rods
v7-252
read comp
'
' UO2 fuel
'
U-234  1 0  6.5539E-06 298.15 end
U-235  1 0  1.6010E-03 298.15 end
U-236  1 0  1.4632E-05 298.15 end
U-238  1 0  2.1296E-02 298.15 end
O      1 0  4.5837E-02 298.15 end
Ag     1 0  9.2319E-09 298.15 end
B      1 0  2.3858E-07 298.15 end
Cd     1 0  1.2380E-08 298.15 end
Co     1 0  2.1620E-08 298.15 end
Cr     1 0  2.5100E-06 298.15 end
Cu     1 0  2.1316E-07 298.15 end
Fe     1 0  1.0311E-05 298.15 end
Mn     1 0  2.8372E-07 298.15 end
Mo     1 0  1.2443E-07 298.15 end
Ni     1 0  3.4989E-06 298.15 end
V      1 0  1.4813E-08 298.15 end
' W      1 0  3.5998E-09 298.15 end
' Neither natural W nor W-180 are in the SCALE 238-group ENDF/B-VII.0 set
'  Source for Isotopic Atom Fractions:  Chart of the Nuclides 16th ed.
' W-180  1 0  4.31976e-12 298.15 end
W-182  1 0  9.53947e-10 298.15 end
W-183  1 0  5.15131e-10 298.15 end
W-184  1 0  1.10298e-09 298.15 end
W-186  1 0  1.02342e-09 298.15 end
'
' 3003 aluminum
'
Al  2 0  5.9668E-02 298.15 end
Si  2 0  1.7561E-04 298.15 end
Fe  2 0  1.0303E-04 298.15 end
Cu  2 0  3.2339E-05 298.15 end
Mn  2 0  3.7407E-04 298.15 end
Zn  2 0  1.2571E-05 298.15 end
'
'  water @ 25 C in core
'
H   3 0  6.6659E-02 298.15 end
O   3 0  3.3329E-02 298.15 end
'
' 6061 aluminum
'
Al  5 0  5.8376E-02 298.15 end
Si  5 0  4.1683E-04 298.15 end
Fe  5 0  1.8051E-04 298.15 end
Cu  5 0  7.9320E-05 298.15 end
Mn  5 0  2.6637E-05 298.15 end
Mg  5 0  6.9574E-04 298.15 end
Cr  5 0  6.2542E-05 298.15 end
Zn  5 0  2.9839E-05 298.15 end
Ti  5 0  6.7918E-06 298.15 end
V   5 0  3.1918E-06 298.15 end
'
' polyethylene
```

```
'
H-POLY 6 0  8.2755E-02 298.15 end
C   6 0  4.1377E-02 298.15 end
'
' SS-304 for springs
'
Fe  8 0  1.2527E-02 298.15 end
Cr  8 0  3.6455E-03 298.15 end
Ni  8 0  1.5724E-03 298.15 end
Mn  8 0  1.8160E-04 298.15 end
C   8 0  3.3225E-05 298.15 end
P   8 0  7.2471E-06 298.15 end
S   8 0  4.6663E-06 298.15 end
Si  8 0  1.7761E-04 298.15 end
N   8 0  3.5613E-05 298.15 end
'
'  water outside of fuel rods
'
H  10 0  6.6659E-02 298.15 end
O  10 0  3.3329E-02 298.15 end
'
' Titanium for experiment rods
'
Ti 11 0  5.6520E-02 298.15 end
C  11 0  2.2423E-05 298.15 end
O  11 0  1.6972E-04 298.15 end
N  11 0  3.8773E-05 298.15 end
H  11 0  1.0776E-04 298.15 end
Fe 11 0  9.9675E-05 298.15 end
end comp
read celldata
  latticecell squarepitch fuelr=0.262814 1 gapr=0.284519 0 cladr=0.317474 2 hpitch=0.40005 3 end
end celldata
read param
 npg=40000 gen=550 tme=500 htm=no
 nsk=50 run=yes flx=yes plt=no
 wrs=35 res=10000
end param
read geom
unit 2
  com=' bottom of driver rod in grid plate '
  cylinder  2 1  0.317474 0.0  -1.27
  cylinder  3 1  0.333375 0.0  -1.27
  cuboid    5 1 4p0.40005 0.0  -2.54
unit 301
  com=' fueled section of driver rod '
  cylinder  1 1  0.262814 48.780      0.0
  cylinder  0 1  0.284519 48.780      0.0
  cylinder  2 1  0.317474 48.780      0.0
  cuboid    3 1 4p0.40005 48.780      0.0
unit 302
  com=' driver rod spring '
  cylinder  0 1  0.17526  50.4952    48.780
  cylinder  8 1  0.22860  50.4952    48.780
  cylinder  0 1  0.284519 50.4952    48.780
  cylinder  2 1  0.317474 50.4952    48.780
  cuboid    3 1 4p0.40005 50.4952    48.780
unit 3
  com=' fueled section and spring '
  array    301   -0.40005 -0.40005    0.0
  cuboid    3 1 4p0.40005 50.4952     0.0
unit 4
  com=' top of driver rod in grid plate '
  cylinder  5 1  0.26289  53.0352    50.4952
  cylinder  0 1  0.284519 53.0352    50.4952
  cylinder  2 1  0.317474 53.0352    50.4952
  cylinder  3 1  0.333375 53.0352    50.4952
  cuboid    5 1 4p0.40005 53.0352    50.4952
unit 5
  com=' poly section of fuel rod in reflector '
  cylinder  6 1  0.26289  68.2752    53.0352
  cylinder  0 1  0.284519 68.2752    53.0352
```

```
  cylinder  2 1  0.317474 68.2752    53.0352
  cuboid   10 1 4p0.40005 68.2752    53.0352
unit 12
  com=' bottom grid plate without rod'
  cylinder  3 1  0.333375 0.0  -1.27
  cuboid    5 1 4p0.40005 0.0  -2.54
unit 13
  com=' fueled section without rod '
  cuboid    3 1 4p0.40005 50.4952     0.0
unit 14
  com=' grid plate without rod'
  cylinder  3 1  0.333375 53.0352    50.4952
  cuboid    5 1 4p0.40005 53.0352    50.4952
unit 15
  com=' poly section without rod '
  cuboid   10 1 4p0.40005 68.2752    53.0352
unit 52
  com=' bottom grid plate without rod'
  cylinder 10 1  0.333375 0.0  -1.27
  cuboid    5 1 4p0.40005 0.0  -2.54
unit 53
  com=' fueled section without rod '
  cuboid   10 1 4p0.40005 50.4952     0.0
unit 54
  com=' grid plate without rod'
  cylinder 10 1  0.333375 53.0352    50.4952
  cuboid    5 1 4p0.40005 53.0352    50.4952
unit 55
  com=' poly section without rod '
  cuboid   10 1 4p0.40005 68.2752    53.0352
unit 92
  com=' bottom of experiment rod in grid plate '
  cylinder 11 1  0.318479 0.0  -1.27
  cylinder 10 1  0.333375 0.0  -1.27
  cuboid    5 1 4p0.40005 0.0  -2.54
unit 93
  com=' in-core section of experiment rod '
  cylinder 11 1  0.318479 50.495      0.0
  cuboid   10 1 4p0.40005 50.495      0.0
unit 94
  com=' experiment rod in upper grid plate'
  cylinder 11 1  0.318479 53.0352    50.4952
  cylinder 10 1  0.333375 53.0352    50.4952
  cuboid    5 1 4p0.40005 53.0352    50.4952
unit 95
  com=' experiment rod above upper grid plate '
  cylinder 11 1  0.318479 68.2752    53.0352
  cuboid   10 1 4p0.40005 68.2752    53.0352
unit 211
  cylinder 10 1  46.8376   16.51     0.0
  cuboid    0 1  46.9  -46.9   46.9  -46.9   16.51     0.0
unit 212
  array   12    -18.00225 -18.00225  0.0
  cylinder  5 1  46.355     2.54     0.0
  cylinder 10 1  46.8376    2.54     0.0
  cuboid    0 1  46.9  -46.9   46.9  -46.9    2.54     0.0
unit 151
  com=' bottom section of detector tube '
  cylinder  0 1  2.8575    0.862      0.735
  cylinder  5 1  3.175     0.862      0.1
unit 152
  com=' poly section of detector tube '
  cylinder  0 1  2.8575   30.8848     0.862
  cylinder  5 1  3.175    30.8848     0.862
  cylinder 10 1  3.30581  30.8848     0.862
  cylinder  6 1  5.75945  30.8848     0.862
unit 153
  com=' section of detector tube above poly in fuel '
  cylinder  0 1  2.875    50.4952    30.8848
  cylinder  5 1  3.175    50.4952    30.8848
unit 213
  array   13    -18.00225 -18.00225    0.0
```

```
  cylinder 10 1  46.8376   50.4952      0.0
  hole    151    32.385     6.4        0.0
  hole    152    32.385     6.4        0.0
  hole    153    32.385     6.4        0.0
  hole    151   -32.385    -6.4        0.0
  hole    152   -32.385    -6.4        0.0
  hole    153   -32.385    -6.4        0.0
  cuboid    0 1  46.9  -46.9   46.9  -46.9   50.4952      0.0
unit 154
  com=' section of detector tube at grid plate '
  cylinder  0 1  2.875    53.0352    50.4952
  cylinder  5 1  3.175    53.0352    50.4952
unit 214
  array   14    -18.00225 -18.00225 50.4952
  cuboid    5 1  4p20.955  53.0352    50.4952
  cylinder 10 1  46.8376   53.0352    50.4952
  hole    154    32.385     6.4        0.0
  hole    154   -32.385    -6.4        0.0
  cuboid    0 1  46.9  -46.9   46.9  -46.9   53.0352    50.4952
unit 155
  com=' bottom section of detector tube '
  cylinder  0 1  2.875    68.2752    53.0352
  cylinder  5 1  3.175    68.2752    53.0352
unit 215
  array   15    -18.00225 -18.00225 53.0352
  cylinder 10 1  46.8376   68.2752    53.0352
  hole    155    32.385     6.4        0.0
  hole    155   -32.385    -6.4        0.0
  cuboid    0 1  46.9  -46.9   46.9  -46.9   68.2752    53.0352
global unit 999
  array    1    -46.9     -46.9    -19.05
end geom
read array
  ara=1
  com=' the whole shebang '
  nux=1   nuy=1   nuz=5
  fill   211  212  213  214  215  end fill
  ara=301
  com=' fueled section of fuel rod '
  nux=1   nuy=1   nuz=2
  fill   301  302  end fill
' 1485 fuel rods 1657 total positions
ara= 12
nux= 45 nuy= 45 nuz= 1 fill
52 52 52 52 52 52 52 52 52 52 52 52 52 52 52 52 52 2 2
2 2 2 2 2 2 2 2 2 2 2 52 52 52 52 52 52 52
52 52 52 52 52 52 52 52 52
52 52 52 52 52 52 52 52 52 52 52 52 52 2 2 2 2 2
2 2 2 2 2 2 2 2 2 2 2 2 2 52 52 52 52
52 52 52 52 52 52 52 52 52
52 52 52 52 52 52 52 52 52 52 52 2 2 2 2 2 2 2
2 2 2 2 2 2 2 2 2 2 2 2 2 2 52 52
52 52 52 52 52 52 52 52 52
52 52 52 52 52 52 52 52 52 2 2 2 2 2 2 2 2 2
2 2 2 2 2 2 2 2 2 2 2 2 2 2 2 2 2
52 52 52 52 52 52 52 52 52
52 52 52 52 52 52 52 52 2 2 2 2 2 2 2 2 2 2
2 2 2 2 2 2 2 2 2 2 2 2 2 2 2 2 2
2 52 52 52 52 52 52 52 52
52 52 52 52 52 52 52 2 2 2 2 2 2 2 2 2 2 2
2 2 2 2 2 2 2 2 2 2 2 2 2 2 2 2 2
2 2 52 52 52 52 52 52
52 52 52 52 52 52 2 2 2 2 2 2 2 2 2 2 2 2
2 2 2 2 2 2 2 2 2 2 2 2 2 2 2 2 2
2 2 2 52 52 52 52 52
52 52 52 52 52 2 2 2 2 2 2 2 2 2 2 2 2 2
2 2 2 2 2 2 2 2 2 2 2 2 2 2 2 2 2
2 2 2 2 52 52 52 52
52 52 52 52 2 2 2 2 2 2 2 2 2 2 2 2 2 2
2 2 2 2 2 2 2 2 2 2 2 2 2 2 2 2 2
2 2 2 2 2 52 52 52 52
52 52 52 2 2 2 2 2 2 2 2 2 2 2 2 2 2
```

```
2 2 2 2 2 2 2 2 2 2 2 2 2 2 2 2 2 2 2
2 2 2 2 2 2 52 52 52
52 52 52 2 2 2 2 2 2 2 2 2 2 2 2 2 2 2 2
2 2 2 2 2 2 2 2 2 2 2 2 2 2 2 2 2 2 2
2 2 2 2 2 2 52 52 52
52 52 2 2 2 2 2 2 2 2 2 2 2 2 2 2 2 2 2
2 2 2 2 2 2 2 2 2 2 2 2 2 2 2 2 2 2 2
2 2 2 2 2 2 2 52 52
52 52 2 2 2 2 2 2 2 2 2 2 2 2 2 2 2 2 2
2 2 2 2 2 2 2 2 2 2 2 2 2 2 2 2 2 2 2
2 2 2 2 2 2 2 52 52
52 2 2 2 2 2 2 2 2 2 2 2 2 2 2 2 2 2 2
2 2 2 2 2 2 2 2 2 2 2 2 2 2 2 2 2 2 2
2 2 2 2 2 2 2 2 52
52 2 2 2 2 2 2 2 2 2 2 2 2 2 2 2 2 2 2
2 2 2 2 2 2 2 2 2 2 2 2 2 2 2 2 2 2 2
2 2 2 2 2 2 2 2 52
52 2 2 2 2 2 2 2 2 2 2 2 2 2 2 2 52 52
52 52 52 52 52 52 52 52 52 52 52 2 2 2 2 2 2 2
2 2 2 2 2 2 2 2 52
2 2 2 2 2 2 2 2 2 2 2 2 2 2 2 52 2 52
2 52 2 52 2 52 2 52 2 52 2 52 2 2 2 2 2 2
2 2 2 2 2 2 2 2 2
2 2 2 2 2 2 2 2 2 2 2 2 2 2 2 52 52 92
52 92 52 92 52 92 52 92 52 92 52 52 2 2 2 2 2 2
2 2 2 2 2 2 2 2 2
2 2 2 2 2 2 2 2 2 2 2 2 2 2 2 52 2 52
2 52 2 52 2 52 2 52 2 52 2 52 2 2 2 2 2 2
2 2 2 2 2 2 2 2 2
2 2 2 2 2 2 2 2 2 2 2 2 2 2 2 52 52 92
52 92 52 92 52 92 52 92 52 92 52 52 2 2 2 2 2 2
2 2 2 2 2 2 2 2 2
2 2 2 2 2 2 2 2 2 2 2 2 2 2 2 52 2 52
2 52 2 52 2 52 2 52 2 52 2 52 2 2 2 2 2 2
2 2 2 2 2 2 2 2 2
2 2 2 2 2 2 2 2 2 2 2 2 2 2 2 52 52 92
52 92 52 92 52 92 52 92 52 92 52 52 2 2 2 2 2 2
2 2 2 2 2 2 2 2 2
2 2 2 2 2 2 2 2 2 2 2 2 2 2 2 52 2 52
2 52 2 52 2 52 2 52 2 52 2 52 2 2 2 2 2 2
2 2 2 2 2 2 2 2 2
2 2 2 2 2 2 2 2 2 2 2 2 2 2 2 52 52 92
52 92 52 92 52 92 52 92 52 92 52 52 2 2 2 2 2 2
2 2 2 2 2 2 2 2 2
2 2 2 2 2 2 2 2 2 2 2 2 2 2 2 52 2 52
2 52 2 52 2 52 2 52 2 52 2 52 2 2 2 2 2 2
2 2 2 2 2 2 2 2 2
2 2 2 2 2 2 2 2 2 2 2 2 2 2 2 52 52 92
52 92 52 92 52 92 52 92 52 92 52 52 2 2 2 2 2 2
2 2 2 2 2 2 2 2 2
2 2 2 2 2 2 2 2 2 2 2 2 2 2 2 52 2 52
2 52 2 52 2 52 2 52 2 52 2 52 2 2 2 2 2 2
2 2 2 2 2 2 2 2 2
52 2 2 2 2 2 2 2 2 2 2 2 2 2 2 2 52 52
52 52 52 52 52 52 52 52 52 52 52 2 2 2 2 2 2 2
2 2 2 2 2 2 2 2 52
52 2 2 2 2 2 2 2 2 2 2 2 2 2 2 2 2 2 2
2 2 2 2 2 2 2 2 2 2 2 2 2 2 2 2 2 2 2
2 2 2 2 2 2 2 2 52
52 2 2 2 2 2 2 2 2 2 2 2 2 2 2 2 2 2 2
2 2 2 2 2 2 2 2 2 2 2 2 2 2 2 2 2 2 2
2 2 2 2 2 2 2 2 52
52 52 2 2 2 2 2 2 2 2 2 2 2 2 2 2 2 2 2
2 2 2 2 2 2 2 2 2 2 2 2 2 2 2 2 2 2 2
2 2 2 2 2 2 2 52 52
52 52 2 2 2 2 2 2 2 2 2 2 2 2 2 2 2 2 2
```

```
2 2 2 2 2 2 2 2 2 2 2 2 2 2 2 2 2 2
2 2 2 2 2 2 2 52 52
52 52 52 2 2 2 2 2 2 2 2 2 2 2 2 2 2
2 2 2 2 2 2 2 2 2 2 2 2 2 2 2 2 2 2
2 2 2 2 2 2 52 52 52
52 52 52 2 2 2 2 2 2 2 2 2 2 2 2 2 2
2 2 2 2 2 2 2 2 2 2 2 2 2 2 2 2 2 2
2 2 2 2 2 2 52 52 52
52 52 52 52 2 2 2 2 2 2 2 2 2 2 2 2 2
2 2 2 2 2 2 2 2 2 2 2 2 2 2 2 2 2 2
2 2 2 2 2 52 52 52 52
52 52 52 52 52 2 2 2 2 2 2 2 2 2 2 2 2
2 2 2 2 2 2 2 2 2 2 2 2 2 2 2 2 2 2
2 2 2 2 52 52 52 52 52
52 52 52 52 52 52 2 2 2 2 2 2 2 2 2 2 2
2 2 2 2 2 2 2 2 2 2 2 2 2 2 2 2 2 2
2 2 2 52 52 52 52 52 52
52 52 52 52 52 52 52 2 2 2 2 2 2 2 2 2 2
2 2 2 2 2 2 2 2 2 2 2 2 2 2 2 2 2 2
2 2 52 52 52 52 52 52 52
52 52 52 52 52 52 52 52 2 2 2 2 2 2 2 2 2
2 2 2 2 2 2 2 2 2 2 2 2 2 2 2 2 2 2
2 52 52 52 52 52 52 52 52
52 52 52 52 52 52 52 52 52 2 2 2 2 2 2 2 2
2 2 2 2 2 2 2 2 2 2 2 2 2 2 2 2 2 2
52 52 52 52 52 52 52 52
52 52 52 52 52 52 52 52 52 52 52 2 2 2 2 2
2 2 2 2 2 2 2 2 2 2 2 2 2 2 52 52
52 52 52 52 52 52 52 52
52 52 52 52 52 52 52 52 52 52 52 52 2 2 2 2
2 2 2 2 2 2 2 2 2 2 2 2 2 52 52 52
52 52 52 52 52 52 52 52
52 52 52 52 52 52 52 52 52 52 52 52 52 52 52 2 2
2 2 2 2 2 2 2 2 2 2 52 52 52 52 52 52
52 52 52 52 52 52 52 52
end fill
ara= 13
nux= 45 nuy= 45 nuz= 1 fill
53 53 53 53 53 53 53 53 53 53 53 53 53 53 53 3 3
3 3 3 3 3 3 3 3 3 3 53 53 53 53 53 53
53 53 53 53 53 53 53 53
53 53 53 53 53 53 53 53 53 53 53 53 3 3 3 3 3
3 3 3 3 3 3 3 3 3 3 3 3 53 53 53 53
53 53 53 53 53 53 53 53
53 53 53 53 53 53 53 53 53 53 3 3 3 3 3 3 3
3 3 3 3 3 3 3 3 3 3 3 3 3 3 3 53 53
53 53 53 53 53 53 53 53
53 53 53 53 53 53 53 53 3 3 3 3 3 3 3 3 3
3 3 3 3 3 3 3 3 3 3 3 3 3 3 3 3 3
53 53 53 53 53 53 53 53
53 53 53 53 53 53 53 3 3 3 3 3 3 3 3 3 3
3 3 3 3 3 3 3 3 3 3 3 3 3 3 3 3 3
3 53 53 53 53 53 53 53 53
53 53 53 53 53 53 53 3 3 3 3 3 3 3 3 3 3
3 3 3 3 3 3 3 3 3 3 3 3 3 3 3 3 3
3 3 53 53 53 53 53 53
53 53 53 53 53 53 3 3 3 3 3 3 3 3 3 3 3
3 3 3 3 3 3 3 3 3 3 3 3 3 3 3 3 3
3 3 3 53 53 53 53 53
53 53 53 53 53 3 3 3 3 3 3 3 3 3 3 3 3
3 3 3 3 3 3 3 3 3 3 3 3 3 3 3 3 3
3 3 3 3 53 53 53 53
53 53 53 53 3 3 3 3 3 3 3 3 3 3 3 3 3
3 3 3 3 3 3 3 3 3 3 3 3 3 3 3 3 3
3 3 3 3 3 53 53 53
53 53 53 3 3 3 3 3 3 3 3 3 3 3 3 3 3
3 3 3 3 3 3 3 3 3 3 3 3 3 3 3 3 3
3 3 3 3 3 3 53 53 53
53 53 3 3 3 3 3 3 3 3 3 3 3 3 3 3 3
```

3 3 3 3 3 3 3 3 3 3 3 3 3 3 3 3 3 3
3 3 3 3 3 3 3 53 53
53 53 3 3 3 3 3 3 3 3 3 3 3 3 3 3 3 3
3 3 3 3 3 3 3 3 3 3 3 3 3 3 3 3 3 3
3 3 3 3 3 3 3 53 53
53 3 3 3 3 3 3 3 3 3 3 3 3 3 3 3 3 3
3 3 3 3 3 3 3 3 3 3 3 3 3 3 3 3 3 3
3 3 3 3 3 3 3 3 53
53 3 3 3 3 3 3 3 3 3 3 3 3 3 3 3 3 3
3 3 3 3 3 3 3 3 3 3 3 3 3 3 3 3 3 3
3 3 3 3 3 3 3 3 53
53 3 3 3 3 3 3 3 3 3 3 3 3 3 3 3 53 53
53 53 53 53 53 53 53 53 53 53 53 3 3 3 3 3 3 3
3 3 3 3 3 3 3 3 53
3 3 3 3 3 3 3 3 3 3 3 3 3 3 3 53 3 53
3 53 3 53 3 53 3 53 3 53 3 53 3 3 3 3 3 3
3 3 3 3 3 3 3 3 3
3 3 3 3 3 3 3 3 3 3 3 3 3 3 3 53 53 93
53 93 53 93 53 93 53 93 53 93 53 53 3 3 3 3 3 3
3 3 3 3 3 3 3 3 3
3 3 3 3 3 3 3 3 3 3 3 3 3 3 3 53 3 53
3 53 3 53 3 53 3 53 3 53 3 53 3 3 3 3 3 3
3 3 3 3 3 3 3 3 3
3 3 3 3 3 3 3 3 3 3 3 3 3 3 3 53 53 93
53 93 53 93 53 93 53 93 53 93 53 53 3 3 3 3 3 3
3 3 3 3 3 3 3 3 3
3 3 3 3 3 3 3 3 3 3 3 3 3 3 3 53 3 53
3 53 3 53 3 53 3 53 3 53 3 53 3 3 3 3 3 3
3 3 3 3 3 3 3 3 3
3 3 3 3 3 3 3 3 3 3 3 3 3 3 3 53 53 93
53 93 53 93 53 93 53 93 53 93 53 53 3 3 3 3 3 3
3 3 3 3 3 3 3 3 3
3 3 3 3 3 3 3 3 3 3 3 3 3 3 3 53 3 53
3 53 3 53 3 53 3 53 3 53 3 53 3 3 3 3 3 3
3 3 3 3 3 3 3 3 3
3 3 3 3 3 3 3 3 3 3 3 3 3 3 3 53 53 93
53 93 53 93 53 93 53 93 53 93 53 53 3 3 3 3 3 3
3 3 3 3 3 3 3 3 3
3 3 3 3 3 3 3 3 3 3 3 3 3 3 3 53 3 53
3 53 3 53 3 53 3 53 3 53 3 53 3 3 3 3 3 3
3 3 3 3 3 3 3 3 3
3 3 3 3 3 3 3 3 3 3 3 3 3 3 3 53 53 93
53 93 53 93 53 93 53 93 53 93 53 53 3 3 3 3 3 3
3 3 3 3 3 3 3 3 3
3 3 3 3 3 3 3 3 3 3 3 3 3 3 3 53 3 53
3 53 3 53 3 53 3 53 3 53 3 53 3 3 3 3 3 3
3 3 3 3 3 3 3 3 3
3 3 3 3 3 3 3 3 3 3 3 3 3 3 3 53 53 93
53 93 53 93 53 93 53 93 53 93 53 53 3 3 3 3 3 3
3 3 3 3 3 3 3 3 3
3 3 3 3 3 3 3 3 3 3 3 3 3 3 3 53 3 53
3 53 3 53 3 53 3 53 3 53 3 53 3 3 3 3 3 3
3 3 3 3 3 3 3 3 3
53 3 3 3 3 3 3 3 3 3 3 3 3 3 3 3 53 53
53 53 53 53 53 53 53 53 53 53 53 3 3 3 3 3 3 3
3 3 3 3 3 3 3 3 53
53 3 3 3 3 3 3 3 3 3 3 3 3 3 3 3 3 3
3 3 3 3 3 3 3 3 3 3 3 3 3 3 3 3 3 3
3 3 3 3 3 3 3 3 53
53 3 3 3 3 3 3 3 3 3 3 3 3 3 3 3 3 3
3 3 3 3 3 3 3 3 3 3 3 3 3 3 3 3 3 3
3 3 3 3 3 3 3 3 53
53 53 3 3 3 3 3 3 3 3 3 3 3 3 3 3 3 3
3 3 3 3 3 3 3 3 3 3 3 3 3 3 3 3 3 3
3 3 3 3 3 3 3 53 53
53 53 3 3 3 3 3 3 3 3 3 3 3 3 3 3 3 3
3 3 3 3 3 3 3 3 3 3 3 3 3 3 3 3 3 3
3 3 3 3 3 3 3 53 53
53 53 53 3 3 3 3 3 3 3 3 3 3 3 3 3 3 3
3 3 3 3 3 3 3 3 3 3 3 3 3 3 3 3 3 3
3 3 3 3 3 3 53 53 53
53 53 53 3 3 3 3 3 3 3 3 3 3 3 3 3 3 3

```
3 3 3 3 3 3 3 3 3 3 3 3 3 3 3 3 3
3 3 3 3 3 3 53 53 53
53 53 53 53 3 3 3 3 3 3 3 3 3 3 3 3 3
3 3 3 3 3 3 3 3 3 3 3 3 3 3 3 3 3
3 3 3 3 3 53 53 53 53
53 53 53 53 53 3 3 3 3 3 3 3 3 3 3 3
3 3 3 3 3 3 3 3 3 3 3 3 3 3 3 3 3
3 3 3 3 53 53 53 53 53
53 53 53 53 53 53 3 3 3 3 3 3 3 3 3 3
3 3 3 3 3 3 3 3 3 3 3 3 3 3 3 3 3
3 3 3 53 53 53 53 53 53
53 53 53 53 53 53 53 3 3 3 3 3 3 3 3 3
3 3 3 3 3 3 3 3 3 3 3 3 3 3 3 3 3
3 3 53 53 53 53 53 53
53 53 53 53 53 53 53 53 3 3 3 3 3 3 3 3
3 3 3 3 3 3 3 3 3 3 3 3 3 3 3 3 3
3 53 53 53 53 53 53 53 53
53 53 53 53 53 53 53 53 53 3 3 3 3 3 3 3
3 3 3 3 3 3 3 3 3 3 3 3 3 3 3 3 3
53 53 53 53 53 53 53 53 53
53 53 53 53 53 53 53 53 53 53 53 53 53 3 3
3 3 3 3 3 3 3 3 3 3 3 3 3 3 3 3 3
53 53 53 53 53 53 53 53 53
53 53 53 53 53 53 53 53 53 53 53 53 53 53 53 3
3 3 3 3 3 3 3 3 3 3 3 3 3 3 3 3 3
53 53 53 53 53 53 53 53 53
53 53 53 53 53 53 53 53 53 53 53 53 53 53 53 53 3 3
3 3 3 3 3 3 3 3 3 3 53 53 53 53 53 53
53 53 53 53 53 53 53 53 53
end fill
ara= 14
nux= 45 nuy= 45 nuz= 1 fill
54 54 54 54 54 54 54 54 54 54 54 54 54 54 54 54 4 4
4 4 4 4 4 4 4 4 4 4 4 54 54 54 54 54 54 54
54 54 54 54 54 54 54 54 54
54 54 54 54 54 54 54 54 54 54 54 54 54 54 4 4 4 4 4
4 4 4 4 4 4 4 4 4 4 4 4 4 4 54 54 54 54
54 54 54 54 54 54 54 54 54
54 54 54 54 54 54 54 54 54 54 54 54 54 54 4 4 4 4 4 4
4 4 4 4 4 4 4 4 4 4 4 4 4 4 4 4 54 54
54 54 54 54 54 54 54 54 54
54 54 54 54 54 54 54 54 54 4 4 4 4 4 4 4 4 4
4 4 4 4 4 4 4 4 4 4 4 4 4 4 4 4 4 4
54 54 54 54 54 54 54 54 54
54 54 54 54 54 54 54 54 54 4 4 4 4 4 4 4 4 4 4 4
4 4 4 4 4 4 4 4 4 4 4 4 4 4 4 4 4 4
4 54 54 54 54 54 54 54 54
54 54 54 54 54 54 54 4 4 4 4 4 4 4 4 4 4 4 4 4
4 4 4 4 4 4 4 4 4 4 4 4 4 4 4 4 4 4
4 4 54 54 54 54 54 54 54
54 54 54 54 54 54 4 4 4 4 4 4 4 4 4 4 4 4 4
4 4 4 4 4 4 4 4 4 4 4 4 4 4 4 4 4 4
4 4 4 54 54 54 54 54 54
54 54 54 54 54 4 4 4 4 4 4 4 4 4 4 4 4 4 4
4 4 4 4 4 4 4 4 4 4 4 4 4 4 4 4 4 4
4 4 4 4 54 54 54 54 54
54 54 54 54 4 4 4 4 4 4 4 4 4 4 4 4 4 4 4
4 4 4 4 4 4 4 4 4 4 4 4 4 4 4 4 4 4
4 4 4 4 4 54 54 54 54
54 54 54 4 4 4 4 4 4 4 4 4 4 4 4 4 4 4 4
4 4 4 4 4 4 4 4 4 4 4 4 4 4 4 4 4 4
4 4 4 4 4 4 54 54 54
54 54 54 4 4 4 4 4 4 4 4 4 4 4 4 4 4 4 4
4 4 4 4 4 4 4 4 4 4 4 4 4 4 4 4 4 4
4 4 4 4 4 4 54 54 54
54 54 4 4 4 4 4 4 4 4 4 4 4 4 4 4 4 4 4
4 4 4 4 4 4 4 4 4 4 4 4 4 4 4 4 4 4
4 4 4 4 4 4 4 54 54
54 54 4 4 4 4 4 4 4 4 4 4 4 4 4 4 4 4 4
4 4 4 4 4 4 4 4 4 4 4 4 4 4 4 4 4 4
4 4 4 4 4 4 4 54 54
54 4 4 4 4 4 4 4 4 4 4 4 4 4 4 4 4 4 4
```

4 4 4 4 4 4 4 4 4 4 4 4 4 4 4 4 4 4
4 4 4 4 4 4 4 4 54
54 4 4 4 4 4 4 4 4 4 4 4 4 4 4 4 4 4 4
4 4 4 4 4 4 4 4 4 4 4 4 4 4 4 4 4 4
4 4 4 4 4 4 4 4 54
54 4 4 4 4 4 4 4 4 4 4 4 4 4 4 4 54 54
54 54 54 54 54 54 54 54 54 54 54 4 4 4 4 4 4 4
4 4 4 4 4 4 4 4 54
4 4 4 4 4 4 4 4 4 4 4 4 4 4 4 54 4 54
4 54 4 54 4 54 4 54 4 54 4 54 4 4 4 4 4 4
4 4 4 4 4 4 4 4 4
4 4 4 4 4 4 4 4 4 4 4 4 4 4 4 54 54 94
54 94 54 94 54 94 54 94 54 94 54 54 4 4 4 4 4 4
4 4 4 4 4 4 4 4 4
4 4 4 4 4 4 4 4 4 4 4 4 4 4 4 54 4 54
4 54 4 54 4 54 4 54 4 54 4 54 4 4 4 4 4 4
4 4 4 4 4 4 4 4 4
4 4 4 4 4 4 4 4 4 4 4 4 4 4 4 54 54 94
54 94 54 94 54 94 54 94 54 94 54 54 4 4 4 4 4 4
4 4 4 4 4 4 4 4 4
4 4 4 4 4 4 4 4 4 4 4 4 4 4 4 54 4 54
4 54 4 54 4 54 4 54 4 54 4 54 4 4 4 4 4 4
4 4 4 4 4 4 4 4 4
4 4 4 4 4 4 4 4 4 4 4 4 4 4 4 54 54 94
54 94 54 94 54 94 54 94 54 94 54 54 4 4 4 4 4 4
4 4 4 4 4 4 4 4 4
4 4 4 4 4 4 4 4 4 4 4 4 4 4 4 54 4 54
4 54 4 54 4 54 4 54 4 54 4 54 4 4 4 4 4 4
4 4 4 4 4 4 4 4 4
4 4 4 4 4 4 4 4 4 4 4 4 4 4 4 54 54 94
54 94 54 94 54 94 54 94 54 94 54 54 4 4 4 4 4 4
4 4 4 4 4 4 4 4 4
4 4 4 4 4 4 4 4 4 4 4 4 4 4 4 54 4 54
4 54 4 54 4 54 4 54 4 54 4 54 4 4 4 4 4 4
4 4 4 4 4 4 4 4 4
4 4 4 4 4 4 4 4 4 4 4 4 4 4 4 54 54 94
54 94 54 94 54 94 54 94 54 94 54 54 4 4 4 4 4 4
4 4 4 4 4 4 4 4 4
4 4 4 4 4 4 4 4 4 4 4 4 4 4 4 54 4 54
4 54 4 54 4 54 4 54 4 54 4 54 4 4 4 4 4 4
4 4 4 4 4 4 4 4 4
4 4 4 4 4 4 4 4 4 4 4 4 4 4 4 54 54 94
54 94 54 94 54 94 54 94 54 94 54 54 4 4 4 4 4 4
4 4 4 4 4 4 4 4 4
4 4 4 4 4 4 4 4 4 4 4 4 4 4 4 54 4 54
4 54 4 54 4 54 4 54 4 54 4 54 4 4 4 4 4 4
4 4 4 4 4 4 4 4 4
54 4 4 4 4 4 4 4 4 4 4 4 4 4 4 4 54 54
54 54 54 54 54 54 54 54 54 54 54 4 4 4 4 4 4 4
4 4 4 4 4 4 4 4 54
54 4 4 4 4 4 4 4 4 4 4 4 4 4 4 4 4 4 4
4 4 4 4 4 4 4 4 4 4 4 4 4 4 4 4 4 4
4 4 4 4 4 4 4 4 54
54 4 4 4 4 4 4 4 4 4 4 4 4 4 4 4 4 4 4
4 4 4 4 4 4 4 4 4 4 4 4 4 4 4 4 4 4
4 4 4 4 4 4 4 4 54
54 54 4 4 4 4 4 4 4 4 4 4 4 4 4 4 4 4 4
4 4 4 4 4 4 4 4 4 4 4 4 4 4 4 4 4 4
4 4 4 4 4 4 4 54 54
54 54 4 4 4 4 4 4 4 4 4 4 4 4 4 4 4 4 4
4 4 4 4 4 4 4 4 4 4 4 4 4 4 4 4 4 4
4 4 4 4 4 4 4 54 54
54 54 54 4 4 4 4 4 4 4 4 4 4 4 4 4 4 4 4
4 4 4 4 4 4 4 4 4 4 4 4 4 4 4 4 4 4
4 4 4 4 4 4 54 54 54
54 54 54 4 4 4 4 4 4 4 4 4 4 4 4 4 4 4 4
4 4 4 4 4 4 4 4 4 4 4 4 4 4 4 4 4 4
4 4 4 4 4 4 54 54 54
54 54 54 54 4 4 4 4 4 4 4 4 4 4 4 4 4 4 4
4 4 4 4 4 4 4 4 4 4 4 4 4 4 4 4 4 4
4 4 4 4 4 54 54 54 54
54 54 54 54 54 4 4 4 4 4 4 4 4 4 4 4 4 4 4

```
4 4 4 4 4 4 4 4 4 4 4 4 4 4 4 4 4 4
4 4 4 4 54 54 54 54 54
54 54 54 54 54 54 4 4 4 4 4 4 4 4 4 4 4 4
4 4 4 4 4 4 4 4 4 4 4 4 4 4 4 4 4 4
4 4 4 54 54 54 54 54 54
54 54 54 54 54 54 54 4 4 4 4 4 4 4 4 4 4
4 4 4 4 4 4 4 4 4 4 4 4 4 4 4 4 4 4
4 4 54 54 54 54 54 54 54
54 54 54 54 54 54 54 54 4 4 4 4 4 4 4 4 4 4
4 4 4 4 4 4 4 4 4 4 4 4 4 4 4 4 4 4
4 54 54 54 54 54 54 54 54
54 54 54 54 54 54 54 54 54 4 4 4 4 4 4 4 4 4
4 4 4 4 4 4 4 4 4 4 4 4 4 4 4 4 4 4
54 54 54 54 54 54 54 54 54
54 54 54 54 54 54 54 54 54 54 54 4 4 4 4 4 4 4
4 4 4 4 4 4 4 4 4 4 4 4 4 4 4 4 54 54
54 54 54 54 54 54 54 54 54
54 54 54 54 54 54 54 54 54 54 54 54 54 4 4 4 4 4
4 4 4 4 4 4 4 4 4 4 4 4 4 4 54 54 54 54
54 54 54 54 54 54 54 54 54
54 54 54 54 54 54 54 54 54 54 54 54 54 54 54 54 4 4
4 4 4 4 4 4 4 4 4 4 4 54 54 54 54 54 54 54
54 54 54 54 54 54 54 54 54
end fill
ara= 15
nux= 45 nuy= 45 nuz= 1 fill
55 55 55 55 55 55 55 55 55 55 55 55 55 55 55 55 5 5
5 5 5 5 5 5 5 5 5 5 55 55 55 55 55 55 55
55 55 55 55 55 55 55 55 55
55 55 55 55 55 55 55 55 55 55 55 55 55 5 5 5 5 5
5 5 5 5 5 5 5 5 5 5 5 5 5 5 55 55 55 55
55 55 55 55 55 55 55 55 55
55 55 55 55 55 55 55 55 55 55 55 5 5 5 5 5 5 5
5 5 5 5 5 5 5 5 5 5 5 5 5 5 5 5 5 55 55
55 55 55 55 55 55 55 55 55
55 55 55 55 55 55 55 55 55 5 5 5 5 5 5 5 5 5 5
5 5 5 5 5 5 5 5 5 5 5 5 5 5 5 5 5 5
55 55 55 55 55 55 55 55 55
55 55 55 55 55 55 55 55 55 5 5 5 5 5 5 5 5 5 5
5 5 5 5 5 5 5 5 5 5 5 5 5 5 5 5 5 5
5 55 55 55 55 55 55 55 55
55 55 55 55 55 55 55 5 5 5 5 5 5 5 5 5 5 5
5 5 5 5 5 5 5 5 5 5 5 5 5 5 5 5 5 5
5 5 55 55 55 55 55 55 55
55 55 55 55 55 55 55 5 5 5 5 5 5 5 5 5 5 5 5
5 5 5 5 5 5 5 5 5 5 5 5 5 5 5 5 5 5
5 5 5 55 55 55 55 55 55
55 55 55 55 55 5 5 5 5 5 5 5 5 5 5 5 5 5 5
5 5 5 5 5 5 5 5 5 5 5 5 5 5 5 5 5 5
5 5 5 5 55 55 55 55 55
55 55 55 55 5 5 5 5 5 5 5 5 5 5 5 5 5 5 5 5
5 5 5 5 5 5 5 5 5 5 5 5 5 5 5 5 5 5
5 5 5 5 5 55 55 55 55
55 55 55 5 5 5 5 5 5 5 5 5 5 5 5 5 5 5 5 5
5 5 5 5 5 5 5 5 5 5 5 5 5 5 5 5 5 5
5 5 5 5 5 5 55 55 55
55 55 55 5 5 5 5 5 5 5 5 5 5 5 5 5 5 5 5 5
5 5 5 5 5 5 5 5 5 5 5 5 5 5 5 5 5 5
5 5 5 5 5 5 55 55 55
55 55 5 5 5 5 5 5 5 5 5 5 5 5 5 5 5 5 5 5
5 5 5 5 5 5 5 5 5 5 5 5 5 5 5 5 5 5
5 5 5 5 5 5 55 55 55
55 55 5 5 5 5 5 5 5 5 5 5 5 5 5 5 5 5 5 5
5 5 5 5 5 5 5 5 5 5 5 5 5 5 5 5 5 5
5 5 5 5 5 5 55 55 55
55 5 5 5 5 5 5 5 5 5 5 5 5 5 5 5 5 5 5
5 5 5 5 5 5 5 5 5 5 5 5 5 5 5 5 5 5
5 5 5 5 5 5 5 55 55
55 5 5 5 5 5 5 5 5 5 5 5 5 5 5 5 5 5 5
5 5 5 5 5 5 5 5 5 5 5 5 5 5 5 5 5 5
5 5 5 5 5 5 5 55 55
55 5 5 5 5 5 5 5 5 5 5 5 5 5 5 5 55 55
```

55 55 55 55 55 55 55 55 55 55 55 5 5 5 5 5 5 5
5 5 5 5 5 5 5 5 55
5 5 5 5 5 5 5 5 5 5 5 5 5 5 5 55 5 55
5 55 5 55 5 55 5 55 5 55 5 55 5 5 5 5 5 5
5 5 5 5 5 5 5 5 5
5 5 5 5 5 5 5 5 5 5 5 5 5 5 5 55 55 95
55 95 55 95 55 95 55 95 55 95 55 55 5 5 5 5 5 5
5 5 5 5 5 5 5 5 5
5 5 5 5 5 5 5 5 5 5 5 5 5 5 5 55 5 55
5 55 5 55 5 55 5 55 5 55 5 55 5 5 5 5 5 5
5 5 5 5 5 5 5 5 5
5 5 5 5 5 5 5 5 5 5 5 5 5 5 5 55 55 95
55 95 55 95 55 95 55 95 55 95 55 55 5 5 5 5 5 5
5 5 5 5 5 5 5 5 5
5 5 5 5 5 5 5 5 5 5 5 5 5 5 5 55 5 55
5 55 5 55 5 55 5 55 5 55 5 55 5 5 5 5 5 5
5 5 5 5 5 5 5 5 5
5 5 5 5 5 5 5 5 5 5 5 5 5 5 5 55 55 95
55 95 55 95 55 95 55 95 55 95 55 55 5 5 5 5 5 5
5 5 5 5 5 5 5 5 5
5 5 5 5 5 5 5 5 5 5 5 5 5 5 5 55 5 55
5 55 5 55 5 55 5 55 5 55 5 55 5 5 5 5 5 5
5 5 5 5 5 5 5 5 5
5 5 5 5 5 5 5 5 5 5 5 5 5 5 5 55 55 95
55 95 55 95 55 95 55 95 55 95 55 55 5 5 5 5 5 5
5 5 5 5 5 5 5 5 5
5 5 5 5 5 5 5 5 5 5 5 5 5 5 5 55 5 55
5 55 5 55 5 55 5 55 5 55 5 55 5 5 5 5 5 5
5 5 5 5 5 5 5 5 5
5 5 5 5 5 5 5 5 5 5 5 5 5 5 5 55 55 95
55 95 55 95 55 95 55 95 55 95 55 55 5 5 5 5 5 5
5 5 5 5 5 5 5 5 5
5 5 5 5 5 5 5 5 5 5 5 5 5 5 5 55 5 55
5 55 5 55 5 55 5 55 5 55 5 55 5 5 5 5 5 5
5 5 5 5 5 5 5 5 5
5 5 5 5 5 5 5 5 5 5 5 5 5 5 5 55 55 95
55 95 55 95 55 95 55 95 55 95 55 55 5 5 5 5 5 5
5 5 5 5 5 5 5 5 5
5 5 5 5 5 5 5 5 5 5 5 5 5 5 5 55 5 55
5 55 5 55 5 55 5 55 5 55 5 55 5 5 5 5 5 5
5 5 5 5 5 5 5 5 5
55 5 5 5 5 5 5 5 5 5 5 5 5 5 5 5 55 55
55 55 55 55 55 55 55 55 55 55 55 5 5 5 5 5 5 5
5 5 5 5 5 5 5 5 55
55 5 5 5 5 5 5 5 5 5 5 5 5 5 5 5 5 5
5 5 5 5 5 5 5 5 5 5 5 5 5 5 5 5 5 5
5 5 5 5 5 5 5 5 55
55 5 5 5 5 5 5 5 5 5 5 5 5 5 5 5 5 5
5 5 5 5 5 5 5 5 5 5 5 5 5 5 5 5 5 5
5 5 5 5 5 5 5 5 55
55 55 5 5 5 5 5 5 5 5 5 5 5 5 5 5 5 5
5 5 5 5 5 5 5 5 5 5 5 5 5 5 5 5 5 5
5 5 5 5 5 5 5 55 55
55 55 5 5 5 5 5 5 5 5 5 5 5 5 5 5 5 5
5 5 5 5 5 5 5 5 5 5 5 5 5 5 5 5 5 5
5 5 5 5 5 5 5 55 55
55 55 55 5 5 5 5 5 5 5 5 5 5 5 5 5 5 5
5 5 5 5 5 5 5 5 5 5 5 5 5 5 5 5 5 5
5 5 5 5 5 5 55 55 55
55 55 55 5 5 5 5 5 5 5 5 5 5 5 5 5 5 5
5 5 5 5 5 5 5 5 5 5 5 5 5 5 5 5 5 5
5 5 5 5 5 5 55 55 55
55 55 55 55 5 5 5 5 5 5 5 5 5 5 5 5 5 5
5 5 5 5 5 5 5 5 5 5 5 5 5 5 5 5 5 5
5 5 5 5 5 55 55 55 55
55 55 55 55 55 5 5 5 5 5 5 5 5 5 5 5 5 5
5 5 5 5 5 5 5 5 5 5 5 5 5 5 5 5 5 5
5 5 5 5 55 55 55 55 55
55 55 55 55 55 55 5 5 5 5 5 5 5 5 5 5 5 5
5 5 5 5 5 5 5 5 5 5 5 5 5 5 5 5 5 5
5 5 5 55 55 55 55 55 55
55 55 55 55 55 55 55 5 5 5 5 5 5 5 5 5 5 5

```
5 5 5 5 5 5 5 5 5 5 5 5 5 5 5 5 5 5 5
5 5 55 55 55 55 55 55 55
55 55 55 55 55 55 55 55 5 5 5 5 5 5 5 5 5 5 5
5 5 5 5 5 5 5 5 5 5 5 5 5 5 5 5 5 5 5
5 55 55 55 55 55 55 55 55
55 55 55 55 55 55 55 55 55 5 5 5 5 5 5 5 5 5
5 5 5 5 5 5 5 5 5 5 5 5 5 5 5 5 5 5 5
55 55 55 55 55 55 55 55 55
55 55 55 55 55 55 55 55 55 55 55 55 5 5 5 5 5 5 5
5 5 5 5 5 5 5 5 5 5 5 5 5 5 5 5 55 55
55 55 55 55 55 55 55 55 55
55 55 55 55 55 55 55 55 55 55 55 55 55 5 5 5 5 5
5 5 5 5 5 5 5 5 5 5 5 5 5 5 55 55 55 55
55 55 55 55 55 55 55 55 55
55 55 55 55 55 55 55 55 55 55 55 55 55 55 55 55 55 5 5
5 5 5 5 5 5 5 5 5 5 5 5 55 55 55 55 55 55
55 55 55 55 55 55 55 55 55
end fill
end array
read plot
  clr=12 180 180  10 end color
  ttl='central few rods'
  xul=-2.  yul= 2.   zul=24.39
  xlr= 2.  ylr=-2.   zlr=24.39
  uax=1    vax=0    wax=0
  udn=0    vdn=-1   wdn=0
  nax=600  ndn=600
  end plt0
  ttl='central "element"'
  xul=-7.7  yul=7.7  zul=24.39
  xlr= 7.7 ylr=-7.7  zlr=24.39
  uax=1    vax=0    wax=0
  udn=0    vdn=-1   wdn=0
  nax=600  ndn=600
  end plt1
  ttl='whole core - midplane'
  xul=-22  yul= 22   zul=24.39
  xlr= 22  ylr=-22   zlr=24.39
  uax=1    vax=0    wax=0
  udn=0    vdn=-1   wdn=0
  nax=600  ndn=600
  end plt2
  ttl='whole core - bottom gridplate'
  xul=-22  yul= 22   zul=-1.2
  xlr= 22  ylr=-22   zlr=-1.2
  uax=1    vax=0    wax=0
  udn=0    vdn=-1   wdn=0
  nax=600  ndn=600
  end plt3
  ttl='whole core - top gridplate'
  xul=-22  yul= 22   zul=51.7
  xlr= 22  ylr=-22   zlr=51.7
  uax=1    vax=0    wax=0
  udn=0    vdn=-1   wdn=0
  nax=600  ndn=600
  end plt4
  ttl='big look - midplane'
  xul=-50  yul= 50   zul=24.39
  xlr= 50  ylr=-50   zlr=24.39
  uax=1    vax=0    wax=0
  udn=0    vdn=-1   wdn=0
  nax=600  ndn=600
  end plt5
  ttl='big look - bottom gridplate'
  xul=-50  yul= 50   zul=-1.2
  xlr= 50  ylr=-50   zlr=-1.2
  uax=1    vax=0    wax=0
  udn=0    vdn=-1   wdn=0
  nax=600  ndn=600
  end plt6
  ttl='big look - top gridplate'
  xul=-50  yul= 50   zul=51.7
```

```
  xlr= 50  ylr=-50   zlr=51.7
  uax=1    vax=0    wax=0
  udn=0    vdn=-1   wdn=0
  nax=600  ndn=600
  end plt7
  ttl='central few rods'
  xul=-2.  yul=0     zul= 26.7
  xlr= 2.  ylr=0     zlr= 22.7
  uax=1    vax=0    wax=0
  udn=0    vdn=0    wdn=-1
  nax=600  ndn=600
  end plt8
  ttl='central few rods - top'
  xul=-4.  yul=0     zul= 53.7
  xlr= 4.  ylr=0     zlr= 45.7
  uax=1    vax=0    wax=0
  udn=0    vdn=0    wdn=-1
  nax=600  ndn=600
  end plt9
  ttl='central few rods - bottom'
  xul=-4.  yul=0     zul= 4.7
  xlr= 4.  ylr=0     zlr=-3.3
  uax=1    vax=0    wax=0
  udn=0    vdn=0    wdn=-1
  nax=600  ndn=600
  end plt10
  ttl='central "element"'
  xul=-7.7 yul= 0.   zul=32.4
  xlr= 7.7 ylr= 0.   zlr=17.0
  end plt11
  ttl='big look'
  xul=-50.  yul=0   zul=  75.
  xlr= 50.  ylr=0   zlr= -25.
  uax=1    vax=0    wax=0
  udn=0    vdn=0    wdn=-1
  nax=600  ndn=600
  end plt12
  ttl='left detector y=6.4'
  xul=-50.  yul= 6.4 zul= 75.
  xlr= 50.  ylr= 6.4 zlr=-25.
  uax=1    vax=0    wax=0
  udn=0    vdn=0    wdn=-1
  nax=600  ndn=600
  end plt13
  ttl='right detector y=-6.4'
  xul=-50.  yul=-6.4 zul= 75.
  xlr= 50.  ylr=-6.4 zlr=-25.
  uax=1    vax=0    wax=0
  udn=0    vdn=0    wdn=-1
  nax=600  ndn=600
  end plt14
end plot
end data
end
```

A.2 MCNP INPUT LISTING

MCNP6.1.1 and the continuous-energy cross section set based on ENDF/B-VII.1 were used. A total of 550 batches of 40,000 neutrons were run. The first 50 batches were skipped. Where necessary, isotopic atom fractions from the Sixteenth Edition of the Chart of the Nuclides[a] were used to subdivide elemental atom densities.

```
MCNP6.1.1 input for Case 24

LCT097 case 24 1485 fuel rod + 36 Ti rod assembly
c
c   fuel rod with grid plates
c
 1     1  6.8772E-02  -1    12   -13       u=1 $ fuel
 2     0              -5    13   -14       u=1 $ inside spring
 3     5  1.8185E-02  -6     5    13   -14 u=1 $ spring
 4     2  5.9877E-02  -7    14   -15       u=1 $ Al spacer
 5     7  1.2413E-01  -7    15   -100      u=1 $ polyethylene spacer
 6     0              -2    12   -100          $ void in clad
                     (1 : 13)                   $ fuel
                     (6 : -13 : 14)             $ spring
                     (7 : -14 : 15)             $ Al spacer
                     (7 : -15 : 100)       u=1  $ poly spacer
 7     3  6.0366E-02  -3    11   -100          $ clad
                     (2 : -12)             u=1  $ void in rod
 8     4  9.9988E-02  -4     3    11   -12 u=1 $ water in lower GP
 9     2  5.9877E-02  10   -12                 $ lower grid plate
                     (4 : -11)              u=1  $ hole
10     4  9.9988E-02 -10                  u=1
11     4  9.9988E-02   3    12   -14       u=1 $ water between GPs
12     4  9.9988E-02  -4     3    14   -15 u=1 $ water in upper GP
13     2  5.9877E-02   4    14   -15       u=1 $ upper grid plate
14     4  9.9988E-02   3    15   -100      u=1 $ water above upper GP
c
c  a water cell
c
114    4  9.9988E-02 -10 -100             u=7 $ water below grid plate
115    2  5.9877E-02  10  -11 :  4   11       $ bottom grid plate
                     -12                  u=7
116    4  9.9988E-02  -4   11  -12        u=7 $ water in lower grid plate
117    4  9.9988E-02  12  -14 -100        u=7 $ water between grid plates
118    4  9.9988E-02  -4   14  -15 -100   u=7 $ water in upper grid plate
119    2  5.9877E-02   4   14  -15        u=7 $ upper grid plate
120    4  9.9988E-02  15 -100             u=7 $ water above grid plate
c
c  Titanium Experiment Rod
c
1920  11  5.6962E-02 -91  11   -100       u=9 $ titanium rod
1926   4  9.9988E-02 -10 -100             u=9 $ water below grid plate
1927   2  5.9877E-02  10  -11 :  4   11       $ lower grid plate
                     -12                  u=9
1928   4  9.9988E-02  -4   91   11  -12   u=9 $ water in lower grid plate
1929   4  9.9988E-02  91   12  -14 -100   u=9 $ water between grid plates
1930   4  9.9988E-02  91   -4   14  -15       $ water in upper grid plate
                    -100                  u=9
1931   2  5.9877E-02   4   14  -15        u=9 $ upper grid plate
1932   4  9.9988E-02  15 -100                $ water above grid plate
                     ( 91 : -11 : 100)   u=9   $ experiment rod
c
c  the array
c
999    4  9.9988E-02 901  -902   903  -904  lat=1  u=10
                   fill -22:23 -22:22  0:0
c  1485 fuel rods 1657 total positions
      7 7 7 7 7 7 7 7 7 7 7 7 7 7 7 1 1 1 1 1 1 1
      1 1 1 1 1 1 7 7 7 7 7 7 7 7 7 7 7 7 7 7 7 7
```

[a] E. M. Baum, et al.,Nuclides and Isotopes, 16th Edition, KAPL, Inc., (2002).

```
7 7 7 7 7 7 7 7 7 7 7 7 7 1 1 1 1 1 1 1 1 1 1
1 1 1 1 1 1 1 1 1 7 7 7 7 7 7 7 7 7 7 7 7 7 7
7 7 7 7 7 7 7 7 7 7 7 1 1 1 1 1 1 1 1 1 1 1 1
1 1 1 1 1 1 1 1 1 1 1 7 7 7 7 7 7 7 7 7 7 7 7
7 7 7 7 7 7 7 7 7 1 1 1 1 1 1 1 1 1 1 1 1 1 1
1 1 1 1 1 1 1 1 1 1 1 1 1 7 7 7 7 7 7 7 7 7 7
7 7 7 7 7 7 7 7 1 1 1 1 1 1 1 1 1 1 1 1 1 1 1
1 1 1 1 1 1 1 1 1 1 1 1 1 1 7 7 7 7 7 7 7 7 7
7 7 7 7 7 7 7 1 1 1 1 1 1 1 1 1 1 1 1 1 1 1 1
1 1 1 1 1 1 1 1 1 1 1 1 1 1 1 7 7 7 7 7 7 7 7
7 7 7 7 7 7 1 1 1 1 1 1 1 1 1 1 1 1 1 1 1 1 1
1 1 1 1 1 1 1 1 1 1 1 1 1 1 1 1 7 7 7 7 7 7 7
7 7 7 7 7 1 1 1 1 1 1 1 1 1 1 1 1 1 1 1 1 1 1
1 1 1 1 1 1 1 1 1 1 1 1 1 1 1 1 1 7 7 7 7 7 7
7 7 7 7 1 1 1 1 1 1 1 1 1 1 1 1 1 1 1 1 1 1 1
1 1 1 1 1 1 1 1 1 1 1 1 1 1 1 1 1 1 7 7 7 7 7
7 7 7 1 1 1 1 1 1 1 1 1 1 1 1 1 1 1 1 1 1 1 1
1 1 1 1 1 1 1 1 1 1 1 1 1 1 1 1 1 1 1 7 7 7 7
7 7 7 1 1 1 1 1 1 1 1 1 1 1 1 1 1 1 1 1 1 1 1
1 1 1 1 1 1 1 1 1 1 1 1 1 1 1 1 1 1 1 7 7 7 7
7 7 1 1 1 1 1 1 1 1 1 1 1 1 1 1 1 1 1 1 1 1 1
1 1 1 1 1 1 1 1 1 1 1 1 1 1 1 1 1 1 1 1 7 7 7
7 7 1 1 1 1 1 1 1 1 1 1 1 1 1 1 1 1 1 1 1 1 1
1 1 1 1 1 1 1 1 1 1 1 1 1 1 1 1 1 1 1 1 7 7 7
7 1 1 1 1 1 1 1 1 1 1 1 1 1 1 1 1 1 1 1 1 1 1
1 1 1 1 1 1 1 1 1 1 1 1 1 1 1 1 1 1 1 1 1 7 7
7 1 1 1 1 1 1 1 1 1 1 1 1 1 1 1 1 1 1 1 1 1 1
1 1 1 1 1 1 1 1 1 1 1 1 1 1 1 1 1 1 1 1 1 7 7
7 1 1 1 1 1 1 1 1 1 1 1 1 1 1 1 7 7 7 7 7 7 7
7 7 7 7 7 7 1 1 1 1 1 1 1 1 1 1 1 1 1 1 1 7 7
1 1 1 1 1 1 1 1 1 1 1 1 1 1 1 7 1 7 1 7 1 7 1
7 1 7 1 7 1 7 1 1 1 1 1 1 1 1 1 1 1 1 1 1 1 7
1 1 1 1 1 1 1 1 1 1 1 1 1 1 1 7 7 9 7 9 7 9 7
9 7 9 7 9 7 7 1 1 1 1 1 1 1 1 1 1 1 1 1 1 1 7
1 1 1 1 1 1 1 1 1 1 1 1 1 1 1 7 1 7 1 7 1 7 1
7 1 7 1 7 1 7 1 1 1 1 1 1 1 1 1 1 1 1 1 1 1 7
1 1 1 1 1 1 1 1 1 1 1 1 1 1 1 7 7 9 7 9 7 9 7
9 7 9 7 9 7 7 1 1 1 1 1 1 1 1 1 1 1 1 1 1 1 7
1 1 1 1 1 1 1 1 1 1 1 1 1 1 1 7 1 7 1 7 1 7 1
7 1 7 1 7 1 7 1 1 1 1 1 1 1 1 1 1 1 1 1 1 1 7
1 1 1 1 1 1 1 1 1 1 1 1 1 1 1 7 7 9 7 9 7 9 7
9 7 9 7 9 7 7 1 1 1 1 1 1 1 1 1 1 1 1 1 1 1 7
1 1 1 1 1 1 1 1 1 1 1 1 1 1 1 7 1 7 1 7 1 7 1
7 1 7 1 7 1 7 1 1 1 1 1 1 1 1 1 1 1 1 1 1 1 7
1 1 1 1 1 1 1 1 1 1 1 1 1 1 1 7 7 9 7 9 7 9 7
9 7 9 7 9 7 7 1 1 1 1 1 1 1 1 1 1 1 1 1 1 1 7
1 1 1 1 1 1 1 1 1 1 1 1 1 1 1 7 1 7 1 7 1 7 1
7 1 7 1 7 1 7 1 1 1 1 1 1 1 1 1 1 1 1 1 1 1 7
1 1 1 1 1 1 1 1 1 1 1 1 1 1 1 7 7 9 7 9 7 9 7
9 7 9 7 9 7 7 1 1 1 1 1 1 1 1 1 1 1 1 1 1 1 7
1 1 1 1 1 1 1 1 1 1 1 1 1 1 1 7 1 7 1 7 1 7 1
7 1 7 1 7 1 7 1 1 1 1 1 1 1 1 1 1 1 1 1 1 1 7
1 1 1 1 1 1 1 1 1 1 1 1 1 1 1 7 7 9 7 9 7 9 7
9 7 9 7 9 7 7 1 1 1 1 1 1 1 1 1 1 1 1 1 1 1 7
1 1 1 1 1 1 1 1 1 1 1 1 1 1 1 7 1 7 1 7 1 7 1
7 1 7 1 7 1 7 1 1 1 1 1 1 1 1 1 1 1 1 1 1 1 7
7 1 1 1 1 1 1 1 1 1 1 1 1 1 1 1 7 7 7 7 7 7 7
7 7 7 7 7 7 1 1 1 1 1 1 1 1 1 1 1 1 1 1 1 7 7
7 1 1 1 1 1 1 1 1 1 1 1 1 1 1 1 1 1 1 1 1 1 1
1 1 1 1 1 1 1 1 1 1 1 1 1 1 1 1 1 1 1 1 1 7 7
7 1 1 1 1 1 1 1 1 1 1 1 1 1 1 1 1 1 1 1 1 1 1
1 1 1 1 1 1 1 1 1 1 1 1 1 1 1 1 1 1 1 1 1 7 7
7 7 1 1 1 1 1 1 1 1 1 1 1 1 1 1 1 1 1 1 1 1 1
1 1 1 1 1 1 1 1 1 1 1 1 1 1 1 1 1 1 1 1 7 7 7
7 7 1 1 1 1 1 1 1 1 1 1 1 1 1 1 1 1 1 1 1 1 1
1 1 1 1 1 1 1 1 1 1 1 1 1 1 1 1 1 1 1 1 7 7 7
7 7 7 1 1 1 1 1 1 1 1 1 1 1 1 1 1 1 1 1 1 1 1
1 1 1 1 1 1 1 1 1 1 1 1 1 1 1 1 1 1 1 7 7 7 7
7 7 7 1 1 1 1 1 1 1 1 1 1 1 1 1 1 1 1 1 1 1 1
1 1 1 1 1 1 1 1 1 1 1 1 1 1 1 1 1 1 1 7 7 7 7
7 7 7 7 1 1 1 1 1 1 1 1 1 1 1 1 1 1 1 1 1 1 1
1 1 1 1 1 1 1 1 1 1 1 1 1 1 1 1 1 1 7 7 7 7 7
```

```
      7 7 7 7 7 1 1 1 1 1 1 1 1 1 1 1 1 1 1 1 1 1 1
      1 1 1 1 1 1 1 1 1 1 1 1 1 1 1 1 1 7 7 7 7 7 7
      7 7 7 7 7 7 1 1 1 1 1 1 1 1 1 1 1 1 1 1 1 1 1
      1 1 1 1 1 1 1 1 1 1 1 1 1 1 1 1 7 7 7 7 7 7 7
      7 7 7 7 7 7 7 1 1 1 1 1 1 1 1 1 1 1 1 1 1 1 1
      1 1 1 1 1 1 1 1 1 1 1 1 1 1 1 7 7 7 7 7 7 7 7
      7 7 7 7 7 7 7 7 1 1 1 1 1 1 1 1 1 1 1 1 1 1 1
      1 1 1 1 1 1 1 1 1 1 1 1 1 1 7 7 7 7 7 7 7 7 7
      7 7 7 7 7 7 7 7 7 1 1 1 1 1 1 1 1 1 1 1 1 1 1
      1 1 1 1 1 1 1 1 1 1 1 1 1 7 7 7 7 7 7 7 7 7 7
      7 7 7 7 7 7 7 7 7 7 7 1 1 1 1 1 1 1 1 1 1 1 1
      1 1 1 1 1 1 1 1 1 1 1 1 7 7 7 7 7 7 7 7 7 7 7
      7 7 7 7 7 7 7 7 7 7 7 7 1 1 1 1 1 1 1 1 1 1 1
      1 1 1 1 1 1 1 1 1 7 7 7 7 7 7 7 7 7 7 7 7 7 7
      7 7 7 7 7 7 7 7 7 7 7 7 7 7 7 1 1 1 1 1 1 1 1
      1 1 1 1 1 1 7 7 7 7 7 7 7 7 7 7 7 7 7 7 7 7 7
c
c
1000   4  9.9988E-02 921  -100   913  -914   915  -916 $ bounds on upper array
           fill=10
1002   2  5.9877E-02 10   -12  -932                    $ bottom grid plate
             (-921 : 912 : -913 : 914 : -915 : 916)      $ the array
1003   2  5.9877E-02 961 -962  963 -964   14   -15     $ top grid plate
             (-921 : 912 : -913 : 914 : -915 : 916)      $ the array
1007   4  9.9988E-02 921 -922 -923 -100                 $ reflector
             (-921 : 912 : -913 : 914 : -915 : 916)      $ the array
                      (-10 : 12 : 932)                   $ bottom grid plate
             (-961 : 962 : -963 : 964 : -14 : 15)        $ top grid plate
             (-803 : 804)                                $-x+y detector tube
             (-803 : 806)                                $+x+y detector tube
             (810 : -811 : 812 : -814)                   $-x-y detector poly
             (810 : -811 : 813 : -815)                   $+x+y detector poly
1030   0             -100   802 -805                     $ -x-y detector well
1031   2  5.9877E-02 -100   803 -804                     $ -x-y detector tube
                    (-802 : 805)                         $-x-y well
1032   7  1.2413E-01 -810   811 -812  814               $ -x-y detector poly
1033   0             -100   802 -807                     $ +x+y detector well
1034   2  5.9877E-02 -100   803 -806                     $ +x+y detector tube
                    (-802 : 807)                         $+x+y well
1035   7  1.2413E-01 -810   811 -813  815               $ +x+y detector poly
1100   0                                                $ external void
                    (-921 : 100 : 923)                   $ water in upper tank

c
c fuel rod surfaces
c
1    cz    0.262814 $ fuel OD
2    cz    0.284519 $ clad ID
3    cz    0.317474 $ clad OD
4    cz    0.333375 $ ID of hole in grid plate at fuel
5    cz    0.17526  $ ID of spring
6    cz    0.22860  $ OD of spring
7    cz    0.26289  $ intermediate plug OD
8    cz    0.26289  $ poly OD
10   pz   -2.54     $ bottom of bottom grid plate
11   pz   -1.27     $ bottom of rod
12   pz    0.0      $ bottom of fuel
13   pz   48.780    $ top of fuel
14   pz   50.4952   $ bottom of upper grid plate
15   pz   53.0352   $ top of upper grid plate
c
c Experiment Rod Surfaces
c
91    cz     0.318479  $ OD of experiment rod
92    pz    78.1812    $ top of experiment rod
c
c     water level
c
100   pz    68.2752        $ top of the water
c
c   detector wells
c
```

```
802   pz     0.735     $ bottom inside of tube
803   pz     0.1       $ bottom of tube
804   c/z   32.385    6.400   3.175  $ OD of tube
805   c/z   32.385    6.400   2.8575 $ ID of tube
806   c/z  -32.385   -6.400   3.175  $ OD of tube
807   c/z  -32.385   -6.400   2.8575 $ ID of tube
810   pz    30.84848                 $ top of poly
811   pz     0.862                   $ bottom of poly
812   c/z   32.385    6.400   5.75945 $ OD poly
813   c/z  -32.385   -6.400   5.75945 $ OD poly
814   c/z   32.385    6.400   3.30581 $ ID poly
815   c/z  -32.385   -6.400   3.30581 $ ID poly
c
c cell boundaries
c
901  px   -0.40005
902  px    0.40005
903  py   -0.40005
904  py    0.40005
c
c array boundaries
c
911  pz  -16.00001
912  pz  145.00001
913  px  -18.00225
914  px   18.00225
915  py  -18.00225
916  py   18.00225
c
c     the water
c
921   pz   -19.05      $ bottom of reflector
922   pz    82.55      $ top of reflector
923   cz    46.83125   $ outside of reflector
932   cz    46.355     $ outside curve of lower grid plate
c
c   upper grid plate
c
961   px   -20.955
962   px    20.955
963   py   -20.955
964   py    20.955

c  Source for Isotopic Atom Fractions:  Chart of the Nuclides 16th ed.
c
c UO2 fuel
c
m1
     92234.80c  6.5539E-06
     92235.80c  1.6010E-03
     92236.80c  1.4632E-05
     92238.80c  2.1296E-02
c  Oxygen 4.5837E-02
      8016.80c 4.57256E-02
      8017.80c 1.74181E-05
c      8018.80c 9.39658E-05
c     47000.xxc  9.2319E-09  $Ag
     47107.80c 4.78572e-09
     47109.80c 4.44618e-09
c      5000.xxc  2.3858E-07  $B
      5010.80c 4.74774e-08
      5011.80c 1.91103e-07
c     48000.xxc  1.2380E-08  $Cd
     48106.80c 1.54750e-10
     48108.80c 1.10182e-10
     48110.80c 1.54626e-09
     48111.80c 1.58464e-09
     48112.80c 2.98729e-09
     48113.80c 1.51284e-09
     48114.80c 3.55677e-09
     48116.80c 9.27262e-10
     27059.80c 2.1620E-08  $Co
```

```
c     24000.xxc  2.5100E-06  $Cr
     24050.80c 1.0906e-07
     24052.80c 2.1031e-06
     24053.80c 2.38475e-07
     24054.80c 5.93615e-08
c     29000.xxc  2.1316E-07  $Cu
     29063.80c 1.47443e-07
     29065.80c 6.57172e-08
c     26000.xxc  1.0311E-05  $Fe
     26054.80c 6.02678e-07
     26056.80c 9.46075e-06
     26057.80c 2.18490e-07
     26058.80c 2.90770e-08
     25055.80c  2.8372E-07  $Mn
c  Molybdenum 1.2443E-07
     42092.80c 1.84654e-08
     42094.80c 1.15098e-08
     42095.80c 1.98093e-08
     42096.80c 2.07549e-08
     42097.80c 1.18831e-08
     42098.80c 3.00250e-08
     42100.80c 1.19826e-08
c     28000.xxc  3.4989E-06  $Ni
     28058.80c 2.38194e-06
     28060.80c 9.17520e-07
     28061.80c 3.98840e-08
     28062.80c 1.27168e-07
     28064.80c 3.23858e-08
c     23000.xxc  1.4813E-08  $V
     23050.80c 3.70325E-11
     23051.80c 1.4776E-08
c     74000.xxc  3.5998E-09  $W
c     74180.70c 4.31976e-12
     74182.80c 9.53947e-10
     74183.80c 5.15131e-10
     74184.80c 1.10298e-09
     74186.80c 1.02342e-09
c
c    6061 aluminum
c
m2
     13027.80c  5.8376E-02
c     14000.xxc  4.1683E-04
     14028.80c 3.84441e-04
     14029.80c 1.95210e-05
     14030.80c 1.28684e-05
c     26000.xxc  1.8051E-04
     26054.80c 1.05508e-05
     26056.80c 1.65625e-04
     26057.80c 3.82501e-06
     26058.80c 5.09038e-07
c     29000.xxc  7.9320E-05
     29063.80c 5.48656e-05
     29065.80c 2.44544e-05
     25055.80c  2.6637E-05
c  Magnesium  6.9574E-04
     12024.80c 5.49565e-04
     12025.80c 6.9574e-05
     12026.80c 7.6601e-05
c     24000.xxc  6.2542E-05
     24050.80c 2.71745e-06
     24052.80c 5.24033e-05
     24053.80c 5.94212e-06
     24054.80c 1.47912e-06
c  Zinc 2.9839E-05
     30064.80c 1.45107E-05
     30066.80c 8.32508E-06
     30067.80c 1.2234E-06
     30068.80c 5.59481E-06
     30070.80c 1.85002E-07
c  Titanium 6.7918e-006
     22046.80c 5.60324e-07
```

```
     22047.80c 5.05310e-07
     22048.80c 5.00691e-06
     22049.80c 3.67436e-07
     22050.80c 3.51815e-07
c  Vanadium 3.1918E-06
      23050.80c 7.9795E-09
      23051.80c 3.18382E-06
c
c    3003 aluminum
c
m3
     13027.80c  5.9668E-02
c     14000.xxc  1.7561E-04
     14028.80c 1.61965e-04
     14029.80c 8.22417e-06
     14030.80c 5.42143e-06
c     26000.xxc  1.0303E-04
     26054.80c 6.02210e-06
     26056.80c 9.45341e-05
     26057.80c 2.18321e-06
     26058.80c 2.90545e-07
c     29000.xxc  3.2339E-05
     29063.80c 2.23689e-05
     29065.80c 9.97011e-06
     25055.80c  3.7407E-04
c  Zinc 1.2571E-05
     30064.80c 6.11328E-06
     30066.80c 3.50731E-06
     30067.80c 5.15411E-07
     30068.80c 2.35706E-06
     30070.80c 7.79402E-08
c
c    water
c
m4
c  Hydrogen 6.6659E-02
      1001.80c 6.66513E-02
      1002.80c 7.66579E-06
c  Oxygen 3.3329E-02
      8016.80c 3.3248E-02
      8017.80c 1.2665E-05
c      8018.80c 6.83244E-05
mt4   lwtr.20t
c
c    stainless steel 304
c
m5
c  Iron 1.2527e-02
     26054.80c 7.32203e-04
     26056.80c 1.14940e-02
     26057.80c 2.65447e-04
     26058.80c 3.53261e-05
c  Chromium 3.6455E-03
     24050.80c 1.58397e-04
     24052.80c 3.05453e-03
     24053.80c 3.46359e-04
     24054.80c 8.62161e-05
c  Nickel 1.5724E-03
     28058.80c 1.07044e-03
     28060.80c 4.12332e-04
     28061.80c 1.79238e-05
     28062.80c 5.71489e-05
     28064.80c 1.45541e-05
     25055.80c  1.8160E-04  $Mn
      6000.80c  3.3225E-05  $C
     15031.80c  7.2471E-06  $P
c  Sulfur 4.6663e-006
     16032.80c 4.42972e-06
     16033.80c 3.54639e-08
     16034.80c 2.00184e-07
     16036.80c 9.33260e-10
c  Silicon 1.7761e-04
```

```
     14028.80c 1.63809e-04
     14029.80c 8.31783e-06
     14030.80c 5.48318e-06
c  Nitrogen 3.5613e-005
      7014.80c 3.54819e-05
      7015.80c 1.31056e-07
c
c    polyethylene (CH2)
c
m7
c  Hydrogen 8.2755E-02
      1001.80c 8.27455E-02
      1002.80c 9.51683E-06
      6000.80c  4.1377E-02
mt7   poly.20t
c
m11
c  Titanium 5.652E-02
      22046.80c 4.6629E-03
      22047.80c 4.20509E-03
      22048.80c 4.16665E-02
      22049.80c 3.05773E-03
      22050.80c 2.92774E-03
c  Carbon
       6000.80c 2.2423E-05
c  Oxygen 1.6972E-04
      8016.80c 1.69308E-04
      8017.80c 6.44936E-08
c      8018.80c 3.47926E-07
c  Nitrogen 3.8773E-05
      7014.80c 3.86303E-05
      7015.80c 1.42685E-07
c  Hydrogen 1.0776E-04
      1001.80c 1.07748E-04
      1002.80c 1.23924E-08
c  Iron 9.9675E-05
      26054.80c 5.826E-06
      26056.80c 9.14558E-05
      26057.80c 2.11211E-06
      26058.80c 2.81084E-07
c
c
imp:n    1 39r 0
mode   n
kcode  40000  1  50  550
ksrc   0 0 24.4
prdmp    0  0  0  1
print    -128
lost   1000 10
kopts  kinetics=yes
ctme 25000
```

A.3 MORET 5 INPUT LISTING

The MORET 5.C.1 code and the continuous-energy cross section set based on ENDF/B-VII.0 were used. A total of420 batches of 10,125 neutrons were run. The first 3 batches were skipped.

MORET5 Input for Case 9

```
DEBUT_MORET
LEU-COMP-THERM-097_case_9


ARRE
  KEFF SIGM 0.00050
FARR

CHIM
PONC
BIBL endf70.xml
TEMP 294

COMP UO2_Fuel CONC
  U234     6.5539E-06
  U235     1.6010E-03
  U236     1.4632E-05
  U238     2.1296E-02
  O16      4.5837E-02
  AG       9.2319E-09
  B        2.3858E-07
  CD       1.2380E-08
  CO       2.1620E-08
  CR       2.5100E-06
  CU       2.1316E-07
  FE       1.0311E-05
  MN       2.8372E-07
  MO       1.2443E-07
  NI       3.4989E-06
  V        1.4813E-08
  W182    9.53947e-10
  W183     5.15131e-10
  W184     1.10298e-09
  W186     1.02342e-09
FINC

COMP 3003_Al CONC
  AL       5.9668E-02
  SI       1.7561E-04
  FE         1.0303E-04
  CU       3.2339E-05
  MN       3.7407E-04
  ZN       1.2571E-05
FINC

COMP Eau CONC
  H1-H2O         6.6659E-02
  O16       3.3329E-02
FINC

COMP 6061_Al CONC
       AL       5.8376E-02
       SI      4.1683E-04
       FE      1.8051E-04
       CU      7.9320E-05
       MN      2.6637E-05
       MG      6.9574E-04
       CR      6.2542E-05
       ZN      2.9839E-05
TI46   5.4293E-07
TI47   4.9542E-07
TI48   5.0085E-06
TI49   3.7326E-07
```

```
TI50    3.6648E-07

        V       3.1918E-06
FINC


COMP POLYETHYLENE CONC
   H1-CH2       8.2755E-02
   C              4.1377E-02
FINC

COMP SS-304 CONC
        FE       1.2527E-02
        CR      3.6455E-03
        NI      1.5724E-03
        MN      1.8160E-04
        C       3.3225E-05
        P       7.2471E-06
        S       4.6663E-06
        SI      1.7761E-04
        N       3.5613E-05
FINC

COMP Air CONC
  N         4.1985E-10
  O16       1.1263E-10
FINC

COMP Titane CONC
C     2.24230E-05
O16   1.69720E-04
N     3.87730E-05
H     1.07760E-04
FE    9.96750E-05
TI    5.65200E-02
FINC

COMP Aluminium_rods CONC
SI      3.35540E-04
FE      5.52780E-05
CU      4.09100E-05
MN      1.47870E-05
MG      5.41480E-04
CR      1.56240E-05
TI      6.78690E-06
GA      2.33030E-06
V       3.18950E-06
AL27    5.90860E-02
FINC

FINChimie

*  ------------------------------------------------------------------------
* MatÃ©riaux
*  1 - Combustible UO2
*  2 - Aluminium 3003
*  3 - Eau
*  4 - Aluminium 6061
*  5 - PolyÃ©thylÃ¨ne
*  6 - SS-304
*  7 - Air
*  8 - Titane
*  9 - Aluminium
*  ------------------------------------------------------------------------

GEOM
MODU 0

*intÃ©rieur cuve (totale)
TYPE 1 CYLZ 46.8376 46.8376
VOLU 1 0 1 7 0. 0. 46.8376
```

```
*intÃ©rieur cuve immergÃ©
*HAUTEUR D'EAU************************************************
TYPE 2 CYLZ 46.8376 46.8376
VOLU 2 1 2 3 0. 0. 46.8376

*RÃ©flecteur bas
TYPE 3 CYLZ 46.8376 8.255
VOLU 3 2 3 3 0. 0. 8.255

*Plaque infÃ©rieure
TYPE 4 CYLZ 46.355 1.27
VOLU 4 2 4 4 0. 0. 17.78

*Plaque supÃ©rieure
TYPE 5 BOITE 20.955 20.955 1.27
VOLU 5 2 5 4 0. 0. 70.8152

*détecteurs
TYPE 6 CYLZ 5.75945 15.0114
TYPE 7 CYLZ 3.30581 15.0114
TYPE 8 CYLZ 3.175 34.0741
TYPE 9 CYLZ 2.8575 33.7566

VOLU 6 1 6 5 32.385 6.4 34.6964 ECRASE 1 2
VOLU 7 6 7 7 32.385 6.4 34.6964
VOLU 8 1 8 4 32.385 6.4 53.1241 ECRASE 3 2 6 7
VOLU 9 8 9 7 32.385 6.4 53.4416

VOLU 10 1 6 5 -32.385 -6.4 34.6964 ECRASE 1 2
VOLU 11 10 7 7 -32.385 -6.4 34.6964
VOLU 12 1 8 4 -32.385 -6.4 53.1241 ECRASE 3 2 10 11
VOLU 13 12 9 7 -32.385 -6.4 53.4416

*Crayons combustibles
TYPE 14 BOIT 18.00225 18.00225 35.4076
TROU 1 1 14 1 0.0 0.0 51.9176 ECRASE 4 3 4 2 5

FINM

MODU 1
* universe
TYPE 1 BOITE 18.00225 18.00225 35.4076
VOLU 1 0 1 3 0. 0. 35.4076

*Volume Maille
TYPE 2 BOITE 0.40005 0.40005 35.4076
VOLU 2 1 2 3 -17.6022 -17.6022 35.4076

*Zone 1
TYPE 3 BOITE 0.40005 0.40005 0.635
VOLU 3 2 3 4 -17.6022 -17.6022 0.635

*Zone 2
*ALU
TYPE 4 BOITE 0.40005 0.40005 0.635
VOLU 4 2 4 4 -17.6022 -17.6022 1.905
*EAU
TYPE 5 CYLZ 0.333375 0.635
VOLU 5 4 5 3 -17.6022 -17.6022 1.905
*ALU3003
TYPE 6 CYLZ 0.317474 0.635
VOLU 6 5 6 2 -17.6022 -17.6022 1.905

*Zone 3
*AIR
TYPE 7 BOITE 0.40005 0.40005 24.39
VOLU 7 2 7 3 -17.6022 -17.6022 26.93
*EAU**********************************************************
TYPE 71 BOITE 0.40005 0.40005 24.34
VOLU 71 7 71 3 -17.6022 -17.6022 26.88
*3003 ALU
TYPE 8 CYLZ 0.317474 24.39
```

```
VOLU 8 7 8 2 -17.6022 -17.6022 26.93 ECRASE 1 71
*VIDE
TYPE 9 CYLZ 0.284519 24.39
VOLU 9 8 9 7 -17.6022 -17.6022 26.93
*UO2
TYPE 10 CYLZ 0.262814 24.39
VOLU 10 9 10 1 -17.6022 -17.6022 26.93

*Zone 4
*VIDE
TYPE 11 BOITE 0.40005 0.40005 0.8576
VOLU 11 2 11 3 -17.6022 -17.6022 52.1776
*3003 ALU
TYPE 12 CYLZ 0.317474 0.8576
VOLU 12 11 12 2 -17.6022 -17.6022 52.1776
*VIDE
TYPE 13 CYLZ 0.284519 0.8576
VOLU 13 12 13 7 -17.6022 -17.6022 52.1776
*303 SS
TYPE 14 CYLZ 0.2286 0.8576
VOLU 14 13 14 6 -17.6022 -17.6022 52.1776
*VIDE
TYPE 15 CYLZ 0.17526 0.8576
VOLU 15 14 15 7 -17.6022 -17.6022 52.1776

*zone 5
*6061 Al
TYPE 16 BOITE 0.40005 0.40005 1.27
VOLU 16 2 16 4 -17.6022 -17.6022 54.3052
*VIDE
TYPE 17 CYLZ 0.333375 1.27
VOLU 17 16 17 3 -17.6022 -17.6022 54.3052
*3003 AL
TYPE 18 CYLZ 0.317474 1.27
VOLU 18 17 18 2 -17.6022 -17.6022 54.3052
*VIDE
TYPE 19 CYLZ 0.284519 1.27
VOLU 19 18 19 7 -17.6022 -17.6022 54.3052
*6061 AL
TYPE 20 CYLZ 0.26289 1.27
VOLU 20 19 20 4 -17.6022 -17.6022 54.3052


*zone 6
*VIDE
TYPE 21 BOITE 0.40005 0.40005 7.62
VOLU 21 2 21 3 -17.6022 -17.6022 63.1952
*3003 AL
TYPE 22 CYLZ 0.317474 7.62
VOLU 22 21 22 2 -17.6022 -17.6022 63.1952
*VIDE
TYPE 23 CYLZ 0.284519 7.62
VOLU 23 22 23 7 -17.6022 -17.6022 63.1952
*CH2
TYPE 24 CYLZ 0.26289 7.62
VOLU 24 23 24 5 -17.6022 -17.6022 63.1952


**************MAILLE SECONDAIRE*************************

*Volume Maille secondaire
VOLU 200 1 2 7 -17.6022 -17.6022 35.4076

*Zone 1
TYPE 300 BOITE 0.40005 0.40005 0.635
VOLU 300 200 300 4 -17.6022 -17.6022 0.635

*Zone 2
*ALU
TYPE 400 BOITE 0.40005 0.40005 0.635
VOLU 400 200 400 4 -17.6022 -17.6022 1.905
*EAU
```

```
TYPE 500 CYLZ 0.333375 0.635
VOLU 500 400 500 3 -17.6022 -17.6022 1.905


*Zone 3
*AIR
TYPE 700 BOITE 0.40005 0.40005 24.39
VOLU 700 200 700 3 -17.6022 -17.6022 26.93
*EAU************************************************************
TYPE 710 BOITE 0.40005 0.40005 24.34
VOLU 710 700 710 3 -17.6022 -17.6022 26.88

*Zone 4
*VIDE
TYPE 110 BOITE 0.40005 0.40005 0.8576
VOLU 110 200 110 3 -17.6022 -17.6022 52.1776

*zone 5
*6061 Al
TYPE 160 BOITE 0.40005 0.40005 1.27
VOLU 160 200 160 4 -17.6022 -17.6022 54.3052
*VIDE
TYPE 170 CYLZ 0.333375 1.27
VOLU 170 160 170 3 -17.6022 -17.6022 54.3052


*zone 6
*VIDE
TYPE 210 BOITE 0.40005 0.40005 7.62
VOLU 210 200 210 3 -17.6022 -17.6022 63.1952


*-----Crayon Titane-----------------------------------------------------------------------------------
-------------

*Volume Maille secondaire
VOLU 201 1 2 7 -17.6022 -17.6022 35.4076

*Zone 1
TYPE 301 BOITE 0.40005 0.40005 0.635
VOLU 301 201 301 4 -17.6022 -17.6022 0.635

*Zone 2
*ALU
TYPE 401 BOITE 0.40005 0.40005 0.635
VOLU 401 201 401 4 -17.6022 -17.6022 1.905
*EAU
TYPE 501 CYLZ 0.333375 0.635
VOLU 501 401 501 3 -17.6022 -17.6022 1.905
*titane
TYPE 411 CYLZ 0.318479 0.635
VOLU 411 501 411 8 -17.6022 -17.6022 1.905


*Zone 3
*EAU
TYPE 701 BOITE 0.40005 0.40005 24.39
VOLU 701 201 701 3 -17.6022 -17.6022 26.93
*titane
TYPE 811 CYLZ 0.318479 24.39
VOLU 811 701 811 8 -17.6022 -17.6022 26.93

*Zone 4
*VIDE
TYPE 111 BOITE 0.40005 0.40005 0.8576
VOLU 111 201 111 3 -17.6022 -17.6022 52.1776
*titane
TYPE 911 CYLZ 0.318479 0.8576
VOLU 911 111 911 8 -17.6022 -17.6022 52.1776

*zone 5
*6061 Al
```

```
TYPE 161 BOITE 0.40005 0.40005 1.27
VOLU 161 201 161 4 -17.6022 -17.6022 54.3052
*VIDE
TYPE 171 CYLZ 0.333375 1.27
VOLU 171 161 171 3 -17.6022 -17.6022 54.3052
*titane
TYPE 181 CYLZ 0.318479 1.27
VOLU 181 171 181 8 -17.6022 -17.6022 54.3052

*zone 6
*VIDE
TYPE 211 BOITE 0.40005 0.40005 7.62
VOLU 211 201 211 3 -17.6022 -17.6022 63.1952
*titane
TYPE 311 CYLZ 0.318479 7.62
VOLU 311 211 311 8 -17.6022 -17.6022 63.1952

* *-----Crayon ALU-----------------------------------------------------------------------------------
------------
* *Volume Maille secondaire
*VOLU 202 1 2 7 -17.6022 -17.6022 35.4076
*
* *Zone 1
*TYPE 302 BOITE 0.40005 0.40005 0.635
*VOLU 302 202 302 4 -17.6022 -17.6022 0.635
*
* *Zone 2
* *ALU
*TYPE 402 BOITE 0.40005 0.40005 0.635
*VOLU 402 202 402 4 -17.6022 -17.6022 1.905
* *EAU
*TYPE 502 CYLZ 0.333375 0.635
*VOLU 502 402 502 3 -17.6022 -17.6022 1.905
* *alu
*TYPE 412 CYLZ 0.319368 0.635
*VOLU 412 502 412 9 -17.6022 -17.6022 1.905
*
*
* *Zone 3
* *EAU
*TYPE 702 BOITE 0.40005 0.40005 24.39
*VOLU 702 202 702 3 -17.6022 -17.6022 26.93
* *alu
*TYPE 812 CYLZ 0.319368 24.39
*VOLU 812 702 812 9 -17.6022 -17.6022 26.93
*
* *Zone 4
* *VIDE
*TYPE 112 BOITE 0.40005 0.40005 0.8576
*VOLU 112 202 112 3 -17.6022 -17.6022 52.1776
* *alu
*TYPE 912 CYLZ 0.319368 0.8576
*VOLU 912 112 912 9 -17.6022 -17.6022 52.1776
*
* *zone 5
* *6061 Al
*TYPE 162 BOITE 0.40005 0.40005 1.27
*VOLU 162 202 162 4 -17.6022 -17.6022 54.3052
* *VIDE
*TYPE 172 CYLZ 0.333375 1.27
*VOLU 172 162 172 3 -17.6022 -17.6022 54.3052
* *alu
*TYPE 182 CYLZ 0.319368 1.27
*VOLU 182 172 182 9 -17.6022 -17.6022 54.3052
*
* *zone 6
* *VIDE
*TYPE 212 BOITE 0.40005 0.40005 7.62
*VOLU 212 202 212 3 -17.6022 -17.6022 63.1952
* *alu
*TYPE 312 CYLZ 0.319368 7.62
*VOLU 312 212 312 9 -17.6022 -17.6022 63.1952
```

```
*-----------------------------------------------------
* CRAYON TITANE : VOLUME 201
* CRAYON ALUMINIUM : VOLUME 202
*-----------------------------------------------------


RESC
 MPRI 2
 DIMR 45 45 1
 INDP 1 1 1
 MSEC 200 432 1 45 1
           1 44 1
           1 43 1
           1 42 1
           1 41 1
           1 40 1
           1 39 1
           1 38 1
           1 37 1
           1 36 1
           1 35 1
           1 34 1
           1 33 1
           1 32 1
           1 31 1
           1 30 1
           1 29 1
           1 28 1
           1 18 1
           1 17 1
           1 16 1
           1 15 1
           1 14 1
           1 13 1
           1 12 1
           1 11 1
           1 10 1
           1 9 1
           1 8 1
           1 7 1
           1 6 1
           1 5 1
           1 4 1
           1 3 1
           1 2 1
           1 1 1
           2 45 1
           2 44 1
           2 43 1
           2 42 1
           2 41 1
           2 40 1
           2 39 1
           2 38 1
           2 37 1
           2 36 1
           2 35 1
           2 34 1
           2 33 1
           2 32 1
           2 14 1
           2 13 1
           2 12 1
           2 11 1
           2 10 1
           2 9 1
           2 8 1
           2 7 1
           2 6 1
           2 5 1
           2 4 1
```

```
2 3 1
2 2 1
2 1 1
3 45 1
3 44 1
3 43 1
3 42 1
3 41 1
3 40 1
3 39 1
3 38 1
3 37 1
3 36 1
3 35 1
3 34 1
3 12 1
3 11 1
3 10 1
3 9 1
3 8 1
3 7 1
3 6 1
3 5 1
3 4 1
3 3 1
3 2 1
3 1 1
4 45 1
4 44 1
4 43 1
4 42 1
4 41 1
4 40 1
4 39 1
4 38 1
4 37 1
4 36 1
4 11 1
4 10 1
4 9 1
4 8 1
4 7 1
4 6 1
4 5 1
4 4 1
4 3 1
4 2 1
4 1 1
5 45 1
5 44 1
5 43 1
5 42 1
5 4 1
5 3 1
5 2 1
5 1 1
6 45 1
6 44 1
6 43 1
6 42 1
6 4 1
6 3 1
6 2 1
6 1 1
7 45 1
7 44 1
7 43 1
7 42 1
7 4 1
7 3 1
7 2 1
7 1 1
```

```
8 45 1
8 44 1
8 43 1
8 42 1
8 4 1
8 3 1
8 2 1
8 1 1
9 45 1
9 44 1
9 43 1
9 42 1
9 4 1
9 3 1
9 2 1
9 1 1
10 45 1
10 44 1
10 43 1
10 42 1
10 4 1
10 3 1
10 2 1
10 1 1
11 45 1
11 44 1
11 43 1
11 42 1
11 4 1
11 3 1
11 2 1
11 1 1
12 45 1
12 44 1
12 43 1
12 3 1
12 2 1
12 1 1
13 45 1
13 44 1
13 2 1
13 1 1
14 45 1
14 44 1
14 2 1
14 1 1
15 45 1
15 1 1
16 45 1
16 1 1
17 45 1
17 1 1
18 45 1
18 1 1
28 45 1
28 1 1
29 45 1
29 1 1
30 45 1
30 1 1
31 45 1
31 1 1
32 45 1
32 44 1
32 2 1
32 1 1
33 45 1
33 44 1
33 2 1
33 1 1
34 45 1
34 44 1
```

```
34 43 1
34 3 1
34 2 1
34 1 1
35 45 1
35 44 1
35 43 1
35 3 1
35 2 1
35 1 1
36 45 1
36 44 1
36 43 1
36 42 1
36 4 1
36 3 1
36 2 1
36 1 1
37 45 1
37 44 1
37 43 1
37 42 1
37 4 1
37 3 1
37 2 1
37 1 1
38 45 1
38 44 1
38 43 1
38 42 1
38 4 1
38 3 1
38 2 1
38 1 1
39 45 1
39 44 1
39 43 1
39 42 1
39 4 1
39 3 1
39 2 1
39 1 1
40 45 1
40 44 1
40 43 1
40 42 1
40 4 1
40 3 1
40 2 1
40 1 1
41 45 1
41 44 1
41 43 1
41 42 1
41 4 1
41 3 1
41 2 1
41 1 1
42 45 1
42 44 1
42 43 1
42 42 1
42 41 1
42 40 1
42 39 1
42 38 1
42 37 1
42 36 1
42 35 1
42 10 1
42 9 1
42 8 1
```

```
42 7 1
42 6 1
42 5 1
42 4 1
42 3 1
42 2 1
42 1 1
43 45 1
43 44 1
43 43 1
43 42 1
43 41 1
43 40 1
43 39 1
43 38 1
43 37 1
43 36 1
43 35 1
43 34 1
43 12 1
43 11 1
43 10 1
43 9 1
43 8 1
43 7 1
43 6 1
43 5 1
43 4 1
43 3 1
43 2 1
43 1 1
44 45 1
44 44 1
44 43 1
44 42 1
44 41 1
44 40 1
44 39 1
44 38 1
44 37 1
44 36 1
44 35 1
44 34 1
44 33 1
44 32 1
44 14 1
44 13 1
44 12 1
44 11 1
44 10 1
44 9 1
44 8 1
44 7 1
44 6 1
44 5 1
44 4 1
44 3 1
44 2 1
44 1 1
45 45 1
45 44 1
45 43 1
45 42 1
45 41 1
45 40 1
45 39 1
45 38 1
45 37 1
45 36 1
45 35 1
45 34 1
45 33 1
```

```
45 32 1
45 31 1
45 30 1
45 29 1
45 28 1
45 18 1
45 17 1
45 16 1
45 15 1
45 14 1
45 13 1
45 12 1
45 11 1
45 10 1
45 9 1
45 8 1
45 7 1
45 6 1
45 5 1
45 4 1
45 3 1
45 2 1
45 1 1
5 41 1
5 40 1
5 39 1
5 38 1
5 37 1
6 41 1
6 40 1
6 39 1
6 38 1
7 41 1
7 40 1
7 39 1
8 41 1
8 40 1
9 41 1
37 41 1
38 41 1
38 40 1
39 41 1
39 40 1
39 39 1
40 41 1
40 40 1
40 39 1
40 38 1
41 41 1
41 40 1
41 39 1
41 38 1
41 37 1
5 9 1
5 8 1
5 7 1
5 6 1
5 5 1
6 8 1
6 7 1
6 6 1
6 5 1
7 7 1
7 6 1
7 5 1
8 6 1
8 5 1
9 5 1
37 5 1
38 6 1
38 5 1
39 7 1
```

```
            39 6 1
            39 5 1
            40 8 1
            40 7 1
            40 6 1
            40 5 1
            41 9 1
            41 8 1
            41 7 1
            41 6 1
            41 5 1
              MSEC 201 36 16 32 1
            16 29 1
            16 26 1
            16 23 1
            16 20 1
            16 17 1
            19 32 1
            19 29 1
            19 26 1
            19 23 1
            19 20 1
            19 17 1
            22 32 1
            22 29 1
            22 26 1
            22 23 1
            22 20 1
            22 17 1
            25 32 1
            25 29 1
            25 26 1
            25 23 1
            25 20 1
            25 17 1
            28 32 1
            28 29 1
            28 26 1
            28 23 1
            28 20 1
            28 17 1
            31 32 1
            31 29 1
            31 26 1
            31 23 1
            31 20 1
            31 17 1

FINR

FINM


FING


GRAP X 0.44 FGRA
PEIN X 0.44 FGRA
GRAP Y 6.4 FGRA
PEIN Y 6.4 FGRA
GRAP Y -6.4 FGRA
PEIN Y -6.4 FGRA
GRAP Z 30 FGRA
PEIN Z 30 FGRA



SORTies
     RESP
          LIST myflux 1 FLUX
    ENDR
```

```
    EBIN
          LIST mybin 1 DEC172_APO2
    ENDE

    LIEUx
         DEFI myloca MODU 0 VOLU 1
    FLIE

    SENS
      EBIN  238 1.0000000E-11 1.0000000E-10 5.0000000E-10 7.5000000E-10 1.0000000E-09 1.2000000E-09
1.5000000E-09 2.0000000E-09
                2.5000000E-09 3.0000000E-09 4.0000000E-09 5.0000000E-09 7.5000000E-09 1.0000000E-08
2.5300000E-08 3.0000000E-08
                4.0000000E-08 5.0000000E-08 6.0000000E-08 7.0000000E-08 8.0000000E-08 9.0000000E-08
1.0000000E-07 1.2500000E-07
                1.5000000E-07 1.7500000E-07 2.0000000E-07 2.2500000E-07 2.5000000E-07 2.7500000E-07
3.0000000E-07 3.2500000E-07
                3.5000000E-07 3.7500000E-07 4.0000000E-07 4.5000000E-07 5.0000000E-07 5.5000000E-07
6.0000000E-07 6.2500000E-07
                6.5000000E-07 7.0000000E-07 7.5000000E-07 8.0000000E-07 8.5000000E-07 9.0000000E-07
9.2500000E-07 9.5000000E-07
                9.7500000E-07 1.0000000E-06 1.0100000E-06 1.0200000E-06 1.0300000E-06 1.0400000E-06
1.0500000E-06 1.0600000E-06
                1.0700000E-06 1.0800000E-06 1.0900000E-06 1.1000000E-06 1.1100000E-06 1.1200000E-06
1.1300000E-06 1.1400000E-06
                1.1500000E-06 1.1750000E-06 1.2000000E-06 1.2250000E-06 1.2500000E-06 1.3000000E-06
1.3500000E-06 1.4000000E-06
                1.4500000E-06 1.5000000E-06 1.5900000E-06 1.6800000E-06 1.7700000E-06 1.8600000E-06
1.9400000E-06 2.0000000E-06
                2.1200000E-06 2.2100000E-06 2.3000000E-06 2.3800000E-06 2.4700000E-06 2.5700000E-06
2.6700000E-06 2.7700000E-06
                2.8700000E-06 2.9700000E-06 3.0000000E-06 3.0500000E-06 3.1500000E-06 3.5000000E-06
3.7300000E-06 4.0000000E-06
                4.7500000E-06 5.0000000E-06 5.4000000E-06 6.0000000E-06 6.2500000E-06 6.5000000E-06
6.7500000E-06 7.0000000E-06
                7.1500000E-06 8.1000000E-06 9.1000000E-06 1.0000000E-05 1.1500000E-05 1.1900000E-05
1.2900000E-05 1.3750000E-05
                1.4400000E-05 1.5100000E-05 1.6000000E-05 1.7000000E-05 1.8500000E-05 1.9000000E-05
2.0000000E-05 2.1000000E-05
                2.2500000E-05 2.5000000E-05 2.7500000E-05 3.0000000E-05 3.1250000E-05 3.1750000E-05
3.3250000E-05 3.3750000E-05
                3.4600000E-05 3.5500000E-05 3.7000000E-05 3.8000000E-05 3.9100000E-05 3.9600000E-05
4.1000000E-05 4.2400000E-05
                4.4000000E-05 4.5200000E-05 4.7000000E-05 4.8300000E-05 4.9200000E-05 5.0600000E-05
5.2000000E-05 5.3400000E-05
                5.9000000E-05 6.1000000E-05 6.5000000E-05 6.7500000E-05 7.2000000E-05 7.6000000E-05
8.0000000E-05 8.2000000E-05
                9.0000000E-05 1.0000000E-04 1.0800000E-04 1.1500000E-04 1.1900000E-04 1.2200000E-04
1.8600000E-04 1.9250000E-04
                2.0750000E-04 2.1000000E-04 2.4000000E-04 2.8500000E-04 3.0500000E-04 5.5000000E-04
6.7000000E-04 6.8300000E-04
                9.5000000E-04 1.1500000E-03 1.5000000E-03 1.5500000E-03 1.8000000E-03 2.2000000E-03
2.2900000E-03 2.5800000E-03
                3.0000000E-03 3.7400000E-03 3.9000000E-03 6.0000000E-03 8.0300000E-03 9.5000000E-03
1.3000000E-02 1.7000000E-02
                2.5000000E-02 3.0000000E-02 4.5000000E-02 5.0000000E-02 5.2000000E-02 6.0000000E-02
7.3000000E-02 7.5000000E-02
                8.2000000E-02 8.5000000E-02 1.0000000E-01 1.2830000E-01 1.5000000E-01 2.0000000E-01
2.7000000E-01 3.3000000E-01
                4.0000000E-01 4.2000000E-01 4.4000000E-01 4.7000000E-01 4.9952000E-01 5.5000000E-01
5.7300000E-01 6.0000000E-01
                6.7000000E-01 6.7900000E-01 7.5000000E-01 8.2000000E-01 8.6110000E-01 8.7500000E-01
9.0000000E-01 9.2000000E-01
                1.0100000E+00 1.1000000E+00 1.2000000E+00 1.2500000E+00 1.3170000E+00 1.3560000E+00
1.4000000E+00 1.5000000E+00
                1.8500000E+00 2.3540000E+00 2.4790000E+00 3.0000000E+00 4.3040000E+00 4.8000000E+00
6.4340000E+00 8.1873000E+00
                1.0000000E+01 1.2840000E+01 1.3840000E+01 1.4550000E+01 1.5683000E+01 1.7333000E+01
2.0000000E+01
    * EBIN  3 1.000000E-11 6.250000E-07 1.000000E-01 2.000000E+01
     ADJO 2
```

```
  ENDS

 SCOR
          * ANNUle TOUS
          DEFI testflux
            EBIN mybin
            LIEU myloca
            REPONSE myflux
FSCOre
FSORties


SOUR
 UNIF 5 MODU 1 VOLU 10 FUNI
FINS


FIND

FIN_MORET
```